Investigation of the cellular and physiological effects of 5 alpha-tetrahydro reduced glucocorticoids *in vitro* and *in vivo*

Chenjing Yang

Doctor of Philosophy

The University of Edinburgh

2009

Contents

Abstract

Glucocorticoids have been the most widely used anti-inflammatory drugs. However, chronic excessive exposure to glucocorticoids causes numerous side effects, including obesity, hypertension and type II diabetes. Thus dissociated steroids with anti-inflammatory efficacy and reduced metabolic side effects are an attractive therapeutic goal. A previous study has shown that 5α-tetrahydro corticosterone (5αTHB), produced by steroid 5α-reductases in rodents, is an activator of glucocorticoid receptor (GR). Therefore, we hypothesized that 5αTHB may possess some of the properties of the parent steroid to transactivate and transrepress genes regulated by GR and have shown it possesses some of the characteristics of a dissociated steroid.

In cultured cells, 5αTHB has weaker effects than corticosterone to induce GR translocation but was synergistic with corticosterone. 5αTHB did not induce the expression of PEPCK or TAT or glucocorticoid responsive reporter genes. In contrast however in bone marrow derived macrophages, 5αTHB increased the secretion of anti-inflammatory cytokine IL-10 and suppressed LPS-induced production of pro-inflammatory cytokines TNFα and IL-6.

In C57BL/6 mice following acute administration of 5αTHB, glucose tolerance and insulin sensitivity were not affected, and hepatic PEPCK and TAT were not increased. In mice that were chronically infused with 5αTHB, body and organ weights, glucose tolerance, insulin sensitivity, or expression of glucocorticoid responsive genes in liver and adipose tissue were not changed. However circulating ACTH was suppressed and in whole blood, LPS-induced production of TNFα was suppressed. In mice suffering from peritonitis induced by LPS, 5αTHB suppressed IL-6 levels in peritoneal fluid to a similar extent as corticosterone.

Therefore the contribution of 5α-reductase type 1 (5αR1) to protect metabolic tissues from adverse metabolic effects of glucocorticoids was tested in 5αR1 deficient mice.

Circulating corticosterone was elevated in animals receiving corticosterone with no difference between genotypes. Infusion of corticosterone induced a greater elevation in insulin and free fatty acids during a glucose tolerance test in 5αR1-null mice, compared to wild-type controls. In the mesenteric adipose tissue, angiotensinogen expression was only increased in 5αR1-null mice receiving corticosterone. However suppression of TNFα and IL-6 by corticosterone in the whole blood was independent of genotype.

In conclusion, 5αTHB is a weak GR ligand, but possesses some anti-inflammatory properties similar to those of corticosterone, potentially acting through GR-protein interactions as opposed to GR-GRE interactions. 5αTHB could be a prototype for a selective anti-inflammatory drug with limited metabolic toxicity. Thus inhibition of 5αR1 may cause detrimental metabolic effects without inducing immune suppression.

List of Figures

List of Tables

Abbreviations

5αDHB	5α-dihydro corticosterone
5αDHF	5α-Dihydrocortisol
5αR	5α-reductase
5αTHB	5α-tetrahydro corticosterone
5βR	5β-reductase
AAP	Aminoantipyrine
ADP	Adenosine diphosphate
AF	Activation function
Agt	Angiotensinogen
AKR	Aldo-keto reductase
ANP	Atrial natriuretic peptide
AP	Activator protein
AT1	Angiotensin II receptor type 1
ATP	Adenosine triphosphate
ATPase	Adenosine triphosphatase
ATT	Aspartate aminotransferase
B	Corticosterone
bp	Base pair
BSA	Bovine serum albumin
BW	Body weight
CBA	Cytometric bead array

CBG	Corticosteroid-binding globulin
cDNA	Complementary DNA
Cp	Crossing point
CRH	Corticotrophin-releasing hormone
CRH R1	CRH receptor 1
DAP	Dihydroxyacetone phosphate
DHBS	Dichloro-2-hydroxybenzene sulfonate
DHC	Dehydrocorticosterone
DMEM	Dulbecco's modified Eagle's medium
DMSO	Dimethyl sulfoxide
DNA	Deoxyribonucleic acid
DPBS	Dulbecco's phosphate buffered saline
EDTA	Ethylene diamine tetraacetic acid
ELISA	Enzyme-linked immunosorbent assay
FDPase	Fructose-1,6-diphosphatase
G6Pase	Glucose-6-phosphatase
GABA	Gamma-aminobutyric acid
GK	Glycerol kinase
GM-CSF	Granulocyte-macrophage colony-stimulating factor
GPO	Glycerol phosphate oxidase
GR	Glucocorticoid receptor
GRE	Glucocorticoid response element
GRE1/2s	Glucocorticoid response element half sites
GRU	Glucocorticoid responsive unit

GTT	Glucose tolerance test
h	Hour
H_2O_2	Hydrogen peroxide
H4IIE	Rat hepatoma cell line
HBSS	Hank's balanced salt solution
HEK293	Human embryonic kidney cell line
Hepes	4-(2-Hydroxyethyl)piperazine-1-ethanesulfonic acid
Hop	Hsp organizing protein
HSD	Hydroxysteroid dehydrogenase
hsp	Heat shock protein
i.p.	Intraperitoneal
IFN	Interferon
IL	Interleukin
IMM	Immunophilins
IκB	Inhibitor of NFκB
K_{Ca}	Calcium-activated potassium channel
KH_2PO_4	Potassium dihydrogen orthophosphate
KO	Knock-out
KOH	Potassium hydroxide
LCM	L929 conditioned medium
LPL	Lipoprotein lipase
LPS	Lipopolysaccharide
MAPK	Mitogen-activated protein kinase
MKP	MAPK phosphatase

MCP	Monocyte chemoattractant protein
M-CSF	Macrophage colony stimulating factor
MFI	Mean fluorescence intensity
mGR	Membrane-bound glucocorticoid receptor
MHC	Histocompatibility complex
MIP	Macrophage inflammatory protein
MW	Molecular weight
NAD	Nicotinamide adenine dinucleotide
NADP	Nicotinamide adenine dinucleotide phosphate
$NaHCO_3$	Sodium bicarbonate
NaOH	Sodium hydroxide
NEFA	Non-esterified fatty acid
NFκB	Nuclear factor-kappa B
NO	Nitric oxide
OFN	Oxygen-free nitrogen
PAR	Peak area ratio
PBS	Phosphate buffered saline
PCR	Polymerase chain reaction
PE	Phycoerythrin
PEPCK	Phosphoenolpyruvate carboxykinase
pHBA	4-hydroxybenzaldehyde
pHPP	4-hydroxybenzaldehyde
POD	Peroxidase
POMC	Pro-opiomelanocortin

SAME	Syndrome of apparent mineralocorticoid excess
SCC	Side-chain cleavage
SHR	Spontaneously hypertensive rats
SIM	Selected ion monitoring
SPA	Scintillation proximity assay
SRC	Steroid receptor coactivator
StAR	Steoidogenic acute regulatory protein
STAT	Signal transducer and activator of transcription
SV	Simian virus
TAT	Tyrosine aminotransferase
TGF	Transforming growth factor
TLR	Toll-like receptor
TMB	Tetramethylbenzidine
TMS	Trimethylsilyl
TMSI	Trimethylsilylimidazole
TNF	Tumor necrosis factor
Tris	Trisma base
VSM	Vascular smooth muscle
WT	Wild-type

Declaration

I declare that this thesis was written by me and that the data presented within it is a result of my own work, except the procedures listed below.

Injection of steroids, termination procedures and dissection of livers of animals with acute administration of steroids were performed by Dr Christopher Kenyon. Surgery for minipump implantation and dissection of organs and adipose tissue of animals receiving chronic infusion treatment were performed by Dr Dawn Livingstone. Instrument support for GCMS analysis was performed by Mrs Alison Rutter. Measurement of NEFAs was performed by Mrs Rachel McDonnell and Mrs Jill Harrison. Plasmid preparation was performed by Mrs Val Kelly. People mentioned above are in the Centre for Cardiovascular Science, Queen's Medical Research Institute, University of Edinburgh.

Injection of steroids and LPS and peritoneal lavage were performed by Dr Rodger Duffin of the Centre of Inflammation Research, Queen's Medical Research Institute, University of Edinburgh.

I declare that this work has not been submitted for any other degree.

Chenjing Yang

Acknowledgement

First of all I would like to express my sincere gratitude to Dr Ruth Andrew, Dr Chris Kenyon and Prof Brian Walker for their extraordinary support and guidance, great kindness and constant encouragement throughout my PhD studies. Further thanks are due especially to Dr Dawn Livingstone who has spent a great deal of time giving me support and advice at all times. I am also very grateful to the Dorothy Hodgkin Postgraduate Awards for their generous support.

Throughout my PhD studies I have received valuable assistance from so many sources. Everyone in the Endocrinology Unit has been so kind and supportive, of whom Rachel, Val, Karen, Paddy and Maggi are thanked specially for their care and guidence with lots of techniques; Dev and Aily of CIR are also thanked for their kind care and assistance.

I am very grateful to my best friends from whom I have gained the most precious friendship in Edinburgh, Tijana, Chiu-ju, Peng, Agnes, Xia, Sanjay, Howard, Shuji and Yumiko, Matt and Laura, Tali and Chris, Shiou and Chris. Their love and kindness have made my life in Edinburgh so beautifully enriched. And now I believe the world is so lovably flat.

I would like to express my heartiest thanks to Dr Xiaojun Liu and his family for their great kindness of being my surrogate family in Edinburgh.

Finally, I am forever indebted to my parents and Dong for their enormous love, understanding and encouragement.

Chapter 1

Introduction

Glucocorticoids are steroid hormones that modulate energy homeostasis in the body, especially during starvation or stress. Over the last fifty years they have been the most widely used agents to control inflammation and immune activation. Their therapeutic significance has drawn enormous amounts of interest in research from a broad range of areas. This thesis will investigate the mechanisms of glucocorticoid action with respect to their metabolic and anti-inflammatory roles. It will focus on one of the 5α-reduced metabolites of glucocorticoids in rodents, 5α-tetrahydro corticosterone (5αTHB), which has been shown to mimic some actions of its 'parent', corticosterone. This chapter will introduce the background information underpinning the investigation of effects of 5αTHB.

1.1 Glucocorticoids

Glucocorticoids are members of the steroid hormone family with 21 carbon atoms. Like all the other steroid hormones, they are derived from the cyclopentanoperhydrophenanthrene structure which is three cyclohexane rings and a single cyclopentane ring, labelled A, B, C, and D, respectively. Each of the 21 carbons is numbered in a standard way (Figure 1.1).

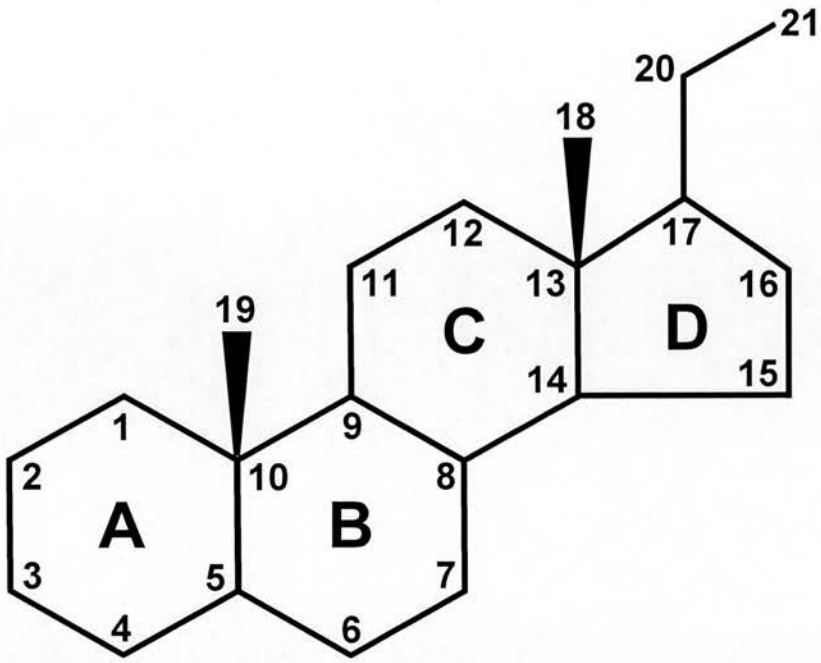

Figure 1.1 The cyclopentanoperhydrophenanthrene structure of glucocorticoid with 21 carbon atoms. The three cyclohexane rings and the single cyclopentane ring are identified by letters and the individual carbon atoms by numbers.

1.1.1 Steroidogenesis in the adrenal cortex

Glucocorticoids are synthesized and released from the cortices of adrenal glands, where mineralocorticoids (aldosterone, deoxycorticosterone (DOC)) and sex steroids (androgens) are also generated. According to cell morphology and function, the adrenal cortex is divided into three zones which are, from outer to inner, the zona glomerulosa, zona fasciculata and zona reticularis.

All adrenocorticosteroids are derived from the same precursor, cholesterol which is either synthesised within the adrenal gland or is taken up from the circulation. Cholesterol circulates in association with lipoproteins and is taken into cells of adrenal cortex by means of receptor-mediated endocytosis in humans (Higashijima, et al. 1987); whereas in rats, receptor-mediated endocytosis and non-endocytotic

pathways are involved (Gwynne, et al. 1984). Then the cholesterol is transported directly to the mitochondrion or it is stored in lipid droplets as cholesterol ester until required. Mitochondrial uptake of free cholesterol is the rate limiting step of steroidogenesis and is regulated by StAR (Steoidogenic Acute Regulatory protein) (Christenson and Strauss 2001). Mitochondrial cholesterol is then cleaved to form pregnenolone by cholesterol side-chain cleavage (SCC) enzyme, cytochrome $P450_{SCC}$ (gene name: *CYP11A1*). The pathways of biosynthesis of glucocorticoids and mineralocorticoids are shown in Figure1.2. A series of cytochrome P450 enzymes are involved. The nomenclature for these enzymes is adopted from their gene names, which are listed in Table 1.1 shown together with their intracellular localizations.

The active glucocorticoid in human circulation is cortisol, while corticosterone is the main glucocorticoid in rodents. Since cortisol is the final product of 17α-hydroxylated pregnenolone or progesterone in zona fasciculata of adrenal cortex, the 17α-hydroxylase (*CYP17*) is a prerequisite enzyme for human glucocorticoid biosynthesis (Chung, et al. 1987; Picado-Leonard and Miller 1987). The zona glomerulosa does not express 17α-hydroxylase, thus cortisol production is excluded from this zone. In rodents, 17α-hydroxylase is absent in adrenal cortex (Luu-The, et al. 2005), and thus corticosterone is the active glucocorticoid instead of cortisol. The final steps in the biosynthesis of glucocorticoids and mineralocorticoids are catalyzed by 11β-hydroxylase and aldosterone synthase, encoded by *CYP11B1* and *CYP11B2*, respectively, that share 95% sequence homology. In rodents, 11-deoxycorticosterone is converted into aldosterone by aldosterone synthase (*CYP11B2*) in the zona glomerulosa and into corticosterone by 11β-hydroxylase (*CYP11B1*) in the zona fasciculata (Domalik, et al. 1991; Ogishima, et al. 1992).

Gene	Enzyme	Localization
CYP11A1	Cholesterol side-chain cleavage enzyme	Mitochondria
CYP11B1	11β-Hydroxylase	
CYP11B2	Aldosterone synthase	
CYP21A2	21-Hydroxylase	Endoplasmic reticulum
CYP17	17α-Hydroxylase	
HSD3B2	3β-Hydroxysteroid dehydrogenase type 2 isozyme (3β-HSD2)	

Table 1.1 Nomenclature of enzymes involved in adrenal steroidogenesis and their intracellular localizations.

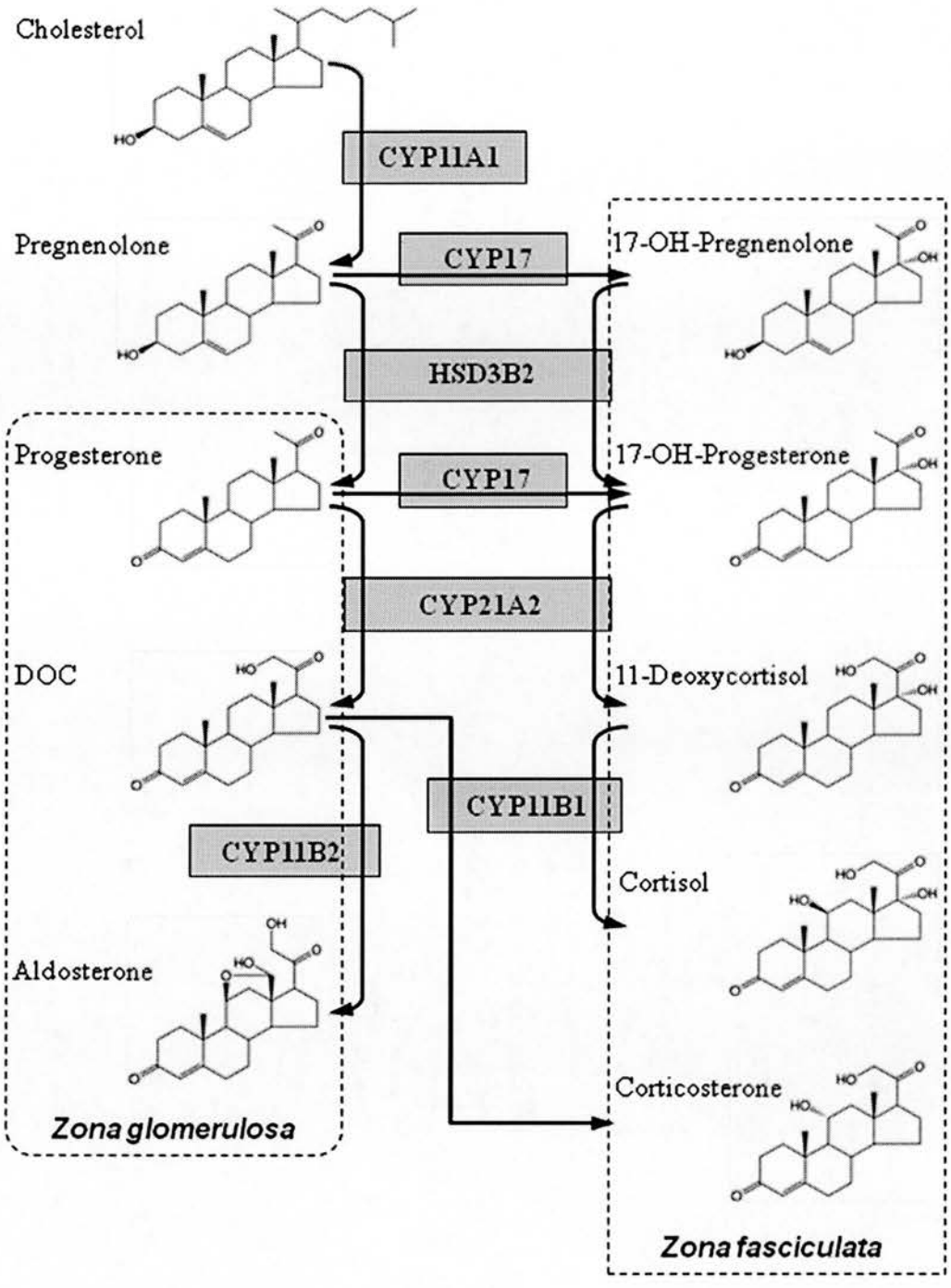

Figure 1.2 The pathways of biosynthesis of glucocorticoids and mineralocorticoids in adrenal cortex. DOC=11-deoxycorticosterone.

1.2 Regulation of glucocorticoids

1.2.1 The hypothalamic-pituitary-adrenal (HPA) axis

Endogenous glucocorticoids, cortisol in humans and corticosterone in rodents, are controlled by the hypothalamic-pituitary-adrenal (HPA) axis. The biosynthesis and secretion of glucocorticoids from the adrenal glands is under the stimulus of adrenocorticotropic hormone (ACTH), released from the anterior pituitary into the circulation. ACTH, a peptide hormone with 39 amino acids, is cleaved from a larger 241-amino-acid precursor, pro-opiomelanocortin (POMC) inside the anterior pituitary cells. Synthesis of POMC and secretion of ACTH into circulation are activated by corticotrophin-releasing hormone (CRH) and arginine vasopressin (AVP). Secretion of CRH, a 41-amino-acid peptide, is stimulated by stressors, produced in neurons within the paraventricular nucleus (PVN) of the hypothalamus and transported through the hypophyseal portal blood to the anterior pituitary where CRH stimulates POMC gene transcription, cleavage, and ACTH secretion.

Elevated circulating cortisol or corticosterone levels exert negative control on POMC transcription and the consequent ACTH secretion from the pituitary and on CRH and AVP transcription in hypothalamus. This completes the negative feedback loop of the HPA axis thereby maintaining the physiological level of glucocorticoids in the body (Dostert and Heinzel 2004; Stewart 2002).

Chronic pharmacological treatment with glucocorticoids causes prolonged suppression of the HPA axis even months after cessation of therapy. Secondary adrenocortical insufficiency is anticipated after withdrawal of steroid treatment which is characterized by glucocorticoid and ACTH deficiency. Primary adrenocortical insufficiency (Addison's disease) is caused by glucocorticoid and mineralocorticoid deficiency, where ACTH levels are markedly elevated (Nieman and Chanco Turner 2006). In contrast when endogenous glucocorticoid levels are high as in Cushing's syndrome due to a cortisol-secreting adrenal adenoma, circulating ACTH levels are hardly detectable (Stewart 2002). Cushing's syndrome

can also arise with elevated ACTH concentrations, as in ectopic ACTH syndrome or ACTH-secreting pituitary adenoma (Howlett, et al. 1986).

1.2.2 The immune-endocrine axis

Control of the immune system by the central nervous system is mediated in part by the HPA axis (Dostert and Heinzel 2004). Various pro-inflammatory cytokines, such as interleukin (IL)-1, IL-2, IL-6, tumor necrosis factor (TNF)-α, and interferon (IFN)-γ are released upon immune stimulation and can activate the HPA axis by increasing the secretion of CRH from hypothalamus and ACTH from pituitary. This in turn increases the release of glucocorticoids to mediate anti-inflammatory events (Sapolsky, et al. 2000).

1.2.3 Circadian rhythm

Under basal conditions, circulating glucocorticoid levels demonstrate a 24-hour circadian rhythm, which is regulated by the pulsatile release of ACTH (Stewart 2002). In humans, cortisol levels are highest in the morning on waking and slowly decline during the day, reaching a trough level in the late afternoon, evening and nocturnal period (Lupien, et al. 2007). In rodents which are nocturnal animals, the circadian peak occurs in the evening with the circadian nadir in the morning (Windle, et al. 1998).

1.3 Glucocorticoid signalling

Glucocorticoids exert their numerous effects through direct interaction with two types of receptors, glucocorticoid receptor (GR, type II corticosteroid receptor) and mineralocorticoid receptors (MR, type I corticosteroid receptor). Both are members of the superfamily of nuclear hormone receptors that includes GR, MR, progesterone receptor (PR), androgen receptor (AR) and estrogen receptor (ER). This thesis

focuses on how glucocorticoid signalling via GRs influences metabolism and inflammation.

1.3.1 Steroid hormone receptors

Steroid hormone receptors are modular proteins that act as transcription factors to transduce the signals of their cognate ligands. According to functional and structural analyses, steroid receptors are composed of a common series of domains, referred to as A to F (Figure 1.3). C includes the DNA-binding domain (DBD); E contains the ligand binding domain (LBD) that controls the receptor's functions. Many actions of steroid hormones require receptors to form a dimer. The critical dimerization domain is within Domain C and consists of two zinc finger regions; the LBD is also involved in dimerization. DNA sequences that recognise and bind to receptors are known as hormone response elements. The amino acids responsible for receptor recognition of the response element are within the P box of the DBD. Many hormone receptors are located in the cytoplasm and are translocated to the nucleus upon ligand binding. Nuclear localization signals (NLS) for nuclear pore recognition are localized in domain C and E. The transcriptional competence of steroid receptors is exerted by two activation functions (AFs), AF-1 (also called τ-1 or enh-1) and AF-2. AF-1 is constitutively active and located in the A/B-domain. AF-2, a ligand-inducible activation function, is in the LBD. Domain F is essential for ligand binding of GR, PR and AR but not ERα (Lazar 2002; Schoneveld, et al. 2004).

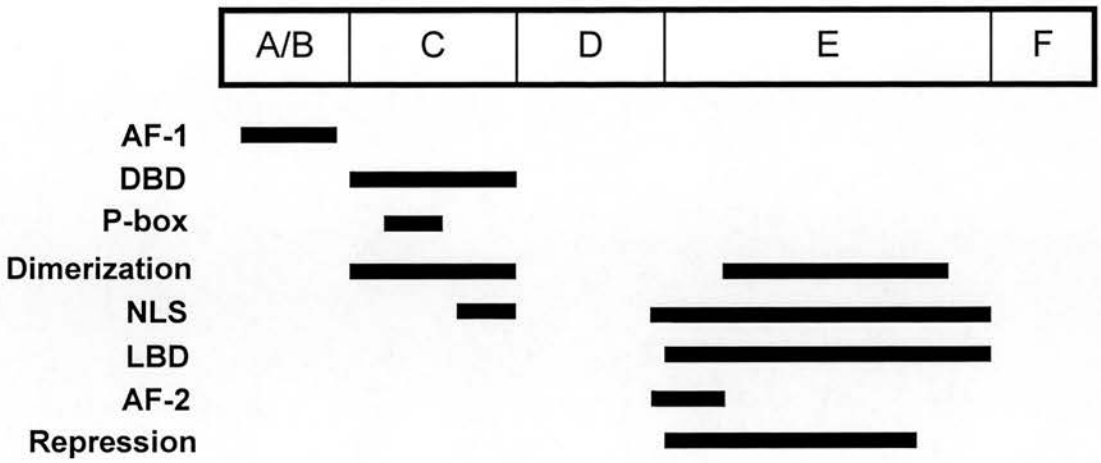

Figure 1.3 Domain structures of nuclear receptors, modified for GR (Beato and Klug 2000; Duma, et al. 2006; Lazar 2002). Domain A/B, N terminal domain; Domain C, DNA binding domain (DBD); Domain D, hinge region; Domain E, ligand binding domain (LBD); Domain F is essential for ligand binding.

1.3.2 GR Trafficking

The intracellular distribution of ER, AR and PR depends on nuclear-cytoplasmic diffusion and ATP-dependent cytoplasmic-nuclear shuttling (Beato and Klug 2000). The nuclear localization signals are the passport for receptors to translocate into the nucleus with or without ligand binding. However, this is not the case for the GR. Ligand-free GR is tethered in the cytoplasm to the heat shock protein (hsp) 90/hsp70 -based chaperone complex (Figure 1.4) (Pratt, et al. 2006). One molecule of GR is bound to a dimer of hsp90 and one molecule of immunophilins (IMM) which includes FKBP51, FKBP52 or CyP-40. The amounts of essential hsp70 are variable but substoichiometric. Hsp90 is characterized by a unique binding pocket for ATP. It binds to the LBD of GR, while other non-essential co-chaperones, such as Hop (hsp organizing protein), hsp40 and p23, are assembled into the complex, whereupon an ATP-dependent hydrophobic cleft is open for steroid binding. This is the rate-limiting step in the overall assembly process, since the preceding stage when GR

binds to hsp90 is rapid (Kanelakis, et al. 2002). Then GR undergoes a conformational change upon assembly of the heterocomplex (Pratt et al. 2006).

Since glucocorticoids are small and highly lipophilic molecules, they can readily pass the cell membrane by passive diffusion and bind to their cytoplasmic cognate receptor. Upon binding of ligand, GR is activated, the hydrophobic pocket closes and the ability to form persistent complexes with hsp90 is lost. The linkage between GR and hsp90 chaperone machinery becomes much more dynamic. The dissociation of GR with hsp90 facilitates the exposure of the NLS of GR, which enables GR to translocate into nucleus (Pratt et al. 2006), however the dynamically bound hsp90 chaperone machinery is also essential in GR trafficking. It has been proposed by Pratt that the hsp90-GR heterocomplexes are moved along microtubules by cytoplasmic dynein, the motor protein with the immunophilins connecting the heterocomplexes to dynein (Pratt et al. 2006).

When they arrive at the nuclear membrane, GR-hsp90 heterocomplexes travel through nuclear pores by means of facilitated diffusion, which involves the transport receptors called importins and exportins to take the signalling proteins in and out of nucleus, respectively (Gorlich and Kutay 1999; Pratt, et al. 2004).

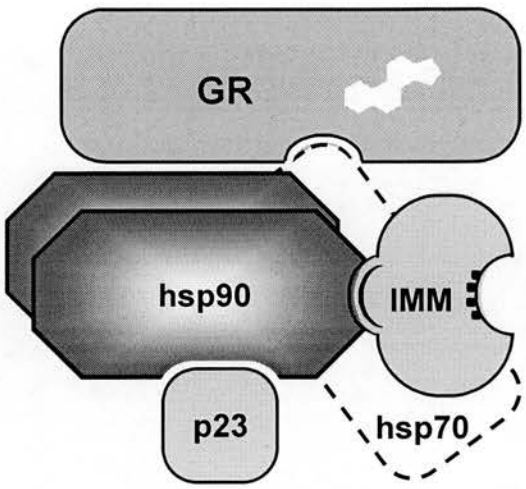

Figure 1.4 The heterocomplex of GR-hsp90-immunophilin in the cytoplasm of glucocorticoid-free cells. One molecule of GR binds to a dimer of hsp90 and one molecule of immunophilin (IMM). The blank steroid structure in the GR indicates that the hydrophobic ligand-binding cleft is open and can be accessed by glucocorticoids. The small co-chaperone p23 helps to stabilize the complex once it is formed.

1.3.3 Molecular mechanisms mediated by GR

Following translocation into nucleus, glucocorticoid bound GRs interact with the regulatory regions of responsive genes by multiple means, and regulate gene expression positively or negatively, which are classified respectively as transactivation or transrepression mechanisms of GR signalling.

1.3.3.1 Transactivation

Glucocorticoid induced transactivation is mediated by GR binding to the glucocorticoid response elements (GREs) in the responsive regions of target genes. A consensus GRE is defined as the 15-bp imperfect palindrome GGTACAnnnTGTTCT (position numbered relative to the dyad axis of symmetry as -6,-5,-4,-3,-2,-1,nnn,1,2,3,4,5,6; n is any nucleotide) in which the 3' half is most conserved and the 5' half highly flexible (Barnes 1998). It has been realized however that only the

nucleotides at the positions -3, -2, +2, +3 and +5 of these are of critical importance. Two GR monomers bind in turn to the 3' and then 5' half sites to form a GR homodimer through the dimerization domain in the GR DNA-binding domain (Schoneveld et al. 2004). The homodimer formation is rate-limiting for high affinity DNA binding by GR and only possible when the GR contacts DNA (Drouin, et al. 1992). In a few genes, it has been found that the GR homodimer binds simply to the GREs, while some other genes require the recruitment of several transcription factors or coactivators, such as C/EBP, FoxA (Schoneveld et al. 2004), CBP/p300, P/CAF and steroid receptor coactivator (SRC)-1 (Smoak and Cidlowski 2004), to bind adjacent to sites other than GREs. The recruited form is referred to as the glucocorticoid responsive unit (GRU). A number of genes are regulated through this model, such as phenylethanolamine N-methyltransferase (PNMT) (Ross, et al. 1990; Tai, et al. 2002) and the genes coding for the enzymes in the gluconeogenesis pathway including phosphoenolpyruvate carboxykinase (PEPCK) (Sugiyama, et al. 1998), tyrosine aminotransferase (TAT) (Grange, et al. 1991), aspartate aminotransferase (AAT) and glucose-6-phosphatase (G6Pase) (Dostert and Heinzel 2004).

Besides the GR homodimer binding to GREs, a monomeric GR can bind the DNA at the GRE half-sites (GRE1/2s) in combination with additional elements, including other transcription factors, GREs or multiple GRE1/2s. For example, the enhancer of the mouse mammary tumor virus (MMTV) gene contains four directly repeated GRE1/2s. The two proximal of those can be bound by two GR monomers to form a homodimer (Truss and Beato 1993). However, this kind of dimerization is different from the one binding to the palindromic GREs because: firstly, the spacer length between the GRE1/2s is less constrained; secondly, the affinity of GR for the GRE1/2s is lower than for a palindromic GRE; thirdly, the dimerization on the directly repeated GRE1/2s is mediated by the ligand binding domain not the DNA binding domain used for binding to the palindromic GREs (Schoneveld et al. 2004; Truss and Beato 1993).

GR can also transactivate the transcription of some anti-inflammatory proteins whose genes have no GRE consensus sequence. Instead GR binds directly to other transcriptional factors to control transcription. IκB (inhibitor of nuclear factor-kappa B (NFκB)) and anti-inflammatory cytokine IL-10 are thought to be activated by GR by this mechanism although the exact transcription factors involved have not been elucidated (Barnes 1998). The only report to date that has confirmed the indirect induction of gene transcription by glucocorticoids is that of the IL-10 gene. GR binds to and increases the transcriptional activity of STAT3 (Signal Transducer and Activator of Transcription 3) to promote IL-10 expression in human B cells (Unterberger, et al. 2008).

1.3.3.2 Transrepression

The transrepression induced by glucocorticoids is mediated through either direct or indirect interaction between GRs and target genes. The direct GR binding to the negatively regulated GRE inhibits the expression of responsive genes. This is often accompanied by recruitment of other transcription factors or co-activators. A consensus sequence of a negative GRE is ATYACnnTnTGATCn, which is more variable than that of a positive GRE (Schoneveld et al. 2004). It is exemplified by the negative control of CRH and POMC by glucocorticoids. GR binds the negative GRE predominantly as monomer in the CRH gene (Malkoski and Dorin 1999) and as a trimer in the POMC gene (Drouin, et al. 1993b).

Glucocorticoid induced repression of inflammatory responses does not involve direct binding of GR to DNA, but interaction of GR with other transcription factors such as NFκB and activator protein-1 (AP-1) that are pro-inflammatory transcription factors. NFκB consists of homodimers or heterodimers assembled from several subunits in which the p65/p50 heterodimer is the predominant combination. GR binds to the p65 subunit by protein-protein interaction and results in the inhibition of the gene transcription mediated by NFκB. Similarly, AP-1 is comprised of a Jun family member (c-Jun, v-Jun, Jun-B, or Jun-D) homodimerized with another Jun protein or heterodimerized with a Fos protein (c-Fos, Fos-B, Fra-1, or Fra-2). GR physically

interacts with the Jun subunit so as to inhibit the gene transcription (Smoak and Cidlowski 2004).

Another model of GR transrepression involves competition for the coactivators of NFκB. The coactivators, such as cAMP response element binding protein (CREB) – binding protein (CBP) and SRC-1, are required for the maximal transcription ability of NFκB. GR can compete with NFκB and thus repress the transcription induced by this transcription factor (Schoneveld et al. 2004; Smoak and Cidlowski 2004).

These models of GR-protein mediated regulation have been shown to be GR dimerization-independent, e.g. through GR monomer (Bledsoe et al. 2002; Heck, et al. 1994).

1.3.4.3 Non-genomic glucocorticoid signalling

Transactivation and transrepression of gene transcription are mediated by the genomic mechanisms of glucocorticoid signalling, in which the translocation of GR into the nucleus and transcription of regulated genes are the most time-consuming steps, requiring 15-150 min to exhibit the effects. However, some rapid glucocorticoid effects, taking place within 5 min or even within seconds, are likely to be mediated by non-genomic mechanisms (Haller, et al. 2008). It is hypothesized that the rapid non-genomic effects are mediated in three ways. Firstly, glucocorticoids themselves may interfere non-specifically with the physico-chemical properties of cellular membranes, e.g. plasma and mitochondrial membranes. High concentrations of glucocorticoids have been shown to intercalate into membranes without binding to GRs, resulting in alteration of the activities of membrane-associated proteins, thereby reducing Ca^{2+} and Na^{+} cycling across plasma membranes, and increasing the proton leak of the mitochondria of immune cells (Buttgereit and Scheffold 2002; Stahn, et al. 2007). These changes could impair ATP production which in turn will contribute to the anti-inflammatory and immunosuppressive effects of glucocorticoids (Song and Buttgereit 2006). Secondly, glucocorticoids may mediate non-genomic effects by binding to membrane-bound glucocorticoid receptors (mGR). The mGR has been identified in human (Gametchu, et al. 1993) and murine (Chen, et al. 1999)

lymphoma cells, and in normal human monocytes in peripheral blood (Bartholome, et al. 2004). It is suggested that the mGR is a variant of the classical cytosolic GR produced by differential splicing or promoter switching or post-translational editing, as overexpression of classical GR did not increase the mGR on the cell surface (Bartholome et al. 2004). Thirdly, the classical cytosolic GR also may mediate non-genomic effects of glucocorticoids. Chaperone proteins, such as SRC, that are released from the GR-chaperone complex upon ligand binding, are shown to contribute to the rapid glucocorticoid effects (Croxtall, et al. 2000). Another example of a GR-dependent (specific GR inhibitor RU486-sensitive) and transcription-independent (actinomycin D-insensitive) process involves the release of arachidonic acid within minutes (an essential mediator for cell growth and metabolic or inflammatory reactions) from cell membrane-associated phospholipids (Croxtall et al. 2000; Song and Buttgereit 2006).

1.3.4 Isoforms of GR

Two human GR have been identified and are termed hGRα and hGRβ. They are 777 and 742 residues long, respectively (Hollenberg, et al. 1985) and are identical up to residue 727 and diverge beyond this point. The two receptor isoforms originate from the same gene and differ by alternative splicing of the final ninth exon. A large portion of the LBD is encoded in exon 8. Exon 9 encodes two alternative extreme carboxyl terminal ends of LBD and the 3' untranslated regions, which results in the additional 50 amino acids of hGRα and additional non-homologues 15 amino acids of hGRβ (Encio and Detera-Wadleigh 1991). The shortened LBD of hGRβ is reported to be unable to bind glucocorticoid agonist, but RU-38486, a glucocorticoid antagonist, has been shown to bind to hGRβ (Lewis-Tuffin, et al. 2007). Both isoforms are widely expressed in virtually all human tissues (Boullu-Ciocca, et al. 2003), although at the transcript level, hGRβ is much less abundant than hGRα, and the ratio varies between 1:40-2800 (DeRijk, et al. 2002). Unlike hGRα, hGRβ is located largely in the nucleus independent of the presence of glucocorticoids. hGRβ will bind to hsp90, although this binding is not affected by addition of ligand (de Castro, et al. 1996).

The isoform hGRα is commonly referred to as *bona fide* hGR, since only hGRα binds hormones and modulates the expression of glucocorticoid-responsive genes in a hormone-dependent fashion. hGRβ cannot affect gene expression by itself but interferes with hGRα activity. hGRβ heterodimerizes with ligand-bound hGRα to decrease the transactivation and transrepression activity of hGRα (DeRijk et al. 2002). Thus hGRβ is thought to function as a dominant negative inhibitor of hGRα and to participate in defining the sensitivity of target tissue to glucocorticoids (Boullu-Ciocca et al. 2003; Oakley, et al. 1996). hGRβ can be up- or down- regulated in different tissues in response to glucocorticoid treatment (DeRijk et al. 2002) and the ratio of hGRα/hGRβ is found to be critical in the modulation of gene transcription (Lewis-Tuffin and Cidlowski 2006). Decreased hGRα/hGRβ ratio in inflammatory cells correlates with the development of glucocorticoid resistance in patients receiving steroid therapy for several diseases including asthma, leukemia, ulcerative colitis and nasal polyposis (Lewis-Tuffin and Cidlowski 2006). In obese patients, the ratio of hGRα/hGRβ is also decreased in circulating monocytes (Boullu-Ciocca et al. 2003).

Until now the β isoform of GR has been found in human and zebrafish only, and the zebrafish GRβ displays similar functions to its human equivalent (Schaaf, et al. 2008). GRβ is not present in mice. Therefore the GR referred to in this thesis is mainly the classically ligand-dependent GR unless otherwise stated.

1.4 Effects of glucocorticoids

Physiologically, glucocorticoids exert a broad range of effects in target systems throughout the body, increasing the availability of substrates for energy supply, and allowing for adaptations to changing demands of the environment, e.g. alterations in behaviour and immune responses.

The pathological effects of glucocorticoids can be exemplified in "Cushing's syndrome" caused by endogenous or exogenous glucocorticoid excess, which was

reported by Harvey Cushing in 1912, and characterized by hypertension, central obesity, insulin resistance and impaired glucose tolerance (Cushing 1912), all of which are risk factors for cardiovascular disease (Haffner 2006). These characteristics are also found in patients with the metabolic syndrome (also known as syndrome X, the insulin resistance syndrome, and the "deadly quartet"). Over the past two decades, there has been a striking increase in the worldwide prevalence of metabolic syndrome (Eckel, et al. 2005). Similarities between the Cushing's syndrome and the metabolic syndrome have stimulated interest in the role of glucocorticoids in the pathogenesis of the metabolic syndrome (Walker 2006).

The anti-inflammatory effects of glucocorticoids were first noticed and reported by Hench in 1949, who won a Nobel Prize for his findings (Hench 1950; Hench and Kendall 1949). From then on, research into glucocorticoids has been extensive and intense. The pharmaceutical industry has developed a number of synthetic glucocorticoids such as dexamethasone, betamethasone, triamcinolone, prednisone, prednisolone and methylprednisolone (Liberman, et al. 2007) which have become the most commonly prescribed agents for the treatment of a wide variety of inflammatory diseases, such as rheumatoid arthritis, inflammatory bowel disease, asthma, psoriasis, vasculitis (Goulding, et al. 1998), polymyalgia rheumatica, chronic obstructive pulmonary disease (Lowenberg, et al. 2008), autoimmune, and allergic diseases. They are also used to reduce organ allotransplant rejection (Liberman et al. 2007).

Chronic and systemic use of glucocorticoids is hampered by severe side effects. Iatrogenic Cushing's syndrome is common in patients who take glucocorticoids chronically (Liberman et al. 2007). Other adverse effects of glucocorticoids include osteoporosis, growth retardation, skin atrophy, myophathy, glaucoma and "steroid psychosis" (Lupien et al. 2007).

1.4.1 Carbohydrate, protein, and lipid metabolism

Glucocorticoids act to provide energy and prepare a man or an animal for a "fight or flight" response when required (e.g. facing a perceived danger or starvation). The

levels of blood glucose and free fatty acids are increased by glucocorticoids through their actions on carbohydrate, protein and lipid metabolism, opposing the effects of insulin (Andrews and Walker 1999; Walker 2007b). In tissues that are important for metabolism, including liver and adipose tissue, glucocorticoids can upregulate the enzyme 11β-hydroxysteroid dehydrogenase type 1 (11β-HSD1, details are in Section 1.6.1) which regenerates the active form of glucocorticoids, thereby amplifying the GR activation in these tissues (Stewart, et al. 1999; Walker 2007a).

In the liver, glucocorticoids activate gluconeogenesis with increased transcription of the key enzymes involved in this pathway, such as PEPCK (the rate-limiting enzyme) (Sugiyama et al. 1998), G6Pase (van Schaftingen and Gerin 2002) and fructose-1,6-diphosphatase (FDPase) (Fleig, et al. 1984) as well as aminotransferases, e.g. TAT and AAT (Dostert and Heinzel 2004). Glucocorticoids increase triglyceride storage (Mantha, et al. 1999) and thereby promote fat accumulation within the liver (Stravitz and Sanyal 2003); they also increase hepatic glycogen synthase and inhibit the glycogen phosphorylase to facilitate glycogen deposition, providing long-term protection against stress and starvation (Bollen, et al. 1998; van Schaftingen and Gerin 2002). Glucocorticoids inhibit glucose uptake and utilization in peripheral tissues including skeletal muscle and adipose tissue, where proteolysis and lipolysis are activated in order to provide glucogenic substrates, e.g. amino acids and free fatty acids respectively, into the circulation (Buren, et al. 2002; Olefsky 1975). Other hormones such as catecholamines, glucagon and epinephrine exert amplified actions through the permissive effects of glucocorticoids (Sapolsky et al. 2000): catecholamines can increase lipolysis in adipose tissue and glycogenolysis in skeletal muscle; glucagon and epinephrine also stimulate gluconeogenesis in the liver. Overall, the efficiency of glucose production is promoted (Exton 1979), causing an elevation in blood glucose and insulin resistance.

In adipose tissue, glucocorticoids stimulate the differentiation of preadipocytes into mature adipocytes which are capable of storing triglycerides (Wiper-Bergeron, et al. 2007). Triglycerides are efficient form to store energy (Hillgartner et al. 1995). They undergo lipolysis to release glycerol and non-esterified (free) fatty acids (NEFAs),

the latter being a major source of fuel for oxidative metabolism (Coppack et al. 1994). Glucocorticoids have important effects on fatty acid metabolism. NEFA release from adipocytes *in vitro* is activated by glucocorticoids (Baxter & Forsham 1972). Lipoprotein lipase (LPL) activity and mRNA expression are also increased by glucocorticoids (Fried et al. 1993; Ong et al. 1992). Effects of glucocorticoids *in vivo* are different between acute and chronic glucocorticoid activations. During fasting and stress with stimulus of elevated catecholamines, elevated glucocorticoids activate LPL, and potentiate NEFA release from circulating triglycerides into the circulation (Samra et al. 1998). If feeding occurs, insulin-stimulated trigs storage in adipose tissue is decreased and NEFA release is sustained. During recovery from stress when catecholamine diminishes while glucocorticoid effects are sustained, re-feeding increases insulin levels when trigs are released from liver, intravascular lipolysis activated, and lipolysis diminished and trigs storage upregulated in adipose tissue (Macfarlane et al. 2008). Chronic exposure to glucocorticoids in human has similar effects to those during recovery from stress, with increased hydrolysis of circulating TAG and NEFAs release from subcutaneous adipose tissue (Krsek et al. 2006) but re-esterification and storage in visceral adipose tissue, resulting in the redistribution of body fat from peripheral fat to central adipose tissues, such as visceral, abdominal, facial, and neck, causing central obesity. Increased cardiovascular morbidity and mortality in human is associated with intra-abdominal adipose deposition, as opposed to subcutaneous fat (Gathercole, et al. 2007; Macfarlane et al. 2008). However, in rodents, chronic glucocorticoid excess results in lose, rather than gain, body weight (Elliott et al. 1971).

1.4.2 Salt and water homeostasis and blood pressure control

Glucocorticoids regulate blood pressure through a variety of actions on kidney and vasculature. In the kidney, glucocorticoids play a critical role in the maintenance of normal glomerular filtration rate and renal blood flow. Excess exposure of glucocorticoids in the kidney causes the nitric oxide-mediated vasodilatation of afferent and efferent arterioles and results in the increase in glomerular plasma flow which is responsible for the increase in glomerular filtration rate (De Matteo and May 1997). In the proximal tubule where GRs not MRs are expressed,

glucocorticoids do not alter sodium transport directly but enhance the activity of ion transporters including apical Na^+-H^+ exchanger (Baum, et al. 1994), basolateral Na^+/K^+-adenosine triphosphatase (Na^+/K^+-ATPase) (Lee, et al. 1995) and $NaHCO_3$ cotransporter (Ruiz, et al. 1995); and they also upregulate angiotensin II receptors in higher mammals such as dogs and humans (Brem 2001). In the distal tubule and cortical collecting duct which is a target of aldosterone (Fuller and Young 2005) enriched with MR (Todd-Turla, et al. 1993), sodium reabsorption can be stimulated by glucocorticoids. This is mediated through both GRs and MRs (Naray-Fejes-Toth and Fejes-Toth 1990) although predominantly MRs. Na^+ entry across the Na^+ channels and the activity of Na^+/K^+-ATPase (Laplace, et al. 1992) are increased. Although MR has 10-fold higher affinity for endogenous glucocorticoids than do GRs and glucocorticoids are present in 100-fold excess to aldosterone in the circulation (Edwards, et al. 1988; Naray-Fejes-Toth and Fejes-Toth 1994; Nishi and Kawata 2007), MRs are protected from glucocorticoids by 11β-hydroxysteroid dehydrogenase type 2 (11β-HSD2) which inactivates glucocorticoids (details are in Section 1.6.1) in this renal segment (Cole 1995; Roland, et al. 1995). When 11β-HSD2 activity is impaired, glucocorticoids induce hypertension because of inappropriate activation of MRs (Edwards et al. 1988; Funder, et al. 1988)

Glucocorticoids exert vasoconstrictive effects in vascular smooth muscle (VSM) mainly via GR mediated processes although MR is also present (Brem 2001). Glucocorticoids enhance pressor responses to other vasoconstrictive hormones, e.g. catecholamines and angiotensin II (Sapolsky, et al. 2000). Glucocorticoids have permissive effects on catecholamine synthesis in vascular and cardiac tissue during stress, since the rate-limiting enzyme in epinephrine synthesis, phenylethanolamine N-methyltransferase (PNMT), is induced by glucocorticoids (Kennedy and Ziegler 1991; Wurtman and Axelrod 1966). Glucocorticoids activate the renin-angiotensin-system by increasing the transcriptional abundance of both angiotensinogen and angiotensin-converting enzyme, and by upregulating the AT1 (angiotensin II receptor type 1) (Sato, et al. 1994). Moreover, the α-adrenergic and vasopressin receptors are also increased. Glucocorticoids also modify cation transport to induce contractile effects in VSM. The expression of calcium-activated potassium channel

(K_{Ca}) in VSM cells, a protein allowing for the potassium efflux from cells causing hyperpolarization and relaxation, is diminished by glucocorticoids, leading to a net increase in vascular tone (Brem, et al. 1999; Nelson and Quayle 1995). Glucocorticoids downregulate the expression of Na^+-Ca^+ exchanger (*Slc8a1*) in VSM cells (Smith and Smith 1994). This decrease reduces exchanger Ca^{2+} efflux from cytosol of VSM cells and potentiates pressor responses to angiotensin II and vasopressin (O'Donnell and Owen 1994). Furthermore, several vasodilatory proteins are downregulated by glucocorticoids: Nitric oxide (NO)-mediated endothelial dilatation is reduced by glucocorticoids by inhibiting the NO synthase (Mitchell and Webb 2002); guanylate cyclase activity induced by natriuretic, diuretic and vasorelaxant atrial natriuretic peptide (ANP) in VSM cells is attenuated (Nuglozeh, et al. 1997; Yasunari, et al. 1990); biosynthesis of vasodilator prostaglandin I2 is reduced (Falardeau and Martineau 1989).

1.4.3 Anti-inflammatory and immunosuppressive actions

Glucocorticoids have profound anti-inflammatory and immunosuppressive effects that are mediated at many levels.

At the molecular level, glucocorticoids inhibit effects of pro-inflammatory transcription factors NFκB and AP-1 that play crucial roles in increasing the transcription of several inflammatory proteins including: (i) cytokines such as IL-1β, IL-2, IL-3, IL-6, IL-11, TNFα, granulocyte-macrophage colony-stimulating factor (GM-CSF); (ii) chemokines that attract inflammatory cells to the inflammatory sites, such as IL-8, RANTES ("Regulated on Activation, Normal T-cell Expressed and Secreted", also known as CCL5), monocyte chemoattractant protein (MCP)-1, MCP-3, MCP-4, macrophage inflammatory protein (MIP)-1α and eotaxin (Barnes 1998); (iii) adhesion molecules involved in lymphocyte extravasation and tissue fibrosis such as endothelial leukocyte adhesion molecule (ECAM)-1 and intracellular adhesion molecule (CAM)-1. The repressive actions of glucocorticoids are exerted either by GR binding directly to a subunit of NFκB or AP-1 to block the gene transcription, or by causing transactivation of IκB, which sequesters NFκB preventing its translocation into the nucleus, thereby inhibiting gene transcription

(Auphan, et al. 1995). The production of inflammatory mediators such as prostaglandins, histamine, nitric oxide, bradykinin, eicosanoids, are also inhibited by glucocorticoids (Sapolsky et al. 2000; Stewart 2002). In addition, glucocorticoids can enhance the expression of anti-inflammatory cytokines such as IL-4, IL-10 and transforming growth factor (TGF)-β (Elenkov and Chrousos 2002; Sorrells and Sapolsky 2007), as well as other anti-inflammatory proteins including annexin-1 (also known as lipocortins-1) and its receptor (Sawmynaden and Perretti 2006), and IL-1 receptor antagonist.

At the cellular level, glucocorticoids inhibit both innate and adaptive immune responses. In innate immunity, glucocorticoids induce cell apoptosis in basophils and eosinophils (Schleimer and Bochner 1994; Yoshimura, et al. 2001). Monocyte differentiation into macrophages, and macrophage phagocytosis and secretion of pro-inflammatory cytokines are suppressed by glucocorticoids (Baybutt and Holsboer 1990). Lymphocyte trafficking and proliferation are inhibited by glucocorticoids (Milad, et al. 1994; Tait, et al. 2008). Glucocorticoids have both positive and negative influences on neutrophils: activation functions of neutrophils, including chemotaxis, adhesion and transmigration, are significantly inhibited (Goulding et al. 1998) whereas glucocorticoids also induce delays in neutrophil apoptosis which potentially prolong inflammatory responses (Cox 1995; Franchimont 2004). In adaptive immunity, glucocorticoids inhibit the production of IL-12 from the antigen-presenting cells (APCs) such as monocyte/macrophages and dendritic cells, resulting in a change in phenotype mode of response of immune cells from Th1 (mediating cellular immunity and secreting IL-2 and IFN-γ) to Th2 (mediating humoral immunity and secreting anti-inflammatory cytokines IL-4 and IL-10) (Elenkov and Chrousos 2002; Franchimont 2004). Glucocorticoids cause dendritic cells to maintain an immature state, which decreases their ability to express histocompatibility complex (MHC) class II and to present antigens to naive and memory T cells (Banchereau and Steinman 1998). Glucocorticoids also induce apoptosis in T-cells, resulting in suppressed inflammation. Moreover, exposure to glucocorticoids causes involution of the thymus. CD4+CD8+ thymocytes are exquisitely sensitive to glucocorticoids and even the physiological increases in

endogenous levels achieved during a stress response can cause apoptosis (Ashwell, et al. 2000).

1.4.4 Bone and calcium metabolism

Glucocorticoids play an important role in the regulation of bone remodelling. Long-term systemic exposure of glucocorticoids increases the risk of developing osteoporosis in adults, and in children leads to growth retardation and delayed puberty. Fractures are common in vertebral bodies and ribs in patients with continued glucocorticoid treatment due to bone loss (more so in cancellous and trabecular than in cortical bone) (Schacke, et al. 2002).

Glucocorticoids regulate bone remodelling in numerous ways. They reduce the number of bone cells by inducing apoptosis in osteoblasts and osteocytes (Silvestrini, et al. 2000), and suppress the proliferation of osteoblasts (Schacke et al. 2002). Transcription of osteocalcin, the main osteoblast-specific non-collageous bone protein (Ducy, et al. 1996) and a key determinant of bone formation, is inhibited by glucocorticoids via GR binding to the negative GRE in the promoter region of the gene (Mancini, et al. 2004; Schoneveld et al. 2004). Glucocorticoids also enhance the differentiation and activation of osteoclasts, favouring bone resorption (Lacey, et al. 1998). Moreover, glucocorticoids suppress the activity of mediators of bone homeostasis including growth hormone, insulin-like growth factor (IGF)-1, and TGF-β (Schacke et al. 2002). Calcium metabolism is also affected by glucocorticoids. As a consequence of decreased gastrointestinal Ca^{2+} absorption and an increased renal Ca^{2+} excretion, glucocorticoids reduce serum Ca^{2+} level which, in turn, stimulates the release of parathyroid hormone, resulting in increased osteoclastic bone resorption (Lane, et al. 1998).

1.4.5 Skin and muscle

Prolonged topical or even systemic and inhaled use of glucocorticoids induces atrophy of the skin. The epidermis, dermis and subcutis are affected, resulting in the irreversible striae rubrae distensae and impaired wound healing. Hypertrichosis in

women and perioral dermatitis are also common after topical use of glucocorticoid on the face (Schacke et al. 2002). Glucocorticoids suppress cell proliferation of keratinocytes and dermal fibroblasts (Perez, et al. 2001), decrease the transcription of tenascin-C (Fassler, et al. 1996), and reduce the biosynthesis of elastin (Russell, et al. 1995), collagen type I and III (Oikarinen, et al. 1992; Oikarinen, et al. 1998), hyaluronic acid and sulphated glycosaminoglycans (Sarnstrand, et al. 1982). A thinner horny layer and decreased synthesis of epidermal lipids account for increased transepidermal water loss.

In the muscle, as described in Section 1.4.1, glucocorticoids exert catabolic effects with decreased glucose uptake and protein synthesis and increased protein degradation. Higher doses and chronic use of glucocorticoid treatment may lead to myopathy (Schacke et al. 2002). At the transcriptional level, glucocorticoids transactivate the expression of glutamine synthetase, which catalyzes the formation of glutamine that is then exported from skeletal muscles (Falduto, et al. 1989; LaPier 1997).

1.4.6 Central nervous system (CNS)

Brain is an important target for glucocorticoids. In rodents, both GRs and MRs are expressed in discrete brain regions including hippocampus, hypothalamus, cerebellum, and cortex (Stewart 2002). In humans, glucocorticoids are of great importance for the control of cognition, memory, arousal, sleep, behaviour and mood (Fietta 2007). Many psychiatric problems occur in patients with glucocorticoid excess or deficiency, such as mania, hallucinations, delusions (Schacke et al. 2002), depression, euphoria, psychosis, apathy, and lethargy (Stewart 2002). Elevated glucocorticoid levels which occur in patients with severe traumatic stress result in brain atrophy (McEwen and Magarinos 2001).

Glucocorticoids exert direct effects on the hippocampus via both GRs and MRs that are highly expressed and co-expressed in single cells in this region (Nishi and Kawata 2007). Thus the hippocampus is a glucocorticoid-sensitive and vulnerable region in the brain. Neuronal serotonin ($5\text{-}HT_{1A}$) receptor gene transcription is down-

regulated by glucocorticoids via interaction with GR-MR heterodimers binding to the negative GRE of the gene in hippocampal CA1 pyramidal cells (Ou, et al. 2001) and may play a critical role in the development of depression (Schacke et al. 2002). Hippocampal CA3 region dentate granule neurons respond differently to glucocorticoids compared with neurons from the CA1 region. Concentrations that activate GRs in the CA1 neurons hardly affect cell function in the dentate. However, dentate granule cells require hormone levels to be within the physiological range. In the absence of glucocorticoids, apoptosis in these cells is dramatically increased (Joels 2007; Mirescu and Gould 2006).

Glucocorticoids are important in both the formation and extinction of memory. Three of the most important brain areas containing GRs are the hippocampus, amygdala and frontal lobes which are known to be involved in learning and memory (Lupien et al. 2007). Elevated glucocorticoid levels partly contribute to impaired memory and cognitive functions (Schacke et al. 2002). Experiments in rodents suggest that continuous predominant MR activation accompanied by additional moderate GR activation by glucocorticoids helps maintain low levels of anxiety and improved cognition. High MR with high GR activation results in high anxiety and a decline in cognition. Therefore, a balanced MR:GR activation system appears to be important for optimum cognitive functions (de Kloet, et al. 2008).

1.5 Dissociated steroids

As stated above, chronic and systemic application of glucocorticoids in treatment of inflammatory diseases is often accompanied with wide range of side effects, in which the metabolic consequences of glucocorticoid excess is associated with significantly increased morbidity and mortality, principally through cardiovascular disease (Lowenberg et al. 2008; Walker 2007b). Therefore, there is an enormous interest in developing new GR ligands with limited side effects during therapy, especially the metabolic side effects.

The term "dissociated steroids" refers to the pharmaceutical design of new glucocorticoids with anti-inflammatory efficacy dissociated from undesirable side effects (Catley 2007; Schacke, et al. 2004). It has been argued that the adverse metabolic effects of glucocorticoids are mediated through the transactivation mechanism of GR whereas anti-inflammatory effects are mainly through transrepression. Moreover, the transrepressive effects of glucocorticoids alone are sufficient to mediate the anti-inflammatory effects (Schacke et al. 2002). Previously a few dissociated steroids have been reported, including RU24858 (Vayssiere et al. 1997) and ZK216348 (Schacke, et al. 2004) that were first shown to have similar anti-inflammatory effects to conventional steroids but reduced side effects. However, subsequent studies have then revealed they were not completely dissociated *in vivo* (reviewed by Catley 2007). Deflazacort (Calcort - Shire Pharmaceuticals Ltd) is the dissociated steroid that has reached patients. It is an oxazoline derivative of prednisolone in clinical trial for 20 years and was licensed in the UK in 1998. However, additional pharmacologic studies are still required to determine the appropriate ratio of bioequivalence for the anti-inflammatory potency in humans in order to compare its potency in respect to side effects including fuel metabolism (Walker 2000).

1.6 Metabolism of glucocorticoids

The activation of GR is dependent on ligand concentrations. Circulating glucocorticoids are principally regulated by secretion of steroid from the adrenal cortex; but are also influenced by the activity of steroid metabolising enzymes. Steroid metabolism can involve hormone inactivation (e.g. cortisol conversion to cortisone), hormone reactivation (e.g. conversion of cortisone to cortisol) or the generation of an active metabolite (e.g. testosterone conversion to 5α-dihydrotestosterone).

The principal metabolic clearance of glucocorticoids takes place in liver via A-ring reduction by A-ring reductases, including 5α- and 5β- reductases and 3α-

hydroxysteroid dehydrogenase (3α-HSD). Glucocorticoids in target cells are also directly metabolized by locally expressed 11β-hydroxysteroid dehydrogenases (11β-HSDs). The major metabolic processes and metabolites involved in corticosterone metabolism in rodents are presented in Figure 1.5. Minor metabolic routes involving the catalysis by 6β-hydroxylase and 20α- and 20β-HSDs are not shown in this figure.

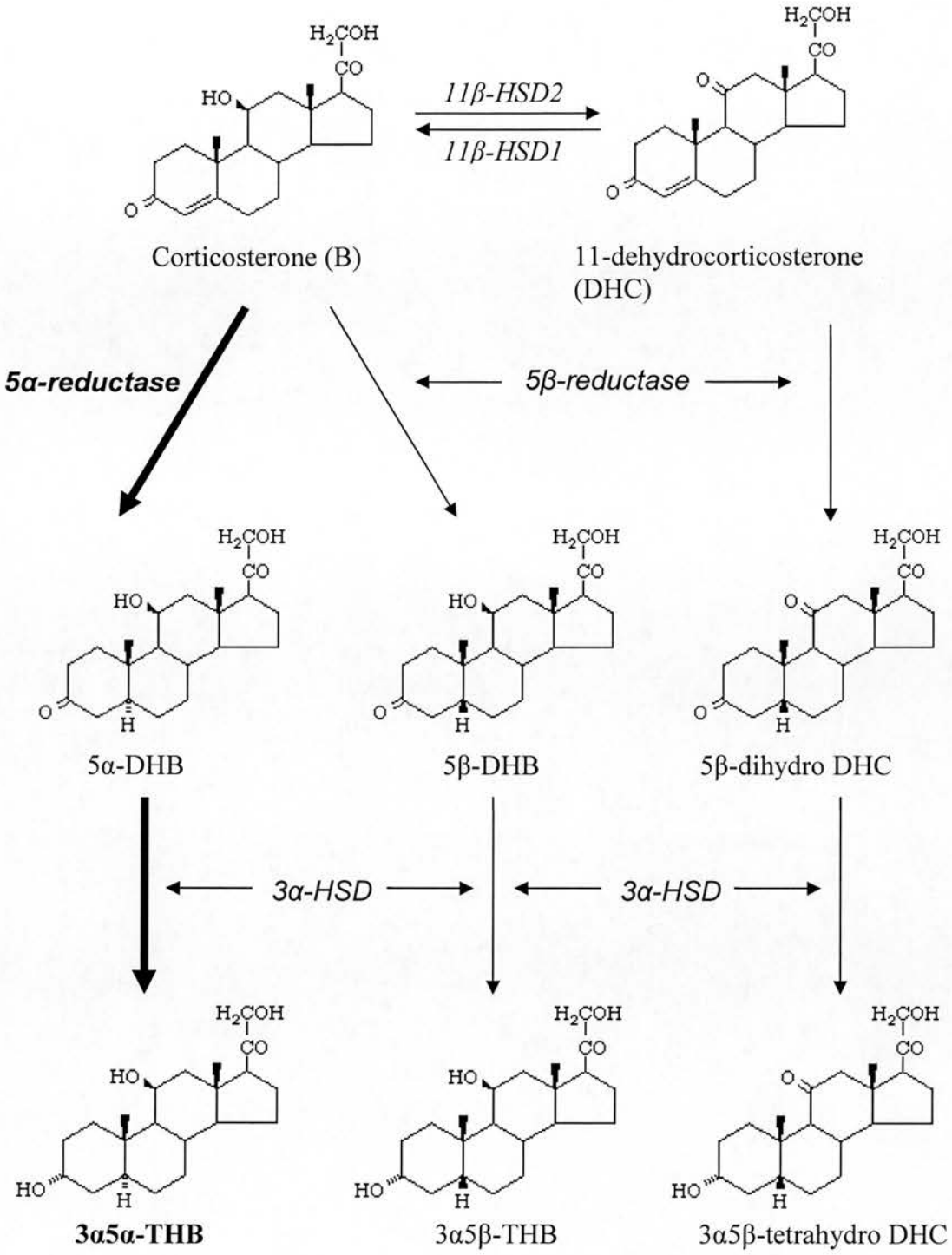

Figure 1.5 Metabolic pathway of corticosterone in rodents. B=corticosterone; DHC = 11-dehydrocorticosterone; DHB = dihydrocorticosterone; THB = tetrahydrocorticosterone.

1.6.1 11β-hydroxysteroid dehydrogenases (11β-HSDs)

As shown in Figure 1.6, 11β-HSDs, type 1 and type 2, catalyse the inter-conversion of active glucocorticoids (cortisol in human and corticosterone in rodents) with their inert 11-keto derivatives (cortisone in human and 11-dehydrocorticosterone (11-DHC) in rodents), thereby modifying local glucocorticoid levels in tissue specific manner. The two enzymes are encoded by two distinct genes. *HSD11B1* is located on chromosome 1 in humans and in mice; and *HSD11B2*, on chromosome 16 in humans and on chromosome 8 in mice. Both enzymes are membrane-bound microsomal enzymes; they are members of short-chain alcohol dehydrogenase superfamily (Grundy, et al. 1997).

1.6.1.1 11β-HSD2

11β-HSD2 is a high affinity (K_m = 10nM) nicotinamide adenine dinucleotide (NAD^+)-dependent dehydrogenase which rapidly inactivates glucocorticoids (Albiston, et al. 1994; Brown, et al. 1996a; Brown, et al. 1996b). 11β-HSD2 is highly expressed in mineralocorticoid target tissues, such as distal nephron, sweat glands, salivary glands and colonic mucosa (Albiston et al. 1994; Edwards et al. 1988; Funder, et al. 1988). Intracellularly, MR is associated with 11β-HSD2 at the endoplasmic reticulum membrane (Odermatt, et al. 2001). This distribution pattern is consistent with two critical roles of 11β-HSD2 in glucocorticoid inactivation. First, 11β-HSD2 protects MR from inappropriate glucocorticoid access. In the absence of 11β-HSD2, glucocorticoids activate mineralocorticoid pathways causing sodium and water retention, hypokalemia and hypertension (Stewart, et al. 1988). These symptoms are seen in transgenic 11β-HSD2 null mice (11β-$HSD2^{-/-}$) (Kotelevtsev, et al. 1999), in patients with an inherited impairment of 11β-HSD2 (the syndrome of apparent mineralocorticoid excess, SAME) (Ulick, et al. 1979), or when patients or animals are treated with an inhibitor of 11β HSD2 (e.g. licorice which contains glycyrrhetinic acid) (Stewart, et al. 1987). Secondly, 11β-HSD2 prevents glucocorticoids from binding to GR. This is important in perinatal development when excess glucocorticoids can cause deleterious effects in tissues like the brain (Holmes, et al. 2006). 11β-HSD2 also acts as a barrier in the placenta and again

offers protection of the fetus from high levels of glucocorticoids in the maternal circulation (Brown et al. 1996a). In utero, exposure to high glucocorticoids programmes offspring to develop hypertension and hyperglycaemia in adult life (Lindsay, et al. 1996a; Lindsay, et al. 1996b).

1.6.1.2 11β-HSD1

11β-HSD1 is predominantly a reductase in intact cells and tissues, regenerating active glucocorticoids from inactive circulating 11-keto derivatives. It has a lower affinity (Km of 100nM for 11-ketosteroids) and uses NADPH as a preferred co-factor (Agarwal, et al. 1989). 11β-HSD1 has been found in liver, adipose tissue, lung, skeletal muscle, bone, vascular smooth muscle, anterior pituitary gland, brain (e.g. PVN of hypothalamus, hippocampus, and cerebral cortex), macrophages and adrenal cortex in humans (Holmes and Seckl 2006). It is also present in rat but not human kidneys (Tomlinson, et al. 2004). The levels of 11β-HSD1, particularly in the liver, are high enough to provide a significant source of circulating active glucocorticoid hormone (Seckl and Walker 2004). 11β-HSD1 helps maintain homeostatic control of metabolism and has been implicated in the development of the metabolic syndrome and cardiovascular disorders. This is exemplified in a number of transgenic modified animal models. Mice with adipose-selective overexpression of 11β-HSD1 (aP2-HSD1 mice) (Masuzaki, et al. 2001) have the metabolic syndrome, i.e. central obesity, glucose intolerance, insulin resistant-diabetes, hyperlipidemia, hyperphagia and hypertension (Masuzaki, et al. 2003). Similarly mice with overexpression of 11β-HSD1 restricted to the liver (apoE-HSD1 mice) exhibit an attenuated metabolic syndrome with modest insulin resistance, fatty liver, dyslipidemia and hypertension with increased expression of hepatic angiotensinogen, but normal glucose tolerance and body weight (Paterson, et al. 2004). In contrast, 11β-HSD1 null mice are protected and resist adverse effects of high fat feeding on glucose intolerance, visceral adiposity, hyperlipidemia and insulin resistance (Kotelevtsev, et al. 1997; Morton, et al. 2001; Morton, et al. 2004).

11β-HSD1 is expressed in a number of immune cells including human myelomonocytic cell line (Gingras and Margolin 2000), T and B lymphocytes in

mice (Zhang, et al. 2005), and murine and human dendritic cells and macrophages (Freeman, et al. 2005; Gilmour, et al. 2006; Zhang et al. 2005). The enzyme may facilitate local production of glucocorticoids as part of the local response in inflammation. In a mouse model of thioglycollate-induced sterile peritonitis, 11β-HSD1 activity is rapidly increased in cells isolated from the peritoneal cavity (Gilmour et al. 2006). These cells also show delayed acquisition of phagocytic capacity and clearance of apoptotic neutrophils from the peritoneum (Gilmour et al. 2006).

Selective 11β-HSD1 inhibitors can reduce blood glucose levels in mice with hyperglycemia (Alberts, et al. 2002). Impaired activity of 11β-HSD1 has been found to be neuroprotective (Holmes and Seckl 2006). In aged animals, chronic elevation of plasma corticosterone results in cognitive impairment and a loss of circadian periodicity (Landfield, et al. 1981; Landfield, et al. 1978) whereas 11β-HSD1-null mice are protected from age-related cognitive decline (Yau, et al. 2001). In humans, elderly patients with type 2 diabetes treated with the 11β-HSD1 inhibitor carbenoxolone show improved cognitive function (Sandeep, et al. 2004); whereas subjects in old age with increased cortisol levels have smaller hippocampus and memory deficits (Lupien, et al. 1998).

Expression of 11β-HSD1 has been found in human adult bone and normal osteoblast cells (Cooper, et al. 2000; Eyre, et al. 2001), whereas 11β-HSD2 is expressed in human and rodents osteosarcoma cell lines, but only where 11β-HSD1 is not present (Bland, et al. 1999). Expression of 11β-HSD1 in osteoblast cells affects glucocorticoid dependent differentiation and bone forming functions (Eijken, et al. 2005; Eijken, et al. 2006). Clinical studies have shown that bone responses to glucocorticoids were strongly correlated to serum cortisone levels rather than cortisol (Pierotti, et al. 2008). Overexpression of 11β-HSD1 in an osteosarcoma cell line results in increased cell differentiation and inhibition of cell proliferation (Rabbitt, et al. 2002). However, osteoblasts from 11β-HSD1-null mice exhibit normal bone mass, cell growth and differentiation potential (Justesen, et al. 2004). Strikingly, 11β-

HSD1-null mice are completely lacking bone marrow adipocytes, though the function of these cells is unknown (Justesen et al. 2004).

1.6.2 A-ring reductases

Steroid A-ring reductases include 5α- and 5β- reductases and 3α-HSD (see Figure 1.6). Reactions catalyzed by 5α- and 5β- reductases involve the irreversible *trans* or *cis* reduction of the double bond at position $\Delta^{4,5}$, yielding *trans* 5α- and *cis* 5β-dihydro glucocorticoids respectively. The 5α- and 5β- reduction is followed promptly with a further reduction by 3α-HSD to produce 5α- and 5β- tetrahydro metabolites. This two-step A-ring reduction, introducing four hydrogens, is common to a variety of other steroid hormones including aldosterone, progesterone, and androgens (testosterone and androstenedione). The interactions between these pathways, particularly that of 5α-reduction, and regulation of glucocorticoid action will form the focus of this thesis.

1.6.2.1 5β-reductase

5β-Reductase is a member of the aldo-keto reductase (AKR) superfamily and catalyses the reduction of the A-ring $\Delta^{4,5}$ double bond, yielding *cis* 5β-dihydro steroids. Only one form of the enzyme has been cloned and purified in human or rat, and it is not homologous to the 5α-reductases (Kondo, et al. 1994; Okuda and Okuda 1984). 5β-Reductase is a cytosolic enzyme, utilising NADPH as a co-factor (Okuda and Okuda 1984). The enzyme is expressed predominantly in liver and much less in kidney (Gorsline, et al. 1988). In the liver, it plays an important role in bile acid and steroids metabolism. Human 5β-reductase has equal affinity for cortisol and bile acid precursors, and higher affinity for progesterone and androgens than cortisol (Okuda and Okuda 1984). Mutations in 5β-reductase results in congenital defects in bile-acid metabolism (Lemonde, et al. 2003; Palermo, et al. 2008; Shneider, et al. 1994).

5β-Reduction is regarded as a catabolic step in steroid metabolism and 5β-reduced metabolites are thought to be biologically inactive (McInnes, et al. 2004). However, the 5β-reduced pregnane type steroids have been found to activate the pregnane-X-

receptor, an orphan nuclear receptor whose endogenous ligands are intermediate metabolites in the bile acid synthetic pathway, suggesting its role in regulating the endogenous biosynthesis of bile acids (Goodwin, et al. 2003).

1.6.2.2 3α-Hydroxysteroid dehydrogenases (3α-HSDs)

3α-HSDs are also members of the AKR superfamily; they catalyse the prompt reduction of the 5α- and 5β- reduced dihydrosteroids, producing 5α- and 5β-tetrahydro derivatives (Penning 1999). They are expressed in cytosolic (soluble) or microsomal sub-fractions and utilize NADPH as preferred co-factor (Degtiar and Kushlinsky 2001).

In human, four isozymes have been cloned from four genes, which are *AKR1C1* (20α(3α)-HSD), *AKR1C2* (3α-HSD type 3), *AKR1C3* (3α(17β)-HSD type 2), and *AKR1C4* (3α-HSD type 1) (Dufort, et al. 1996; Khanna, et al. 1995; Lin, et al. 1997). They share at least 84% sequence identity (Penning, et al. 2000). In humans the four isozymes are differentially expressed in different tissues. Liver expresses high equal levels of all four isozymes, and is the main site of AKR1C4. Lung expresses high levels of three isozymes but low levels of AKR1C4. AKR1C2 and AKR1C3 are dominant isozymes in prostate and uterus; within the latter all four isozymes are expressed in low levels. In brain, four isozymes are also present in low levels with AKR1C1 and AKR1C2 being higher. AKR1C1 is the major isozyme in testes and AKR1C3 is dominant in mammary gland (Penning, et al. 2000). The 3α-HSD enzymes are also found in other tissues such as kidney, small intestine and colon (Lin et al. 1997). However, in the rat, only one isozyme (AKR1C9) has been identified and cloned (Lin, et al. 1999).

In human liver, AKR1C4 plays an important catabolic role in steroid metabolism acting as a reductase to protect from circulating steroid excess; for instance, active 5α-DHT is reduced to the inactivated 5α-tetrahydro form (Khanna et al. 1995). AKR1C2 (type 3 isozyme) is identical to the bile acid binding protein and is inhibited by bile acids (Hara, et al. 1996; Khanna et al. 1995). In contrast, the prostate AKR1C2 functions in the reverse direction as an oxidative enzyme, forming

the active 5α-DHT (Penning, et al. 2000). In the rat liver, the single isozyme AKR1C9 functions as a reductase to catalyze steroid metabolism and as a bile acid binding protein (Degtiar and Kushlinsky 2001). It does not catalyze the HSD activities on 17β- or 20α- keto as the human isozymes do, nor does it act as a dehydrogenase (Penning, et al. 1986).

1.6.2.3 5α-reductases

5α-Reductases are hydrophobic proteins, and are located in the microsomal and plasma membrane/nuclear fractions of cells (Andersson and Russell 1990). They catalyze the nicotinamide adenine dinucleotide phosphate (NADP(H))-dependent reduction of $\Delta^{4,5}$ double bonds in a number of steroid substrates containing 3-keto at $\Delta^{4,5}$ double bonds . Two isozymes, type 1 and type 2 (5αR1 and 5αR2, respectively), have been cloned from different genes, *SRD5A1* and *SRD5A2*. Rat and human sequences of the two isozymes share 60% and 77% homology in amino acid sequence respectively (Normington and Russell 1992; Russell and Wilson 1994).

The two isozymes differ in their biochemical properties, tissue distribution, and affinity to substrates. When examined *in vitro*, the 5αR1 has broad neutral to basic pH optimum range of 6.0 - 8.5, while the 5αR2 has distinct pH optima that are narrow and acidic around pH 5.0 (Normington and Russell 1992). 5αR2 has Km values in nanomolar range for steroid substrates, whereas 5αR1 has micromolar affinities (Normington and Russell 1992). The isozymic proteins are detected in different tissues, and this distribution is species specific. In humans, both isozymes are present in liver, adipose tissue and brain (Doering, et al. 2002; Mackenzie, et al. 2008); 5αR1 is found in nongenital skin and 5αR2 is mostly present in tissues of male reproductive system including prostate, epididymis, seminal vesicle and genital skin. However in rats, 5αR1, but not 5αR2, is found in liver (Normington and Russell 1992). Both isozymes are detected in brain and epididymis; and within the ventral prostate, 5αR1 is found in basal epithelial cells and 5αR2 in stromal cells (Russell and Wilson 1994; Torres and Ortega 2003). The two isozymes have different affinity for steroids. In rats 5αR1 has 10-20 fold higher affinity for androgens, progesterone, and corticosterone than 5αR2 (Normington and Russell 1992).

Different properties of the isozymes result in diverse physiological significance. 5αR2 is essential for development of normal male sexual characteristics in humans as it is primarily responsible for converting testosterone to 5α-dihydrotestosterone (5α-DHT), the latter being a more potent androgen than its parent hormone. Mutations in 5αR2 in human results in male pseudohermaphroditism characterized by normal male internal urogenital tracts but feminised external genitalia in childhood (Andersson, et al. 1991). This disorder is however species specific as male mice with deficiency in 5αR2 or in both isozymes have fully formed internal and external genitalia and are fertile, but have smaller prostates and seminal vesicles than wild type controls (Mahendroo, et al. 2001). Congenital syndrome of deficiency in 5αR1 has not been reported in humans. Normington and Russell (1992) suggest 5αR1 plays a largely catabolic role in the metabolism of steroid hormones. Some clues to its role may be inferred from mice with transgenic disruption of the gene. In the female 5αR1 knockout mice, two thirds exhibit parturition disturbances (Mahendroo, et al. 1996). This is due to the failure of cervical ripening because of prolonged exposure to elevated progesterone levels (Mahendroo, et al. 1999). Moreover, approximately half of embryos die in the type 1-null mice, caused by chronic elevated levels of plasma estrogen (Mahendroo, et al. 1997) through diversion of testosterone in the absence of 5αR1. Female mice lacking both isozymes show parturition defects and fecundity defects similar to those in the mice without 5αR1 (Mahendroo et al. 2001).

1.7 5α-Reduction of glucocorticoids in Metabolic Syndrome

1.7.1 5α-Reduced metabolites of glucocorticoids

It is known that some 5α-reduced metabolites of steroid hormones have biological activity. While A-ring reduced androgens are recognised as more active than the parent steroid, 5α-reduced products of other steroids are less active than the parent. The 5α-reduced metabolites of aldosterone have anti-natriuretic and kaliuretic

activities of aldosterone that regulate water and electrolyte metabolism in adrenalectomized rats (Kenyon, et al. 1985; Kenyon, et al. 1983), and have the capacity to increase blood pressure in adrenalectomized spontaneously hypertensive rats (SHR) (Gorsline, et al. 1986). In the case of progestogens, 5α-tetrahydro progesterone acts like a sedative and activates the GABA(A) receptor (gamma-aminobutyric acid (A) receptor, the brain's major inhibitory neurotransmitter), decreasing anxiety and reducing seizure activity (Smith, et al. 1998).

Previous work has suggested that 5α-reduced glucocorticoids are biologically active. 5α-Dihydrocortisol (5αDHF) was capable of competing with dexamethasone for specific cytoplasmic binding sites in hepatoma tissue culture cells (Baxter and Tomkins 1971). When male rats were administered for seven days with 5α-dihydro corticosterone (5αDHB) and 5αDHF, hepatic activities of PEPCK and FDPase were significantly decreased; and the treatment of 5αDHB also decreased blood insulin (Golf, et al. 1984). However, it has been reported that 5αDHB had very limited ability to compete with dexamethasone for binding sites on GR and was practically devoid of glucocorticoid activity (Carlstedt-Duke, et al. 1977). Recent work by McInnes et al. (2004) has also shown that 5αDHB was less effective than 5α-tetrahydro corticosterone (5αTHB) in displacing dexamethasone from binding sites in rat hepatocytes and increasing the induction of MMTV reporter gene in transiently transfected Hela cells. Moreover, when 5αTHB was administered to adrenalectomised rats, it was active to transactivate gluconeogenic genes (e.g. PEPCK and TAT) *in vitro*, and to suppress the circulating ACTH levels (McInnes et al. 2004). These intriguing findings create interest about the potential effects of 5α-reduced glucocorticoids on GR activation in tissues where the enzyme is expressed, and suggest that 5α-reduced metabolites could contribute to the metabolic or anti-inflammatory effects of its parent hormone, although the effects of 5α-reduced metabolites on the immune system have as yet not been reported. If this hypothesis is true, selective inhibition of 5α-reductase might have a role in reducing endogenous glucocorticoid action, for example in metabolic syndrome, by removing the component mediated by 5α-reduced glucocorticoid metabolites.

1.7.2 5αR1 in Metabolic Syndrome

Research by our group and others has found increased 5α-reduction of glucocorticoids in obese subjects that correlate with insulin concentrations (Andrew, et al. 1998; Tomlinson, et al. 2008a). Analogous findings have been observed in rodents. Transcription and activity of both 5αR1 and 5β-reductase in liver are increased in obese Zucker rats, with 5αR1 being induced to a greater extent. Insulin sensitization can ameliorate the increase in A-ring reductases in rats (Livingstone, et al. 2000a; Livingstone, et al. 2005). Furthermore, decreased 5α-reductase activity is associated with weight loss in obese humans (Tomlinson et al. 2008a; Tomlinson, et al. 2008b). These findings are consistent with the concept that 5α-reduced glucocorticoids contribute to GR signalling, e.g. in liver: if increased 5α-reductase activity increases concentrations of 5α-reduced metabolites and these increase GR signalling, this could contribute to the metabolic syndrome in obesity. However, there are several unknowns. Without knowing the relative contribution of 5α-reduced glucocorticoids and the parent steroid to GR signalling, it is unclear whether the effects of upregulation are harmful or protective. If 5α-reduced metabolites are fully biologically active, increased 5α-reductase activity would exacerbate the adverse effects of glucocorticoids; however, if 5α-reduced metabolites are inactive, or partially active (as partial agonists), then increased 5α-reductase activity would reduce GR activation and act as a more conventional clearance mechanism for the active parent hormone. The concentrations of 5α-reduced metabolites that are available for GR binding are unknown; these may be rapidly conjugated and excreted.

Against this background, more recent findings in our lab (within the tenure of this thesis) have demonstrated that 5αR1 deficient mice with high-fat diet exhibited metabolic syndrome characterised by glucose intolerance and fatty liver, suggesting that inhibition of 5αR1 may cause detrimental metabolic side effects, probably by allowing accumulation of the parent glucocorticoid which then plays the major role in GR activation (Livingstone, et al. 2008). Similar data with 5αR1 inhibitors are not yet available in humans. The physiological contribution of 5α-reduced glucocorticoid metabolites therefore needs to be studied further.

This thesis has focused on the potential pharmacological role for 5α-reduced glucocorticoid metabolites, and has investigated the effects of 5αTHB compared to the parent hormone corticosterone.

1.8 Hypothesis and Aims

The hypothesis of this thesis is that 5α-reduced glucocorticoids modify GR action. The primary aim of this thesis is to investigate the effects of 5αTHB, which will be addressed as follows:

1. To investigate the effects of 5αTHB on GR translocation *in vitro* using transiently transfected green fluorescent protein (GFP)-tagged GR by fluorescent microscopy;

2. To investigate the effects of 5αTHB on transactivation and transrepression of glucocorticoid regulated genes *in vitro*;

3. To investigate the effects of acute or chronic administration of 5αTHB *in vivo* on HPA axis, fuel metabolism and immune responses in mice;

4. To investigate the pharmacological effects of 5αTHB *in vivo* on inflammation induced by intraperitoneal administration of lipopolysaccharide (LPS);

5. To investigate the role of 5αR1 to modulate the adverse effects of corticosterone.

Chapter 2

Materials and Methods

2.1 Materials

All chemicals and reagents were purchased from Sigma, Poole, UK unless otherwise stated. All enzymes for molecular biology were purchased from Promega, Southampton, UK. All tissue culture media used for cell culture were purchased from Lonza (previously Cambrex), Verviers, Belgium. All flasks and plates were either Corning® or Costar®, both purchased from Corning Incorporated, NY, USA. All radioactively labelled steroids and radioactive isotopes were purchased from Amersham (now GE Healthcare), Little Chalfont, UK. All HPLC grade solvents were purchased from Rathburn Chemicals, Walkerburn, UK. All epi-steroids were from Steraloids, Newport, USA. Sources other than these are indicated in parenthesis. Room temperature (RT) was 18-20 °C.

2.2 Buffers and Solutions

2.2.1 Preparations for animal experiments

2.2.1.1 Glucose (20% w/v) in saline for intraperitoneal (i.p.) injection

Glucose (1 g) was dissolved in saline (5ml; 0.9% NaCl w/v, B.Braun Melsungen AG, Germany).

2.2.1.2 Mini-pump loading solutions

Corticosterone or 5αTHB (8.33 mg) were weighed and dissolved in glass vials in a mixture (2 ml) of DMSO and propylene glycol (1:1 v/v) and mixed thoroughly by sonicating for approximately 15 min. The solution was prepared immediately before use. The loaded mini-pumps were kept at RT.

2.2.1.3 Lipopolysaccharide (LPS) solutions

LPS (1 g) was dissolved in Dulbecco's phosphate buffered saline (DPBS, 1 ml, without Mg^{2+} or Ca^{2+}), mixed thoroughly and stored in -20 °C. This stock LPS solution was diluted with DPBS to 0.001, 0.01, 0.1, 1 and 10 ng/µl, on the day before treatment (stored in 4 °C).

2.2.2 Preparations for molecular biology

2.2.2.1 DEPC-treated water

Diethylpyrocarbonate (DEPC; 5 drops) was added to distilled water (500 ml), shaken gently and allowed to remain at RT for 16-24 hours prior to sterilisation in an autoclave.

2.2.2.2 EDTA buffer

Ethylene diamine tetraacetic acid (EDTA, 0.5 M) was dissolved in distilled water, adjusted to pH 8.0 by addition of NaOH (10 M), sterilised in an autoclave and stored at RT.

2.2.2.3 10×TBE buffer

Trizma base (108 g), boric acid (55 g) and EDTA buffer (0.5 M, 40 ml, see 2.2.2.2) were dissolved in distilled water, the pH was adjusted to 8.0 by addition of NaOH (10 M), and the volume adjusted to 1 L. The solution was sterilised in an autoclave and stored at RT.

2.2.2.4 0.5×TBE buffer

The 10×TBE buffer (50 ml) was diluted with distilled water (950 ml) and stored at RT.

2.2.2.5 Loading buffer

Bromophenol blue (0.25% w/v), xylene cyanol (0.25% w/v) and Ficoll® (a nonionic synthetic polymer of sucrose, 25% w/v) were dissolved in DEPC-treated water and stored at 4 °C.

2.2.3 Preparations for enzymology

2.2.3.1 Potassium phosphate buffer (0.2 M)

KH_2PO_4 (27.22 g) was dissolved in distilled water (800 ml). The pH was adjusted to 7.3 by addition of KOH (10 M), and volume adjusted to 1 L. The buffer was stored at 4 °C.

2.2.3.2 Glucose/Hepes buffer

Hepes (4-(2-Hydroxyethyl)piperazine-1-ethanesulfonic acid, 1.19 g, 5 mM) and sucrose (85.58 g, 250 mM) were dissolved in distilled water. The pH was adjusted to 7.4 with HCl (1 M), and volume adjusted to 1 L. The solution was stored at 4 °C.

2.2.3.3 Tyrosine (10 M)

Tyrosine (0.186g) was dissolved in 0.2 M potassium phosphate buffer (150 ml) by heating at 60-70°C for 1.5 h until the solution became clear.

2.2.3.4 α-Ketoglutarate (0.3 M)

α-Ketoglutarate (0.2216g) was dissolved in 0.2M potassium phosphate buffer (8 ml), mixed thoroughly and kept on ice immediately prior to use.

2.2.3.5 Pyridoxal phosphate (1.33 M)

Pyridoxal phosphate (0.003g) was dissolved in potassium phosphate buffer (10ml, see 2.2.3.1), placed on ice and protected from direct light.

2.2.3.6 NaOH (10 M)

NaOH (40g) was dissolved in distilled water (100ml), allowed to cool and stored at RT.

2.2.4 Preparations for biochemical assays

2.2.4.1 Borate buffer

Boric acid (8.25 g), NaOH (2.70 g) and HCl (1 M, 3.5 ml) were dissolved in distilled water. The pH was adjusted to 7.4 with HCl (1 M) before bovine serum albumin (BSA, 5.0 g, Fraction V) was added and dissolved in the solution. The final volume was adjusted to 1 L. The buffer was stored at -20°C and thawed at RT immediately before use.

2.2.4.2 Phosphate buffered saline (PBS)

Five PBS tablets were dissolved in distilled water (1 L), yielding phosphate buffer (0.01 M) containing KCl (2.7 mM) and NaCl (137 mM), pH 7.4, sterilised in an autoclave and stored at RT.

2.3 General animal husbandry

2.3.1 Maintenance of animals

Animals were maintained under controlled conditions of light (lights on 07:00–19:00) and temperature (18-20 °C) and allowed access to standard chow (Special Diet Services, Witham, UK) and drinking water *ad libitum*. All experiments were performed under the project licence (JR Seckl, PPL No: 60/01562) and personal licence (Yang, PIL No: 60/10364) and under the guidelines of the UK Home Office.

2.3.2 Mini-osmotic pump implantation

2.3.2.1 Loading of mini-osmotic pumps

Mini-osmotic pumps (Model 2002; Alzet®, Cupertino, US, 0.5 µl/h, 14 days) were fully loaded (approximately 247 µl) with the steroid solutions (see 2.2.1.2) following the manufacturer's instructions and kept in a cool and dry place at RT before surgery.

2.3.2.2 Implantation of the mini-osmotic pumps

The surgical procedures were carried out by Dr. Dawn Livingstone, Centre for Cardiovascular Science, Queen's Medical Research Institute. Animals were injected subcutaneously with buprenorphine (Alstoe Animal Health, York, UK; 0.05 mg/kg body weight, 1 in 10 diluted in saline (0.9% w/v, B.Braun Melsungen AG, Germany)), and anaesthetised with isoflurane (Merial Animal Health Ltd, Essex, UK). The loaded mini-osmotic pumps were implanted subcutaneously through dorsal incisions which were then closed with staples. Following surgery, mice were allowed to recover under observation in a warm box (30 °C) before being transferred to individual clean cages.

2.4 Specific animal procedures

2.4.1 Systolic blood pressure measurement

Mice were pre-warmed in a hot box (33 °C, 5 min) prior to measurement of systolic blood pressure using a computerised tail cuff plethysmography system (Evans, et al. 1994). Each mouse was restrained in a darkened perspex tube mounted on a platform (Harvard Instruments) designed to position the pressure transducer at the base of the tail. The pressure transducer is a combined computer controlled compression cuff with photoelectric pulse detector. On inflation, blood flow through the tail was prevented, and upon deflation the return of blood flow was detected by the

transducer (Evans et al. 1994). The program software (written in Turbo Pascal v 6.0) controlled the pressure and detected the pulsation signals, which were amplified and filtered before being digitised. The blood pressure trace, shown as amplitude on the screen, was generated. On deflation, a threshold of the minimum amplitude was estimated by the program to be the value of systolic blood pressure (mmHg). The final value of pressure was the mean of four successful measurements.

2.4.2 Glucose tolerance test

Food was withdrawn from animals for six hours from 08.00h. Glucose (20% w/v in saline) was administered by intraperitoneal injection (10 µl per gram body weight) to give a total dose of 2 g of glucose per kg. Blood was collected via tail nicks before injection and at 15, 30, 60 and 90 min post-injection. Food was restored immediately after collection of the last sample. Blood was taken into EDTA microvettes (Sarstedt, Germany), and plasma was prepared immediately by centrifugation (1000 g, 5 min, 4 °C) then stored at -20 °C for later analysis.

2.4.3 Terminal procedures for animals with glucocorticoid infusions

Animals were decapitated in the morning of the last day of infusion within 1 min of disturbing of the home cage. Trunk blood was collected immediately into tubes containing either heparin (1 unit/ml) or EDTA (0.5 M). Five pads of adipose tissue (omental, retroperitoneal, epididymal, mesenteric and subcutaneous) and six organs (thymus, kidneys, left adrenal, liver, spleen and right quadriceps muscle) were dissected, weighed and snap frozen on dry ice. Two pieces of liver (<100 mg) were snap frozen, and the remainder was immersed in ice cold glucose/Hepes buffer for preparation of cytosol. The right adrenal was fixed in formalin (10% v/v). After fixation for 24 hours, it was weighed following removal of associated fat tissue. An aliquot of heparinized blood was used for LPS activation. Plasma was collected by centrifugation (1000 g, 5 min, 4 °C) then frozen (-80 °C) and used to measure corticosterone, ACTH and 5αTHB concentrations.

2.4.4 Activation of whole blood by LPS

A series of solutions of LPS were prepared in DPBS (10 μl), containing 0 (DPBS alone), 0.01, 0.1, 1, 10 and 100 ng of LPS, and added to six 2 ml-round-bottom tubes respectively. Heparinized aliquots of whole blood collected from each animal were dispensed into the six tubes (90 μl for each). Then they were gently mixed and incubated in a shaking water bath (18 h, 37 °C). Supernatant from each tube was collected after centrifugation (1,000 g, 5 min, 4 °C) and stored at -80 °C until required for quantification of cytokines.

2.5 Molecular Biology

2.5.1 RNA extraction

2.5.1.1 RNA extraction from tissues and cultured cells

TRIzol® reagent (Invitrogen, Paisley, UK) was used for isolation of total RNAs from cells and tissues. It contains phenol and guanidine isothiocyanate, which disrupts cells and dissolves cell components but maintains the integrity of RNA during homogenization or lysis.

Freshly collected tissues were snap frozen on dry ice immediately after dissection from the animal. Each sample was cut into small pieces (50-100 mg) and homogenized in TRIzol reagent (1 ml) (Model Ultra-Turrax T8 homogenizer, IKA Labortechnik, Germany). Homogenised samples were used directly or stored at -80°C until required.

Cells incubated in six-well plates were washed with PBS and then lysed in the TRIzol® reagent (1 ml per 10 cm^2 growth area) by shaking the plates and passing the

lysate through a pipette. The cell lysate was harvested from each experiment and stored at -80°C until required.

Tissue homogenates or cell lysates were allowed to equilibrate to RT. After 5min at RT to allow complete dissociation of the nucleoprotein complexes, chloroform (0.2 ml) was added; samples were vortexed (15 sec) and then incubated at RT for a further 3 min. The mixture was separated by centrifugation (12,000 g, 15 min, 4 °C,) into three phases, a lower red, phenol-chloroform phase containing proteins, an interphase containing DNAs, and a colourless upper aqueous phase containing RNA.

This upper phase was transferred into another Eppendorf tube and RNA was precipitated by adding isopropanol (500 µl per ml TRIzol®) with incubation (10 min, RT) following centrifugation (12,000 g, 10 min, 4 °C). The supernatant was removed and ethanol (75% v/v in DEPC-treated water, 1 ml per ml TRIzol®) was added to the white RNA pellet. RNA was re-suspended by vortexing and then re-precipitated by centrifugation (7,500 g, 5 min, 4 °C). The ethanol supernatant was removed and the RNA pellet was air-dried briefly before being dissolved in DEPC-treated water (40 µl for tissues, 20 µl for cells) by pipetting and incubation (10 min, 60 °C). Samples were stored at -80 °C until required.

2.5.1.2 RNA extraction from adipose tissue

Extraction of RNAs from adipose tissue was carried out using RNeasy Lipid Tissue Mini Kit (Qiagen Ltd, West Sussex, UK), which integrates phenol/guanidine-based lysis and silica-gel membrane purification of total RNA.

Fresh subcutaneous fat and retroperitoneal fat were snap frozen on dry ice immediately after removal from mice. Adipose tissue (<100 mg) was homogenized in QIAzol Lysis Reagent (1 ml), a monophasic solution of phenol and guanidine thiocyanate. Sample homogenate was either used directly or stored at -80 °C until required.

When the homogenate was equilibrated to RT, chloroform (200 µl) was added following vortexing. The mixture was separated by centrifugation (12,000 g, 15 min, 4 °C) into an upper aqueous phase containing RNA, a white interphase with DNA, and lower organic phases where protein remained. The aqueous supernatant (600 µl) was collected into another Eppendorf tube and ethanol (70% v/v in DEPC-treated water, 600 µl) was added to the aqueous supernatant to provide appropriate binding conditions. Then the samples were applied to an RNeasy Mini Spin Column where the total RNA bound to the membrane, while phenol and other contaminants were eluted by two reagents applied successively (Buffer RW1 and Buffer RPE) by centrifugation (15 sec, >8000 g, RT). Purified RNA was then dissolved in RNase-free water (20 µl) by direct addition of water to the column membrane, and eluted into a fresh tube by centrifugation (1 min, >8000 g, RT).

2.5.1.3 RNA extraction from mouse pituitary

RNAs from mouse pituitaries were isolated using the RNeasy Mini Kit (Qiagen Ltd, West Sussex, UK), which is a technology for purification of total RNA by a silica-based membrane.

Fresh pituitaries were dissected from animals and snap frozen on dry ice. When required, each pituitary was ground with a little dry ice (twice the volume of tissue) in a mortar which was also cooled with dry ice. The pituitary powder was transferred into an Eppendorf and mixed with the supplied Buffer RLT (350 µl, containing guanidine thiocyanate) in which the ground tissue was soaked, protecting the RNA. The mixture was transferred directly into a QIAshredder spin column (Qiagen Ltd, West Sussex, UK) which was placed in a collection tube then centrifuged (12,000 g, 2 min, RT) to fully disrupt the tissue. The lysate was cleared of very small amounts of insoluble materials by further centrifugation (12,000 g, 3 min, RT) without the QIAshredder, and the resultant supernatant was carefully removed and transferred into a new Eppendorf.

Ethanol (70% v/v in DEPC-treated water, 350 µl) was added to the lysate. The subsequent processes were the same as described above in 2.5.1.2.

2.5.2 RNA quantification

RNA (1 µl) was diluted in DEPC-treated water (99 µl) and mixed by brief vortexing before quantification using a GeneQuant spectrophotometer (Pharmacia Biotech, Sweden). The RNA concentration was determined by the absorbance at 260nm wavelength (A260), and the purity by the ratio of RNA/DNA (A260/A280). Low ionic strength and low pH solutions (such as water) increase the absorbance at 280 nm (Wilfinger, et al. 1997). Therefore, RNA samples with the A260/A280 ratio of their dilutions between 1.5 and 1.8 were deemed suitable for use.

2.5.3 Reverse transcription

First strand complementary DNA (cDNA) synthesis was performed using the Reverse Transcription System (Promega). RNA samples were diluted in DEPC-treated water to 0.1 µg/µl in a final volume of 10 µl. Then the diluted RNA (5 µl) was incubated with DEPC-treated water (4.5 µl) and master mix (9.5 µl) which contains the reagents provided as follows:

$MgCl_2$ (25 mM, 4 µl)
Random primers (0.5 µg/µl, 1 µl)
Reverse transcription 10× buffer (2 µl)
PCR nucleotide mix (containing dATP, dCTP, dGTP and dTTP, 10 mM each, 2 µl)
AMV (Avian Myeloblastosis Virus)-reverse transcriptase (22 units/µl, 1 µl)
RNasin (RNase inhibitor, 40 units/µl, 1 µl)

Negative control reactions to confirm the absence of contaminating genomic DNA were performed in parallel for each RNA sample. These controls were prepared as above but with DEPC-treated water replacing AMV-reverse. Additionally, a negative control reaction containing water instead of RNA was performed to demonstrate that Reverse Transcriptase System reagents were not contaminated with RNA.

The reverse transcription system for each sample was incubated in a 200 µl Eppendorf tube in a PCR machine (G-Storm, GRI Lid, Essex, UK). Samples were

heated at 42 °C for 15 min and 99 °C for 5 min, and then chilled to 4°C. The resultant cDNA was stored at -20 °C until required.

2.5.4 Polymerase Chain Reaction (PCR)

The polymerase chain reaction (PCR) was carried out using the TaqBead™ Hot Start Polymerase kit (Promega). cDNA template was first diluted 1 in 5 in the nuclease-free water provided, and then 5 µl of the dilution was added to each PCR reaction containing the following reagents:

TaqBead™ Hot Start Polymerase (1.25 u/bead, 1 bead)
Nuclease-free water (32 µl)
Magnesium-free 10× reaction buffer (5 µl)
$MgCl_2$ (25 mM, 3 µl)
PCR nucleotide mix (containing dATP, dCTP, dGTP and dTTP, 10 mM each, 1 µl)
Primers (forward and reverse, 20 pmol/µl, 2 µl each)

A negative control reaction containing nuclease-free water instead of cDNA was prepared in parallel to confirm the absence of cDNA contamination in the PCR reagents.

Thermal cycling was performed using the G-Storm PCR machine with the lid heated to 100 °C. Samples were heated to 95 °C for 5 min for initial denaturation, then underwent 35 cycles of PCR amplification, which consisted of denaturation at 95 °C for 45 sec, primer annealing at 55 °C for 45 sec, and elongation at 72 °C for 1.5 min. Upon completion of the PCR programme, samples were incubated at 72 °C for a further 5 min to ensure elongation of products to full length and chilled to 10 °C prior to gel electrophoresis. The details of primer sequences were listed in Table 2.1.

The PCR products (5 µl) were separated by electrophoresis on an agarose gel (2.0% w/v in 0.5×TBE buffer). For each gel, the DNA fragments of known fragment sizes (100 bp (base pair) ladder; Promega), shown on a photo taken under UV light, were

resolved to identify the bands equivalent in size to those anticipated for the genes of interest.

2.5.5 Real-time PCR

Quantification of transcript abundance was performed using the LightCycler®480 (Roche Diagnostics, Mannheim, Germany). Sample cDNA was diluted 1 in 32 in DEPC-treated water, except for those from adipose tissue (1 in 8) and pituitary (1 in 16). Intron-spanning primers and probes for TAT, PEPCK and Agt were designed, and other primer-probe sets for the genes of interest were purchased from TaqMan® Gene Expression Assays (AppliedBiosystems, UK) (Table 2.2). All probes had a FAM reporter dye at the 5' end and a nonfluorescent quencher at the 3' end.

The diluted cDNA sample or standard (2 µl) was added into a 384-well plate before addition of the freshly prepared master mix (8 µl) which consisted of the following components:

Primers (forward and reverse, 12 pmol/µl, 0.5 µl each)
The corresponding probe (4 pmol/µl, 0.5 µl)
LightCycler®480 Probes Master (2×conc.) (5 µl, Roche Diagnostics)
Water provided (2.5 µl)

Samples were heated to 95 °C for 5 min for initial denaturation, and underwent 50 cycles of PCR amplification which included denaturation at 95 °C for 10 sec, primer annealing at 60 °C for 30 sec and elongation at 72 °C for 1 sec. Once these cycles were completed, samples were cooled to 40°C for 30sec prior to completion. During the amplification, relative DNA concentrations presented were determined by plotting fluorescence against cycle number on a logarithmic scale, thus a straight line was constituted to show the increase of DNA quantity during the exponential phase when DNA quantity doubled every cycle.

The LightCycler®480 Software (Version LCS480, Roche Diagnostics) determines the value of the crossing point (Cp), which represents the cycle at which the rate of

increase of fluorescence is highest and where the logarithmic phase of a PCR begins, by calculating the second derivatives of entire amplification curves where the maximum is determined as Cp (Molenkamp, et al. 2007). The standard curve for each primer-probe set was generated in triplicate by serial dilution of cDNAs pooled from different samples representing all groups under study. Individual samples were analysed in duplicate and the mean was used to calculate the transcript abundance. The corresponding amounts of RNA from each sample were determined by interpolating the results onto the standard curve, and then abundances were divided by the amount of RNA from a housekeeping gene, cyclophilin, measured in the same sample; this process normalized for the variations in the amount and quality of RNAs between samples. RT negative controls were used to confirm the absence of contamination with genomic DNA.

Table 2.1 Details of primer sequences and PCR products (For=forward; Rev=reverse).

Gene Accession No. (Mouse)	Amplicon Region	Primer sequence		Product (bp)
SRD5A1 (5α-reductase 1) NM_175283	160-281	For	CTA CAG GAG CTG CCT TCA AT	122
		Rev	CTT TGC ACG TAG TGG ATC AG	
SRD5A2 (5α-reductase 2) NM_053188	113-272	For	AAC ACA GCG AGA GTG TGT CG	160
		Rev	GAG AAG AGA CCC AGC AGC AC	
AKR1D1 (5β-reductase) NM_145364	157-656	For	ATG GCG CCT ATG TTT ACC AC	500
		Rev	ATG TGC GAC AAT GAC GAT GT	
AKR1C6 (3αHSD) NM_030611	281-688	For	AAT TGG TCC GAT CTT GCT TG	408
		Rev	CCA CCC AGA TTT TGT CTC GT	
Emr1 (F4/80) NM_010130	1282-1927	For	AAC AAA AGT GCC CCA GTG TC	646
		Rev	AGT TTG CCA TCC GGT TAC AG	

Table 2.2 Primers and probes designed for genes (with Accession number) or purchased for Real-Time PCR

TAT	Primers	Rat (NM_ 012668)	For	CCG GTC CGC CCT TCT G
			Rev	TCC GGG AAA TGC TCC ATC T
		Mouse (NM_146214)	For	GCC AGT CCG CCC ATC TG
			Rev	TCT GGG AAG TGC TCC ATC T
	Probe	AGC CAT GTA CCT TAT GGT GGG AAT T		
PEPCK	Primers	Rat (NM_198780)	For	AGT TGA ATG TGT GGG TGA TGA CA
			Rev	CTG GGT TGA TGG CCC TTA AG
		Mouse (NM_011044)	For	GTC GAA TGT GTG GGC GAT GAC
			Rev	CTG GGT TGA TAG CCC TTA AG
	Probe	CCT GGA TGA AGT TTG ATG CCC AAG GC		
AGT	Primers	Rat (NM_134432)	For	CTG GGC AAG ATG GGT GAC A
			Rev	GGA GTT CAA GGA GGA TGC TGTT
		Mouse (NM_007428)	For	CTG AAC AAC ATT GGT GAC ACC
			Rev	TGA GTT CGA GGA GGA TGC TATT
	Probe	CCC CCG AGT GGG AGA GGT TCT		
ID of TaqMan® Gene Expression Assays purchased from Applied BioSystems				
11βHSD 1	Mm00476182_m1			
TNFα	Mm00443258_m1			
IL-6	Mm00446190_m1			
MCP-1	Mm00441242_m1			
POMC	Mm00435874_m1			
CRF Receptor 1	Mm00432670_m1			

2.6 Biochemical assays

2.6.1 Quantification of corticosterone by radioimmunoassay (RIA)

Borate buffer (pH 7.4) was prepared as previously described (see 2.2.4.1), and thawed at RT immediately before use. Plasma samples were diluted (10% v/v) in borate buffer and denatured (30 min, 80 °C) to release corticosterone from its binding proteins. A series of solutions representing a range of concentrations of corticosterone was prepared (0, 0.63, 1.25, 2.5, 5, 10, 20, 40, 80, 160 and 320 nM dissolved in borate buffer) to constitute a standard curve. Samples and standards (20 µl each) were mixed with 50 µl of tritiated corticosterone (1,2,6,7-[^{3}H]$_4$-B; 80 Ci/mmol, final concentration was 1.5 nM; Amersham, Bucks, UK) plus corticosterone antibody (final concentration 1:10,000), a kind gift from Dr Christopher Kenyon, University of Edinburgh (MacPhee, et al. 1989), and then adjusted up to a total volume of 70 µl on a 96-well plate with the borate buffer. Anti-rabbit scintillation proximity assay (SPA) beads (50 µl, Amersham, Bucks, UK) were added to each well, and the plate was allowed to incubate (16-20 h, RT). Scintillation occurred when the SPA beads bound to that fraction of primary antibody which was associated with [^{3}H]$_4$-B. Due to the competition between binding of unlabelled and labelled corticosterone to the primary antibody, the extent of scintillation decreases as the concentration of unlabelled corticosterone increases. The degree of scintillation was quantified using a liquid scintillation counter (Microbeta Plus, Wallac 1450, Turku, Finland), and data (Bound/Bound at zero) used to construct a semi-log standard curve from which the concentration of corticosterone in each sample was calculated. Standard curves were acceptable if $R>0.99$, and data acceptable if duplicate values differed by less than the coefficient of variation, i.e. <10%. The detection limit of the assay was 0.6 nM.

2.6.2 Quantification of glucose by hexokinase assay

Plasma glucose was determined quantitatively using Infinity Glucose Hexokinase Liquid Stable Reagent (Thermo Electron, Melbourne, Australia). A series of solutions representing a range of concentrations of glucose (0, 2.8, 5.6, 8.3, 11.1, 13.9, 16.7, 22.2, 33.3 and 44.4 mM in distilled water) was prepared to construct a standard curve. Standards and samples were incubated with reagent at a ratio of 1:125 in a 96-well plate (3 min, RT) during which time hexokinase catalysed the phosphorylation of glucose by ATP producing ADP and glucose-6-phosphate. The latter was then oxidised to 6-phosphogluconate with the associated reduction of NAD^+ to NADH by glucose-6-phosphate dehydrogenase. The amount of NADH formed was proportional to the concentration of glucose in the sample and standards. The absorbance (340 nm) of the reaction product was measured by OPTImax^{TM} Tunable Microplate Reader (Molecular Devices, Sunnyvale, CA, USA). The concentrations of glucose in plasma samples were calculated from the standard curve obtained by plotting the absorbance versus the concentrations of glucose standards. The R values of the acceptable standard curves were >0.99. Samples were assayed in duplicate. The intra-assay coefficients of variation were <10%. The limit of detection of this assay was 0.038 mM.

2.6.3 Quantification of insulin by enzyme-linked immunosorbent assay (ELISA)

Insulin was quantified using Ultra Sensitive Rat Insulin ELISA Kit (Crystal Chem Inc., Downers Grove, USA) by means of anti-rat/mouse insulin antibody and standard rat insulin, which was also suitable for determination of mouse insulin concentration. A series of solutions representing a range of rat insulin concentrations (0, 0.1, 0.2, 0.4, 0.8, 1.6, 3.2 and 6.4 ng/ml in sample diluent provided) was prepared to construct a standard curve in which supplied sample diluent was used as control. Samples and standards were diluted (5 µl in 95 µl diluent) and incubated (2 h, 4 °C) in a 96-well plate coated with guinea pig anti-insulin antibody allowing plasma insulin to bind to the antibody. Then wells were washed five times with washing buffer supplied to remove unbound insulin. The immobilized guinea pig anti-insulin

antibody/insulin complex was then incubated with horse-radish peroxidase (HRP)-conjugated anti-insulin antibody (100 µl, 30 min, RT). Wells were washed for five times again to remove excess HRP-conjugate. The bound HRP conjugate on the microplate well was detected following incubation (40 min, RT) with tetramethylbenzidine (TMB) substrate solution (100 µl) in the dark. This enzymatic reaction was stopped by addition of sulphuric acid (0.5 M, 100 µl). Absorbances at 450 nm and 630 nm (measuring absorbance at 450 nm, subtracting absorbance at 630 nm) were measured with an OPTImax^{TM} Tunable Microplate Reader (Molecular Devices, USA). Insulin concentrations were evaluated against the standard curve obtained by plotting the resultant absorbance difference versus corresponding concentrations of insulin standards. The R values of the acceptable standard curves were >0.99. The minimum detection limit of this assay is 0.1ng/ml. The intra-assay precision was <6%.

2.6.4 Quantification of ACTH by ELISA

Mouse plasma ACTH was quantified by an ACTH ELISA kit (Biomerica, Newport Beach, USA). This is a two-site ELISA for the specific measurement of the biologically active 39 amino acid chain of ACTH, in contrast to an alternative ACTH radioimmunoassay (RIA) which is known to react with proopiomelanocortin (POMC), pro-ACTH, ACTH and some fragments of ACTH.

Plasma samples, controls and a series of ACTH standards representing a range of concentrations (0, 7.1, 18.5, 70, 215 and 515 pg/ml, 200 µl each), respectively, were simultaneously incubated with a biotin coupled goat polyclonal antibody to C-terminal ACTH 34-39 (25 µl) and a HRP labelled mouse monoclonal antibody to N-terminal ACTH 1-24 (25 µl) in a streptavidin-coated microplate well without exposure to light on an orbital shaker (170 ± 10 rpm, 4 h ± 30 min, RT). Following incubation, the complexes of biotinylated antibody – ACTH - HRP conjugated antibody were bound to the wells.

At the end of the incubation, the wells were washed five times to remove unbound components and the immobilized complex was incubated with the substrate TMB

(150 µl) without exposure to light on an orbital shaker (170 ± 10 rpm, 30 ± 5 min, RT). An acidic stopping solution (sulphuric acid, 0.5 M, 100 µl) was then added, generating a yellow coloured product. The absorbance (λ450 nm) of the solution in the wells was measured by OPTImax™ Tunable Microplate Reader (Molecular Devices, USA) against a blank of distilled water. A calibration curve of resultant absorbance versus concentration was constructed using results obtained from the standards. The R values were >0.99 for the standard curves to be accepted. Concentrations of ACTH present in the samples were determined from the curves. Samples were assayed in singlicate due to paucity of sample. The minimum detection limit of this assay is 0.46 pg/ml.

2.6.5 Quantification of NEFAs

NEFAs in plasma samples were quantified by the 96-well Serum/Plasma Fatty Acid Kit (Zen-Bio, Research Triangle Park, NC, US) based on the following reactions. NEFAs and CoA were firstly converted to fatty acyl-CoA thiol esters, in the presence of acyl-CoA synthetase, which subsequently reacted with oxygen in the presence of acyl-CoA oxidase, producing hydrogen peroxide. Thereafter 3-methyl-N-ethyl-N-(β-hydroxyethyl) -aniline and 4-aminoantipyrine were oxidized by hydrogen peroxide in the presence of peroxidase and produced a purple product with an absorbance of 550 nm. The concentrations of NEFAs in plasma were determined by spectrophotometry.

The kit standard solution was reconstituted and diluted with the Dilution Buffer to give a range of concentrations (1.4, 4.1, 12.3, 37, 111, 333 and 1000 µM) with Dilution Buffer as the zero standard. Standards and samples (5 µl) were pipetted into a 96-well plate with Dilution Buffer (48 µl) followed by FFA Reagent A (50 µl, reconstituted with FFA Diluent A). The plate was gently shaken and allowed to incubate (10 min, 37 °C) prior to addition of FFA Reagent B (100 µl) to each well. Then the plate was shaken gently and incubated again (10 min, 37 °C), and equilibrated to RT for 5 min before the absorbance was measured by OPTImax™ Tunable Microplate Reader at 540 nm (Molecular Devices, USA). The value of the zero standard was subtracted from all values including the standards. The results were then calculated from the standard curve, plotting the corrected absorbance

versus concentrations of standards. The R values were >0.99 for the standard curves to be acceptable. Samples were assayed in singlicate due to paucity of sample. The limit of detection of this kit was 0.68 μM.

2.6.6 Quantification of cytokines by Cytometric Bead Array

The amount of cytokines in biological fluids was determined by flow cytometry, an analysis tool that discriminates different particles on the basis of size and colour, using the BD Cytometric Bead Array (CBA) Mouse Inflammation Kit (BD BioSciences, Oxford, UK).

The CBA kit applied six different microparticles (7.5 μm polystyrene beads) that were dyed to give discrete fluorescence signals which could be amplified and detected by the FL3 detection channel of a flow cytometer (BD FACSArray™ BioAnalyzer, BD BioSciences Immunocytometry Systems, San Jose, CA). The six beads in the Mouse Inflammation Kit were coated with capture antibodies specific for IL-6, IL-10, MCP-1, IFN-γ, TNFα and IL-12p70 proteins. The fluorescence intensity characteristics of each type of bead were distributed from brightest to dimmest in this order. Each antibody-bound bead captured a given cytokine which could be detected as a discrete population with unique FL3 intensity that could be distinguished in a mixture of beads with different antibodies. The specifically captured cytokines were detected via a direct immunoassay using six specific detection antibodies conjugated with phycoerythrin (PE), providing a fluorescent signal that could be detected by the FL2 detection channel (Figure 2.1). This signal was proportional to the concentrations of the cytokines in the test matrix. Therefore the concentrations of the six analytes in a single sample could be determined.

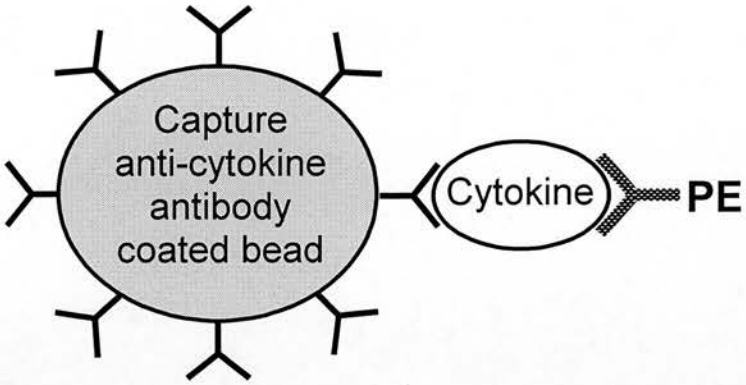

Figure 2.1 A schematic of the "cytokine sandwich" in a CBA assay. Beads of different fluorescence intensity, coated with specific cytokine antibodies and detector cytokine antibodies coupled to phycoerythrin (PE), were incubated with sample or standards and analyzed by flow cytometry.

One pre-mixed vial of lyophilized standards containing the six recombinant proteins was reconstituted in the Assay Diluent provided (0.2 ml) and equilibrated for 15 min before dilutions to achieve a series of solutions containing 20, 40, 80, 156, 312.5, 625, 1250, 2500 and 5000 pg/ml of protein respectively with the Assay Diluent used as a blank. The appropriate amount of Capture Beads were pooled together and mixed by vortexing before adding to all the assay wells (25 µl per well) in a 96-well plate. The dilutions of standards (25 µl) were added to the control assay wells and the test samples (25 µl) to the test assay wells. The PE Detection Reagent (25 µl) provided, containing six specific antibodies, was added to all wells prior to incubation of the plate (2 hours, RT, without light) in order to form sandwich complexes. After incubation, Wash Buffer (120 µl per well) was added before centrifugation (330 g, 5 min, RT). Thereafter the supernatant was discarded by inversion and the plate dried carefully on paper tissues. The bead pellets were resuspended in Wash Buffer (120 µl) before analysis on BD FACSArray™ Bioanalyzer.

Data were acquired and analyzed using BD CBA Analysis software. The parameters FSC (forward light scatter) and SSC (side light scatter) were employed to exclude

any sample particles other than the 7.5μm polystyrene beads. Using a BD FACSArray flow cytometer, the Yellow detection channel (FL2, 564-606 nm, measuring fluorescence following excitation by 532nm laser) was used to measure the PE-labeled reporter reagent, and bead populations were identified from the emissions in the Red (FL3, 653-669 nm, measuring fluorescence excited by 635 nm laser) and Far Red (>685 nm, measuring fluorescence excited by 532 nm laser) detector channels. The fluorescence intensity data from each bead in each of the two detector channels were plotted in a two-dimensional dot-plot (FL2 vs FL3) by the BD CellQuest™ Analysis Software, such that the six discrete FL3 microparticle dye intensities were distributed along the Y-axis.

The results were calculated by interpolation onto the six standard curves, plotting cytokine concentrations of standards versus the mean fluorescence intensity (MFI) of FL2 using a four-parameter logistic curve fitting model. Standard curves were accepted if the R values were >0.99. The assay sensitivity of IL-6, IL-10, MCP-1, TNFα, (IFN)-γ and IL-12p70 were 5, 17.5, 52.7, 7.3, 2.5 and 10.7pg/ml, respectively. The samples were assayed in singlicate due to paucity of sample.

2.7 Statistics

Data were analysed statistically by one-way or two-way ANOVA, or repeated measures ANOVA, followed by Holm-Sidak post-hoc test where appropriate. The statistics was performed by the program of SigmaStat 3.5 (Dundas Software Ltd, Germany).

Chapter 3

Investigation of the effects of 5αTHB *in vitro* on GR translocation, transactivation and transrepression

3.1 Introduction

Glucocorticoids exert many of their numerous actions via GRs. GRs are ligand-activated transcription factors which regulate gene transcription, either through transactivation or transrepression. Previous work has suggested that 5α-reduced glucocorticoids may mimic their parent steroid at GR and hence may play a role in the magnitude of activation of the receptor (Baxter and Tomkins 1971; Dubrovsky et al. 1987; Golf et al. 1984; McInnes et al. 2004). This may be of importance in disorders where expression of 5α-reductases are altered e.g. obesity (Andrew et al. 1998; Livingstone et al. 2000; Livingstone et al. 2005). However, the molecular mechanisms underlying the effects of 5α-reduced metabolites have not been clearly elucidated, although McInnes et al suggested that the time course of effects may differ from that of corticosterone. Therefore in this chapter the intracellular responses to 5αTHB will be investigated.

Without ligand binding, GRs stay in cytoplasm, associated with the heat shock protein based chaperone machinery. Upon ligand binding, the nuclear localization signals (NLSs) are exposed which enable GRs to translocate into the nucleus (Smoak and Cidlowski 2004). It has previously been reported that 5αTHB, the 5α-reduced tetrahydro metabolite of corticosterone, is effective in displacing dexamethasone from binding sites in hepatocytes and increasing the transcription of MMTV reporter gene in transfected Hela cells as well as hepatic PEPCK and TAT in hepatoma cells *in vitro* (McInnes et al. 2004). However, the ability and efficiency of 5αTHB in driving GR translocation have not been studied specifically. This chapter will investigate the effects of 5αTHB on this process by utilising fluorescent microscopy to monitor the movement of green fluorescent protein (GFP) -tagged GR (GFP-GR) in living cells, and further detect the mobility of GFP-GR post-translocation by means of fluorescence recovery after photobleaching (FRAP).

Following GR translocation, activated GRs regulate gene transcription via transactivation or transrepression mechanisms. Glucocorticoid induced transactivation can be mediated by GR homodimer binding to palindromic GRE in

the promoter or enhancer regions of target genes or by non-palindromic dimer binding to GRE half sites. (Schoneveld et al. 2004). McInnes et al. demonstrated that 5αTHB activated the induction of mRNA expression of TAT and PEPCK (palindromic GRE) in H4IIE hepatoma cells, which was inhibited by GR antagonist, RU486 (McInnes et al. 2004). Moreover, 5αTHB increased the expression of MMTV reporter gene (GRE half sites) in transiently transfected Hela cells (McInnes et al. 2004), and the effect was additive to that of corticosterone (McInnes et al. 2004). This chapter will further investigate the time course and dose response to 5αTHB in transactivation of glucocorticoid target genes in H4IIE cells. Furthermore, the effects of 5αTHB on gene transactivation via different GR binding mechanisms (binding to GRE or GRE1/2s) will also be investigated and compared in transiently transfected Hela cells.

Glucocorticoids induce transrepressive actions by direct or indirect interaction of GR with target genes. It has been demonstrated in rats that plasma ACTH was suppressed following intraperitoneal administration of 5αTHB (McInnes et al. 2004). This suppression of ACTH was possibly a transrepressive effect of 5αTHB on mRNA expression of POMC, regulated via GR binding to the negative GRE (Drouin, et al. 1993a). Therefore, in this chapter the effects of 5αTHB on POMC transcription will be investigated in AtT20 cells, the mouse pituitary corticotroph tumor cell line.

Lastly glucocorticoids have profound anti-inflammatory and immunosuppressive effects, one of which is to alter the secretion of a variety of cytokines, increasing anti-inflammatory cytokines such as IL-10 and suppressing pro-inflammatory cytokines including TNFα, IL-6 and MCP-1 (Schoneveld et al. 2004). These actions are mediated via GR-protein binding mechanisms. GR binds to the subunits of pro-inflammatory transcription factors NFκB and AP-1, thereby inhibiting the gene transcription of pro-inflammatory cytokines. GR has also been shown to bind directly to the transcription factor STAT3 to activate the expression of anti-inflammatory cytokines (Unterberger et al. 2008). The ability of 5αTHB to initiate these responses has not been previously studied and the work presented here will

investigate the ability and efficiency of 5αTHB to affect cytokine secretion in bone marrow derived macrophages.

Aims

The aims of this chapter were to investigate the effects of 5αTHB on

1) GR translocation and nuclear mobility;

2) Gene transactivation;

3) Gene transrepression.

3.2 Methods and materials

3.2.1 Maintenance of cell lines

3.2.1.1 H4IIE (rat hepatoma cells)

H4IIE cells were cultured in 75 cm^2 flasks in normal-serum medium, which was Dulbecco's modified Eagle's medium (DMEM) supplemented with 10% (v/v) heat-inactivated foetal bovine serum (FBS), penicillin (100 IU/ml), streptomycin (100 μg/ml) and L-glutamine (200 mM). Serum-free medium was also prepared with the same components omitting the FBS. Cells were incubated in a humidified atmosphere in 95% air and 5% CO_2 at 37 °C.

Cells were routinely passaged when confluent, usually twice a week. For subculturing, cells were washed with serum-free medium (7 ml) and trypsin/EDTA (trypsin (0.05% w/v) and EDTA (0.01% w/v); 2 ml), and then cells incubated with trypsin/EDTA (2 ml, 1-2 min, 37 °C). The flasks were shaken until cells were released from the flask surface. Cells were resuspended in normal-serum medium (10 ml). 1/10 to 1/4 of cells were left for maintenance in the flasks, and the rest were aspirated or transferred to other containers. The normal-serum medium (12 ml final volume) was added to the flasks before cells were incubated in the conditions described above, unless otherwise stated.

3.2.1.2 HEK293 (human embryonic kidney cells)

HEK293 cells were cultured and passaged under the same conditions as those described for H4IIE cells (see 3.2.1.1) except for the nature of the growth surface. The culture flasks were coated with poly-d-lysine before use (see 3.2.1.6).

3.2.1.3 AtT20 (mouse pituitary corticotroph tumor cells) and Hela (human cervical carcinoma cells)

AtT20 cells were cultured in 162 cm^2 flasks under the same conditions as those described for H4IIE cells (see 3.2.1.1). The volume of media and trypsin/EDTA was increased by a factor of 2 for washing, passaging and maintenance. Cells were passaged every five days and diluted 1 in 5 in normal-serum medium.

3.2.1.4 Preparation for stripped-serum medium

Heat-inactivated FBS (500 ml) was mixed with dextran-coated charcoal (5 g) and stirred for 16-24 hours at 4 °C. The serum was filtered using 5 µm and 0.45 µm filters (Sartorius, Germany) successively and sterilized by filtration (0.20 µm filter (Nalgenec, Nalge Nunc International, NY, USA)). The filtered serum was dispensed into 50 ml aliquots and stored at -20 °C. The stripped-serum medium was prepared with the same components as the normal culture medium (see 3.2.2.1) with the normal FBS replaced by the stripped-serum, to avoid interference from background concentrations of glucocorticoids found in FBS.

3.2.1.5 Quantification of cells by haemocytometry

The haemocytometer was prepared by breathing on the slide and gently pushing the edges of the coverslip on either side of the chamber until the coverslip was firmly attached to the chamber where Newton's rings appeared. Cell suspension was added to both sides of the chamber (10 µl to each). Cells were counted in the four corner quadrants of each side of the chamber along two of the four edges. For each side, the total number was divided by four, and the average of both sides equated to the number of cells per mm^2. This value was multiplied by 10^4 to give the number of cells per ml of the cell suspension. The appropriate number of cells was added accordingly to the size of the multiple-well plates.

3.2.1.6 Preparation of poly-d-lysine coated flasks and plates

Poly-d-lysine (BD Biosciences, Bedford, MA, USA; MW (molecular weight) 500,000 – 550,000 daltons) is a synthetic molecule used as a thin coating to enhance

the attachment of cells to plastic and glass surfaces. Diluted poly-d-lysine in DPBS was added to flasks or 6-well plates (5.0 μg per cm^2 of growth surface) and allowed to incubate (1h, RT). The remaining solution was aspirated before washing the flasks or plate wells with DPBS following aspiration. They were either ready to use or air dried (RT) with sterility maintained.

3.2.1.7 Preparation of steroid treatments

Corticosterone, 5αTHB or dexamethasone was dissolved separately in ethanol to make a stock (1 M). Solutions were stored in -20 °C. A series of dilutions of each steroid were prepared with ethanol.

3.2.2 Quantification of GFP-GR translocation in HEK293 cells

3.2.2.1 Transient transfection of GRs in HEK293 cells

HEK293 cells (see 3.2.2.2) were transiently transfected with plasmid DNAs of pGEM (Promega, Madison, US), pEGFP-N1 or pGFP-rGR (Prima, et al. 2000). pGEM (inert DNA, Promega) was transfected as a mock transfection which would not induce fluorescence in cells, and additionally to confirm the absence of fluorescent contamination formed from any reagent. pEGFP-N1 (N stands for N terminus, meaning that it is designed to fuse proteins to the N terminus of EGFP) transfection was used as positive control which would confirm the success of transfection and induce fluorescence in the whole cell including cytoplasm and nucleus, regardless of the position of GRs. All the plasmids were prepared from two batches to avoid false results caused by mutations during bacterial cloning.

The day before transfection, HEK293 cells were plated at a density of $2\text{-}3\times10^5$ cells per well in poly-d-lysine coated (see 3.2.1.6) six-well plates and incubated in the atmosphere of 95% air and 5% CO_2 at 37 °C overnight in normal-serum medium (2 ml per well). On the day of transfection when they were 80-90% confluent, cells were washed and cultured in antibiotic-free medium (2 ml per well) with stripped-serum for one hour prior to transfection.

For each well to be transfected, FuGENE HD transfection reagent (5 µl, Roche Applied Science, Indianapolis, IN, USA) was incubated (5 min, RT) in reduced-serum medium Opti-MEM (100 µL, GIBCO, Parsley, UK) in a microtube. Then the plasmid DNA, pGEM, pGFP-GR or pEGFP-N1 (2 µg each) was added respectively to the FuGENE/Opti-MEM mixture prior to incubation (15 min, RT). The entire volume of mixture was added to the corresponding wells, and then the cells were incubated under the same conditions as described above.

3.2.2.2 Observation and quantification of GFP-GR translocation in transiently transfected HEK293 cells

Twenty-four hours after transfection, HEK293 cells were first checked using fluorescent microscopy (Model: Axiovert 25, Carl Zeiss, Germany; objective, Zeiss LD Achrostigmat 40×/0.50 Ph2 Var2; ocular lens, E-Pl 10×/20) which was connected to a camera and a computer with the imaging programme MCID Basic 7.0 (Imaging Research Inc., Canada). Photos were taken prior to steroid treatment if transfection efficiency met requirements, i.e. fluorescence in the cells was bright enough to be visible and cells were not initially contaminated with steroid (this was noted as nuclear translocation without addition of steroid). Cells were then incubated with glucocorticoid or vehicle (ethanol only, 0.1-0.2% volume of medium). Three fields were chosen randomly per well and photos were taken at chosen time points. Cells were counted afterwards from the archived photographs.

All the fluorescent cells in the photographs were counted and recorded in a semi-quantitative manner (Galigniana, et al. 1998). Cells where the fluorescence in the nucleus was distinctly stronger than in the cytoplasm were recorded as nuclear-translocated cells. Where the fluorescence was equally strong in nucleus and cytoplasm, they were not included in the count of nuclear-translocated cells. The percentage of nuclear-translocated cells was consequently calculated. The experiments were performed in triplicate.

3.2.2.3 Time course study of GR translocation

HEK293 cells which had been successfully transfected with GFP-GR were incubated with 5αTHB, corticosterone, dexamethasone (1 μM each) or vehicle (ethanol, 2 μl). Photographs of fluorescent cells were taken at 15 min, 30 min, 2 h, 5 h and 24 h.

3.2.2.4 GR nuclear export

HEK293 cells were transfected with GFP-GR and first incubated with medium containing 5αTHB, corticosterone, dexamethasone (1 μM each) or vehicle (ethanol, 2 μl) for 24 hours. Then the culture medium containing the steroid treatment was aspirated, and cells were washed twice and replaced with fresh steroid-free medium. Photographs of fluorescent cells were taken at 30 min, 2 h, 5 h and 24 h after washing.

3.2.2.5 Dose response to corticosterone

GFP-GR transfected HEK293 cells were incubated with increasing concentrations of corticosterone (3, 10, 30, 100 nM), and photographs were taken at 15 min, 30 min, 2 h, 5 h and 24 h.

3.2.2.6 Co-incubation with corticosterone and 5αTHB

HEK293 cells transfected with GFP-GR were incubated with varying amounts of corticosterone (0.3, 1 or 3 nM) plus a higher concentration of 5αTHB (100, 300 nM or 1 μM). Cells were observed and photographs taken at 45min post transfection.

3.2.3 Fluorescence recovery after photobleaching (FRAP)

FRAP analysis allows measuring the mobility of the fluorescence-labelled proteins (e.g. GFP-GR) by confocol microscopy. In FRAP, a small area of living cell is beached, without damage to the protein, by a short laser pulse, and the fluorescence intensity in the bleached and nonbleached areas before and after bleaching is measured using time-lapse microscopy. Following the bleach, the fluorescence in the bleached area recovers immediately as a result of fast exchange of GFP-GR between

bleached and nonbleached areas. Subsequently, the fluorescence in the two areas becomes completely balanced. The recovery kinetics of GFP-GR is dependent on their mobility; immobile proteins show no recovery (Phair and Misteli 2001).

HEK293 cells were seeded and transfected in a 35 mm dish with a glass bottom (10 mm diameter) in the centre of the culture area (MatTek Corporation, MA, USA) in order to produce high-resolution microscopic images. Cells were incubated with 5αTHB or corticosterone (1 μM each) for 24 hours before FRAP analysis was performed while the dish was maintained warm on a hot plate (37 °C) stacked on top of the observation platform. Cells were observed by a Zeiss LSM 510 (Axiovert 100M) confocal laser scanning microscope, using a Plan-Neofluar 40× oil immersion objective (1.3 numeric aperture).

Cells were excited with an argon laser at 488 nm, and emission was collected using a 505 nm long-pass filter through a pinhole of 66 μm. Images were taken every 500 ms at a resolution of 512 by 512 pixels (45.0 by 45.0 μm). After the first image, a selected rectangular region of fixed size (90 by 15 pixels) in the nucleus was bleached at a set laser power of maximal 15.0 mW. Fluorescence intensity in either bleached or unbleached region in the nucleus was quantified at every 500 ms using LSM software. In each experiment, two dishes, including 20 cells in total, were analyzed per treatment.

The FRAP data curve was created from the data of fluorescence intensity. To correct for differences in expression level between individual cells, fluorescence data for the bleached region and unbleached region in the nucleus were normalized to the level before bleaching. In addition, at all time points data were normalized to the fluorescence in unbleached region in the nucleus in order to correct for the loss in fluorescence due to the bleach pulse and the imaging. Thus, in mathematical terms FRAP curves were created using the following equation:

$$F_t = (N_0 \cdot B_t) / (N_t \cdot B_0)$$

Where F_t is the normalized fluorescence at time point t; N_0 and N_t are the fluorescence in the non-bleached region in the nucleus at time points 0 and t, respectively, and B_0 and B_t are the fluorescence in the bleached region at time points 0 and t.

Subsequently, the normalized FRAP curve was plotted as a non-linear regression model using GraphPad Prism 4, described by the equation:

$$F_t = Fmax \times (1 - e^{-kt})$$

The half life ($t_{1/2}$) of maximal recovery was determined, which is defined as the time point after bleaching at which the normalized fluorescence has increased to half the amount of the maximal recovery.

$$t_{1/2} = \ln 0.5 / (-k) = 0.69 / k$$

3.2.4 Quantification of transcription by reporter assays

3.2.4.1 Transient transfection in Hela cells

Hela cells were transiently transfected with plasmids encoding rat GR and a reporter gene, MMTV-LTR-luciferase (Lefebvre, et al. 1991) or rPNMT-998/-466-luciferase (Adams, et al. 2003). The process of transfection was the same as described for HEK293 cells (see 3.2.2.1) except that: 1) Hela cells were seeded in non-coated six-well plates; 2) the volume of FuGENE HD transfection reagent used for Hela cells was 4μl; 3) the total amounts of plasmid DNAs transfected were 2.2 μg per transfection.

The components of each transfection were shown in Table 3.1. The transfection of pGEM (inert DNA) was the negative control; and pGL3-basic (Promega) was an empty vector control which was a luciferase reporter vector without promoter or enhancer. Simian virus (SV) 2-luc was a luciferase expression vector not requiring

induction by glucocorticoids, used as positive control (de Wet, et al. 1987) to confirm the success of each batch of transfection. When the luciferase activity of cells transfected with pSV2 was 500 times higher than that of pGL3-basic, the transfection was deemed successful. The plasmid DNA of pVL342 was designed to be representative as either rat or mouse GR; KC275 was a reporter gene of β-galactosidase used as internal control to normalize for transfection efficiency. These latter two plasmids were kind gifts from Karen Chapman (Centre for Cardiovascular Science, Queen's Medical Research Institute, the University of Edinburgh, UK). Each transfection was performed in triplicate, and the experiment was carried out in six replicates, on separate days assaying with two batches of plasmids.

Table 3.1 Components of each transfection.

Transfection / DNA (μg)	pGEM	pSV2	pGL3	MMTV-LTR	PNMT
pGEM	2.2	0.2	0.2	--	--
pSV2-luc	--	1	--	--	--
pGL3-basic	--	--	1	--	--
MMTV-LTR-luc	--	--	--	1	--
rPNMT-998/-466-luc	--	--	--	--	1
pVL342	--	--	--	0.2	0.2
KC275	--	1	1	1	1

3.2.4.2 Glucocorticoid treatment

One hour after transfection, cells were incubated for 48 h with corticosterone, 5αTHB (1 μM each) or vehicle (ethanol, 0.1% v/v) before being assayed for luciferase and β-galactosidase activity.

3.2.4.3 Luciferase assay

The luciferase activity of the samples from the transient transfection experiment was assayed by a Luciferase Assay System (Promega, UK).

3.2.4.3.1 Preparation of cell lysates

The 5× lysis buffer provided, containing Bicine buffer and Tween detergents, was diluted to 1×buffer in distilled water and equilibrated to RT before use. The growth medium from cells was removed, and then cells were rinsed carefully with PBS which was aspirated as much as possible after washing. The diluted lysis buffer (100 µl per well) was added and the culture plates rocked to ensure complete coverage of the cells with lysis buffer. The cells were then scraped from wells and transferred to an Eppendorf tube prior to centrifugation (12,000 g, 2 min, RT) to precipitate any remaining undissolved cell lysate. The transparent supernatant was used in subsequent assays of luciferase and β-galactosidase.

3.2.4.3.2 Luciferase assay

The reconstituted Luciferase Assay Reagent was prepared by adding the Luciferase Assay Buffer provided to the lyophilized Luciferase Assay Substrate (luciferin). The cell lysate (20 µl per well) was transferred to a 96-well plate (Nunclon Surface, Denmark). The plate was placed into a Microplate Luminometer (Orion II, Berthold Detection Systems GmbH, Germany), in which the Luciferase Assay Reagent (100 µl) was injected to each well. The reaction between the substrate luciferin and cosubstrate ATP Mg^{2+} was catalyzed by the firefly luciferase produced within the cells, forming the product of oxyluciferin. During the oxidation of luciferin, light was produced by converting the chemical energy derived from an electron transition. The luminescence from each well was read with a 2.05 sec delay after injection, and each measurement lasted for 10 sec. The values of luminescence were calculated by a computer programme, Simplicity 4.1 (Berthold Detection Systems, Germany). The light intensity was proportional to luciferin concentrations in the range of 10^{-20} to 10^{-30} moles, according to the manufacturer's instruction. Assays were performed in singlicate.

3.2.4.4 β-Galactosidase assay

β-Galactosidase was used in conjunction with luciferase reporter genes to normalize for transfection efficiency. The activity of the β-galactosidase was determined by a chemiluminescent assay using Galacto-Light Plus (Applied Biosystems, UK) which provides the chemiluminescent substrate for β-galactosidase.

When the cell lysates were ready and the reagents provided had been equilibrated (RT), Galacton-Plus substrate diluent (67 µl, 1% v/v in the Reaction Buffer Diluent) was added to a 96-well plate (Nunclon Surface). The cell lysate (10 µl) was added, and the plate was allowed to incubate (15-60 min, RT) prior to measurement of the luminescence using the Orion II Microplate Luminometer, by which the Light Emission Accelerator (105 µl, light emission triggering solution with luminescence enhancer) was injected into each well. The luminescence was read immediately after injection, and each measurement lasted for 5 sec. Luminescence values were calculated by the programme, Simplicity 4.1 (Berthold Detection Systems). Assays were performed in singlicate.

3.2.4.5 Data analysis

Data for the transient transfection study were analysed using the raw data of luminescent intensity of luciferase assay and β-galactosidase assay. The values of the luciferase activity and β-galactosidase activity were the mean of triplicates of the experimental values, followed by subtraction of the corresponding mean values of the background that were produced by transfections with pGEM only. The resultant luciferase activity was normalized against the associated β-galactosidase activity.

3.2.5 Investigation of transactivation effects of 5αTHB in H4IIE cells

3.2.5.1 Time Course of transactivation of GR responsive genes in H4IIE cells incubated in culture medium with stripped serum

H4IIE cells were incubated in six-well plates with the presence of 5αTHB, corticosterone (1 μM each) or vehicle (ethanol, 2 μl) for 0, 1, 2, 4, 8, 16 and 24 h. The incubation was performed in the medium (2ml per well) with stripped serum. Total RNAs were extracted (see 2.5.1.1) and the transcript abundance of glucocorticoid responsive genes TAT and PEPCK were quantified by real-time PCR (see 2.5.5). Their transcript abundances were normalized to that of cyclophilin.

3.2.5.2 Time course of transactivation of GR responsive genes in H4IIE cells incubated in normal-serum medium

H4IIE cells were incubated in normal culture medium (2 ml per well) with the addition of the same glucocorticoid or vehicle treatment and processed as above (see 3.2.5.1) for 0, 2, 4, 8, 16 and 24h.

3.2.5.3 Dose response of induction of GR responsive genes in H4IIE cells incubated in normal-serum medium

H4IIE cells were incubated in normal-serum medium (2 ml per well) with varying concentrations (3, 10, 30, 100, 300, 1000nM) of 5αTHB or corticosterone or with vehicle (ethanol, 2 μl) for 16 h. The transcript abundance of TAT mRNA was quantified as above (see 3.2.5.1).

3.2.6 Investigation of the transrepression of GR responsive genes by 5αTHB in AtT20 cells

AtT20 cells are a mouse corticotroph pituitary tumor cell line, which expresses POMC, the precursor to ACTH and endorphins, before they are secreted. In these

cells, processing of POMC is suppressed by glucocorticoids (Ooi, et al. 2004), and the secretion of ACTH may be stimulated by CRH (Aoki, et al. 1997).

The cells were seeded in six-well plates with normal medium (2 ml per well) two days before the glucocorticoid treatment. Then the medium was removed and replaced with the stripped-serum medium (2 ml per well). One hour later, cells were given one of eight treatments, which were 5αTHB, corticosterone, dexamethasone (1 μM each) or vehicle (ethanol, 0.01%) alone and the same treatments with CRH (100 nM). Cells were incubated for 48 h and performed in triplicate. Thereafter the transcript abundance of POMC and CRH receptor 1 was quantified by real-time PCR (see 2.5.5). The experiment was replicated six times.

3.2.7 Effects of 5αTHB on cytokine release by transactivation and transrepression mechanisms in bone marrow derived macrophages (BMDMØs)

3.2.7.1 Bone marrow preparation and macrophage culture

C57BL/6 mice (25 g, 8 weeks old) were acclimatised to housing as described in 2.3.1 for one week before being euthanized by CO_2. Femurs with half hipbone and half tibiae attached were removed and immersed in Hank's balanced salt solution (Lonza). The following procedures were performed inside a Class II biosafety cabinet. The femur was separated from the attached bones and surrounding muscle by scraping with a scalpel and rubbing with bactericidal disinfectant wipes (Premier®, Shermond, Brighton, England; fluid containing ethanol (70% v/v) and chlorhexidine digluconate (1% w/v)), and wetting with a few drops of ethanol (70% v/v) for disinfection. Both ends of the femur were cut off with a scalpel and the marrow flushed with L929 conditioned medium (LCM, 10 ml) into a 60 ml Teflon pot (Roland Vetter Laborbedarf OHG, Germany) using a syringe adapted with a 25 Gauge needle (BD Microlance 3, Spain). LCM consisted of L929 culture medium (20% v/v) (Hosoe, et al. 1989) and DMEM/F12 medium (80% v/v) supplemented with 10% FBS, L-glutamine (200 mM), penicillin (100 U/ml) and streptomycin (100 mg/ml). Marrow

cell clusters within the suspension were dissociated by vigorous pipetting using the syringe adapted with a 21 Gauge needle. After addition of another 20 ml of the LCM, the marrow cells were incubated at 37 °C in a humidified atmosphere of 95% air and 5% CO_2. During incubation, the culture medium was changed twice (every second day) by removing half of the old medium (15 ml) and replacing with the fresh LCM medium (15 ml).

After six days incubation in the Teflon pots, the matured macrophages were resuspended in the pots by pipetting and then transferred into a 50 ml-tube (CellStar, Greiner Labortechnik, Germany) prior to centrifugation (220 g, 5 min, RT). Cells were then resuspended in fresh LCM (1 ml per well) and placed in 12-well plates at a density of 5×10^5 cell/ml per well, and incubated at 37°C for 16-24 hours before use.

3.2.7.2 LPS activation of the BMDMØs

When desired, the culture medium in the 12-well plates of the macrophages was replaced by the fresh LCM containing stripped-serum. Then the macrophages were primed for 1h with dexamethasone, corticosterone, 5αDHB, 5αTHB (1 μM each) or vehicle (ethanol, 0.01% v/v), and then incubated with LPS (100 ng/ml) for 24h. Each treatment was performed in triplicate. Thereafter the supernatant was removed and centrifuged (350 g, 5 min, RT) to remove dead cells that form pellets followed by another centrifugation (10,000 g, 5 min, RT). Samples were stored at -80°C until required for the quantification of cytokines using CBA (see 2.6.6).

3.2.7.3 Dose response of glucocorticoid effects on the release of cytokines stimulated by LPS

BMDMØs were primed for 1h by corticosterone or 5αTHB (3, 10, 30, 100, 300 and 1000 nM) or vehicle (ethanol, 0.01% v/v) before they were stimulated by LPS (10 or 100 ng/ml) for another 24 h. Each treatment was performed in triplicate. Then the supernatant was clarified and samples assayed using the same procedures described as above (see 3.2.7.2).

3.2.8 Statistics

Data are presented as mean ± SEM and were analysed by Student's t test, or one-way, two-way ANOVA, or repeated measures ANOVA, followed by Holm-Sidak post-hoc test where appropriate.

3.3 Results:

3.3.1 Investigation of the effects of 5αTHB on GFP-GR translocation in transiently transfected HEK293 cells

3.3.1.1 Controls for transfection

HEK293 cells transfected with plasmid DNA pGEM (inert DNA) did not induce fluorescence within cells, confirming the absence of fluorescent contamination from any reagent. The transfection of pEGFP-N1 as a positive control confirmed the success of transfection and induced fluorescence to the whole cell including cytoplasm and nucleus, regardless of the position of GRs. Non-transfected cells in the pEGFP-N1 transfection remained dark (Figure 3.1).

3.3.1.2 Time course study of GR translocation

GRs shuttle between the cytoplasm and the nucleus, dependent on their association with glucocorticoids. This dynamic performance can be observed under a fluorescent microscope in HEK293 cells transfected with GFP-GR.

Without the addition of glucocorticoids, the fluorescent GRs were distinctly excluded from nuclei of cells (see Figure 3.2, vehicle). Incubation for up to 24 h with 0.1% ethanol (vehicle) did not affect the localization of GRs or stability of transfection. However particular care had to be taken to maintain cleanliness of incubators to ensure a "glucocorticoid-free environment".

When glucocorticoids were added to the medium, GRs were activated and started to translocate into the nucleus. With the addition of dexamethasone (1 μM), GR translocation was complete within 15 min (Figure 3.3). Similarly, corticosterone (1 μM) induced translocation of GRs into the nucleus within 30 min (Figure 3.4). In both cases, GRs remained exclusively in the nucleus for periods up to 24 h, and the cytoplasm was ultimately clear of fluorescence.

With the addition of 5αTHB (1 μM), the process of GR translocation was much slower and incomplete (Figure 3.5). Nuclear localization of GRs was not observed until 2 hours after the treatment of 5αTHB, with both nucleus localization and nucleus exclusion of GRs observed in some cells throughout the course of observation up to 24 hours. Nuclear translocation induced by 5αTHB was incomplete as faint but visible cytoplasm could be observed.

The difference in efficacy between the glucocorticoid treatments was quantified as the percentage of cells demonstrating nuclear localisation of GFP-GR. Corticosterone and dexamethasone were effective in inducing rapid and complete translocation of GRs (Figure 3.6). 5αTHB mimicked the effect but in a much slower and less efficient manner as described above. After incubation for 24 hours, only 82.7±1.5% of cells showed nuclear localization.

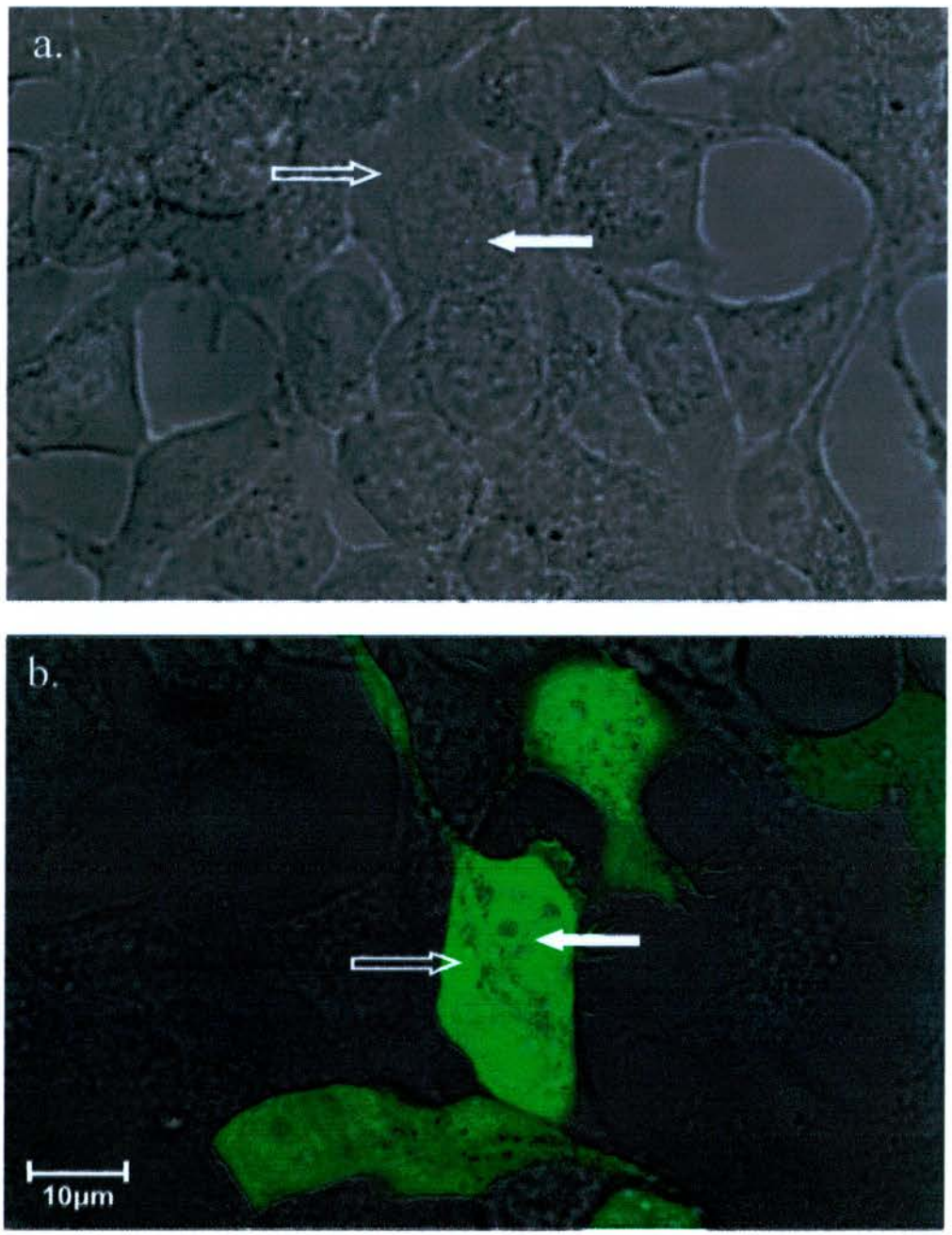

Figure 3.1 Controls for transfection in HEK293 cells. Cells were transfected with (a) pGEM or (b) pEGFP-N1 (2 μg each). pGEM was transfected as mock transfection, which did not induce fluorescence within cells. pEGFP-N1 transfection was used as positive control which induced fluorescence in both cytoplasm (open arrows) and nucleus (solid arrows).

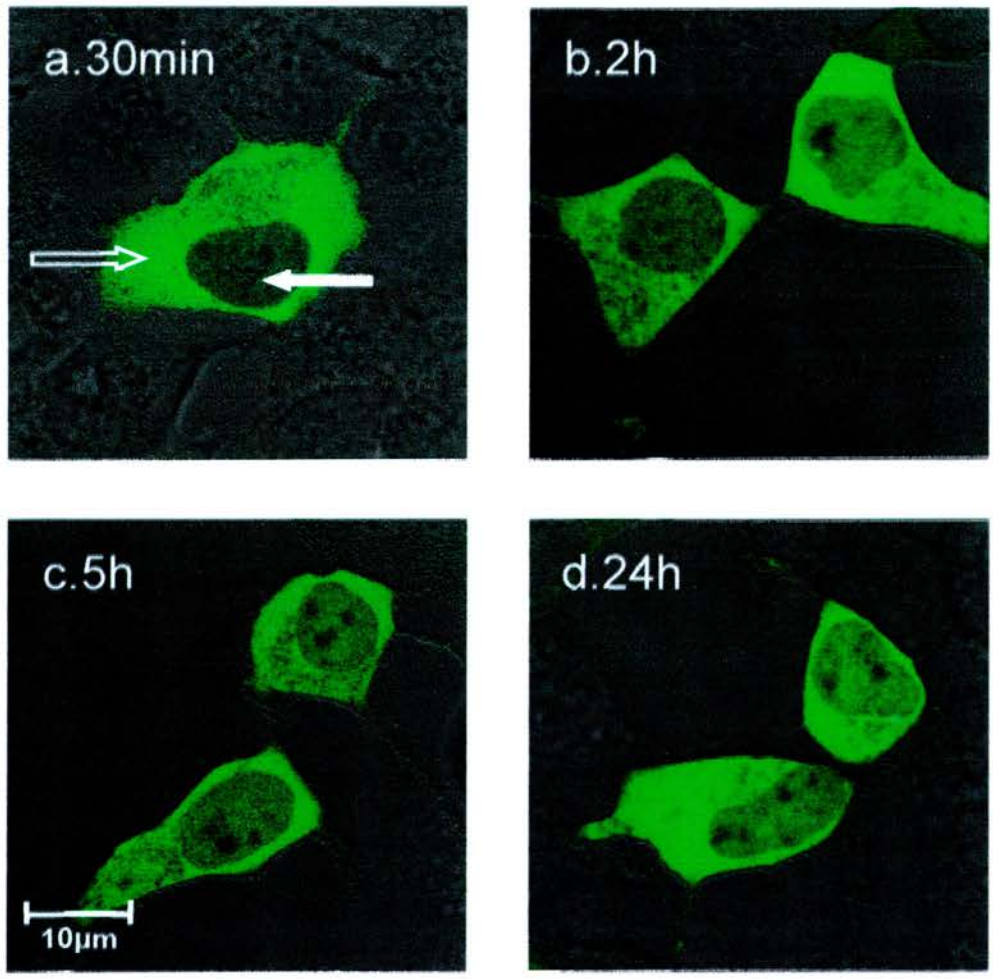

Figure 3.2 GFP-GR stayed in cytoplasm without presence of steroids. HEK293 cells were transfected with GFP-GR (2 μg) and incubated with vehicle (0.1% ethanol) for (a) 30 min; (b) 2 h; (c) 5 h or (d) 24 h. Fluorescent GRs were in cytoplasm (open arrow) excluded from nucleus (solid arrow). Incubation for up to 24 h with vehicle treatment did not affect the localization of GRs or stability of transfection.

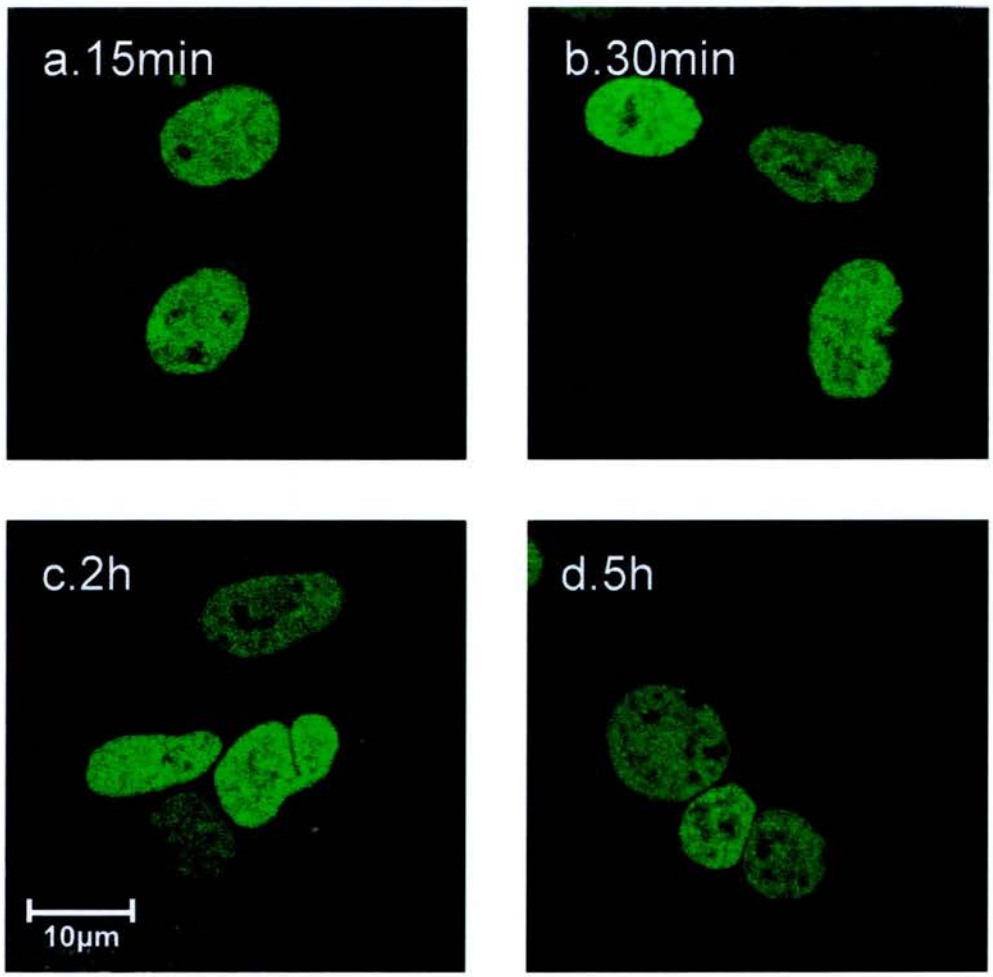

Figure 3.3 Time course of GR translocation induced by dexamethasone (Dex). HEK293 cells were transfected with GFP-GR (2 μg) and incubated with Dex (1 μM) for (a) 15 min; (b) 30 min; (c) 2 h or (d) 5 h. Dex induced complete translocation of GRs within 15 min. Thereafter, GRs remained exclusively in the nucleus (solid arrow) for up to 24 h.

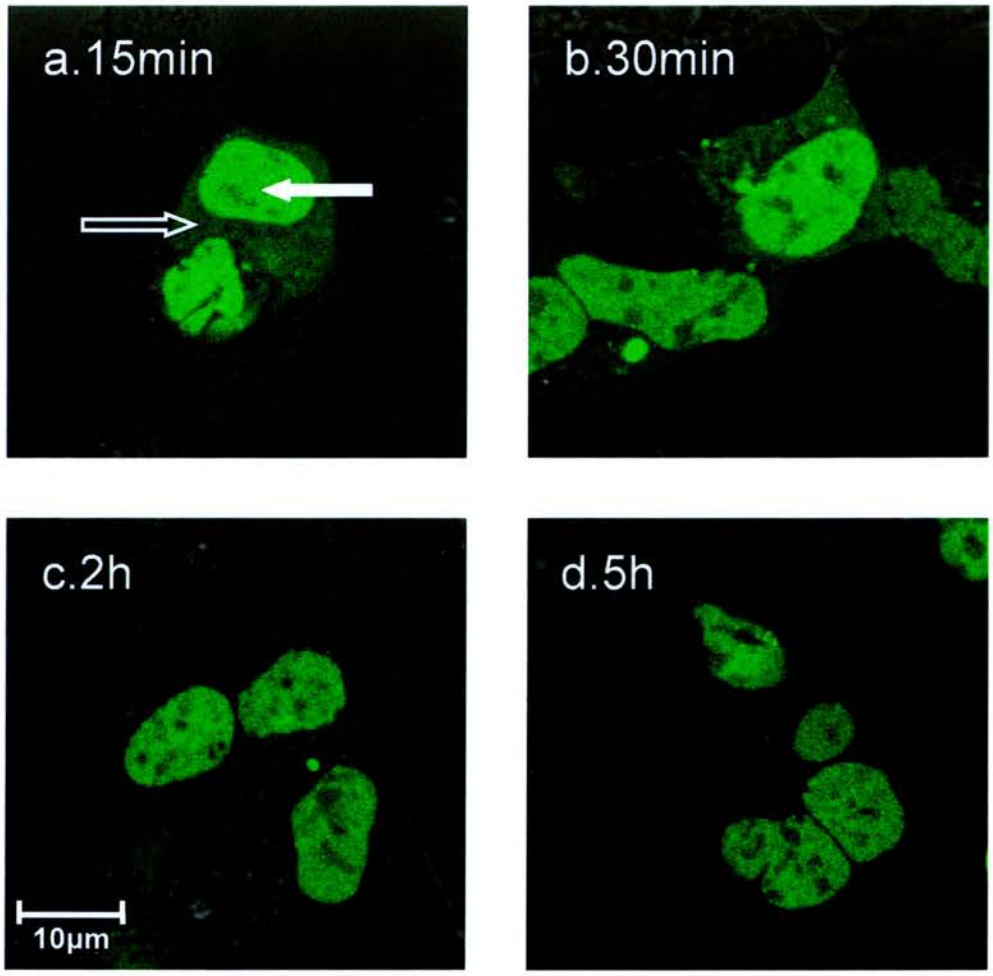

Figure 3.4 Time course of GR translocation induced by corticosterone. HEK293 cells were transfected with GFP-GR (2 μg) and incubated with corticosterone (B, 1 μM) for (a) 15 min; (b) 30 min; (c) 2 h or (d) 5 h. Translocation of GRs by B was evident within 15 min, but not complete until 30 min. GRs remained exclusively in the nucleus (solid arrow) thereafter until 24 h. Open arrow indicates cytoplasm.

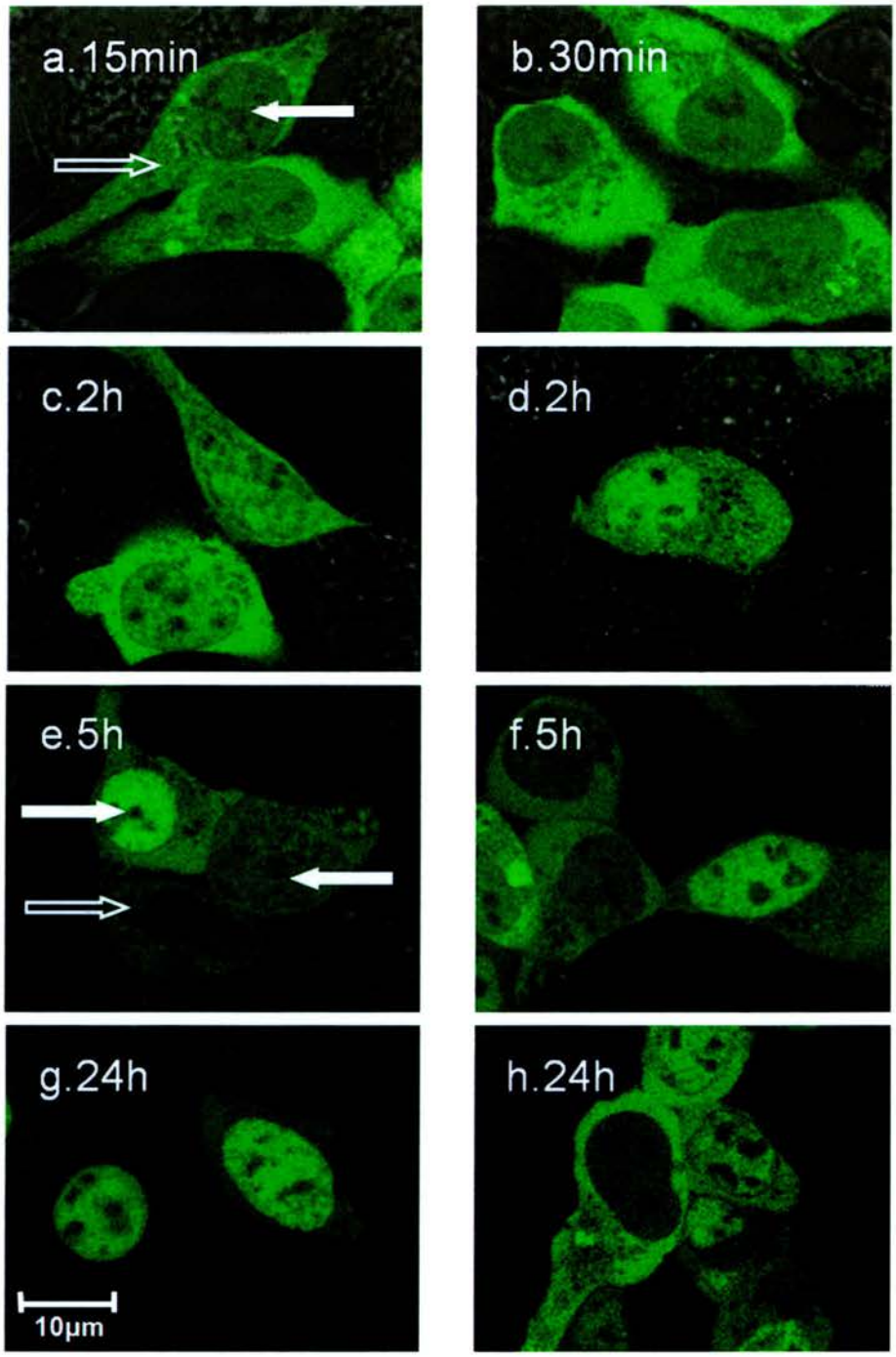

Figure 3.5 Time course of GR translocation induced by 5αTHB. HEK293 cells were transfected with GFP-GR (2 μg) and incubated with 5αTHB (1 μM) for (a) 15 min; (b) 30 min; (c, d) 2 h; (e, f) 5 h or (g, h) 24 h. Most GRs did not move into the nucleus in the first 30min after treatment (a, b). Partial GR translocation was observed up until 2 h but to a variable degree. Maximal extent of translocation was observed within 5 h but this was not complete, even after 24 h, with cytoplasmic fluorescence still evident. Nuclear (solid arrow) translocation induced by 5αTHB was incomplete as faint but visible figure of cytoplasm (open arrow) could be observed.

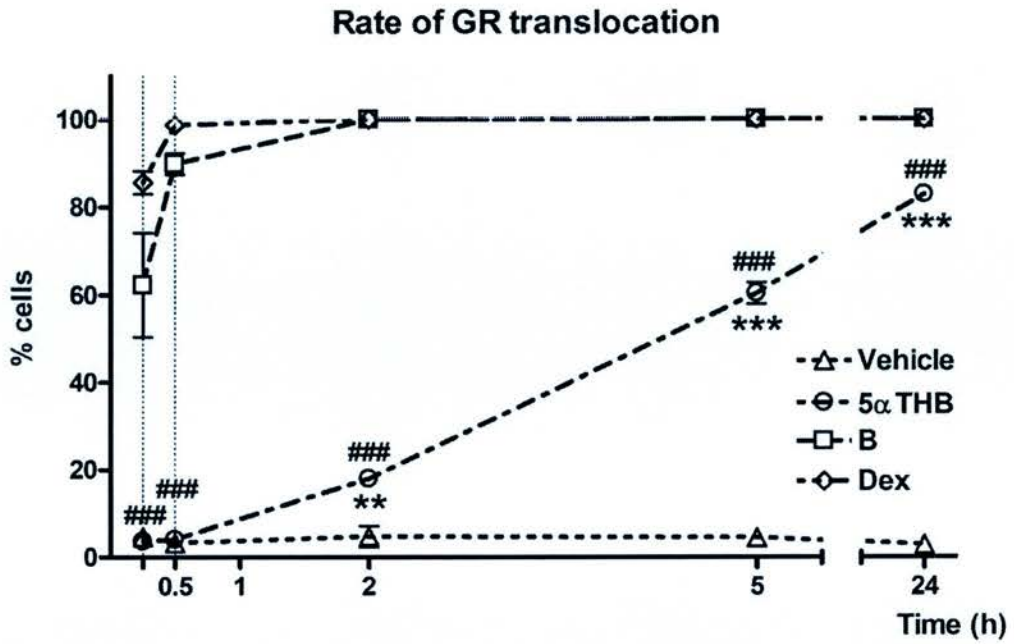

Treatment, p<0.0001; Time, p<0.0001; Interaction, p<0.0001.

Figure 3.6 Rate of GR translocation. HEK293 cells were transfected with GFP-GR and incubated with 1 μM of either 5αTHB, B or Dex or with vehicle (ethanol). Cells were observed under a fluorescent microscope and translocation counted in three fields per well at 15 min, 30 min, 2 h, 5 h and 24 h. Data were plotted as the percentage of cells observed with nuclear translocation of GRs. 5αTHB only started to exert its effect of translocation after 2h when nuclear translocation induced by Dex or B was already complete. After 24 h incubation, nuclear localization was only observed in 82.7±1.5% of cells in the presence of 5αTHB. Data are mean ± SEM of three experiments with triplicate measurements at every time point for each experiment. **p<0.01, ***p<0.001 versus vehicle; ###p<0.001 versus B, analyzed for the effect of 5αTHB by two-way repeated measures ANOVA (one factor repetition) with Holm-Sidak post-hoc tests.

3.3.1.3 GR nuclear export

After the medium was replaced (see Figure 3.7), GRs in the 5αTHB-treated cells started to move out of nucleus into cytoplasm. Five hours later, the number of the cells with nuclear localisation induced by 5αTHB decreased from a maximum of 82.0±2.3% to 45.6±2.9% post- medium replacement. After 24 hours, only 32.1±6.1% cells had more GRs in nucleus than in cytoplasm. Unlike 5αTHB, dexamethasone and corticosterone (1 μM) maintained GRs exclusively in nucleus over 24 hours, despite replacement of medium.

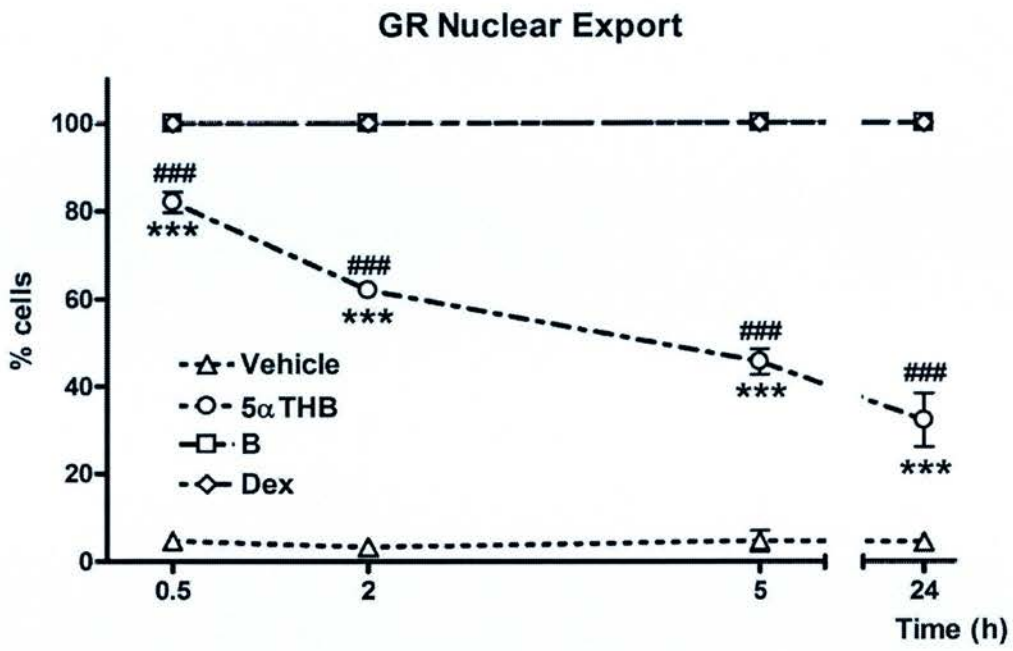

Treatment, p<0.0001; Time, p<0.0001; Interaction, p<0.0001.

Figure 3.7 GR nuclear export. HEK293 cells transfected with pGFP-GR were incubated with 1 μM of 5αTHB, B, Dex or vehicle (ethanol) for 24 h before the culture medium was washed away and replaced with steroid-free medium; thereafter the changes of GR localization were recorded and plotted as percentage of GR translocated cells at 30 min, 2 h, 5 h and 24 h post-medium replacement. GR was maintained in the nucleus in cells treated with Dex and B but not in those treated with 5αTHB. GRs in the 5αTHB treated cells started to move out of nucleus slowly into the cytoplasm, leaving only 32.1±6.1% of cells with more GRs in nucleus than in cytoplasm at 24 h. Data are mean ± SEM of three experiments with triplicate measurements at every time point for each experiment. ***p<0.001 versus vehicle, ###p<0.001 versus B, analyzed for effect of 5αTHB by two-way repeated measures ANOVA (one factor repetition) with Holm-Sidak post-hoc test.

3.3.1.4 Dose response to corticosterone

Rat GR has a higher affinity for dexamethasone and corticosterone than 5αTHB. A study of the time and concentration-dependent effects of corticosterone on GR translocation was undertaken to establish the relative potency of 5αTHB (see Figure 3.8).

The efficacy could be compared at 30 min when the velocity of GR translocation increased with the concentration of corticosterone (Figure 3.9) and was sub-maximal. GRs were translocated into nucleus to 7.2±1.2%, 66.4±3.6% and 77.9±0.8% by concentrations of corticosterone of 10, 30 and 100 nM, respectively, at 30 min. GR demonstrated nuclear-localization at 2 h which remained until 24 h, as shown in Figure 3.9, except for those incubated with 3 nM.

With the presence of 3 nM of corticosterone, GR translocation could not be observed within 30 min, similarly to 5αTHB (1 μM). The percentage of cells with GR translocation increased dramatically from 30 min to 2 h to 85.1±0.5%, and continued to increase slowly to the maximum of 90.8±0.8% at 5 h (Figure 3.10). Between 5 h to 24 h, GRs moved out of nucleus, leaving 40.6±0.4% of cells with nuclear localisation of GR at 24 h (Figure 3.8), similar to 5αTHB (1μM).

Therefore, for further studies, investigating synergism or additive effects on GR translocation by 5αTHB in the presence of corticosterone, corticosterone concentrations were maintained at lower than 3 nM, to avoid maximal stimulation and incubations performed for 45 min.

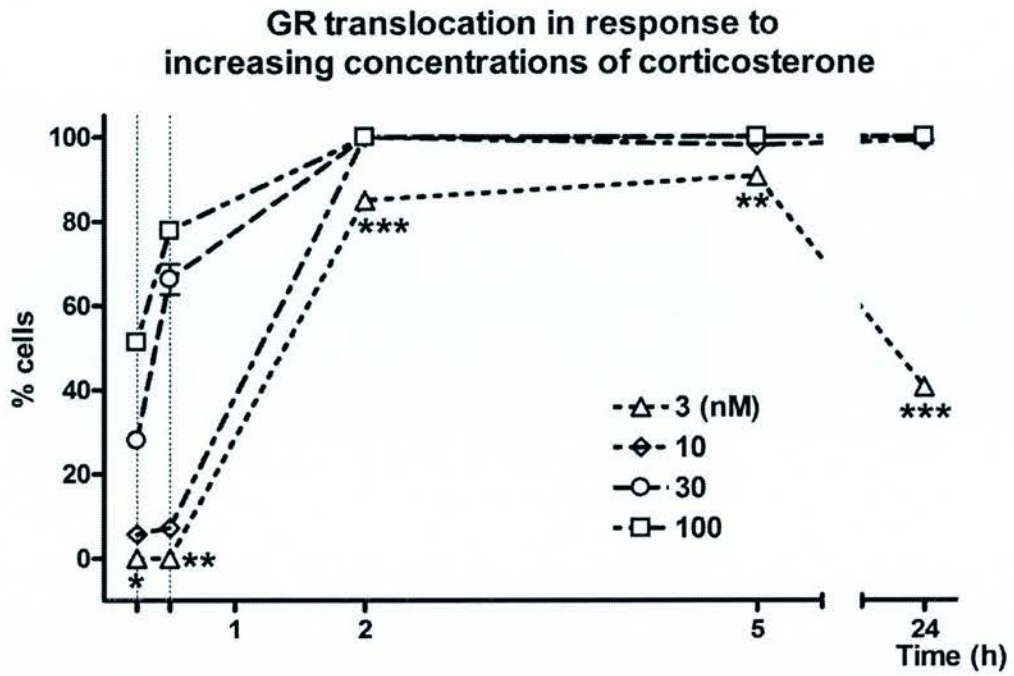

Treatment, p<0.0001; Time, p<0.0001; Interaction, p<0.0001.

Figure 3.8 GR translocation in response to increasing concentrations of B. pGFP-GR transfected HEK293 cells were incubated with 3, 10, 30 or 100 nM of B. Cells were observed under fluorescent microscope and counted from three fields per well at 15 min, 30 min, 2 h, 5 h and 24 h. Data were plotted as the percentage of cells observed with nuclear translocation of GRs. The velocity of GR translocation increased with the concentration of B. Concentrations of B of 10 nM and higher could induce translocation of GRs to the nucleus in all the cells by 2 h and maintain them there over 24 h. However, in the presence of 3 nM of B, GR translocation was only observed in 85.1±0.5% of cells at 2 h and 90.8±0.8% at 5 h, and GRs moved out of the nucleus at 24 h, leaving 40.6±0.4% of cells with nuclear localisation of signal. Data are mean ± SEM of three experiments with triplicate measurements at every time point for each experiment. *p<0.05, **p<0.01, ***p<0.001 versus 10 nM, analyzed by two-way repeated measures ANOVA (one factor repetition) with Holm-Sidak post-hoc test.

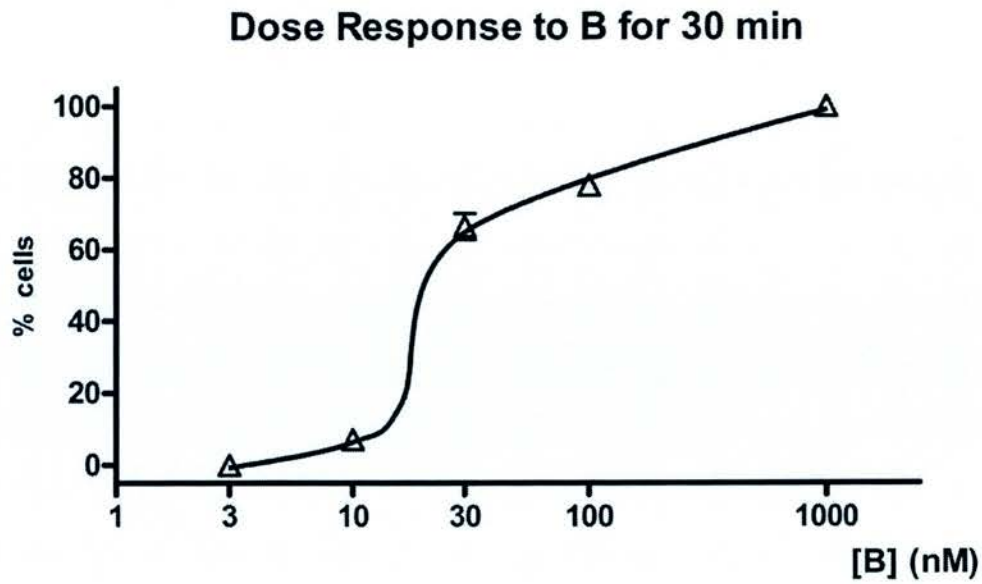

Figure 3.9 Log dose response curve of B to induce GR translocation in the GFP-GR transfected HEK293 cells. Cells were observed under fluorescent microscope and counted from three fields per well at 30 min. The percentage of cells showing GR translocation increased with the concentrations of B (3, 10, 30, 100 and 1000 nM). Data are mean ± SEM, n=3, triplicates.

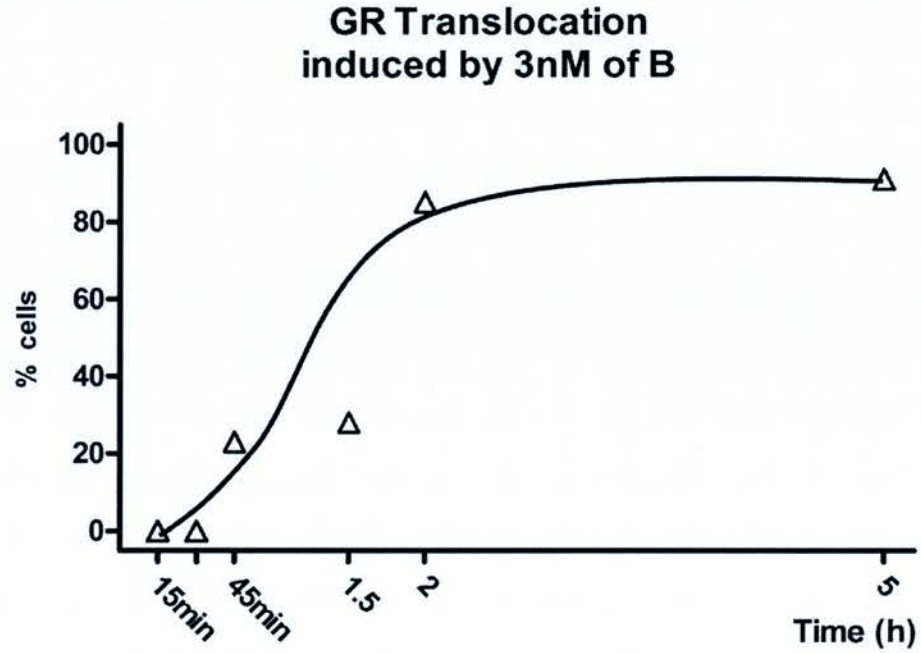

Figure 3.10 The time course curve of GR translocation induced by 3 nM of corticosterone over 5 h in GFP-GR transfected cells. Cells were observed under fluorescent microscope and counted from 3 fields per well at 15 min, 30 min, 45 min, 2 h, 5 h and 24 h. From 45 min to 1.5 h, approximately a quarter of the cells transfected with GFP-GR demonstrated nuclear localization. Half an hour later, % cells showing GRs translocated cells increased dramatically to a higher plateau from 2 h to 5 h. Data are mean ± SEM, n=3, triplicates.

3.3.1.5 Co-incubation with corticosterone and 5αTHB

Since the progress of GR translocation induced by 3 nM of corticosterone was submaximal between 45 min to 1.5 h, and the translocation by 1 μM of 5αTHB was not evident until 2 h, a co-incubation of a small amount of corticosterone (0.3, 1 or 3 nM) with higher dose of 5αTHB (100, 300 or 1000 nM) was performed to determine whether synergistic or additive effects exist (Figure 3.11).

Without the addition of corticosterone in any dose, GRs remained nuclearly excluded at 45 min, as described before. With corticosterone alone, GR translocation started to be observed only with a concentration of 3 nM at this time point. With the presence of both corticosterone and 5αTHB, their effects on GR translocation were synergistically magnified. The co-incubation with 5αTHB and corticosterone accelerated the process of translocation.

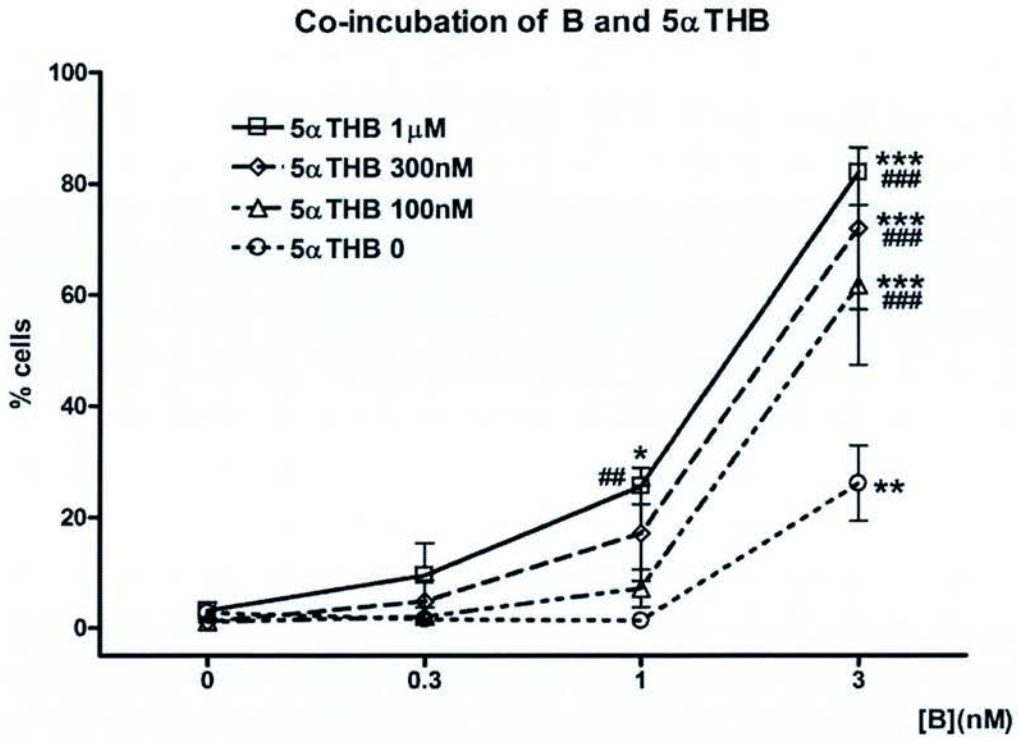

Figure 3.11 GFP-GR translocation induced by co-incubation of B and 5αTHB. GFP-GR transfected HEK293 cells were co-incubated with corticosterone (0, 0.3, 1, or 3 nM) and 5αTHB (0, 100, 300 nM or 1 μM) for 45 min. Cells were observed under fluorescent microscope and counted from 3 fields per well. Data were plotted as the percentage of GR translocated cells. The co-incubation with 5αTHB and corticosterone accelerated the process of translocation. Their combined effects on GR translocation were synergistically magnified. Data are mean ± SEM, n=3, triplicates. *p<0.05, **p<0.01, ***p<0.001 versus [B]=0; ##p<0.01, ###p<0.001 versus [5αTHB]=0; analyzed by two-way repeated measures ANOVA with Holm-Sidak post-hoc test.

3.3.1.6 FRAP analysis of GFP-GR

FRAP was applied to quantitatively assess the mobility of GFP-GR within the nucleus of HEK293 cells after the translocation induced by corticosterone and 5αTHB (Figure 3.12-13). The difference of half-life of maximal recovery ($t_{1/2}$) in the FRAP analysis between corticosterone and 5αTHB suggested that corticosterone decreased the mobility of GFP-GR to a greater extent than 5αTHB. However maximal recovery did not differ following addition of both steroids (Figure 3.14).

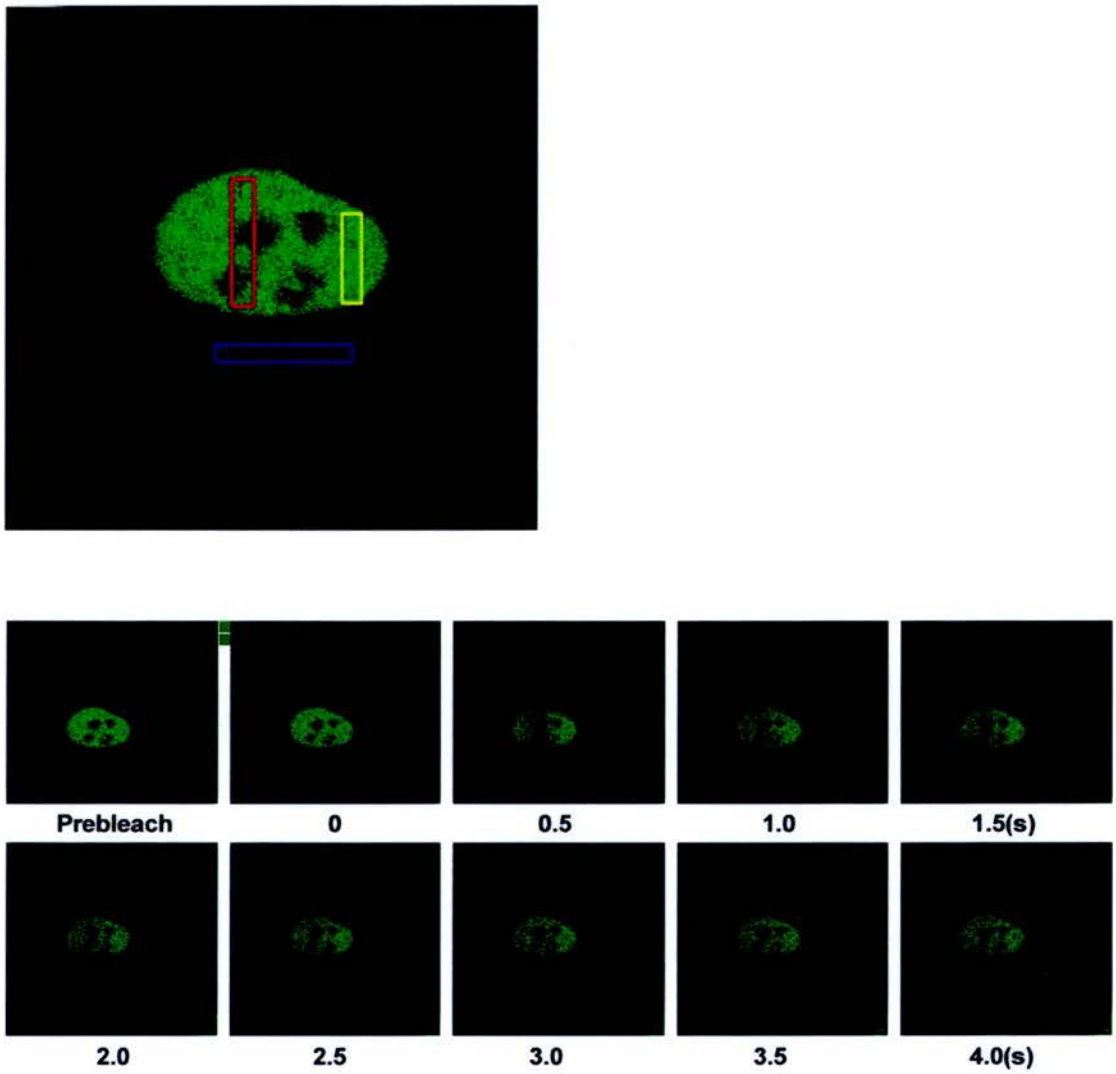

Figure 3.12 Cells undergoing FRAP analysis of nuclear GFP-GR. HEK293 cells were transfected with GFP-GR and incubated with corticosterone (1 μM) for 24 h. A small area of the cell (red rectangular area) was bleached and fluorescence started to recover immediately as a result of the mobility of GR protein. The background (blue area) was also detected as control. Fluorescence intensity in either bleached (red area) or unbleached region (represented by the yellow area) was quantified at every 500 ms.

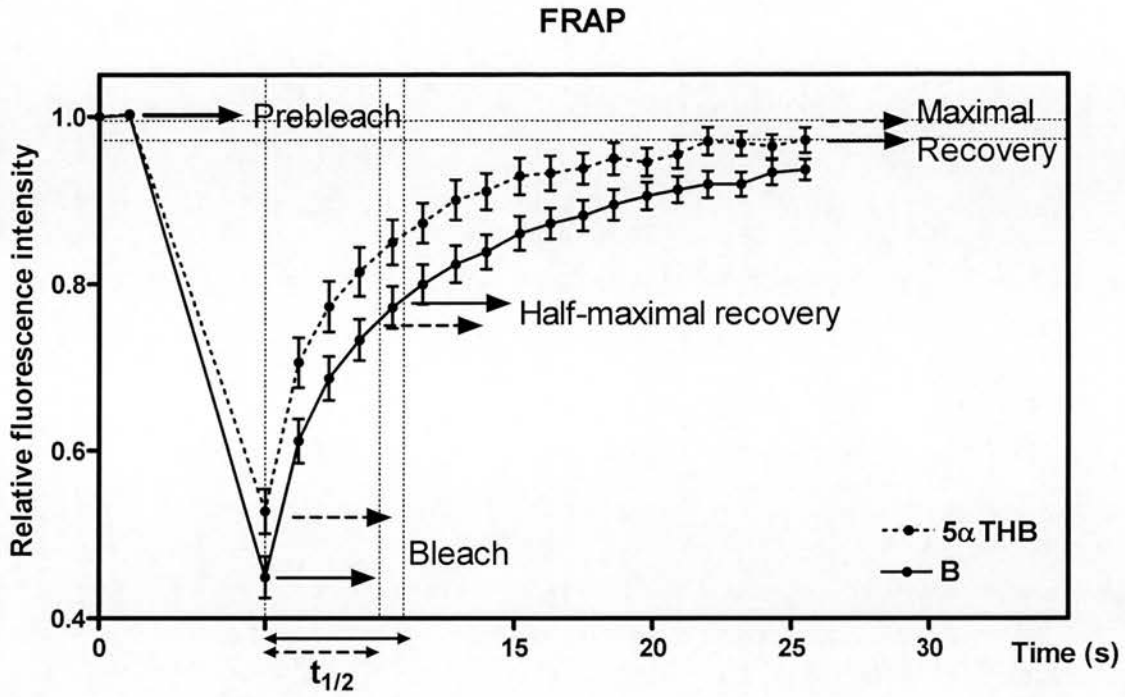

Figure 3.13 Schematic superimposed on experimental data to demonstrate FRAP analysis of GFP-GR. HEK293 cells were transfected with GFP-GR and incubated with corticosterone (solid line and arrows) or 5αTHB (dotted line and arrows; 1 μM each) for 24 h. Fluorescence in bleached area was corrected for the change in non-bleached area. $t_{1/2}$ was determined, which is the time when the fluorescence reached half of the maximal recovery.

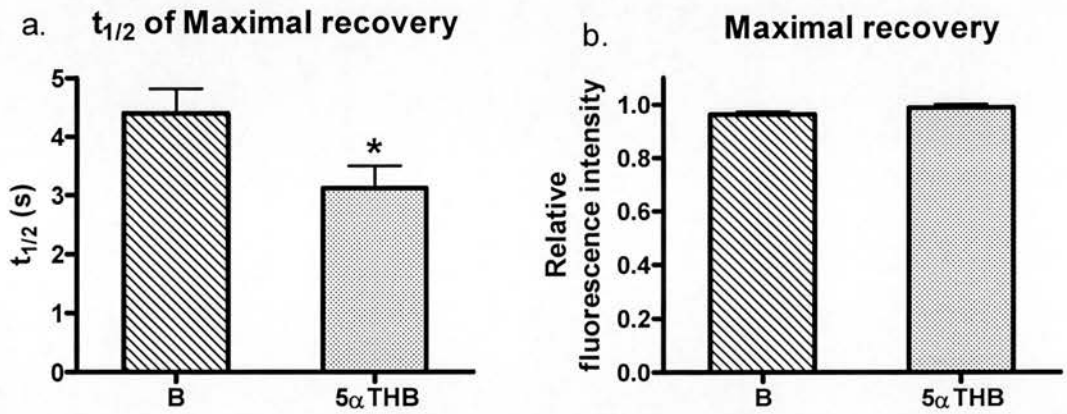

Figure 3.14 Maximal recovery in the FRAP analysis. Addition of B decreased the mobility of nuclear GFP-GR to a greater extent than 5αTHB (a). The maximal recovery was not different between treatments (b). HEK293 cells were transfected with GFP-GR and incubated with corticosterone or 5αTHB (1 μM) for 24 h. Fluorescence in bleached area was corrected for the change in non-bleached area. Three individual experiments were performed by analyzing 18-20 cells in total in each experimental group. Data are mean ± SEM, n=18-20, *$p<0.05$, analyzed by Student's *t* test.

3.3.2 Investigation of transactivation effects of 5αTHB in H4IIE cells

3.3.2.1 Time course of the transactivation effects in H4IIE cells incubated in culture medium with stripped serum

Corticosterone induced a time dependent increase in mRNA expression of TAT and also PEPCK although with less efficiency. However, 5αTHB did not significantly influence the transcript abundance of genes tested (Figure 3.15). The abundance of mRNA for the house-keeping gene, cyclophilin was not significantly changed by treatment ($p>0.05$).

3.3.2.3 Time course of the transactivation effects in H4IIE cells incubated in normal-serum medium

The same experiment was performed in normal medium with non-stripped serum, but once again 5αTHB did not increase the abundance of mRNAs of TAT or PEPCK (Figure 3.16).

3.3.2.4 Dose response of induction of GR responsive genes in H4IIE cells incubated in normal-serum medium

A dose response in TAT mRNA abundance was observed with corticosterone, with a significant increase starting from the dose of 30 nM of corticosterone, but no response was induced by 5αTHB (Figure 3.17).

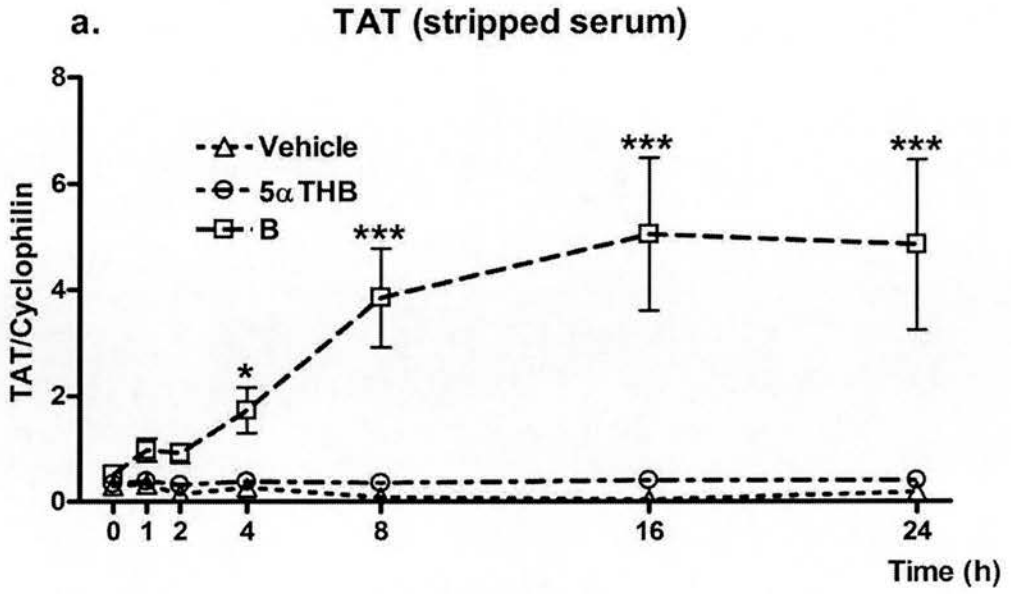

TAT: Treatment, p<0.001; Time, p<0.001; Interaction, p<0.001.

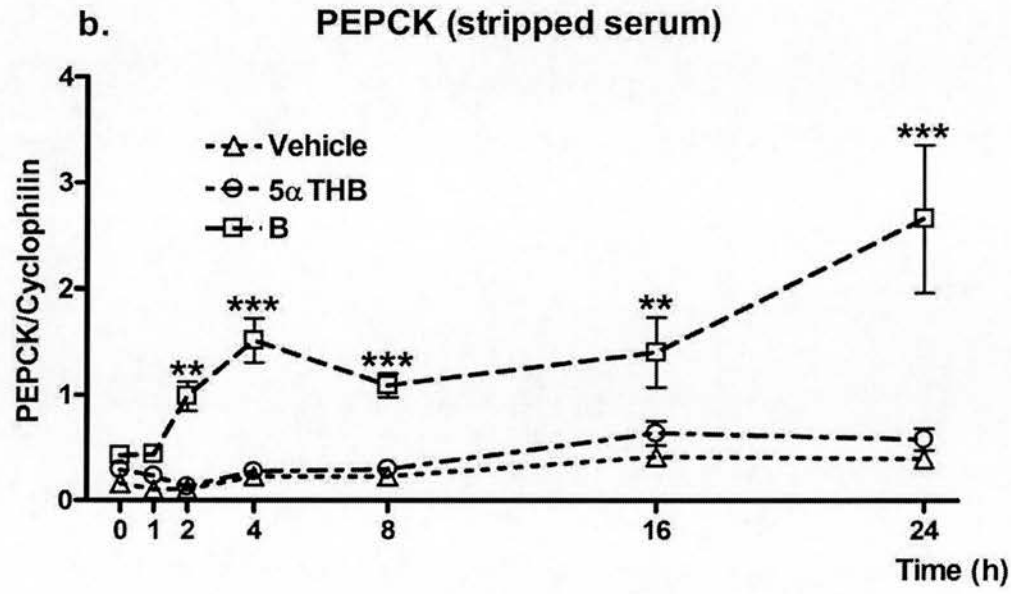

PEPCK: Treatment, p<0.001; Time, p<0.001; Interaction, p<0.001.

Figure 3.15 The abundance of mRNAs of (a) TAT and (b) PEPCK in H4IIE cells incubated in stripped-serum medium with the presence of 5αTHB, B (1μM each) or vehicle (ethanol) for 0, 1, 2, 4, 8, 16 and 24 h. The transcript abundance was quantified by real-time PCR and normalized for cyclophilin. B induced a time-dependent increase ($p<0.001$ vs. vehicle) in the abundance of mRNA of both genes however 5αTHB failed to stimulate the transcription. Data are mean ± SEM, n=6. *$p<0.05$, **$p<0.01$, ***$p\leq0.001$ versus vehicle, analyzed by two-way repeated measures ANOVA with Holm-Sidak post-hoc tests.

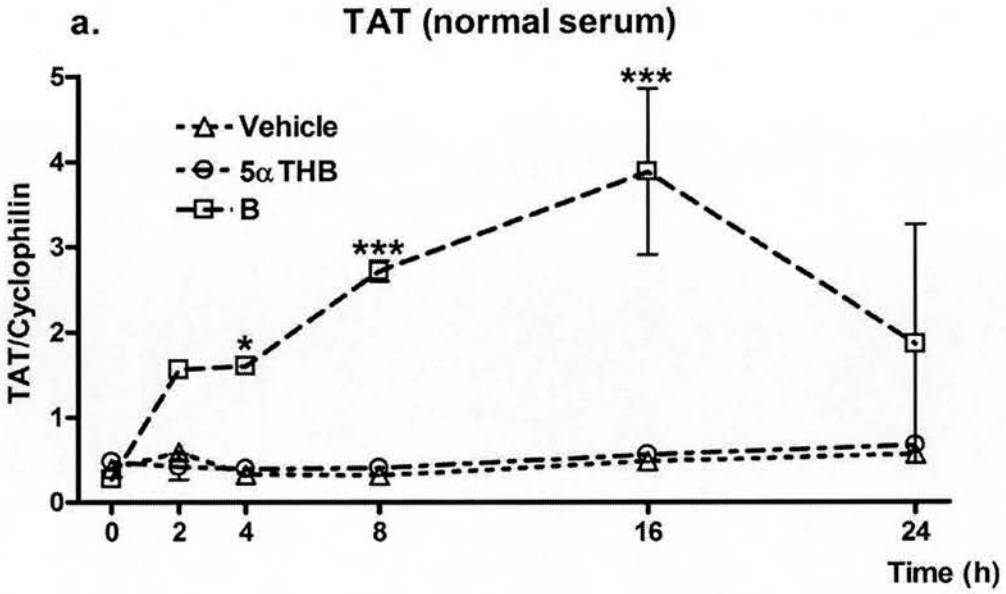

TAT: Treatment, p<0.001; Time, p=0.041; Interaction, p=0.027.

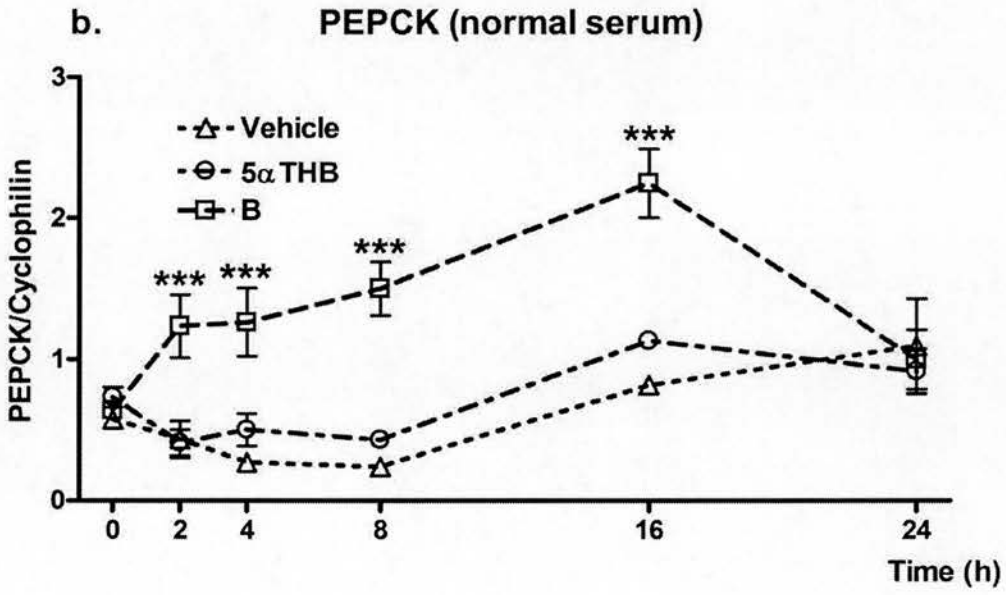

PEPCK: Treatment, p=0.002; Time, p<0.001; Interaction, p<0.001.

Figure 3.16 The abundance of mRNAs of (a) TAT and (b) PEPCK in H4IIE cells incubated in normal medium with the presence of 5αTHB, B (1 μM each) or vehicle (ethanol) for 0, 2, 4, 8, 16 and 24 h. The transcript abundance was quantified by real-time PCR and normalized for cyclophilin. B increased the transcript abundance of both genes whereas 5αTHB did not. Data are mean ± SEM, n=3. *p<0.05, **p<0.01, ***p≤0.001 versus vehicle, analyzed by two-way repeated measures ANOVA with Holm-Sidak post-hoc tests.

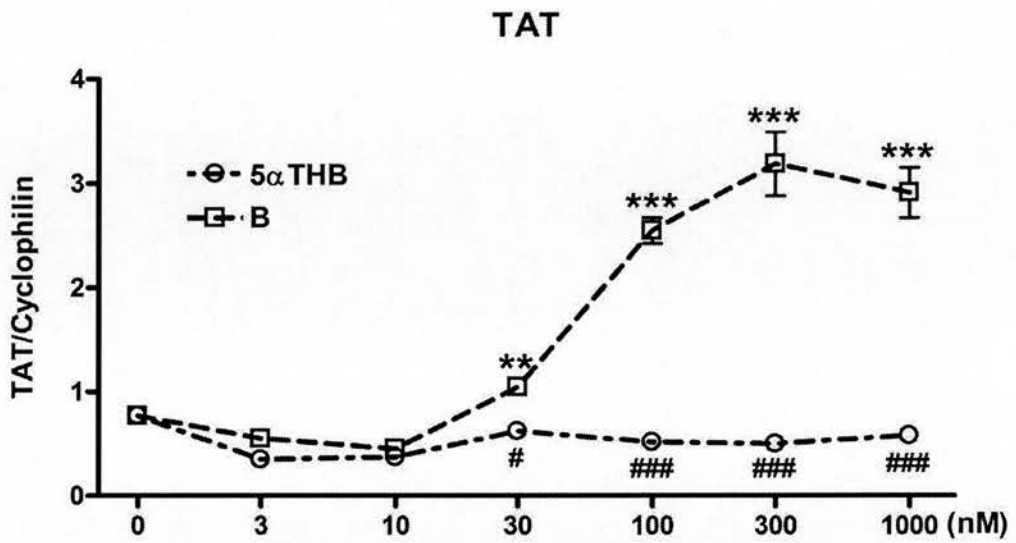

Treatment, p<0.001; Time, p<0.001; Interaction, p<0.001.

Figure 3.17 Induction of mRNA of TAT in H4IIE cells incubated in normal culture medium with different doses of 5αTHB or B (0 (ethanol), 3, 10, 30, 100, 300 and 1000 nM) over 16 h. A log dose response in TAT abundance was observed with B but not 5αTHB, with significant increase starting from the dose of 30 nM of B. Data are mean ± SEM, n=3, shown with logarithm X axis; **p<0.01, ***p<0.001 versus [steroid]=0; #p<0.05, ###p<0.001, 5αTHB versus B; analyzed by two-way repeated measures ANOVA (one factor repetition) with Holm-Sidak post-hoc tests.

3.3.3 Investigation of transactivation induced by 5αTHB in transiently transfected Hela cells

The expression of the reporter genes with promoters of MMTV and PNMT were stimulated by corticosterone (1 μM) and increased substantially by 30 to 40 fold. However, 5αTHB (1 μM) did not exert a significant effect on the gene transcription (Figure 3.18).

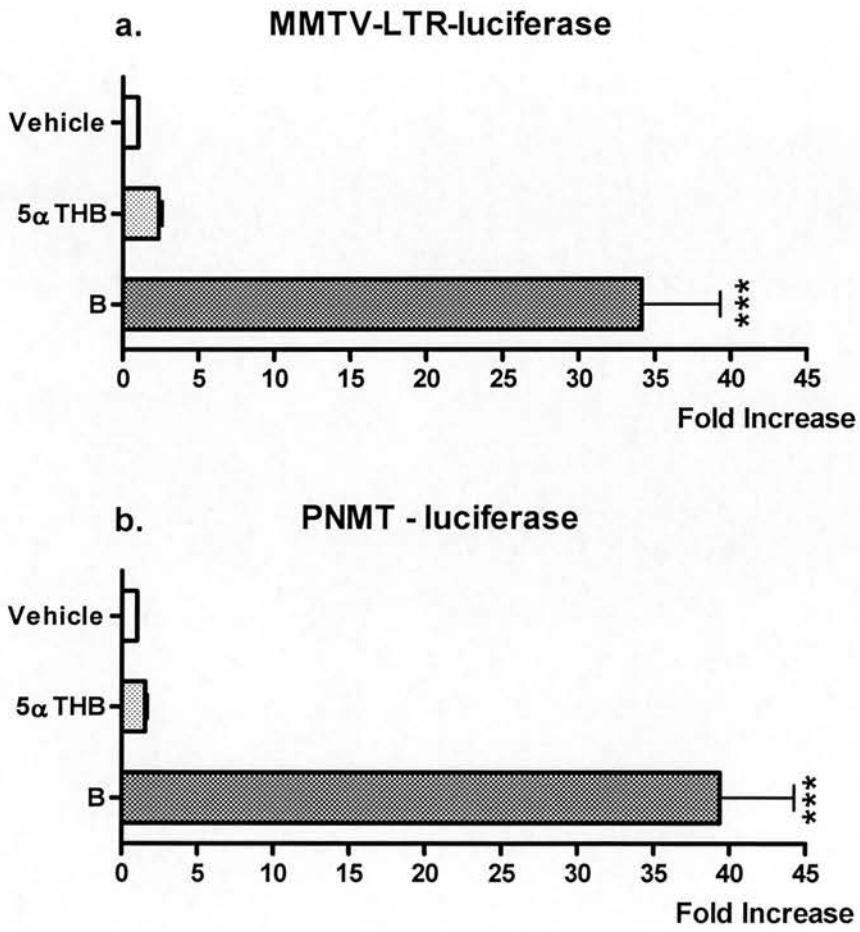

Figure 3.18 Induction of transiently transfected reporters driven by promoters of MMTV or PNMT. (a) MMTV-LTR-luc and (b) PNMT-luc were transfected into Hela cells and incubated with 5αTHB, B (1 μM each) or vehicle (ethanol) for 24 h. Both reporters were substantially induced by B but not 5αTHB. Data are mean ± SEM, shown as the fold increase normalized to the luciferase activities of vehicle; n=6; ***$p<0.001$ versus vehicle, analyzed by one-way ANOVA with Holm-Sidak post-hoc tests.

3.3.4 Investigation of the transrepressive effects of 5αTHB in AtT20 cells

As shown in Figure 3.19, the basal level of the transcription of POMC was significantly increased by CRH; whereas the increase was not detected in that of CRH receptor 1. During the 48 h long incubation, the transcript abundance of POMC was potently inhibited by corticosterone and dexamethasone but not influenced by 5αTHB, with and without the presence of CRH. CRH receptor 1 expression was significantly decreased by dexamethasone and corticosterone when cells were treated by CRH, but was not affected by 5αTHB either.

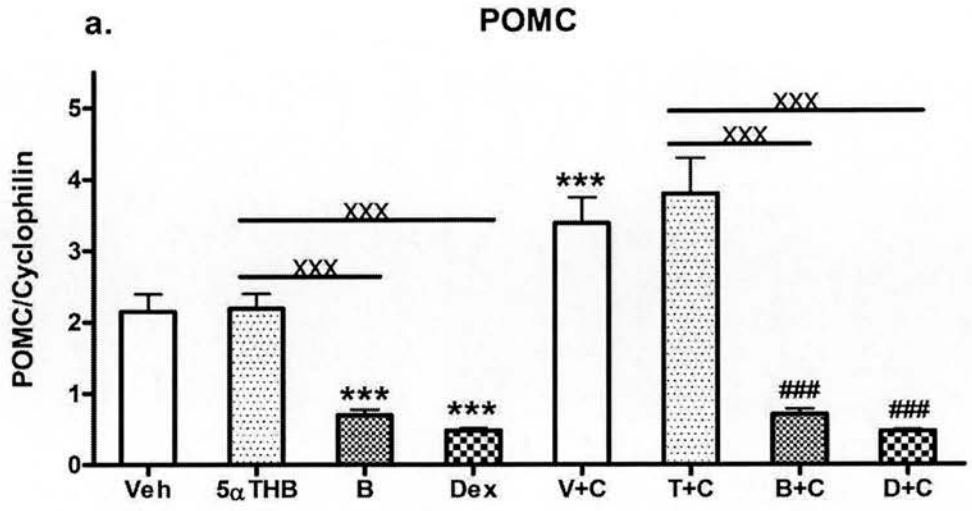

Treatment, p<0.001; CRH, p<0.001; Interaction, p=0.002.

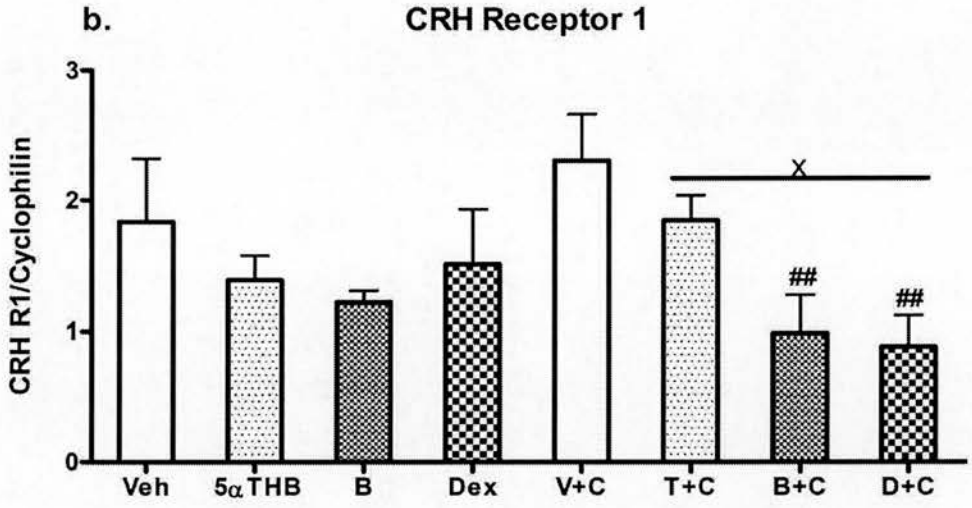

Treatment, p=0.012; CRH, p=0.936; Interaction, p=0.224.

Figure 3.19 Effects of 5αTHB to suppress abundance of mRNAs for (a) POMC and (b) CRH receptor 1 (CRH R1) in AtT20 cells. AtT20 cells were incubated with 5αTHB, B, Dex (1μM each) or vehicle (Veh; ethanol), or each of the four treatments together with CRH (100nM), abbreviated as T+C, B+C, D+C and V+C, respectively, for 48 hours. The transcript abundance of POMC was quantified by real-time PCR. The basal level of POMC transcription was increased by CRH; POMC expression was down regulated by B and Dex, not 5αTHB, with or without the addition of CRH. Data are mean ± SEM, n=6; ***$p<0.001$ versus Veh; ###$p<0.001$ versus V+C; $^{X}p<0.05$, $^{XXX}p<0.001$ versus other steroid treatment indicated by the bar; analyzed by two-way ANOVA with Holm-Sidak post-hoc tests.

3.3.5 Cytokine release from bone marrow derived macrophages (BMDMØs):

3.3.5.1 Expression of A-ring reductases in BMDMØs

The presence of mRNAs of A-ring reductases, e.g. 3α-HSD, 5α-reductase type 1, type 2, and 5β-reductase, was investigated in un-stimulated BMDMØs (Figure 3.20), using mouse liver as the positive control for 3α-HSD, 5α-reductase type 1, and 5β-reductase, and prostate as the positive control of 5α-reductase type 2. None of these genes were transcribed in BMDMØs. F4/80, which is expressed in macrophages, was detected as the positive control to ensure the integrity of the mRNA harvested from BMDMØs.

3.3.5.2 Transactivation of the anti-inflammatory cytokine IL-10

In un-stimulated BMDMØs, both 5αTHB and 5αDHB, along with dexamethasone and corticosterone (1 μM each), induced the release of IL-10 compared to vehicle. When the BMDMØs were stimulated by LPS (100 ng/ml), the secretion of IL-10 was substantially increased, and this response was significantly suppressed following the addition of dexamethasone or corticosterone but not 5αTHB or 5αDHB (Figure 3.21).

3.3.5.3 Suppression of IL-6, TNFα and MCP-1 from LPS stimulated BMDMØs

Glucocorticoids suppress the secretion of selected cytokines through a transrepression mechanism. As shown in Figure 3.22, the release of proinflammatory cytokines IL-6 and TNFα and chemokine MCP-1 were substantially increased by LPS but not by glucocorticoids alone. Dexamethasone and corticosterone significantly reduced the cytokine production following stimulation by LPS, and also suppressed MCP-1 in un-stimulated macrophages. 5αTHB and 5αDHB suppressed the releases of IL-6 and TNFα to a much lesser extent, and 5αDHB was more potent than the tetrahydro reduced form, 5αTHB. The same pattern of data was observed for MCP-1 but 5αTHB was too weak to reduce the chemokine release following such a high dose of LPS (100 ng/ml). Therefore, to further elucidate the potency of 5αTHB,

the dose response of 5αTHB to induce suppression of cytokine release by LPS was investigated.

The inhibition of LPS-stimulated IL-6 secretion by dexamethasone and corticosterone was attenuated by RU486, the specific GR antagonist. However, addition of RU486 did not affect the suppressive effects of 5αDHB, and potentiated the inhibition induced by 5αTHB (Figure 3.23).

3.3.5.4 Dose response to the release of cytokines and chemokine stimulated by different doses of LPS

As shown in Figure 3.24, after incubation with a higher dose of LPS (100 ng/ml) for 24 hours, the production of proinflammatory cytokine IL-6 was reduced by corticosterone from concentrations above 10nM and by 5αTHB above 300 nM. When stimulated by a lower dose of LPS (10 ng/ml), 30nM of 5αTHB was able to reduce the release of IL-6, in contrast to 3nM of corticosterone, indicating a 10 - 30 fold difference in potency.

The suppressive effect of B and 5αTHB on IL-10 secretion post-stimulation by LPS was much weaker. 1 μM of 5αTHB only demonstrated an effect compared to a lower dose of 3-30 nM of corticosterone.

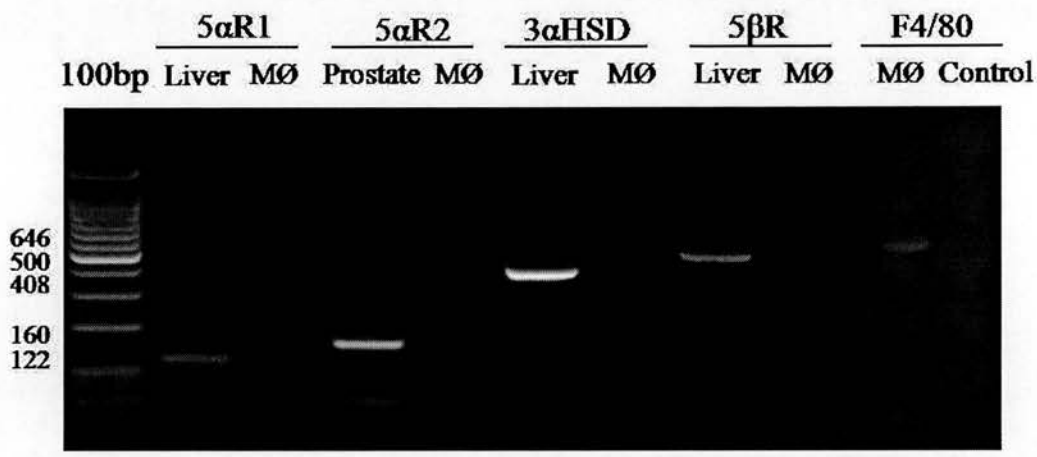

Figure 3.20 Expression of mRNA of A-ring reductases in BMDMØs. Total RNA (1 μg) isolated from mouse BMDMØs was amplified by reverse transcription with specific primers to detect expression of A-ring reductases. 5α-Reductase type 1 (5αR1), type 2 (5αR2), 3α-HSD, and 5β-reductase were not detected in un-stimulated BMDMØs. Mouse liver and prostate were used as positive controls where appropriate. F4/80 was the positive controls for BMDMØs, and was normally expressed in cells. A reaction without the presence of reverse transcriptase was used as a negative control.

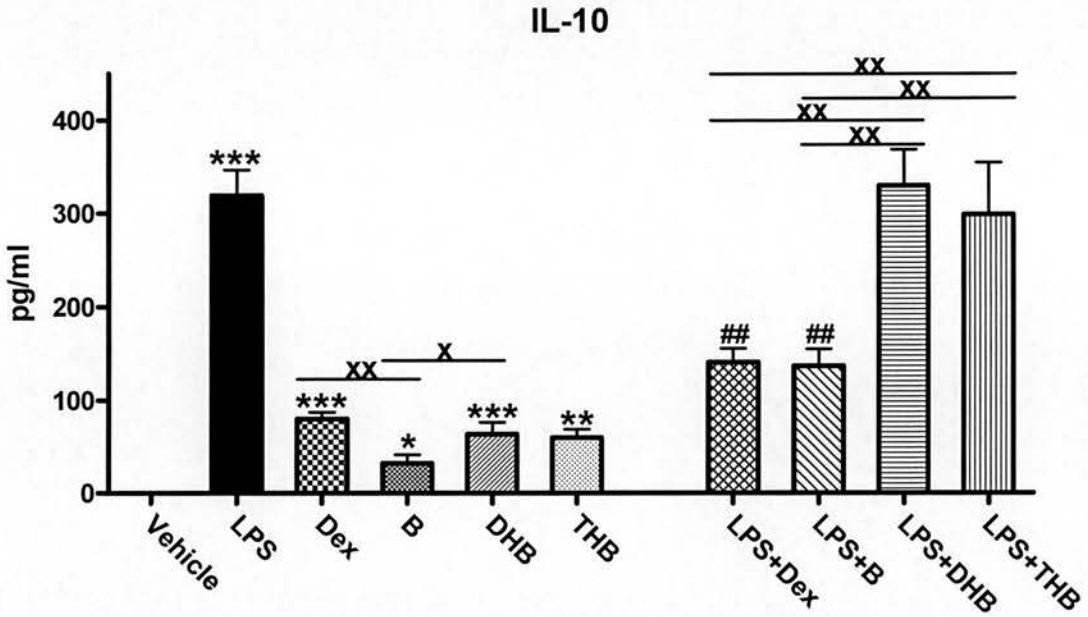

Figure 3.21 Secretion of IL-10 from BMDMØs. Matured BMDMØs were primed by glucocorticoids (dexamethasone (Dex), corticosterone (B), 5αDHB (DHB) or 5αTHB (THB)) for 1h prior to the stimulation by LPS for 24h or incubation with vehicle. Vehicle samples were BMDMØs incubated with ethanol only. The IL-10 released into the culture medium was quantified by CBA. All these four steroid solutions increased the secretion of IL-10 versus vehicle; LPS stimulated the release of IL-10 substantially, and this increase was suppressed by Dex and B but not DHB or THB. Data are mean ± SEM, n=3; *$p<0.05$, **$p<0.01$, ***$p<0.001$ versus vehicle; ##$p<0.01$ versus LPS; $^{X}p<0.05$, $^{XX}p<0.01$ versus another steroid treatment indicated by the bar; analysed by one-way ANOVA with Holm-Sidak post tests.

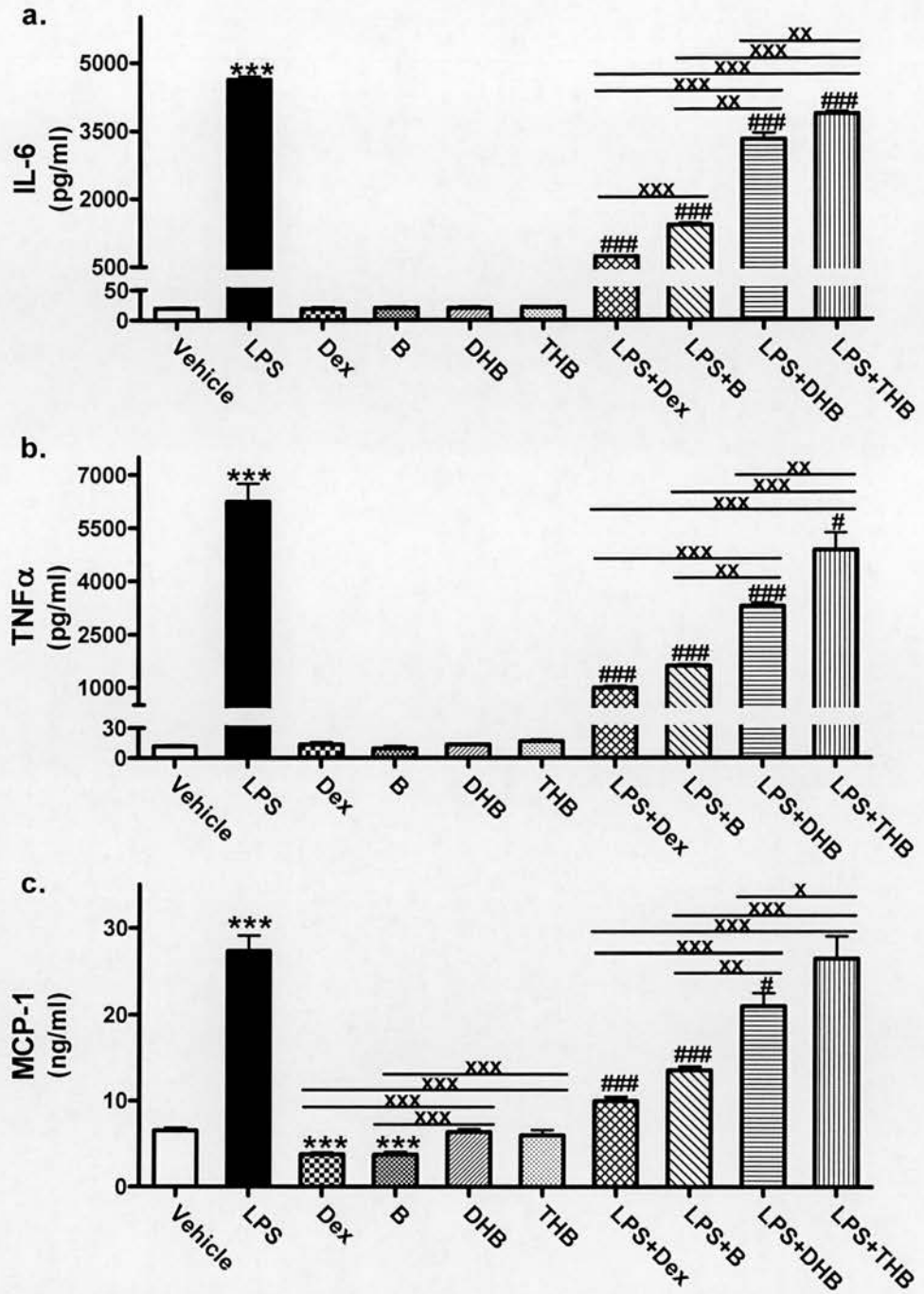

Figure 3.22 Secretion of (a) IL-6, (b) TNFα and (c) MCP-1 from BMDMØs. Matured BMDMØs were primed by glucocorticoids (dexamethasone (Dex), corticosterone (B), 5αDHB (DHB) or 5αTHB (THB)) for 1h prior to the stimulation by LPS for 24h. Vehicle samples were BMDMØs incubated with ethanol only. The cytokines and chemokine released into the culture medium were quantified by CBA. Dex and B reduced their release following the stimulation by LPS, while 5αTHB and 5αDHB suppressed the release to a lesser extent. Data are mean ± SEM, n=3; ***p<0.001, versus vehicle; #p<0.05, ###p<0.001 versus LPS; ^{X}p<0.05, ^{XX}p<0.01 versus another steroid treatment indicated by the bar; analysed by one-way ANOVA with Holm-Sidak post tests.

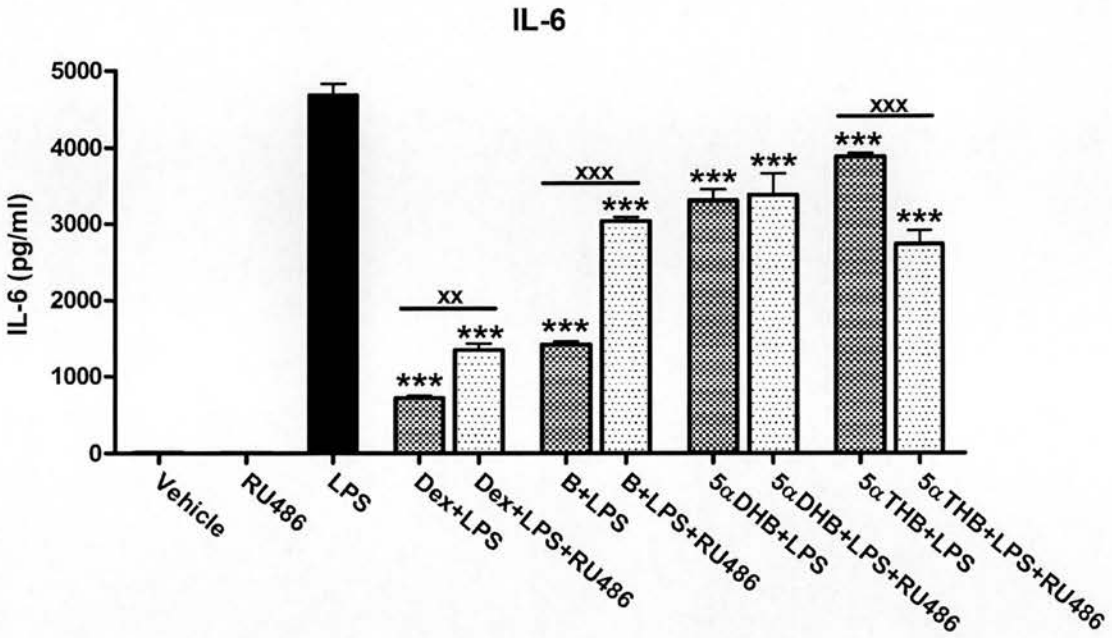

Treatment, p<0.001; RU486, p=0.216.

Figure 3.23 Secretion of IL-6 from LPS-stimulated BMDMØs, with or without the presence of RU486. BMDMØs were primed by Dex, B, 5αDHB or 5αTHB (1 μM) or vehicle (ethanol) before they were stimulated by LPS (100 ng/ml) for 24 h. IL-6 in the culture medium were quantified by CBA. LPS induced IL-6 secretion was suppressed by all the steroid treatments. RU486 antagonized the suppression induced by Dex and B but not by 5αDHB and potentiated that of 5αTHB. Data are mean ± SEM, n=3; Impact of RU486 was analyzed by two-way ANOVA; ***p<0.001 versus LPS; ^{xx}p<0.01, ^{xxx}p<0.001, analyzed by one-way ANOVA with Holm-Sidak post-hoc tests.

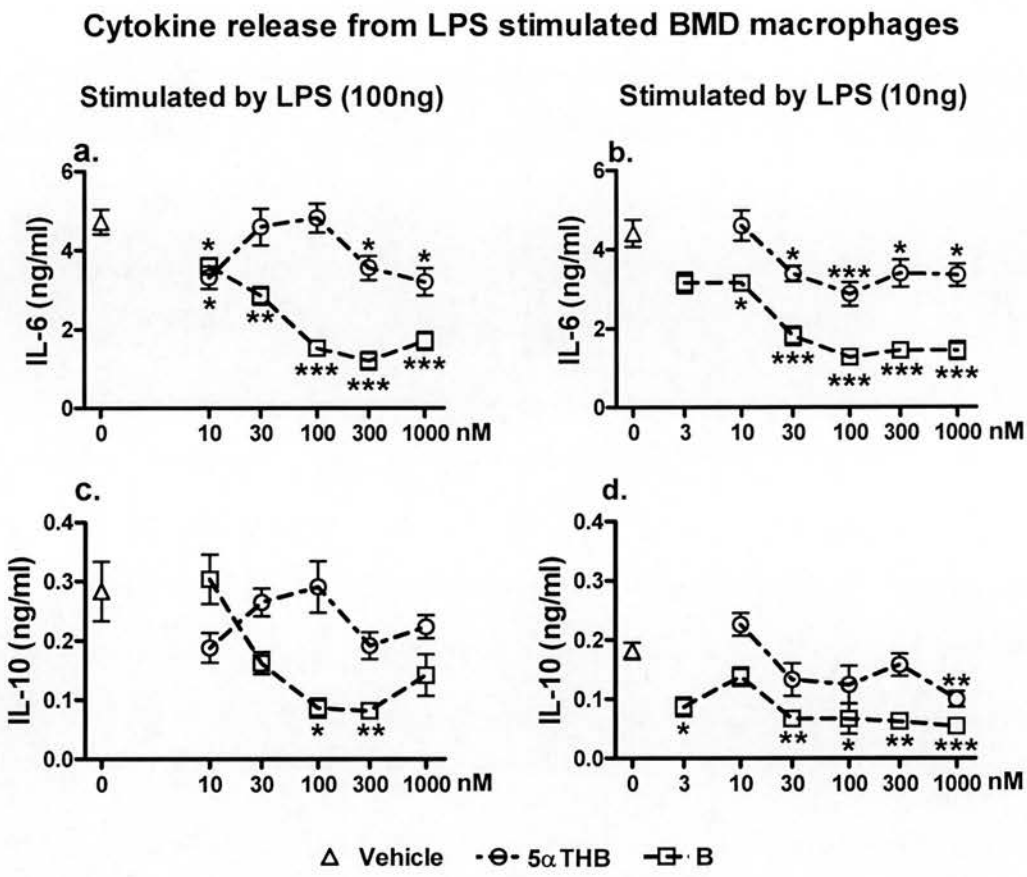

Figure 3.24 Suppression of LPS-induced production of IL-6 and IL-10 from BMDMØs, that were primed by B, 5αTHB (3, 10, 30, 100, 300 and 1000 nM) or vehicle (ethanol) before they were stimulated by LPS (10 or 100 ng/ml) for 24 h. The cytokines and chemokine released into the culture medium were quantified by CBA. When incubated with a higher dose of LPS (100 ng/ml), the production of IL-6 was reduced by B at concentrations of 10 nM and above and by 5αTHB upward of 300nM. When stimulated by a lower dose of LPS (10 ng/ml), 30 nM of 5αTHB was able to reduce the release of IL-6 (a, b). The suppressive effect of 5αTHB on IL-10 secretion post-stimulation by LPS was much weaker, whereby 1 μM of 5αTHB could only exert an effect on secretion induced by low-dose LPS (10 ng/ml) (c, d). Data are mean ± SEM, n=3; *p<0.05, **p<0.01, ***p<0.001 versus vehicle; analysed by one-way ANOVA with Holm-Sidak post-hoc tests.

3.4 Discussion:

In this chapter, the cellular properties of 5αTHB, i.e. GR translocation, transactivation and transrepression of glucocorticoid responsive genes, have been investigated. In HEK293 cells that were transiently transfected with GFP-GR, 5αTHB-bound GR showed prolonged process of nuclear translocation, and accelerated nuclear export following steroid withdrawl. 5αTHB also increased the nuclear mobility of GFP-GR in the FRAP analysis. However 5αTHB was synergistic with corticosterone in GR translocation. To investigate the activity of 5αTHB to transactivate glucocorticoid responsive genes, a number of model systems have been used. In the H4IIE cells that were cultured in normal medium or the medium with stripped-serum, 5αTHB did not alter the expression of PEPCK or TAT. In the transiently transfected Hela cells, 5αTHB did not increase the expression of the MMTV and PNMT reporter genes which represent two distinct ways of GR dimerization. In the aspects of gene transrepression, 5αTHB did not suppress the expression of POMC or CRH receptor 1 in AtT20 cells. However, 5αTHB had significant anti-inflammatory properties. It induced the release of IL-10 from non-stimulated BMDMØs, and suppressed the LPS-induced production of TNFα and IL-6 from BMDMØs.

3.4.1 Effects of 5αTHB on GFP-GR translocation

Natural glucocorticoids, such as cortisol and corticosterone, circulate either as the free steroid or approximately 70-90% of total in the circulation bound to serum corticosterone-binding globulin (CBG) or albumin. However, synthetic dexamethasone mostly remains as free in circulation and hardly binds to these proteins (Stewart, et al. 2002). Thus cells were treated with 1 μM of steroids which is a high concentration to investigate the actions of both dexamethasone and corticosterone. They both were used as positive controls; however, it was not possible to compare directly the activities between them since the active free concentrations were unknown. McInnes et al. (2004) has shown that 5αTHB was able to compete with dexamethasone for its binding sites in hepatocytes with affinity

similar to that of corticosterone. Therefore, in this section, the binding activities of 5αTHB to GRs or chromatin binding sites were mainly compared to those of corticosterone.

Glucocorticoids exert their activities via GRs that are ligand-activated nuclear receptors. GR protein is composed of domain structures, the major ones being the C-terminal ligand binding domain (LBD) that serves as hormone binding sites and also contains the nuclear localization signals (NLSs) and ligand-dependent activation function domain (AF-2); the central DNA binding domain (DBD) that is essential for target gene binding and GR dimerization; the N-terminal AF-1 activation domain required for transcriptional activation and association of GR with other transcription factors (Smoak and Cidlowski 2004). Without ligand binding, GRs are associated with the heat shock protein based chaperon machinery in the cytoplasm. Upon ligand binding, GRs are activated and translocate into nucleus. Intracellular GR distribution and trafficking can be monitored and analyzed in living cells, into which the chimera of GFP-GR is transfected so that the ligand-dependent GR trafficking between cytoplasm and nuclei is visible under fluorescent microscope (Htun, et al. 1996). The effects of 5αTHB versus corticosterone and dexamethasone on GR translocation from cytoplasm into nucleus have been investigated in the HEK293 cells transiently transfected with GFP-GR. Compared to dexamethasone and corticosterone, 5αTHB translocated GRs in a much slower and weaker manner, according to our 24-hour observation. Additionally, when ligands were washed away after 24 hours incubation (1 μM), GRs were 'locked' in the nucleus by dexamethasone and corticosterone, whereas they 'escaped' into cytoplasm following incubation with 5αTHB. As the GFP-GR translocation was performed using decreasing concentrations of corticosterone, it was found that 3nM of corticosterone was equivalent to 1 μM of 5αTHB achieving a similar efficacy of translocation within 5 hours. Furthermore, the interaction between corticosterone and 5αTHB has been revealed by means of co-incubation of the two ligands, that they have synergetic effects on GR translocation. To explain the differences between 5αTHB and its parent hormone on the above observations, the mechanisms of ligand binding and GR translocation need to be further clarified.

In the absence of ligand, GR is tethered in the cytoplasm by association with chaperone proteins that bind to the ligand binding domain (LBD). The LBD has multiple functions including ligand binding, chaperone association, nuclear location and transcription regulation. Crystallographic analysis shows the GR LBD contains a ligand binding pocket which is a feature unique to the GR LBD among other nuclear hormone receptors. This pocket allows for the selective binding of glucocorticoids and some mineralocorticoids that have larger substituents at the C17α position than other steroids (Necela and Cidlowski 2003). In rodents, 5α-reductase catalyzes the *trans* reduction of corticosterone at the double bond of position $\Delta^{4,5}$, yielding 5αDHB, which is further reduced promptly by 3α-HSD to 5αTHB (Russell and Wilson 1994) (the structures of 5αDHB and 5αTHB are in Figure 1.6). The 5α-reduction of corticosterone does not change the structure at the C17α position, which allows 5αTHB to bind with GR. However, the polar substituents, at positions C3 or C17 of the glucocorticoid structure, also affect the specific GR-ligand interaction. Interestingly, GR, as well as AR, PR and MR preferentially bind the steroid hormones with a ketone at the C3 position. Analysis of the dexamethasone bound ligand binding pocket reveals that the hydrophobic residues within GR protein contact nearly every atom of the steroid core of dexamethasone, and all hydrophilic groups of dexamethasone form hydrogen bonds with the GR protein (Bledsoe, et al. 2002). The hydrogen bond network between GR and the ligand is likely to contribute to the high affinity binding of dexamethasone, and an important interaction is with the C3 ketone group. Indeed, in the structures of GR, PR and AR, there is a conserved structure from which the C3 ketone is ready to accept hydrogen bonds; however, ER prefers to be presented a hydrogen bond donated from its ligand. Therefore, ER prefers a hydroxyl group at the C3 position whereas GR, AR and PR select the steroid hormones with a ketone group at C3 (Bledsoe, et al. 2002). This finding suggested that 5αDHB would be a better ligand for GR than 5αTHB, since 5αDHB has a ketone group at C3 position whereas 5αTHB has a hydroxyl group produced in the 3αHSD reductive process. However this is in contrast with McInnes' findings that 5αDHB had higher K_d value than 5αTHB, and is less efficient in displacing dexamethasone from binding sites in hepatocytes (McInnes et al. 2004).

Following from those findings, in this thesis the efficiency of 5αDHB in GR translocation was not tested, and the course of GR translocation induced by 5αTHB showed significant lag in initiation, suggesting that 5αTHB had difficulty in interacting with GR, and that 5αTHB was not a preferred ligand for GR. Nonetheless 5αTHB was able to translocate conventional GR to the nucleus of the cell where it may be transcriptionally active.

Upon ligand binding, the GR protein favours closure of the steroid binding pocket, promoting enough conformational change in the receptor to expose the nuclear localization signals (NLSs) (Pratt et al. 2006) that are essential for nuclear translocation. Given a much slower rate of translocation induced by 5αTHB compared to dexamethasone and corticosterone, it is possible that 5αTHB may not be as efficient in inducing conformational changes in GR to reveal NLSs. However, co-incubation with corticosterone and 5αTHB showed intriguingly synergetic effects on GR translocation in a concentration-dependent manner, suggesting the interaction between the two ligands induced functional changes in NLSs. Possibly, the NLS on GR that were activated by corticosterone opened the nuclear pore more efficiently, which then leaves a way for the 5αTHB-bound GR to pass through. Alternatively, perhaps the presence of 5αTHB allosterically enabled binding of corticosterone. However, the detailed mechanism underpinning the synergetic effects between 5αTHB and corticosterone on GR translocation needs further investigation.

Within the nucleus, GR binds to chromatin binding sites and induces transcriptional actions. The interaction between the GR and chromatin is an extremely dynamic rather than a static process (McNally et al. 2000). Then the ligand dissociates from GR which is released from chromatin by the hsp90/hsp70-based chaperone machinery. Unligated GRs are collected in a subnuclear compartment which serves as a nuclear export staging area with binding to the chaperone machinery, and recycle to chromatin upon rebinding the ligand without exiting the nucleus to regain functionality (Yang et al. 1997). It is known that after steroid withdrawal, the active nuclear retention of GR plays an integral role in its ability to transactivate the transcription of MMTV reporter gene (Carrigan et al. 2007); and the ability to bind

DNA is an important determinant for both nuclear localization and accelerated nuclear retention (Sackey et al. 1996). In the present study in this chapter, 5αTHB not only slowed the nuclear import of GR, but also prolonged the process of nuclear retention after steroid withdrawal. These findings indicated that 5αTHB induced a conformational change of GR that may have lower affinity for the chaperone machinery, weaker ability to bind DNA and to activate gene transcription than the GRs ligated by dexamethasone or corticosterone.

Nuclear mobility of GFP-GRs ligated with 5αTHB or corticosterone was detected by FRAP analysis. The mobility of GR is affected by the nature of the ligand bound to GR which may induce a specific conformational change of GR to facilitate the binding to GRE (Meijsing et al. 2007). Dexamethasone, the high-affinity GR ligand, dramatically decreases the mobility of GRs in a concentration-dependent manner, whereas corticosterone with lower affinity decreases GR mobility to a much lesser extent (Schaaf and Cidlowski 2003). Additionally, previously reported studies on the effects of geldanamycin (disrupting the assembly of GR-chaperone complex) on GFP-GR mobility, faster GFP-GR mobility indicated that the chaperone machinery stabilizes GR binding to chromatin rather than promoting its removal (Pratt et al. 2006). In the present study, increased mobility of GFP-GR by 5αTHB suggested lower affinity of 5αTHB for GR and incompetent ability of 5αTHB to induce the conformational change of GR, which lead to much weaker binding of GR to GRE and to the chaperone proteins. It is possible that 5αTHB induced GR may hardly bind to GRE at all. Furthermore, a number of GRs with a mutant in the LBD have the transcriptional activities to induce MMTV expression that correlate positively with the half life ($t_{1/2}$) of maximal recovery; thus increased nuclear mobility of GR is an integrated indicator of decreased signalling ability (Kino et al. 2004). Therefore it is suggested that 5αTHB has weaker transcriptional ability than corticosterone.

Taken together, all these findings discussed above suggest that 5αTHB ligated GR may have transformed to the receptor that has less exposed NLSs, weaker abilities of nuclear retention and DNA binding, and thus weaker transactivation ability than dexamethasone and corticosterone.

3.4.2 Effects of 5αTHB on GR transactivation

The effects of 5αTHB on GR transactivation were investigated in a number of *in vitro* culture systems, anticipating initial confirmation of the findings of McInnes et al.

Transcriptional induction of two glucocorticoid responsive genes encoding for the gluconeogenic enzymes PEPCK and TAT in the hepatoma cell line, H4IIE cells, was quantified following incubation with corticosterone or 5αTHB. Corticosterone induced a time and dose dependent increase in mRNA abundance; however 5αTHB had little influence on the gene transcription. This result opposed the previous findings, in which 5αTHB induced transcription of these genes (McInnes et al. 2004). Further experiments of McInnes were revisited to confirm the results of GR transactivation induced by 5αTHB. Effects of 5αTHB or corticosterone on expression of another two glucocorticoid response elements, MMTV-LTR and PNMT, were quantified by reporter assay in transiently transfected HEK293 cells. MMTV and PNMT represent two distinct dimerization mechanisms of GR binding with the regulatory regions of the gene. To transactivate PNMT, which is similar to TAT and PEPCK, GRs dimerize through the DNA binding domain and bind to the consensus GRE and increase transcription; whereas for the MMTV promoter, GRs bind as monomer to the GRE1/2s where GRs form dimer through the ligand binding domain at the directly repeated GRE1/2s (Schoneveld et al. 2004; Truss and Beato 1993). As a result, corticosterone substantially activated transcription of both promoters; however again, 5αTHB did not transactivate these genes.

There are three major differences in methodology between McInnes' study and the ones in this thesis which may explain these contrasting findings and were considered: 1) McInnes investigated the mRNA induction after 16 hours (only one time point) incubation using Northern blotting as opposed Real time-PCR which was used here to allow processing of a larger number of samples at multiple time points; 2) here the two housekeeping genes, cyclophilin and 18S, were used for internal controls, which are commonly used in real-time PCR, whereas U1 was used as a correction in Northern blotting; 3) here the cells were incubated and treated with stripped-serum

medium at least initially, as opposed to McInnes who used medium contained normal serum.

To address these experimental confounders, the mRNAs used to detect the transactivation of TAT and PEPCK in the archived samples from McInnes' study were re-quantified by real-time PCR using cyclophilin as an internal control, and results were consistent between methods (data not shown), indicating it was not the quantification approach that brought about the distinction. Furthermore, the internal control genes in both experiments were not significantly changed by treatment. Finally the experiment was re-performed in culture medium containing normal serum instead of stripped serum. However, again, 5αTHB did not induce transcription of the two genes.

Although a concrete answer has not been found to explain the discrepancy, at a later stage in the execution of the work presented in this thesis, the synergetic effects of 5αTHB and corticosterone (at very low concentrations) on GR translocation were revealed. Thus there is the possibility that the synergism may also exist in responses to gene transcription. 5αTHB might induce higher levels of transactivation of these genes in the presence of corticosterone or cortisol (fetal bovine serum contains cortisol of about 30 nM, diluted 1 in 10 to prepare culture medium). This assumption may explain the increased transcription in McInnes' study if batch to batch variation in concentrations of glucocorticoids in culture medium occurs. However, against this argument, McInnes et al only found additive effects of 5αTHB and corticosterone on induction of MMTV reporter gene but not synergetic effects (McInnes et al. 2004). Nonetheless further studies are underway to revisit these effects on gene transactivation in H4IIE cells. Taken together, in this thesis 5αTHB can poorly induce GR binding to the GREs in chromatin to regulate transactivation but may synergise with corticosterone.

In H4IIE cells (rat hepatoma cells) and Hela cells (human cervical carcinoma cells), 3α-HSD is expressed (Penning et al. 1986; Zheng, et al. 2005) and will convert the 5α-dihydro derivatives of glucocorticoids rapidly to 5α-tetrahydro forms. Therefore,

in these cells the effects of 5αDHB were not investigated. Whereas in bone marrow derived macrophages, A-ring reductases, e.g. 3α-HSD, 5αR1, 5αR2, and 5β-reductase were not expressed. In the study performed in the macrophages, 5αTHB as well as 5αDHB increased IL-10 secretion from unstimulated bone marrow derived macrophages incubated in stripped-serum medium, and 5αDHB was more efficient than 5αTHB, which supported the theoretical concept that 5αDHB is a better ligand for GR than 5αTHB but was contrary to McInnes' findings. Binding constants were assessed in the previous study in hepatic cytosol which contains 3αHSD; if there was any endogenous NADPH within this preparation then 5αDHB may have been converted to 5αTHB rapidly. 5β-Reductase is also present in cytosol and may also have accepted corticosterone as a substrate under the incubation conditions, however this enzyme is rate-limiting, unlike 3αHSD whose reaction proceeds nearly 100-1000 times more rapidly.

Glucocorticoids mediated increase in IL-10 production is regulated by GR binding to the transcription factor STAT3 via GR-protein binding mechanism instead of GR binding to GRE (Unterberger et al. 2008). Given the findings that 5αTHB increased IL-10 secretion but did not increase the other glucocorticoid transactivated genes discussed above, e.g. TAT, PEPCK, PNMT, and MMTV, it seems 5αTHB activated GRs favour interaction with proteins rather than chromatin. In our study, corticosterone and dexamethasone significantly suppressed LPS-induced IL-10 secretion whereas only high dose of 5αTHB (1 μM) suppressed low dose LPS (10 ng/ml) -induced IL-10 release. Although it is known that glucocorticoids increase IL-10 production, the mechanism underpinning the suppressive effects of glucocorticoids on LPS-induced IL-10 is unclear. The production of LPS-induced IL-10 in Kupffer cells is autoregulated at the transcriptional level by a negative feedback mechanism involving the IL-10 receptor (Knolle, et al. 1998), and it has been demonstrated that TNFα increases the production of lipoprotein-induced IL-10 in THP-1 cells (macrophage-like cell line) (Giambartolomei, et al. 2002). Thus the results in our study may be due to the decreased production of TNFα in the steroid-treated LPS-activated macrophages (which appears more sensitive to dexamethasone and corticosterone as discussed below) that contribute to the decrease in IL-10.

3.4.3 Effects of 5αTHB on GR transrepression

The effects of 5αTHB on GR transrepressive actions on POMC and pro-inflammatory cytokines have been investigated. GR transrepression is mediated through either direct or indirect interaction between GRs and target genes.

McInnes et al previously showed suppression of ACTH release in rats in response to intraperitoneal administration of 5αTHB, and this may be explained by a decrease in transcription of POMC. Thus the effects of 5αTHB on POMC mRNA expression were investigated in AtT20 cells, the mouse pituitary corticotroph tumor cell line. AtT20 cells are able to secret ACTH permanently; POMC, the ACTH precursor, is expressed, synthesized and processed into ACTH before its secretion. Glucocorticoids inhibit ACTH secretion, while CRH and cytokines, such as IL-6 and IL-1, upregulate its secretion (Ooi et al. 2004). Studies on the inhibition of ACTH secretion by glucocorticoids in AtT20 cells often involve the treatment of cells with CRH to amplify the magnitude of ACTH levels as well as POMC synthesis. The actions of glucocorticoids in the pituitary gland occurs in two main phases, the early (0.5-2 h) and slow (>6-8 h) feedback inhibition; both are GR mediated processes, and both have been studied using the AtT20 cells as a model system. The early inhibitory action of glucocorticoids is caused by suppression of CRH-evoked intracellular free calcium transients (Antoni, et al. 1992; Loechner, et al. 1999) and thereby inhibiting CRH-induced synthesis of POMC mRNA and protein; and the slow inhibition involves the repression of the synthesis of POMC (Antoni et al. 1992; Woods, et al. 1992), in which activated GRs bind as a trimer to the negative GRE in the regulatory region of POMC and inhibit gene transcription (Drouin, et al. 1993b). As shown in our study, dexamethasone and corticosterone dramatically decreased POMC transcription with or without stimulation of CRH, and also decreased that of CRH receptor 1 only in the presence of CRH, in AtT20 cells with continuous incubation for 48 h. However, 5αTHB did not decrease the transcription of both genes, suggesting that 5αTHB did not induce transrepressive effects through GR binding to the negative GRE. The effects of these steroids on calcium transients were not studied and may still explain the effects observed previously in rats, although the time course was slower rather than rapid.

Dexamethasone inhibits ACTH secretion in 2 h from the AtT20 cells following a short-term incubation with CRH (30 min). However, corticosterone does not induce any effect under these conditions unless used at the high concentration of 10 μM and in the presence of glycyrrhetinic acid (inhibitor of 11β-HSDs) (Woods et al. 1992). The equilibrium of metabolism of dexamethasone by 11β-HSD2 in contrast favours reduction, thus maintaining high levels of active steroid (Best, et al. 1997). Therefore, the 11β-HSD present in the AtT20 cells should be the type 2 isozyme rather than type 1, so that corticosterone was inactivated rapidly by 11β-HSD2. However A-ring reduced steroids may be maintained in these cells since they too are not substrates for 11β-HSD2 and this metabolic route does therefore not explain the lack of effect.

A further consideration was whether the cells had been studied over the correct time interval to observe an effect. CRH can constantly induce POMC mRNA expression as well as ACTH secretion over 24 h, and the increase in POMC mRNA abundance continues for another 24 h after CRH withdrawal (Affolter and Reisine 1985). Additionally, the inhibitory effects of corticosterone last for more than 4 h to suppress the abundance of mRNA of CRH receptor 1 in AtT20 cells without the presence of 11β-HSD inhibitor (Iredale and Duman 1997). Therefore, it is likely that corticosterone can exert repressive effects at the transcriptional level with a long-term co-incubation of CRH, and the activity of 11β-HSD2 may possibly only have a brief impact. In our study the experiment has also used dexamethasone as a guaranteed positive control, although the effects of corticosterone together with 5αTHB on the slow inhibitory manner were also investigated.

Apart from direct binding to DNA, GR can bind to the subunit of a second transcription factors such as the pro-inflammatory transcription factors NFκB and AP-1 in a GR-protein manner and transrepress the gene transcription regulated by these transcription factors (Schoneveld et al. 2004). LPS-stimulated macrophages are activated through the Toll-like receptor (TLR) 4 which plays a critical role in the innate immune reactions to recognize the microbial products such as LPS. TLR4 is predominantly expressed on the cell surface of macrophages, dendritic cells and B

cells (Zhang and Daynes 2007). Once stimulated by LPS, TLR4 signalling triggers the activation of NFκB, AP-1 and mitogen-activated protein kinase (MAPK) cascades, all of which are essential for the LPS-induced production of various cytokines (Fang, et al. 2004; Fukao and Koyasu 2003). Glucocorticoids suppress the genomic activity of NFκB and AP-1 via direct GR binding and thereby inhibit the synthesis and secretion of cytokines. Glucocorticoids also suppress LPS-induced activation of p38 MAPK by transactivating the induction of MAPK phosphatase (MKP) -1 that is known to inhibit MAPK activation (Bhattacharyya, et al. 2007), and this induction does not require GR dimerization (Abraham, et al. 2006). Therefore, glucocorticoid suppression of the LPS-stimulated cytokine production in macrophages involves transrepression mediated by GR-protein binding mechanism as well as transactivation that is GR-dimerization-independent.

In our study, dexamethasone, as the most potent anti-inflammatory agent to date, decreased substantially the production of TNFα, IL-6 and MCP-1 from LPS-stimulated bone marrow derived macrophages, and corticosterone decreased the release to a lesser extent. 5αTHB also suppressed the release of cytokines TNFα and IL-6 from macrophages although to a much lesser extent; and 5αDHB again exerted a stronger effect than 5αTHB. However, the detailed mechanism through which 5αTHB exerted its effects (i.e. the transrepression or transactivation mechanism described above) is not known. Moreover, RU486 impaired the suppressive effects of dexamethasone and corticosterone on IL-6 secretion but did not affect the effects of 5αDHB, and in the contrast potentiated the effects of 5αTHB. This finding suggested an interesting novel mechanism for 5αTHB-mediated inhibition of TLR4 activated inflammation however it needs further investigation.

Besides, it is known that 11β-HSD1 is expressed in mouse macrophages, amplifying the intracellular activities of glucocorticoids and promoting their anti-inflammatory effects (Gilmour et al. 2006). Since A-ring reduced steroids are not substrates for 11β-HSD1 (Tomlinson and Stewart 2001), the activities of 5αDHB and 5αTHB were not amplified.

3.4.4 Summary

In summary, 5αTHB, with a hydroxyl group at the C3 position, may be an unfavourable ligand for GR. Thus 5αTHB ligated GR may undergo an insufficient conformational change that have exhibited prolonged process of nuclear translocation and accelerated nuclear export following steroid withdrawl, indicating its weak ability to activate gene transcription. 5αTHB also increased the nuclear mobility of GR suggesting its lower affinity for the receptor than corticosterone. 5αTHB was synergistic with corticosterone in GR translocation however this property has not been investigated at the transcriptional level.

5αTHB did not induce the expression of the glucocorticoid responsive genes tested, such as PEPCK, TAT, MMTV and PNMT, which are transactivated dependent on GR-GRE binding. 5αTHB also did not transrepress the expression of POMC or CRH receptor 1, which also requires GR binding to the negative GRE. However, 5αTHB had anti-inflammatory properties. It induced the release of IL-10 from BMDMØs which involves GR-protein binding, and suppressed the LPS-induced production of TNFα and IL-6 from BMDMØs which may involve transrepression mechanism mediated by GR-protein binding and transactivation mechanism independent of GR-dimerization. These findings suggest that GR by 5αTHB can induce responses that are relatively selective for GR-protein rather than GR-GRE interactions.

Chapter 4

Investigation of the effects of 5αTHB on transactivation and transrepression *in vivo*

4.1 Introduction

Glucocorticoids exert a wide range of effects in target systems throughout the body, among which they modulate energy homeostasis, increase blood pressure, execute negative feedback on the HPA axis, and also suppress immune responses. If elevated glucocorticoids secretion is sustained, such as in the naturally occurring Cushing's Syndrome or chronic intake of glucocorticoids in the therapy of inflammatory diseases, these effects can be aggravated and result in impaired glucose tolerance, insulin resistance, central obesity, hypertension, dyslipidemia, and HPA axis dysfunction (Walker 2006). Therefore, there is an enormous interest in developing "dissociated steroids" which control specific pathophysiological functions with limited metabolic side effects during therapy (Catley 2007; Schacke et al. 2004). If 5α-reduced metabolites of glucocorticoids can be shown to selectively target key areas of metabolism but not others, they may have therapeutic potential. This thesis is concerned with testing the *in vivo* effects of 5α-THB.

As shown from the *in vitro* findings in Chapter 3, 5αTHB did not induce the expression of glucocorticoid responsive genes, including the ones encoding for the gluconeogenic enzymes, PEPCK and TAT. However, 5αTHB induced IL-10 secretion and suppressed the production of TNFα and IL-6. Taken together, 5αTHB might be an anti-inflammatory steroid lacking metabolic effects. Additionally, McInnes et al. have shown that administration of 5αTHB *in vivo* suppressed the levels of plasma ACTH, suggesting its negative feedback effect of glucocorticoids on the HPA axis, although repression of POMC was not observed in AtT20 cells. Thus this steroid has some of the desirable characteristics of a dissociated steroid *in vitro*. This chapter will investigate whether this pattern of effects of 5αTHB are recapitulated *in vivo*.

The hypothesis of this chapter is that 5αTHB will not activate transcription of genes regulating fuel metabolism but has anti-inflammatory effects, and may suppress the HPA axis.

Aims

The aims of this chapter are to investigate:

1) The effects of 5αTHB on fuel metabolism following acute administration;

2) The effects of 5αTHB on the HPA axis and fuel metabolism following chronic infusion;

3) The anti-inflammatory effects of 5αTHB following chronic treatment.

4.2 Methods and materials

4.2.1 Maintenance of animals

Male C57BL/6 mice (Charles River, Kent, UK) were obtained at 8 weeks of age and used when their body weights were ≥ 25 g. Mice were maintained as described in Section 2.3.1. Upon arrival, they were allowed to acclimatise to the new environment for at least one week before any experiments were performed.

4.2.2 Study of acute administration of glucocorticoids

4.2.2.1 Preparations of injection solutions

4.2.2.1.1 Glucocorticoid solutions dissolved in DMSO: ethanol: saline (13:1:6 v/v)

Corticosterone or 5αTHB (0.003 g) were dissolved in dimethyl sulfoxide (DMSO, 1.56 ml) and mixed thoroughly in a glass vial. Ethanol (120 µl) was added slowly. The solution was stored in -20 °C until required when it was thawed at RT and saline (720 µl, 0.9 % w/v) was added slowly to mix. The final solution was examined for clarity before administration.

4.2.2.1.2 Glucocorticoid solutions dissolved in DMSO

Appropriate amounts of corticosterone or 5αTHB were weighed and dissolved in DMSO in glass vials and mixed thoroughly by sonicating for approximately 15 min.

4.2.2.2 Terminal procedures

Animals were decapitated under controls of minimum achievable stress. Trunk blood was collected into EDTA microvettes (Sarstedt, Germany), and plasma was prepared immediately by centrifugation (1000 g, 5 min, 4 °C). Livers were removed. Two pieces of liver (<100 mg) were snap frozen, and the remainder was immersed in glucose/Hepes buffer for preparation of cytosol.

4.2.2.3 Time course of induction of hepatic TAT expression in C57BL/6 mice

C57BL/6 mice (n=5) were injected subcutaneously (s.c.) with 5αTHB, corticosterone (25 μg/mouse, 100 μl each) or vehicle (DMSO: ethanol: saline (0.9 % w/v) = 13:1:6 v/v) at 08:30 h on each day of experiment. Once treated, mice were either culled immediately (0 h) following the terminal procedures above (see 4.2.2.2) or put back to clean cages and removed for culling after 1 h, 3 h or 6 h. TAT activity in hepatic cytosol was measured by the TAT assay (see 4.2.5.3).

4.2.2.4 TAT activity in response to different vehicle injections

Four mice were injected (s.c.) with Treatment A (vehicle solution (100 μl) used in 4.2.2.3) by syringes (BD Micro-Fine, 29G, BD Medical-Diabetes Care, France) or Treatment B (DMSO only, 20 μl) by Insulin Pens (NovoPen®3, 30G, Novo Nordisk A/S, Bagsvaerd, Denmark), while Group 'V' were left quietly without disturbance. They were all culled at 3 h after injections. Hepatic TAT activity was assayed afterwards (see 4.2.5.3).

4.2.2.5 Optimisation of injection volumes

Corticosterone (25 mg/ml in DMSO, 20 or 50 μl, n=3) and vehicle (20, 50, 100 μl of DMSO, n=2) were injected s.c. into C57BL/6 mice by Insulin Pen. Mice were culled 3h post-injection. Hepatic TAT activity was measured by TAT assay afterwards (see 4.2.5.3).

4.2.2.6 Dose response of glucocorticoids delivered in low volume

C57BL/6 mice (n=3-7) were injected s.c. by Insulin Pens with 20 μl of either corticosterone (25, 75, 250, 750 mg/ml), 5αTHB (75, 250 mg/ml) or vehicle (DMSO). The maximum dose was limited by the solubility of the steroids. Three hours after injections, mice were culled and hepatic TAT activity was measured (see 4.2.5.3).

4.2.3 Investigation of transactivation and transrepression effects of 5αTHB following chronic infusion in C57BL/6 mice

4.2.3.1 Experimental design

Two pre-treatment blood pressure measurements were carried out in order to acclimatise animals to the measurements. After surgery to implant minipumps (Day 0), animals (12 mice per group) were infused with corticosterone, 5αTHB (50 μg/day) or vehicle (DMSO: propylene glycol = 1:1, v/v) using osmotic pumps. Animals were weighed on Day 0, 1, 4, 6 and 11, and blood pressure measured on Day 1, 4, 6 and 11. Glucose tolerance tests were carried out on Day 7. Animals were culled; blood and tissue collected on Day 14. A second series of mice were infused with the same treatments but did not undergo the above procedures to provide sufficient blood for analysis of plasma ACTH.

4.2.3.2 Mini-osmotic pump implantation

Mini-osmotic pumps were loaded with solutions of corticosterone, 5αTHB or vehicle (see 2.2.1.2, 50 μg/day). C57BL/6 mice were operated on Day 0 using the surgical procedures described in Section 2.3.2.

4.2.3.3 Measurement of systolic blood pressure

On mornings of Day 1, 4, 6 and 11, systolic blood pressure of each animal was measured as described in Section 2.4.1.

4.2.3.4 Glucose tolerance/insulin sensitivity

A glucose tolerance test was performed on Day 7 as described in Section 2.4.2.

4.2.3.5 Terminal procedures

Animals were culled, and trunk blood and tissues were collected as described in Section 2.4.3.

4.2.4 Activation of whole blood by LPS

Heparinized trunk blood was activated by increasing doses of LPS to study the impact of 5αTHB on cytokine release from white blood cells. The experiment was performed as described in Section 2.4.4.

4.2.5 Enzymology

4.2.5.1 Preparation of cytosol

Fresh liver samples were immersed in glucose/Hepes buffer before being cut into small pieces and homogenized using a mechanical homogeniser (Model PRO 200, PRO Scientic Inc, Monroe, CT, USA). Homogenates were centrifuged (1,000 g, 10 min, 4 °C) to precipitate unhomogenized tissue and heavy membranes (Livingstone, et al. 2000b). The supernatant was removed and subject to further centrifugation (124,000 g, 45 min, 4 °C; Optime TLX Ultracentrifuge, Beckman, Palo Alto, CA, USA). The subsequent clear supernatant was the cytosol which was transferred carefully into fresh tubes without the upper fatty layer and stored at -80 °C until required.

4.2.5.2 Determination of protein concentrations

The protein concentrations of cytosolic samples were determined using the Bio-Rad® protein assay kit (BioRad, Hemel Hempstead, UK) which is a dye-binding assay, based on the shift of absorbance maximum for an acidic solution of Coomassie® Brilliant Blue G-250 from 465 nm to 595 nm upon binding to proteins. The concentration of protein present in the sample is proportional to the increase of absorbance at 595nm.

A series of solutions of bovine serum albumin (BSA, fraction V) representing a range of concentrations (0, 0.1, 0.2, 0.4, 0.6, 0.8, 1.0 and 1.2 mg/ml) were prepared in duplicate with distilled water. Protein assay dye reagent (1 in 5) and cytosolic samples (1 in 50) were diluted in distilled water. Protein standards or cytosol dilutions (20 µl) were added respectively to diluted dye (2 ml), vortexed and

incubated (RT, 10 min). The mixtures were dispensed in duplicate into a flat-bottom 96-well plate (CellStar, Greiner Labortechnik, Germany). Thereafter, the absorbances of solutions resulting from the standards and samples were measured at λ595 nm using OPTImaxTM Tunable Microplate Reader (SOFTmax PRO, Molecular Device, Ismaning, Germany). The concentrations of protein in each sample were calculated from the standard curve, obtained from the linear relationship between absorbance against concentration. The intra-assay coefficients of variation were <10 %, and the values of R of acceptable standard curves were >0.99.

4.2.5.3 Tyrosine aminotransferase (TAT) activity assay

TAT is a cytosolic enzyme which contributes to the pathway involved with hepatic gluconeogenesis. It is significantly upregulated by the glucocorticoids (Grange, et al. 2001). TAT activity was determined by the spectrophotometric method of Diamondstone (1966), which was based on the reactions consisting of following two steps, and had been optimised for TAT in rat liver. The structures relating to the key reagents are shown below in Figure 4.1. However, here the assay described as follows was optimised to measure the hepatic TAT activity in mice.

Reaction 1: L-Tyrosine + α-ketoglutarate $\xrightarrow{\text{TAT}}$ pHPP+ L-glutamate

Reaction 2: pHPP + OH^- ⟶ pHBA+oxalate

Figure 4.1 The structural formula of the chemical compounds in TAT assay

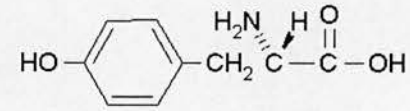

---------- L-Tyrosine

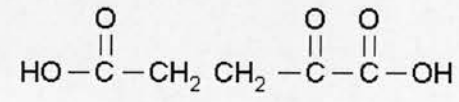

------ α-Ketoglutarate

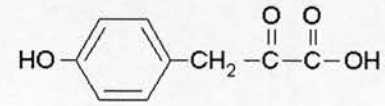

---------- 4-Hydroxyphenylpyruvate (pHPP)

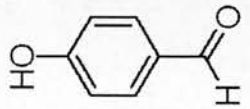

---------- 4-Hydroxybenzaldehyde (pHBA)

All the following solutions except NaOH were prepared with potassium phosphate buffer (0.2 M, pH 7.3). Tyrosine solution (10 M, 2.8 ml), pyridoxal phosphate (1.33 M, 0.1 ml), and diluted sample (0.5 mM, 0.2 ml) were successively added into a 10-ml glass tube (Fisher Scientific, Pittsburgh, PA, US) and incubated in a water-bath (30 min, 37 °C) before addition of α-ketoglutarate (0.3 M, 0.1 ml). Then the cytosol samples were added and well mixed, and incubated in the water-bath for another 10min (Reaction 1) before NaOH (10 M, 0.2 ml) was added and mixed immediately on a vortex. The reaction system was then allowed to stand at RT (Reaction 2), yielding pHBA with maximal absorbance at 331 nm. After 70 min, the absorbance (λ331 nm) was recorded using a spectrophotometer (UV-160A, Shimadzu Europa GmbH). The reference solution for the absorbance reading was prepared by adding the NaOH just before α-ketoglutarate to inactivate the enzyme.

The following equation was used to calculate TAT activity from absorbance values (the absorption coefficient for pHBA under the conditions of this assay is 1.99 $L \times mmol^{-1} \times mm^{-1}$):

$$\text{TAT activity (mmol/mg/min)} = 1030 \times \text{absorbance} / 19.9$$

4.2.5.4 Optimisation of TAT assay

The TAT assay was optimised to measure the activity of TAT in livers of mice. Before the final method (see 4.2.5.3) was determined, a series of validation experiments were performed to establish suitable reaction conditions.

4.2.5.4.1 Optimisation of Reaction Time 2 in mock system

The time of Reaction 2 was determined by investigating the kinetics of pHBA formation in alkali. NaOH (10 M, 0.1 ml) was added to pHPP (4.85×10^{-5} M, 2.8 ml) and tube shaken immediately. The mixture was transferred into silica cells ($1 cm^3$) without delay. Absorbance (λ331 nm) was recorded every minute for 100 min using the UV-visible spectrophotometer (UV-160A, Shimadzu Europa GmbH).

4.2.5.4.2 Linearity of absorbance with changes in pHPP concentration in mock system

Conditions as described in section 4.2.5.4.1 were used except for variation of pHPP concentrations: 0 (vehicle, water), 5, 10, 20, 40, 60, 80, 100 μM and absorbance recorded after 70 min.

4.2.5.4.3 Optimisation of Reaction Time 2 in enzyme system

The length of Reaction Time 2 was checked again when pHPP was generated using diluted mouse cytosol. This experiment was performed by the same procedure as described in the final protocol (see 4.2.5.3), except for

1) Concentration of cytosol (0.5 mg/ml);

2) Absorbance was recorded every minute for 80 min.

4.2.5.4.4 Optimisation of Reaction Time 1 in enzyme system

The procedure was the same as described in the final protocol (see 4.2.5.3) except for

1) Reaction Time 1 was varied from 0 to 18 min;

2) Concentration of cytosol was 0.5 mg protein/ml.

4.2.5.4.5 Linearity of absorbance with changes in protein concentrations

Various dilutions of the same cytosol sample (0.5, 1, 2, 4 and 6 mg/ml) were prepared in potassium phosphate buffer (0.2 M, pH 7.3). Conditions remained the same as above (see 4.2.5.4.4), with 10min for Reaction Time1.

4.2.6 Molecular biology: quantification of mRNA abundance of genes of interest

Total RNAs were isolated from snap frozen livers (see 2.5.1.1), pituitaries (see 2.5.1.3), subcutaneous fat and retroperitoneal fat (see 2.5.1.2) before RNA quantification (see 2.5.2). First strand cDNA was synthesised by reverse transcription (see 2.5.3). The mRNA abundances of TAT, PEPCK and angiotensinogen (Agt) in

liver, POMC and CRH receptor 1 in pituitary, 11β-HSD1, Agt, IL-6, TNFα and MCP-1 in subcutaneous and retroperitoneal fat were quantified by real-time PCR (see 2.5.5) and normalised against levels of the house-keeping gene cyclophilin A.

4.2.7 Biochemical assays

4.2.7.1 Quantification of plasma corticosterone

Corticosterone in plasma prepared from trunk blood was quantified by RIA (see 2.6.1).

4.2.7.2 Quantification of plasma glucose

Glucose in plasma collected during the glucose tolerance test was quantified by hexokinase assay as described in Section 2.6.2.

4.2.7.3 Quantification of plasma insulin

Insulin in plasma collected during the glucose tolerance test was quantified by ELISA as described in Section 2.6.3.

4.2.7.4 Quantification of plasma ACTH

ACTH in plasma prepared from trunk blood was quantified by ELISA (see 2.6.4).

4.2.7.5 Quantification of plasma NEFAs

NEFAs in plasma collected during the glucose tolerance test were quantified by spectrophotometry as described in Section 2.6.5.

4.2.7.6 Quantification of cytokines

Cytokines in samples collected in LPS-activated whole blood were quantified by CBA assay as described in Section 2.6.6.

4.2.7.7 Quantification of steroids by gas chromatography / mass spectrometry (GCMS)

Plasma 5αTHB was quantified from the remaining plasma samples (10-20 µl remaining) when other assays had been complete. Since it was not possible to test 5αTHB in individual samples, the plasma of animals receiving the same treatment was pooled (yielding 150 µl), allowing the determination of an average concentration.

Corticosterone and 5αTHB in the remainder of solutions used for the chronic infusion treatment were quantified by GCMS to confirm that both steroids neither degraded nor had precipitated out of solution.

4.2.7.7.1 Extraction of steroids from plasma

Glass tubes were prepared containing internal controls epi-corticosterone (epi-B) and epi-THB (containing 10 µg of both steroids in ethanol; Steraloids, Newport, RI, USA) prior to reduction to dryness under oxygen-free nitrogen (OFN) at RT. Standards of corticosterone and 5αTHB (0, 1, 2, 5, 10, 15, 20 ng of both in ethanol) or samples were added respectively to the tubes, and water (HPLC grade) was added to make the final volume to 200 µl. Then ethyl acetate (2 ml) was added and mixed so that steroids were extracted into the upper organic phase from lower water phase. Supernatant was transferred to glass vials and reduced to dryness under OFN. The remaining steroids in the water phase were extracted again by adding to another 2 ml of ethyl acetate, and supernatant was transferred to the same vials and reduced to dryness.

4.2.7.7.2 Derivatisation of steroids

The extracted steroids exhibit poor peak shapes and poor resolution if analysed in their natural state by GCMS. Thus they were derivatised so that they were more amenable to this method (more volatile and thermally stable). The steroids underwent a two-step derivatisation.

Firstly, methoxyamine (2%, v/v) in dry pyridine (50 µl) was added to each vial, and incubated (60 °C, 30 min) with the dried residues. Under these conditions, the carbonyl groups formed oxime derivatives ($CH_3ON=R$) that improved chromatographic performance and separation. Samples were reduced to dryness under OFN at 60 °C.

Secondly, trimethylsilylimidazole (TMSI, 50 µl), a strong silyl donor, was added and incubated (100 °C, 2 h) in capped vials; under these conditions, the hydroxyl groups were silylated where active hydrogen was replaced by trimethylsilyl (TMS).

4.2.7.7.3 Isolation of derivatised steroids

Derivatised steroids were isolated from residues by passing through Lipidex 5000 columns. Lipidex 5000 (1 ml; Perkin Elmer, UK) was added to a Pasteur pipette plugged with silanised glass wool, and prepared with mobile phase (cyclohexane: hexamethyldisilazane: pyridine, 98:1:1, v/v) by passing the mobile phase three times (1 ml each) through the columns. Eluate was discarded.

Samples and standards were reconstituted with mobile phase (1 ml) and applied to columns and allowed to pass through. Vials were also washed twice with mobile phase (0.5 ml each) and these washings were also passed through columns. Lastly fresh mobile phase (1 ml) was passed through columns. All eluate was collected into the fresh vials and reduced to dryness under OFN at 60 °C. Dried samples were reconstituted in hexane (200 µl), half of which was transferred to auto sampler vials and ready for GCMS analysis. Otherwise samples were stored at -20 °C until required.

4.2.7.7.4 Quantification of 5αTHB by GCMS

Gas chromatographic mass spectrometric (GCMS) analysis was performed in selected ion monitoring (SIM) mode using a Polaris Q GC-ion trap gas chromatography/mass spectrometer GC/MS (Thermo Finnigan, UK), fitted with a Db5MS capillary column (crossbond, 5 % diphenyl, 95 % dimethyl polysiloxane; length, 30 m; internal diameter, 0.25 mm; film thickness, 0.25 µm; Alltech, Camforth,

UK). Epi-corticosterone and epi-tetrahydrocorticosterone (epi-THB) were used as internal standards for the corticosterone and 5αTHB being measured. The initial oven temperature was 150 °C which was maintained for 1 min; then it was increased by 30 °C/min to 200°C and then by 8 °C/min to 300 °C and maintained for 8 minutes. Injection temperature was 240 °C, with a flow rate of helium of 1.0 ml/min; the ion source was heated at 200 °C; and MS transfer line was kept at 280 °C. The mass (*m/z*) and typical retention times of the ions monitored are shown in Table 4.1. Corticosterone and 5αTHB were quantified by integrating the area under each derivatised steroid peak and calculating the ratio of each peak relative to the peak of the relevant internal standard. The concentrations of steroid were determined by interpolation onto a linear calibration line of peak area ratio (PAR) versus concentrations of standards where R>0.99 was deemed acceptable. The minimum detection level for steroids was less than 1 nM.

Table 4.1 The masses and retention time of ions used for detection of derivatised steroids

Compound	**Retention time when isomers formed (min)**	**Ion monitored (*m/z*)**
Corticosterone	18.83, 18.95	548
Epi-corticosterone	18.32, 18.85	548
5αTHB	16.55, 16.96	564
Epi-5αTHB	16.31, 16.94	564

4.2.8 Statistics

Data are presented as mean ± SEM and were analysed by one-way, two-way, or three-way ANOVA, or repeated measures ANOVA, followed by Holm-Sidak post-hoc test where appropriate.

4.3 Results

4.3.1 Method development:

Hepatic TAT and PEPCK were measured as indicators of the metabolic effects of the positive effects of glucocorticoids on gene transcription mediated via GR binding to GREs. The following steps were performed to optimise the assay to quantify TAT in mouse liver.

4.3.1.1 Optimisation of Reaction Time 2 in mock system

The absorbance had reached a plateau by 70 min, when the coefficient of variation within 5 min was <5 %. This was selected as the time of incubation in routine assays (Figure 4.2).

4.3.1.2 Linearity of absorbance with changes in pHPP concentration in mock system

The absorbance of the production pHBA was proportional to the concentrations of pHPP, within the range of 0 – 100 μM, under the mock conditions (Figure 4.3).

4.3.1.3 Optimisation of Reaction Time 2 in enzyme system

Following the addition of NaOH in the presence of enzyme, the absorbance was maximal after 30 min remained stable for up to 80 min (Figure 4.4). The Reaction Time 2 was confirmed as 70 min.

4.3.1.4 Optimisation of Reaction Time1 in enzyme system

With fixed concentrations of reactants and a Reaction Time 2 of 70 min, the absorbance of pHBA increased linearly with time of Reaction 1, and was more reproducible when absorbance values were greater than 0.1 (Figure 4.5). Accordingly, the value of absorbance was not reliable if the reaction time was less than 6 min. Therefore, 10 min was used as the Reaction Time1 in the subsequent experiments.

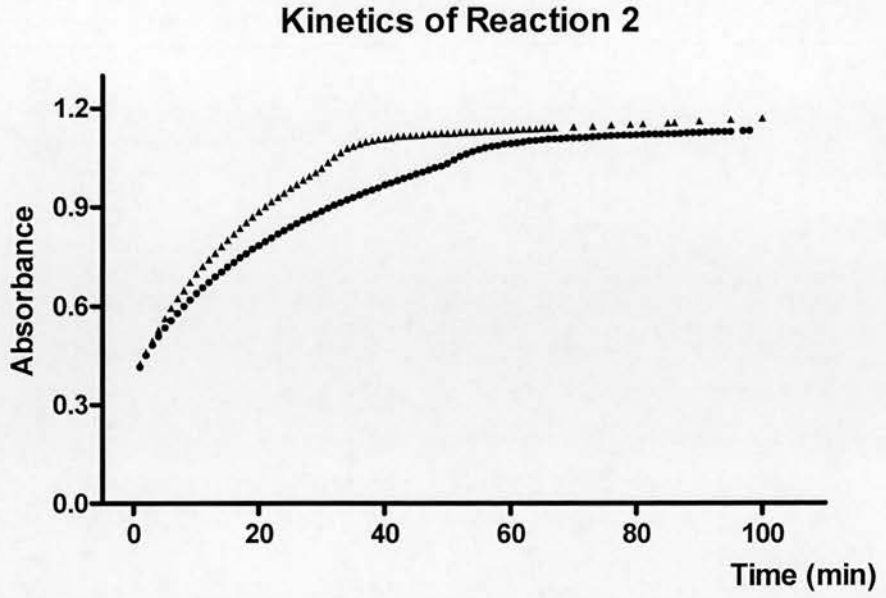

Figure 4.2 Kinetics of pHBA production (Reaction 2) was investigated in a mock system. With addition of NaOH (10 M, 0.1 ml) to pHPP (4.85×10^{-5} M, 2.8 ml), pHBA was produced and quantified spectrophotometrically at 331nm. The experiment was performed in duplicate.

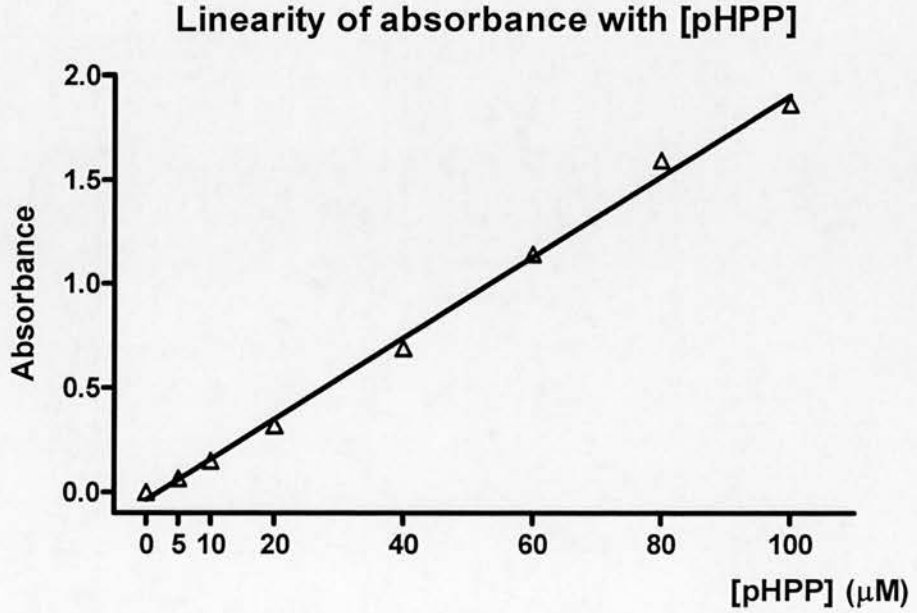

Figure 4.3 The amount of pHBA formed (measured by absorbance) was linear with increasing concentration of pHPP (0, 5, 10, 20, 40, 60, 80, 100 μM), R=0.998. The absorbance was recorded 70 min after addition of NaOH.

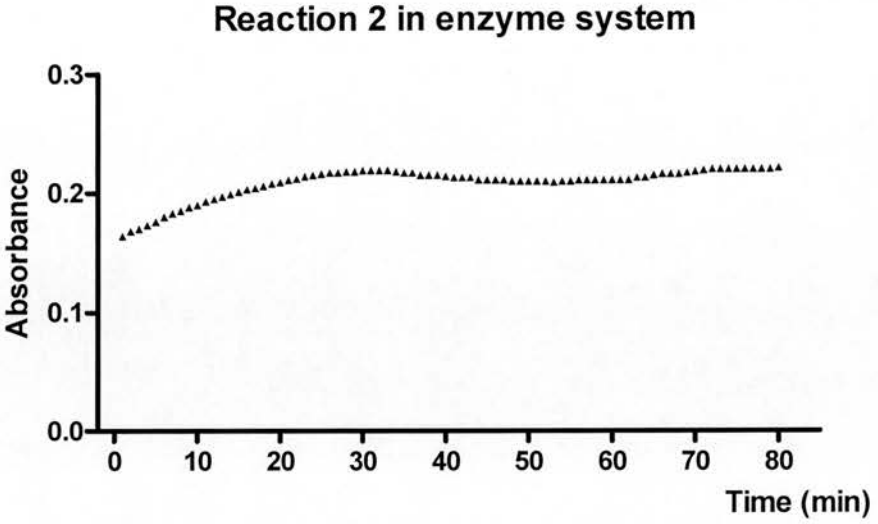

Figure 4.4 The kinetics of enzymatic production of pHBA (Reaction 2). Tyrosine (10 M, 2.8 ml), pyridoxal phosphate (1.33 M, 0.1 ml), and diluted cytosol (0.5 mg/ml, 0.2 ml) were successively added and incubated (37 °C, 30 min) before incubation with α-ketoglutarate (0.3 M, 0.1 ml) for 10min. NaOH (10 M, 0.2 ml) was added and mixed immediately, and then absorbance at 331 nm recorded every minute for 80 min at RT. The absorbance increased and remained stable after 30 min and up to 80 min.

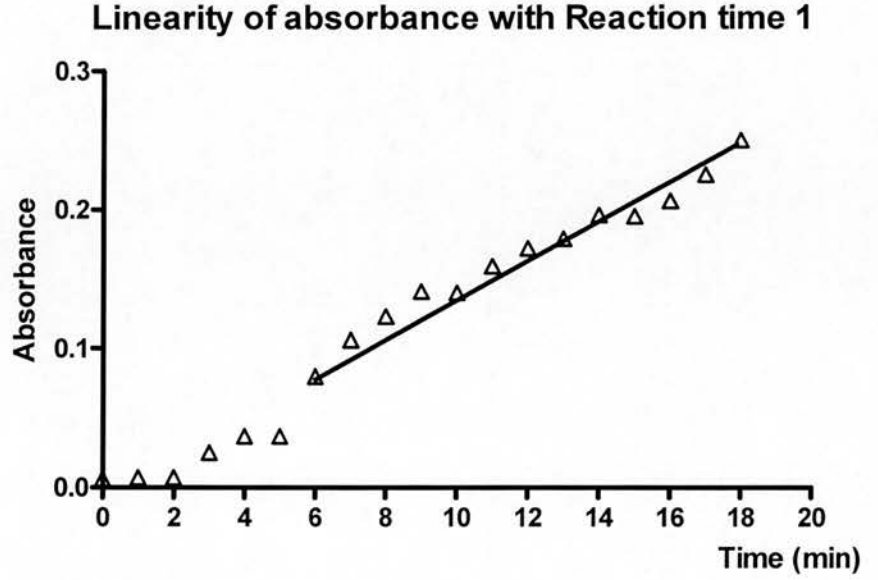

Figure 4.5 Absorbance was linear with the time length of Reaction 1. Tyrosine (10 M, 2.8 ml), pyridoxal phosphate (1.33 M, 0.1 ml), and diluted cytosol (0.5 mg/ml, 0.2 ml) were successively added and incubated (37 °C, 30 min) before incubation with α-ketoglutarate (0.3 M, 0.1 ml) for 0 - 18 min. NaOH (10 M, 0.2 ml) was added and mixed immediately, and then absorbance at 331nm was recorded after 70 min at RT. R=0.988.

4.3.1.5 Linearity of absorbance with protein concentrations

Absorbance increased linearly with protein concentrations within the range of 0.5 - 6 mg/ml, and absorbance at 331 nm from 0.1 - 2.0 (Figure 4.6). Absorbance data were not available with protein concentration higher than 6 mg/ml in this assay because the relevant value of absorbance exceeded the maximum range of the spectrophotometer.

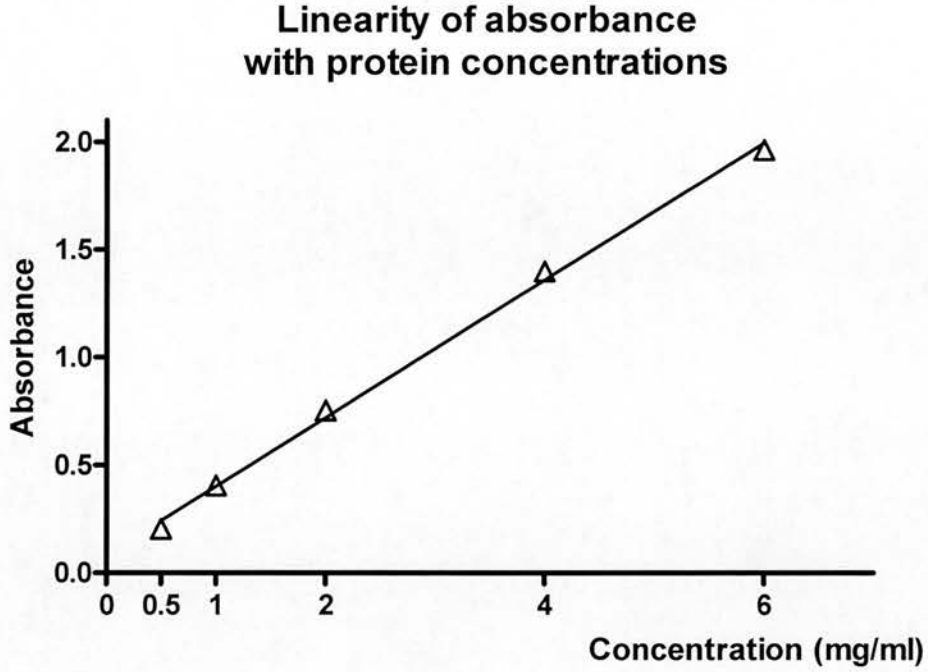

Figure 4.6 Absorbance increased linearly with protein concentrations of cytosol samples within the range of 0.5 – 6 mg/ml, and absorbance at 331 nm from 0.1-2.0, R=0.999. Conditions were the same as described in Figure 4.5 except for the concentrations of cytosol.

4.3.2 Investigation of transactivation effects of 5αTHB by acute administration of glucocorticoids to C57BL/6 mice

4.3.2.1 Time course of TAT induction following acute administration of glucocorticoids

Plasma corticosterone, glucose and insulin, and hepatic TAT activity, were assessed following acute administration of glucocorticoids.

Since the process of injection may induce an acute stress, circulating corticosterone levels were initially measured to ensure to the concentration of corticosterone achieved exceeded any stress response induced by the injection. As shown in Figure 4.7 (1), following injection of corticosterone, plasma corticosterone was elevated immediately, reached peak level at 1 h following the injection, and was cleared from circulation afterwards. In the animals receiving vehicle and 5αTHB, corticosterone levels also increased significantly at 1 h and returned to basal level afterwards. However, circulating corticosterone in these two groups was significantly lower than in those animals receiving corticosterone; and prolonged clearance of corticosterone was seen in animals receiving 5αTHB. Plasma 5αTHB was below the limits of detection in the GCMS assay in the small blood volumes from individual mice and was therefore measured in a sample pooled from several mice.

In the same animals, hepatic TAT activity was increased by injection of corticosterone reaching a peak at 3h. Although a similar time course was evident with 5αTHB, the extent of induction was less and indistinguishable from vehicle (Figure 4.7 (1)) which itself induced TAT expression and could be attributed to the increase in endogenous corticosterone caused by injection. These changes in TAT activity were not manifest in changes of circulating glucose but corticosterone alone caused an increase in plasma insulin at 6 h (Figure 4.7 (2)).

The effects of vehicle treatment on plasma corticosterone could be due to either the injection itself or the irritation induced by the injection solution, indirectly inducing adrenal synthesis of corticosterone. Alternatively, the vehicle itself could have induced changes in hepatic metabolism, perhaps in a response to eliminate the xenobiotic solvents. Therefore, before proceeding with further assessment of steroids, efforts were made to suppress the vehicle response. A time point of 3 h was selected since this reflected the peak response of TAT induction.

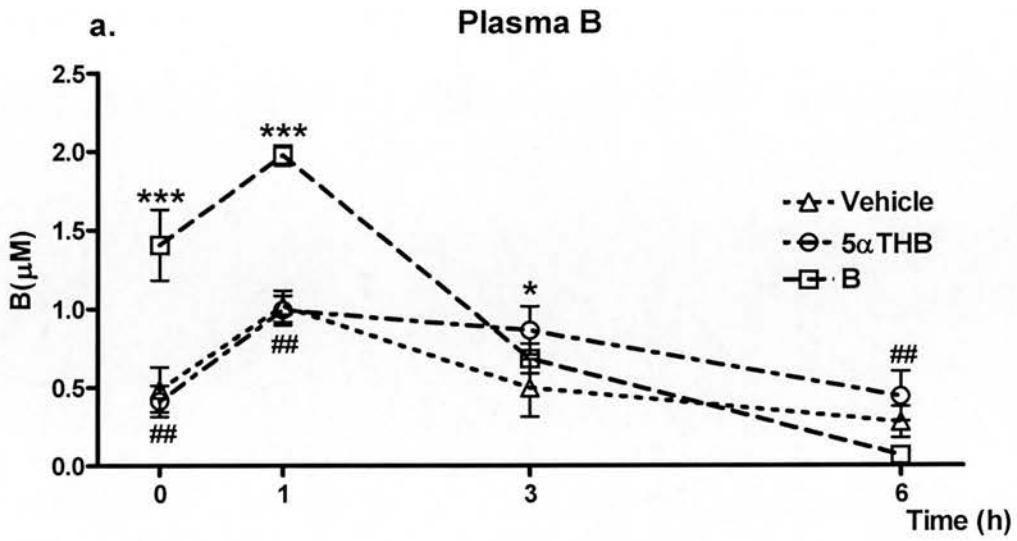

Plasma B: Treatment, p<0.001; Time, p<0.001; Interaction, p<0.001.

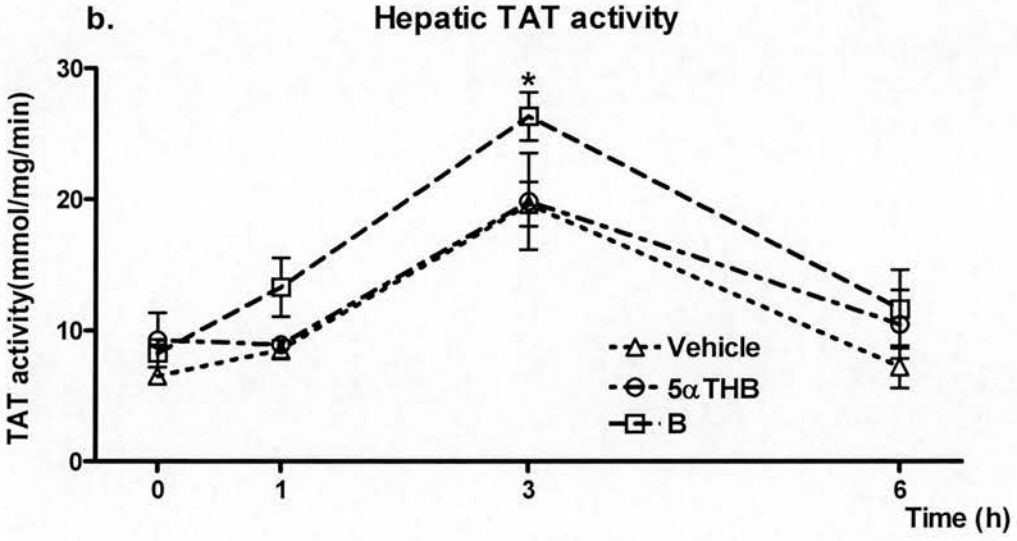

TAT: Treatment, p=0.066; Time, p<0.001; Interaction, n.s.

Figure 4.7 (1) (a) plasma B and (b) hepatic TAT activity in C57BL/6 mice 0, 1, 3 and 6 h after animals had been injected s.c. with 5αTHB, B (25 μg/mouse) or vehicle (100 μl each) in the solution of DMSO: ethanol: saline (0.9% w/v) = 13:1:6 v/v. The maximum effect of B to induce TAT activity was observed at 3 h, however vehicle also showed a significant response, making it difficult to interpret the impact of 5αTHB. Data are mean ± SEM, n=5. *p≤0.05, **p<0.01, ***p<0.001 versus vehicle, ##p<0.05, 5αTHB versus B; analyzed by two-way repeated measures ANOVA (one factor repetition) with Holm-Sidak post-hoc tests.

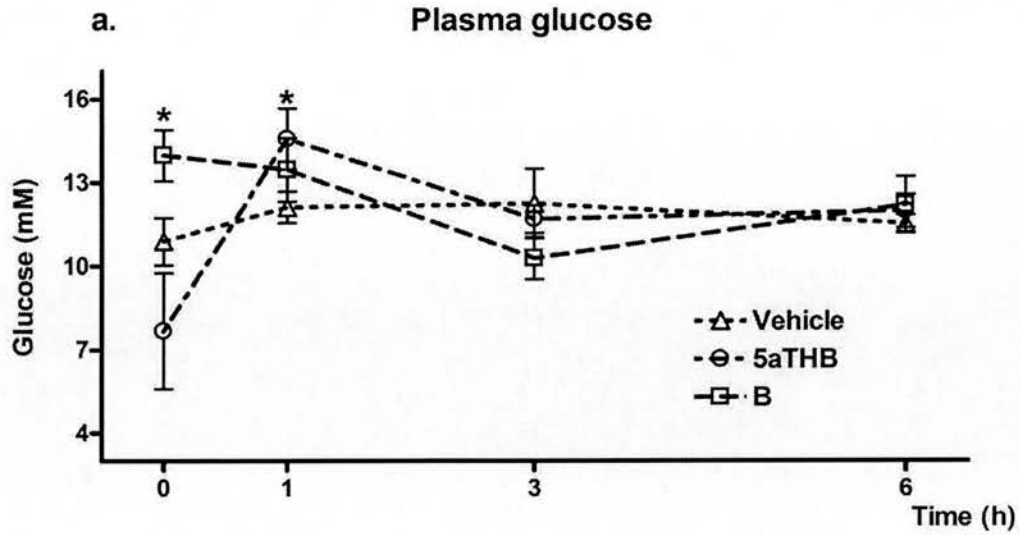

Glucose: Treatment, n.s.; Time, p=0.023; Interaction, p=0.017

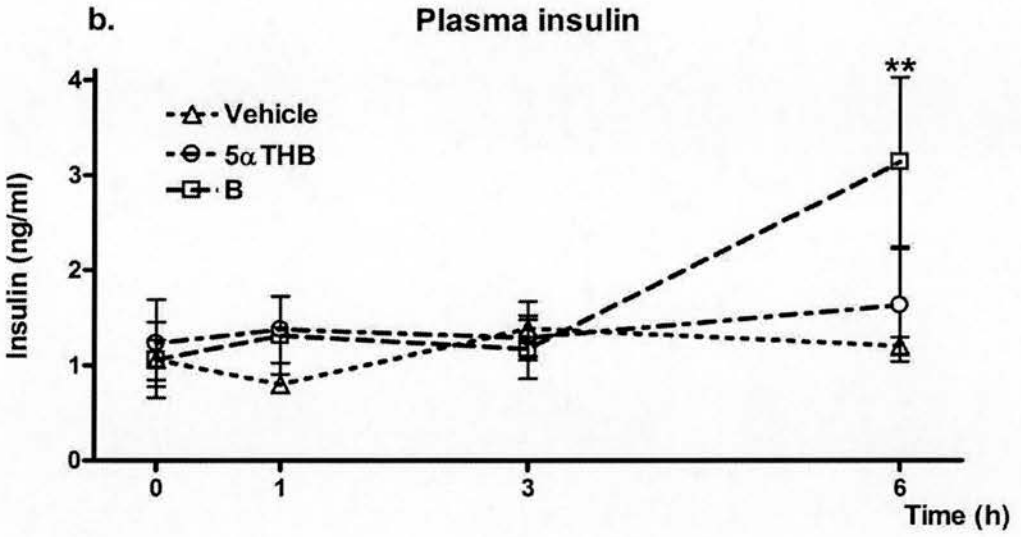

Insulin: Treatment, n.s.; Time, p=0.037; Interaction, n.s.

Figure 4.7 (2) (a) Plasma glucose and (b) insulin in C57BL/6 mice 0, 1, 3 and 6h after animals had been injected s.c. with 5αTHB, B (25μg/mouse) or vehicle (100μl each) in the solution of DMSO: ethanol: saline (0.9% w/v) = 13:1:6 v/v. Data are mean ± SEM, n=5. *p≤0.05, **p<0.01, ***p<0.001 versus vehicle; analyzed by two-way repeated measures ANOVA (one factor repetition) with Holm-Sidak post-hoc tests.

4.3.2.2 TAT activity in response to different vehicle injections

An experiment was performed to assess the effect of injection of different volumes of vehicle (Figure 4.8). Compared to the undisturbed mice as control, the hepatic TAT activity from mice injected with a small volume of DMSO (20μl) remained at the base line, while the vehicle solution used in 4.3.2.1 (DMSO: ethanol: saline (0.9% w/v) = 13:1:6 v/v; 100μl) was able to induce increased TAT activity at 3h (peak induction in previous experiment). Therefore the injection method was changed to reduce the volume of solutions.

4.3.2.3 Determination of injection volumes

Since it was planned to investigate the log dose response of corticosterone and 5αTHB, it was anticipated that up to ×100 of the basal dose would be dissolved into solution. Based on the vehicle test above and in consideration of the limited solubility of steroids in DMSO, the injection volume was increased marginally, which would have enabled administration of higher doses. However a stress response to vehicle was already apparent at 50μl and therefore 20μl was chosen for further experiments (Figure 4.9).

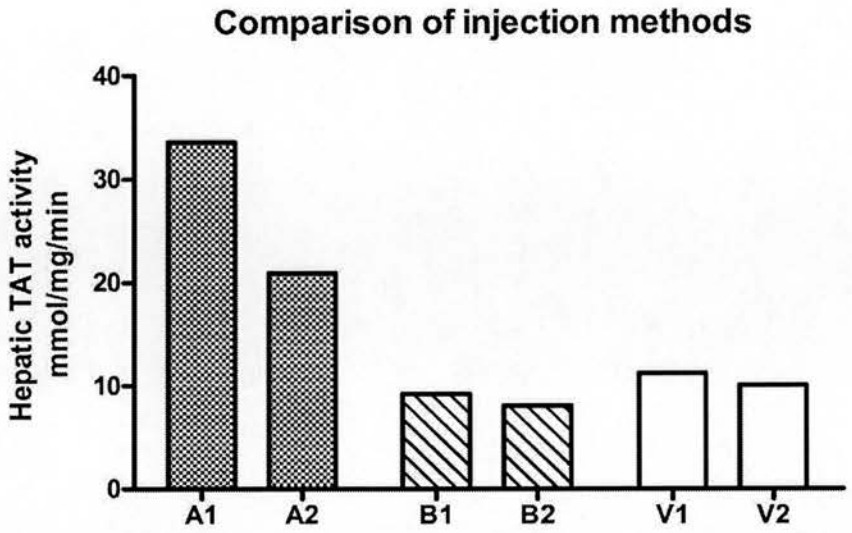

Figure 4.8 Hepatic TAT activity in response to different vehicle injections. Two mice in each group were given s.c. injection, either with (A) the vehicle solution (100 µl, DMSO: ethanol: saline (0.9% w/v) = 13:1:6 v/v) or (B) DMSO (20 µl) by Insulin Pen. (V) Two mice were undisturbed. TAT activity in livers collected at 3h post-injection was measured by TAT assay. Treatment A increased TAT activity while Treatment B kept TAT at the basal level.

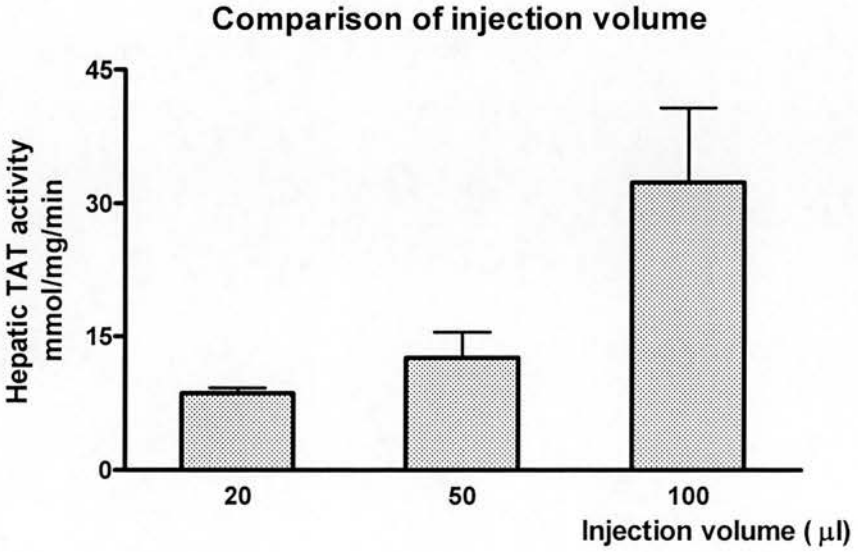

Figure 4.9 Hepatic TAT activity in response to different injection volumes of DMSO. Vehicle (20, 50, 100µl of DMSO) were injected s.c. by Insulin Pen. TAT activity in livers collected at 3h post-injection was measured by TAT assay. Data are mean±SEM, n=2. Injection volumes > 20µl vehicle increased hepatic TAT activity more than basal levels.

4.3.2.4 Dose response of glucocorticoids

Using the approach determined above, false positives caused by stress of injection could be successfully avoided, allowing detection of smaller changes induced by test steroids. Indeed, under these conditions, plasma corticosterone increased with the increasing dose of injected corticosterone, but reassuringly this was only observed in animals receiving this hormone (Figure 4.10 (1)); animals receiving 5αTHB had circulating corticosterone not significantly different from vehicle. All doses of corticosterone increased hepatic TAT activity, although this effect was observed over a narrow dynamic range. However, 5αTHB failed to increase TAT activity (Figure 4.10 (1)). Plasma glucose or insulin was not significantly affected by either glucocorticoid treatments (Figure 4.10 (2)).

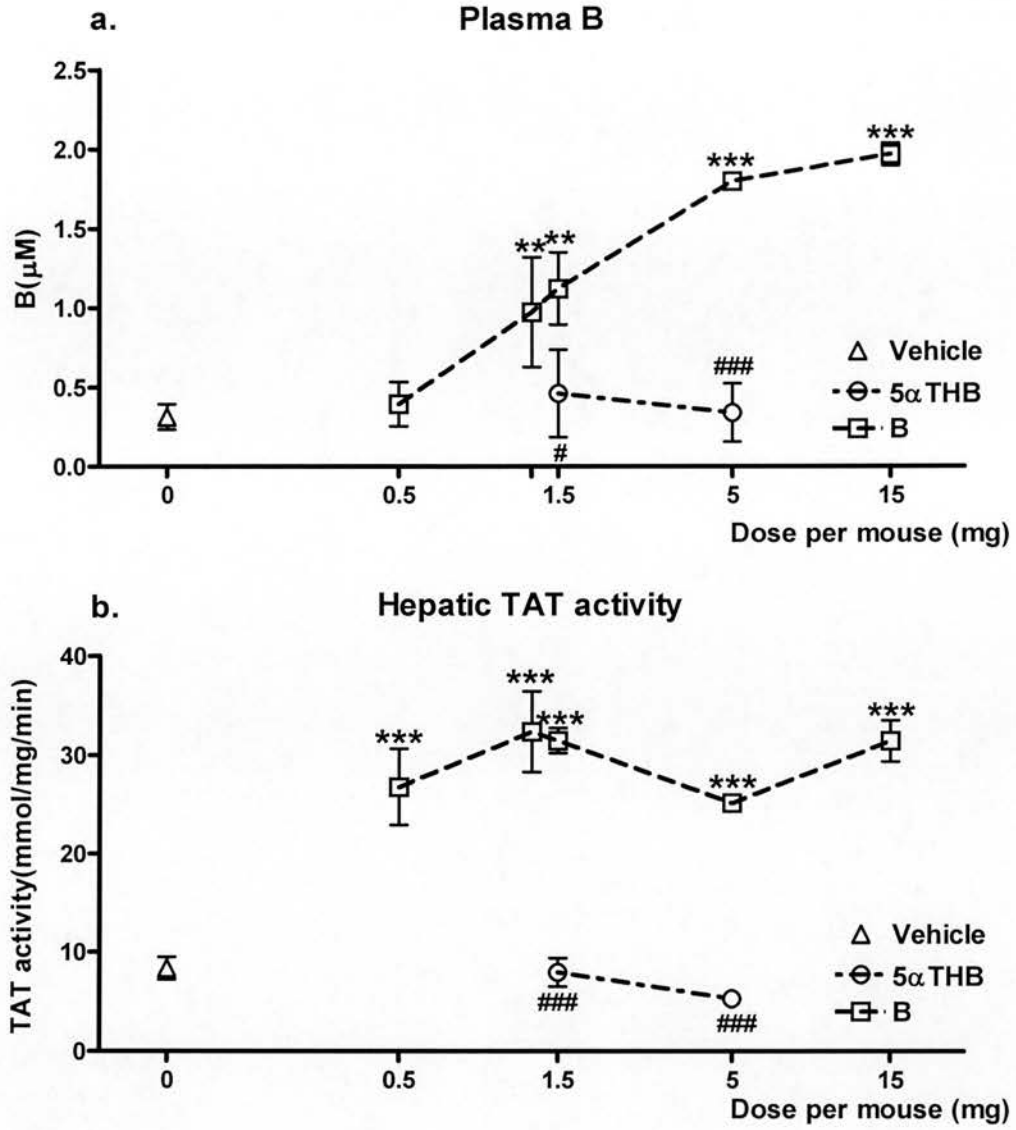

Figure 4.10 (1) Dose responses of (a) plasma B and (b) hepatic TAT activity to B and 5αTHB. C57BL/6 mice (n=3~7) were injected s.c. with 20 μl of either B (25, 75, 125, 250, 750 mg/ml), 5αTHB (75, 250 mg/ml) or vehicle (DMSO). Mice were culled 3 h following injection. Plasma B was quantified by RIA, and hepatic TAT activity by TAT assay. A dose response of B was observed in the circulation; hepatic TAT activity was increased over a narrow dynamic range. 5αTHB did not alter plasma B, and failed to increase TAT activity. **p<0.01, ***p<0.001 versus vehicle; #p<0.05, ###p<0.001 versus B; analysed by one-way ANOVA with Holm-Sidak post-hoc tests.

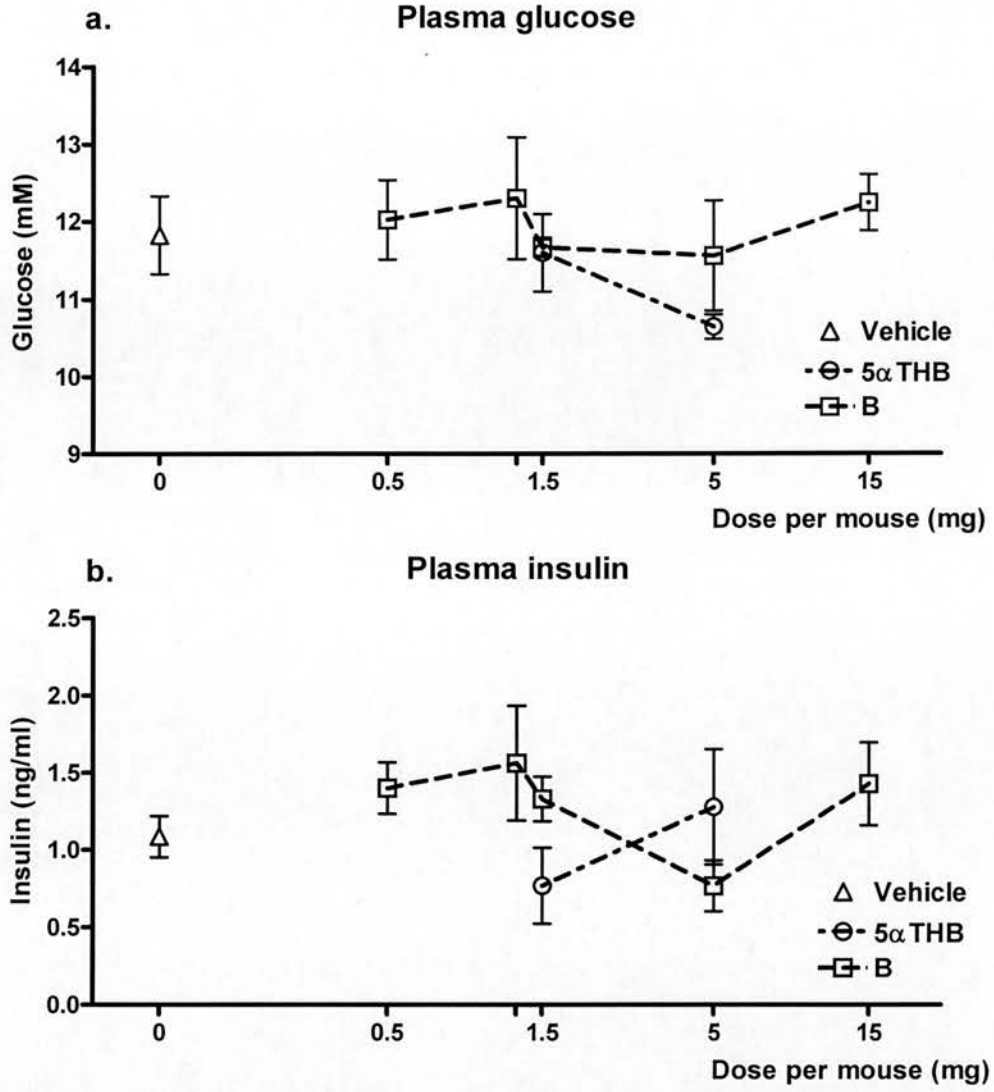

Figure 4.10 (2) Dose responses of (a) plasma glucose and (b) insulin to B and 5αTHB. C57BL/6 mice (n=3~7) were injected s.c. with 20 µl of either corticosterone (25, 75, 125, 250, 750 mg/ml), 5αTHB (75, 250 mg/ml) or vehicle (DMSO). Mice were culled 3 h following injection. Plasma glucose was measured by glucose assay, and plasma insulin by insulin ELISA. No significant changes were observed with either steroid at 3 h, analysed by one-way ANOVA.

4.3.3 Investigation the effects of 5αTHB on GR transactivation and transrepression by chronic infusion in C57BL/6 mice

It was possible that the effect of 5αTHB had been missed following acute injections of steroids, since 5αTHB might exert a slower action than corticosterone, based on our *in vitro* findings in Chapter 3. Therefore, the steroids were administered over a two week time period, performed by chronic infusion. Effects were sought in aspects of glucocorticoid action on the HPA axis, fuel metabolism, and inflammation.

4.3.3.1 Infusion of steroids

4.3.3.1.1 Glucocorticoids in circulation

Increased plasma corticosterone concentrations were observed only in the animals receiving this infusion but not in those receiving vehicle or 5αTHB. Basal corticosterone levels in the vehicle group confirmed that animals were not stressed before cull, and in 5αTHB group confirmed that 5α-reduction of corticosterone is an irreversible metabolic pathway (Figure 4.11a).

It was not possible to test 5αTHB in individual plasma samples (10-20 μl remaining). Therefore all remaining plasma samples were pooled when other assays had been complete to allow the determination of an average concentration by GCMS. Circulating 5αTHB in animals receiving this steroid was detectable but 10-fold lower than the circulating corticosterone in animals on corticosterone treatment (Figure 4.11a). Plasma 5αTHB in animals on other treatments was under the minimum detection limit.

4.3.3.1.2 Glucocorticoids in infusion solution

The remainder of the infusion solution was measured for concentrations of corticosterone and 5αTHB after the course of infusion in animals. The concentrations of steroids in theory (prepared as described in Section 2.2.1.2) and measured in solution were listed in Table 4.2. These are not substantially different.

Table 4.2 Concentrations of steroids in the remaining of infusion solution

	Measured Concentration	Concentration in theory
Corticosterone	3.271 mg/ml (9.4 mM)	4.165 mg/ml (12.0 mM)
5αTHB	4.238 mg/ml (12.1 mM)	4.165 mg/ml (11.9 mM)

4.3.3.1.3 Indices of HPA axis activity

Administration of corticosterone was accompanied by suppression of the HPA axis reflected in smaller adrenal glands (Figure 4.11c), while 5αTHB did not induce this effect. However, plasma ACTH was suppressed by both steroid treatments (Figure 4.11b). In pituitaries, the transcript abundances of POMC and CRH receptor were not significantly affected by any glucocorticoid infusion (Figure 4.11d, e).

4.3.3.2 Body weight and blood pressure

During the experiment, body weight increased with time ($p<0.001$) and there was a significant effect of corticosterone but not 5αTHB to reduce body weight on Day 11 (Figure 4.12a), whereas animals on vehicle treatment continued to gain weight.

Treatment with corticosterone or 5αTHB infusion did not induce significant difference in blood pressure, although a trend for corticosterone induced hypertension was observed on Day 11 ($p=0.08$). Some of the systolic blood pressures were stressed measurements e.g. the increased blood pressures of vehicle cohorts on Day 6 (Figure 4.12b).

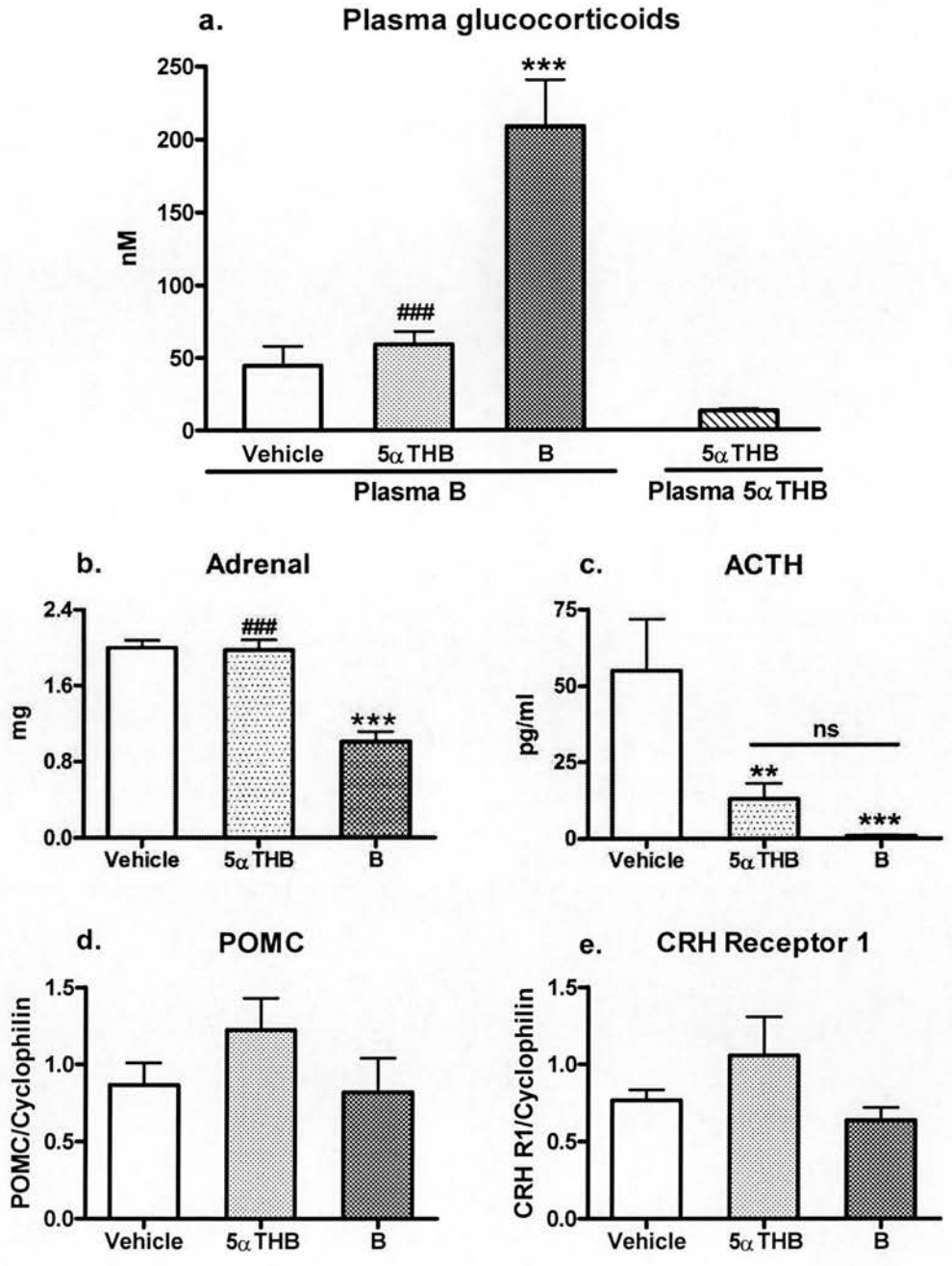

Figure 4.11 Indices of circulating glucocorticoids and HPA feedback following infusion (0.5 µl/h, 14d) of 5αTHB or B (50 µg/day) or vehicle (DMSO / propylene glycol, 1:1), n=12. (a), Plasma B (quantified by RIA) and 5αTHB (quantified by GCMS) was increased only in the group receiving the relevant steroids (plasma 5αTHB in animals receiving vehicle or B was not detectable). (b), Formalin fixed right adrenal weights, were reduced only in the group receiving B. (c), Plasma ACTH (n=10) was suppressed by treatment with both 5αTHB and B. (d, e), Pituitary mRNA of POMC and CRH receptor 1 (quantified by real-time PCR), was not affected by any steroid. Data are mean ± SEM, **p<0.01, ***p<0.001 versus vehicle; ###p<0.001 versus B, analysed by one-way ANOVA with Holm-Sidak post tests.

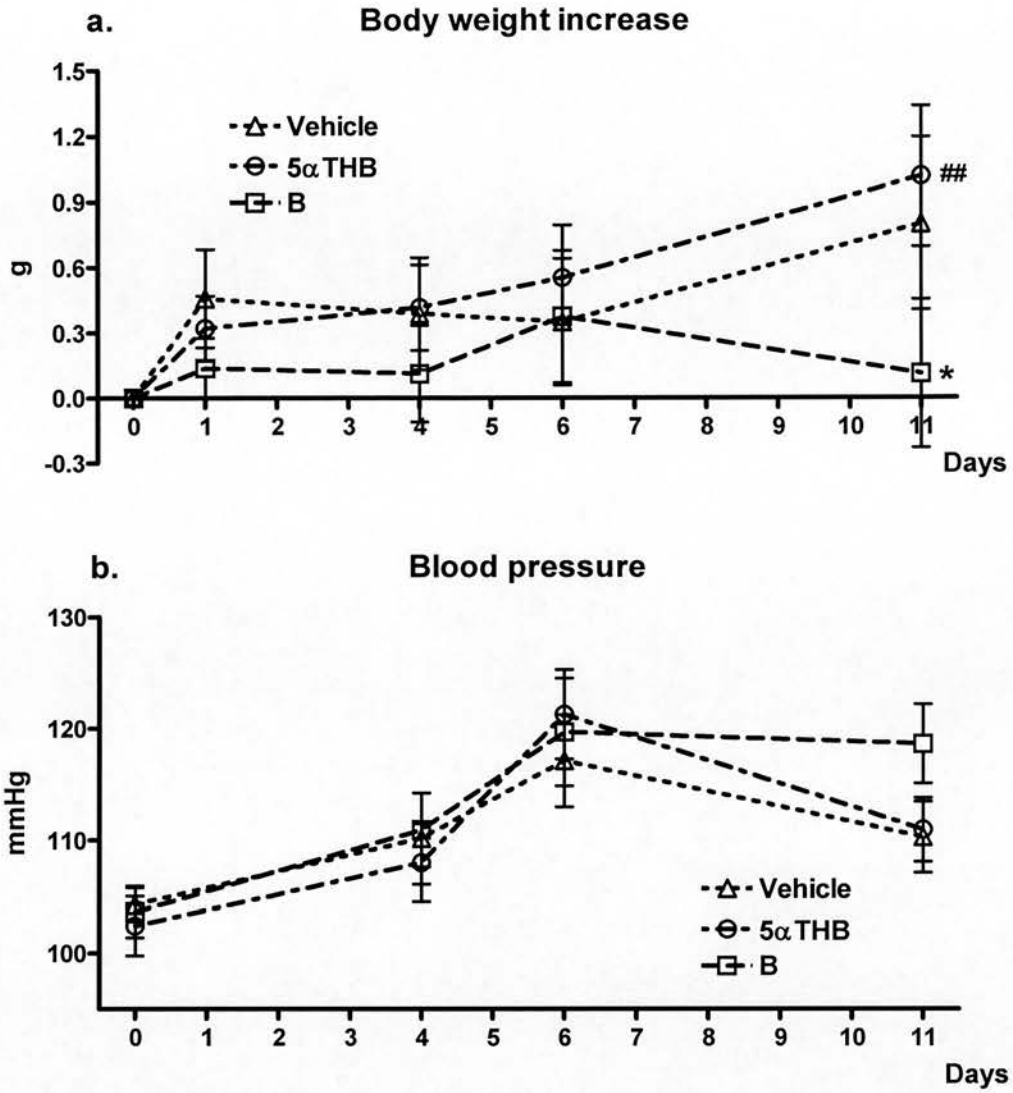

BW increase: Treatment, p=0.473; Time, p<0.001; Interaction, p=0.188.
Blood pressure: Treatment, p=0.626; Time, p<0.001; Interaction, p=0.629.

Figure 4.12 (a) Body weight increase, recorded on Day 0, 1, 4, 6 and 11 after the surgery of mini-pump implantation. A significant effect of B to reduce body weight was shown on Day 11. (b) Systolic blood pressure measured by tail cuff prior to (Day 0) and after (Day 4, 6 and 11) steroid infusions was not altered by any treatment. Blood pressure data on Day 0 were the average values from two pre-treatment measurements. Systolic blood pressure was not affected by steroid treatment although blood pressure of both steroids and vehicle-treated controls tended to be higher after minipump implantation. Data are mean ± SEM, n=12, *p<0.05 versus vehicle, analysed by two-way repeated measures ANOVA (one factor repetition) with Holm-Sidak post-hoc tests.

4.3.3.3 Weights of organs

Smaller thymus glands were seen only in animals receiving corticosterone (Figure 4.13a), consistent with higher circulating levels of plasma corticosterone detected in these animals. Other organ weights were unaffected (expressed as weight in Figure 4.13(1), or in relation to body weight in Figure 4.13(2)). Subtle redistribution of fat to subcutaneous depots was observed following infusion of corticosterone only (Figure 4.14a), while other adipose tissues were not affected (expressed as weight in Figure 4.14(1) or in relation to body weight in Figure 4.14(2)).

4.3.3.4 Glucose tolerance tests

Following fasting for six hours, basal plasma glucose was not altered by either steroid infusion. Circulating glucose was elevated soon after intraperitoneal administration of glucose in all animals and was cleared after 15 min (Figure 4.15a) in response to insulin action. However glucose tolerance was not significantly altered by either treatment. Animals receiving corticosterone infusion showed increased plasma insulin at 15 min (Figure 4.15b) and NEFAs at 90min (Figure 4.15c) following glucose administration; however 5αTHB did not exert any significant effects.

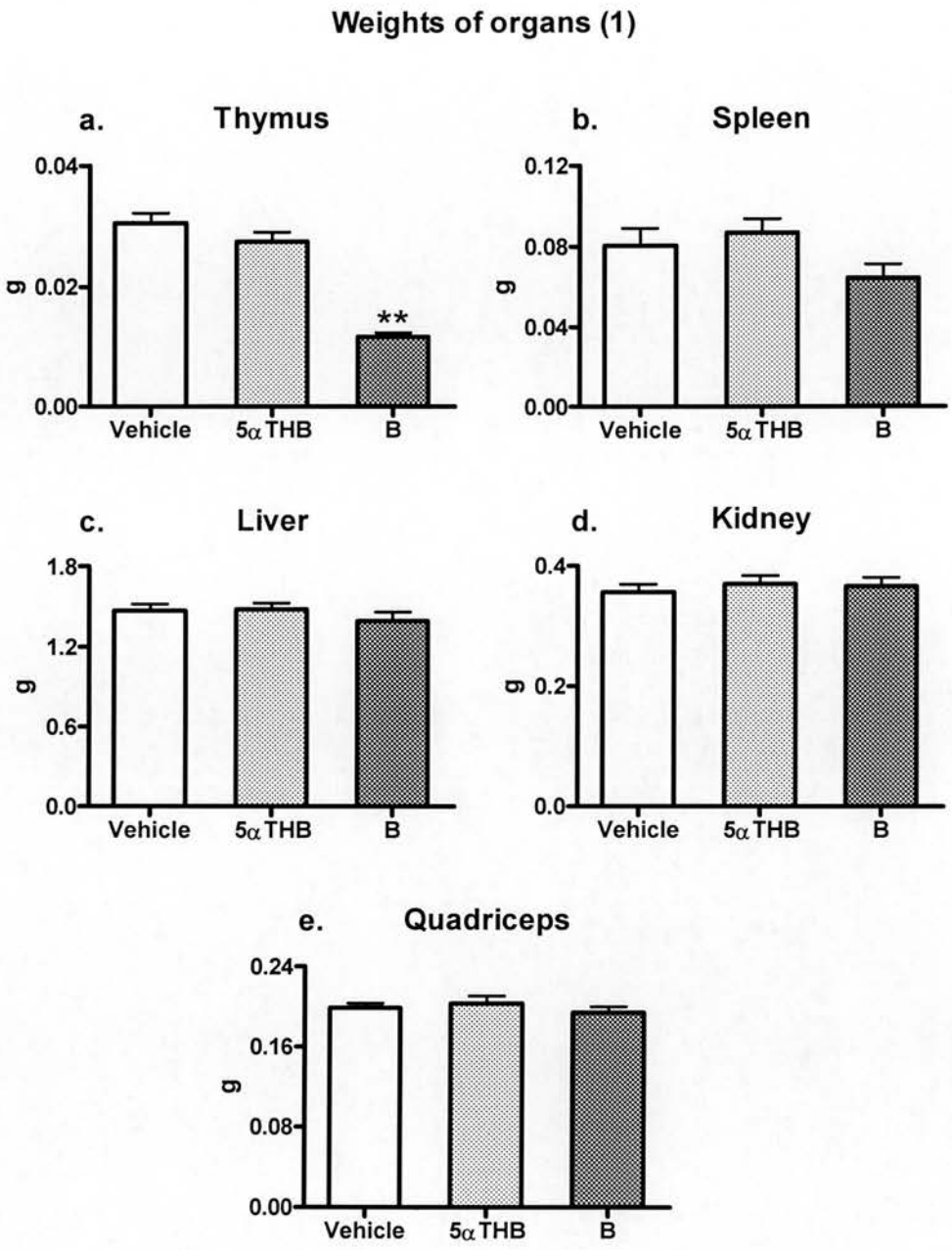

Figure 4.13 (1) Organ weights. (a) Thymus weights were reduced only in the group receiving B. Weights of (b) spleens, (c) livers, (d) kidneys and (e) quadriceps were not affected by either treatment. These organs were weighed immediately after dissection on Day 14. Data are mean ± SEM, n=12, **p<0.01, analysed by one-way ANOVA with Holm-Sidak post-hoc tests.

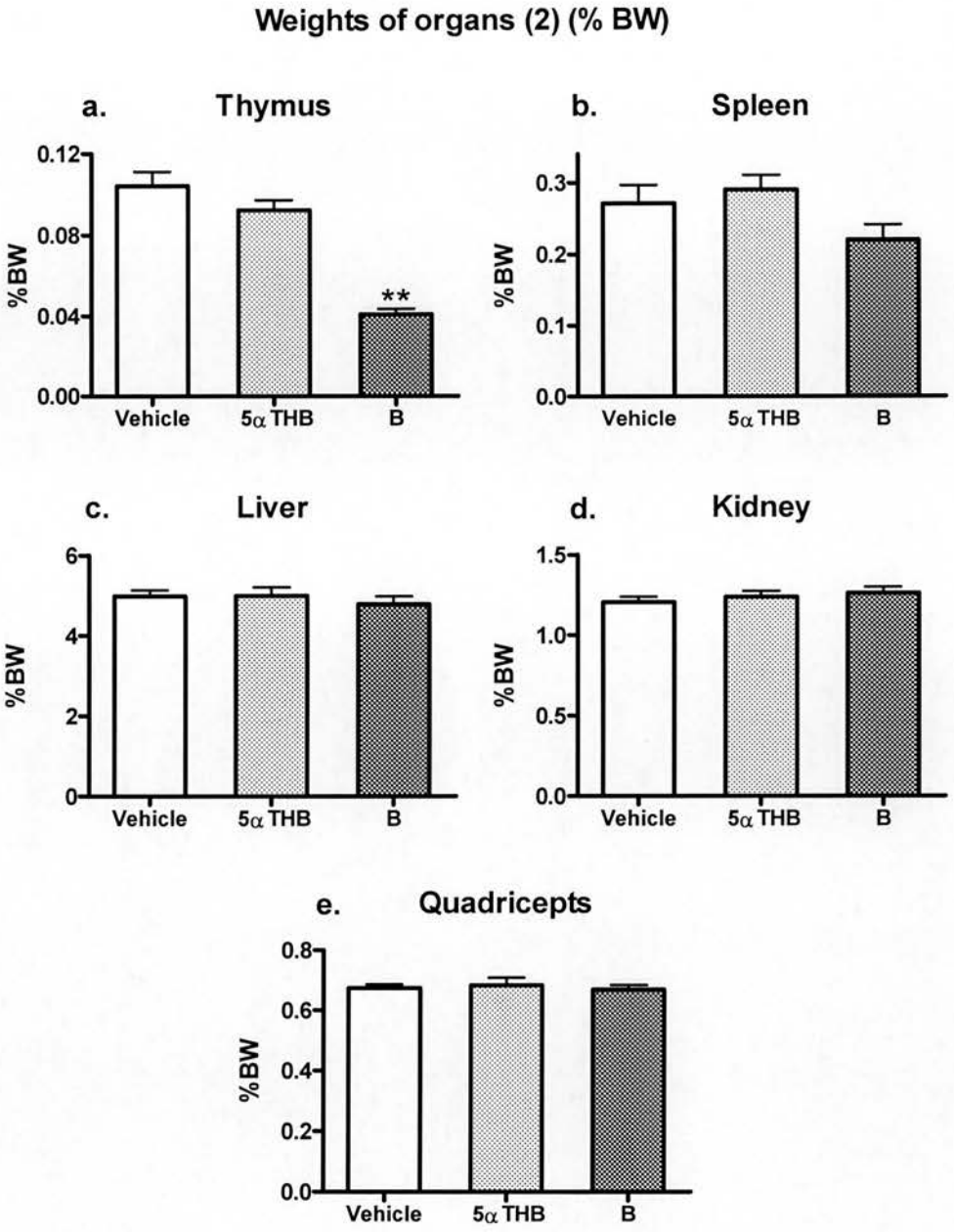

Figure 4.13 (2) Organ weights presented as percentage of body weights. (a) Thymus weights were reduced only in the group receiving B. Weights of (b) Spleens, (c) livers, (d) kidneys, and (e) quadriceps were not affected by either treatment. These organs were weighed immediately after dissection on Day 14. Data are mean ± SEM, n=12, **p<0.01, analysed by one-way ANOVA with Holm-Sidak post-hoc tests.

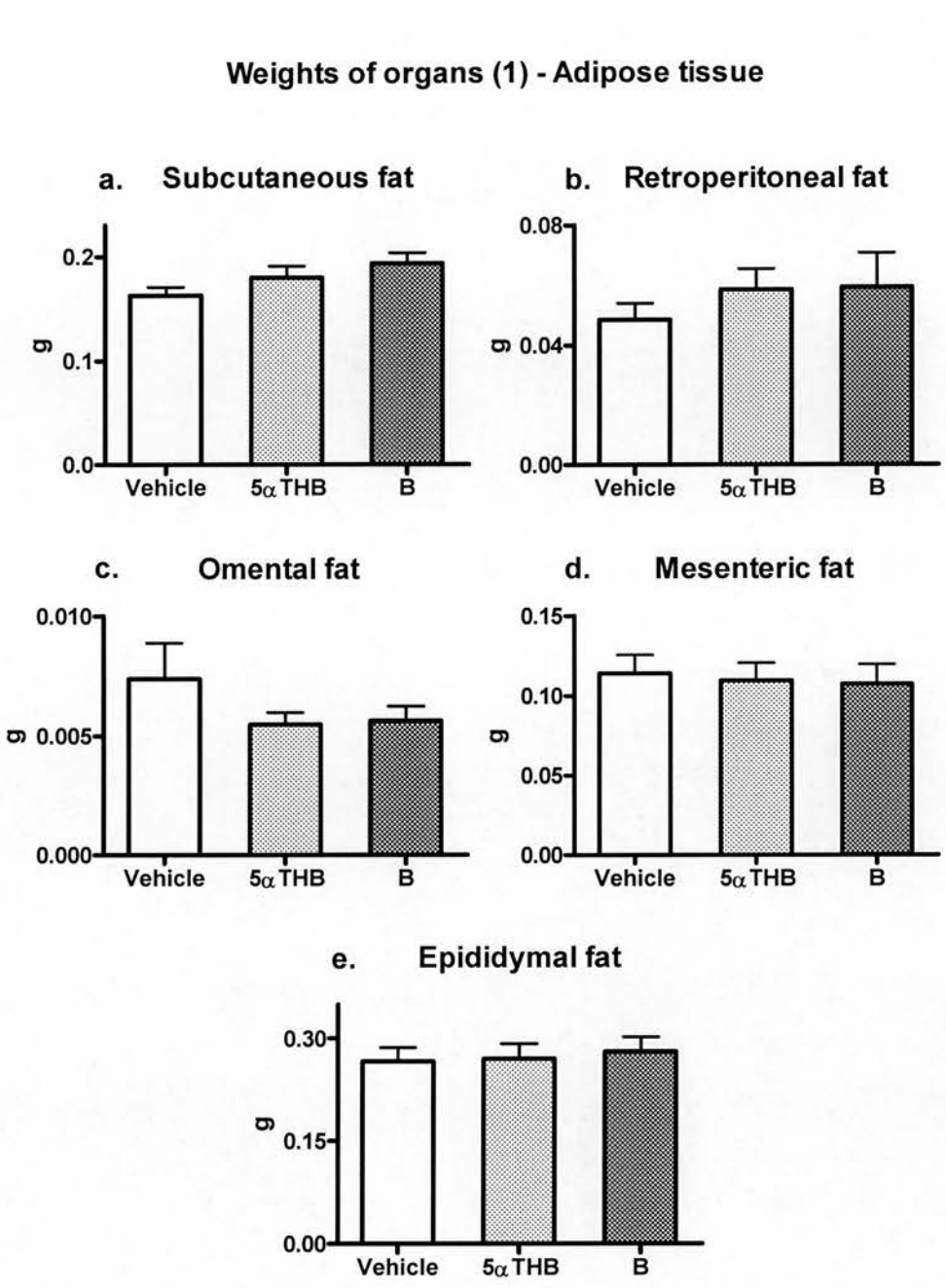

Figure 4.14 (1) Weights of adipose depots, (a) subcutaneous, (b) retroperitoneal, (c) omental, (d) mesenteric, and (e) epididymal fat. Five pads of adipose tissue were weighed immediately after dissection on Day 14. Only the weight of subcutaneous fat increased upon treatment with B (See Figure 4.14(2)). Other fat pads were unaffected. Data are mean ± SEM, n=12, analysed by one-way ANOVA with Holm-Sidak post-hoc tests. *$p<0.05$ versus vehicle.

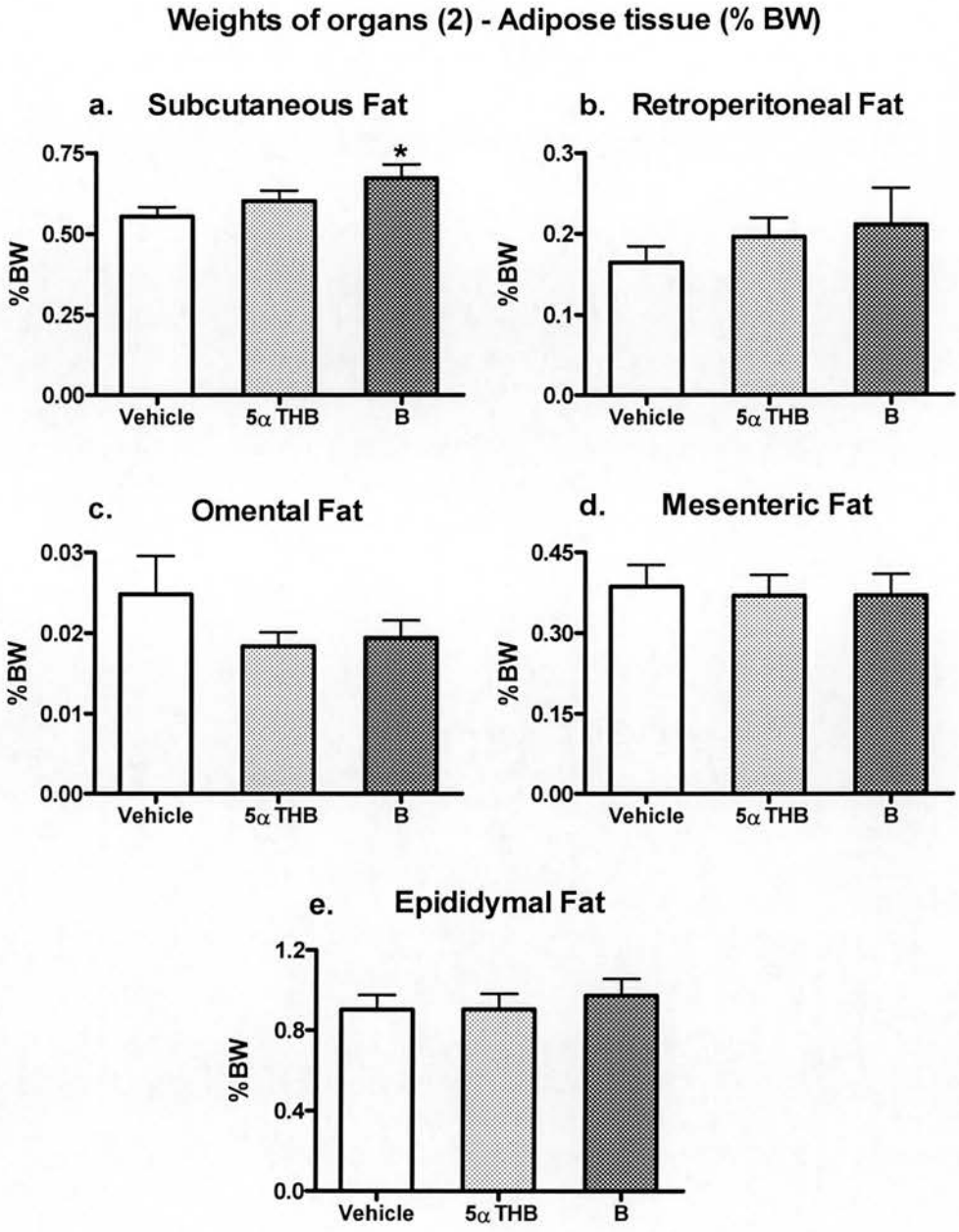

Figure 4.14 (2) Weights of adipose depots presented as percentage of body weights. (a) Subcutaneous, (b) retroperitoneal, (c) omental, (d) mesenteric, and (e) epididymal fat. Five pads of adipose tissue were weighed immediately after dissection on Day 14. Only the weight of subcutaneous fat increased upon treatment with B. Other fat pads were unaffected. Data are mean ± SEM, n=12, analysed by one-way ANOVA with Holm-Sidak post-hoc tests. *$p<0.05$ versus vehicle.

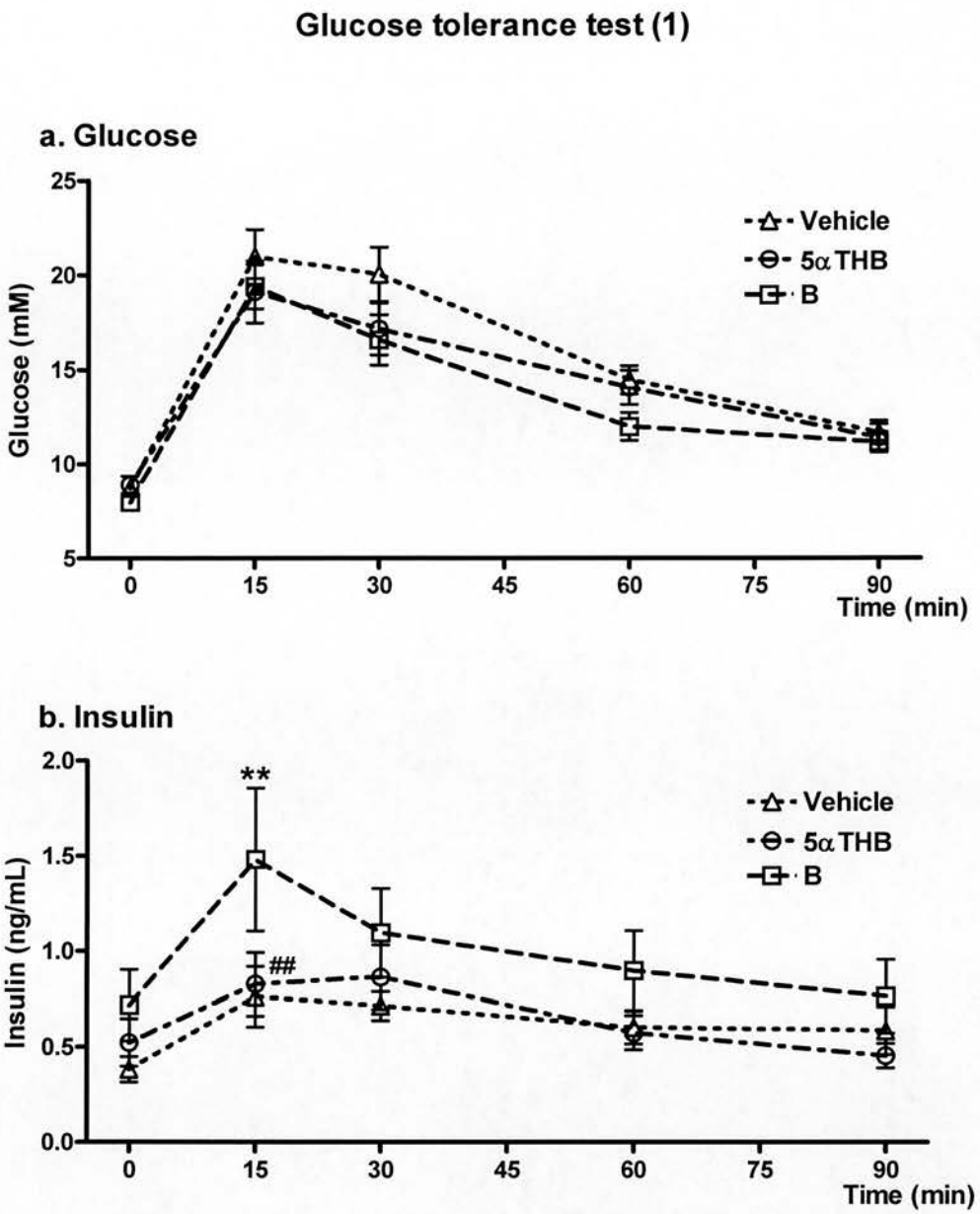

Figure 4.15 (1) (a) Plasma glucose and (b) insulin in glucose tolerance test (GTT). Mice were fasted for 6 h before they were injected i.p. with 2 g/kg BW of glucose, and blood samples were collected at 0, 15, 30, 60 and 90 min. (a) Plasma glucose and (b) insulin are presented in time course curves. Glucose concentrations were not significantly different between each group during the time course of GTT. Animals receiving B infusion showed elevated plasma insulin at 15 min following glucose administration however 5αTHB did not exert such significant effect. Data are mean ± SEM, n=12, **p<0.01, ***p<0.001 versus vehicle, #p<0.05, ##p≤0.01 5αTHB versus B, analysed by two-way repeated measures ANOVA (one factor repetition) with Holm-Sidak post-hoc tests.

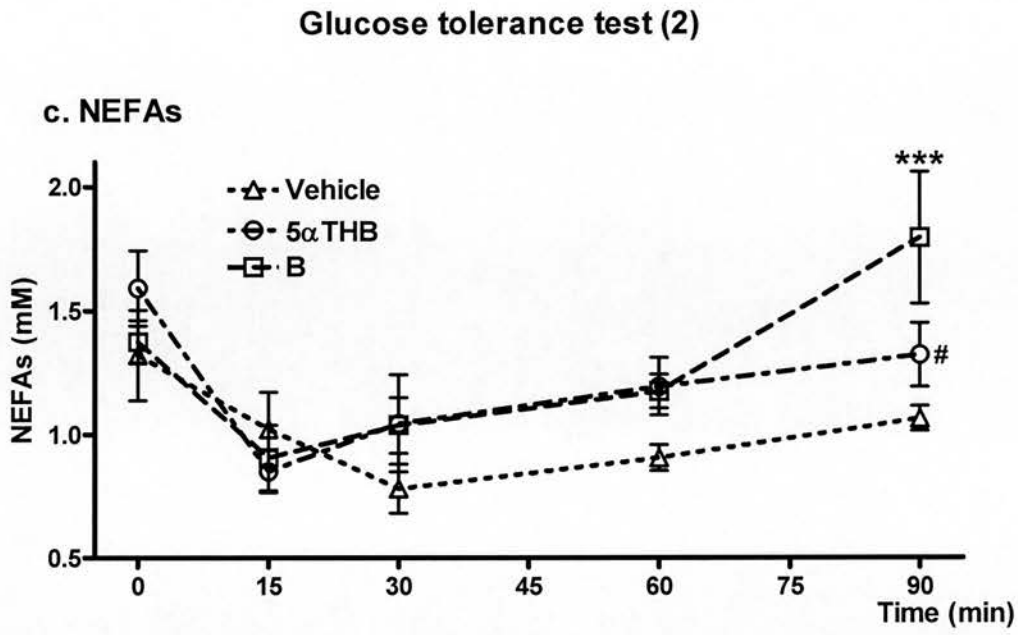

NEFAs: Treatment, p=0.071; Time, p<0.001; Interaction, p=0.043.
B vs. vehicle, p=0.025.

Figure 4.15 (2) (c) Plasma NEFAs in glucose tolerance test. Mice were fasted for 6 h before they were injected i.p. with 2g/kg BW of glucose, and blood samples were collected at 0, 15, 30, 60 and 90 min. Animals receiving B infusion showed elevated plasma NEFAs at 90 min following glucose administration however 5αTHB did not exert such significant effect. Suppression from basal level (0 min) to 15 min following glucose injection was not significantly different between treatments. Data are mean ± SEM, n=12, ***p<0.001, versus vehicle, #p<0.05, 5αTHB versus B, analysed by two-way repeated measures ANOVA (one factor repetition) with Holm-Sidak post-hoc tests.

4.3.3.5 Glucocorticoid responsive genes in liver

Changes were not observed in either hepatic TAT activity or in abundance of transcript for TAT, PEPCK or angiotensinogen following either corticosterone or 5αTHB infusion (Figure 4.16).

4.3.3.6 Glucocorticoid responsive genes in adipose tissues

The glucocorticoid responsive gene transcripts in adipose tissue, 11β-HSD1, was significantly increased in both subcutaneous and retroperitoneal fat pads in response to infused corticosterone, while increased angiotensinogen expression was only detected in retroperitoneal fat following the same treatment. However, changes in expression of these target genes were not induced by 5αTHB (Figure 4.17).

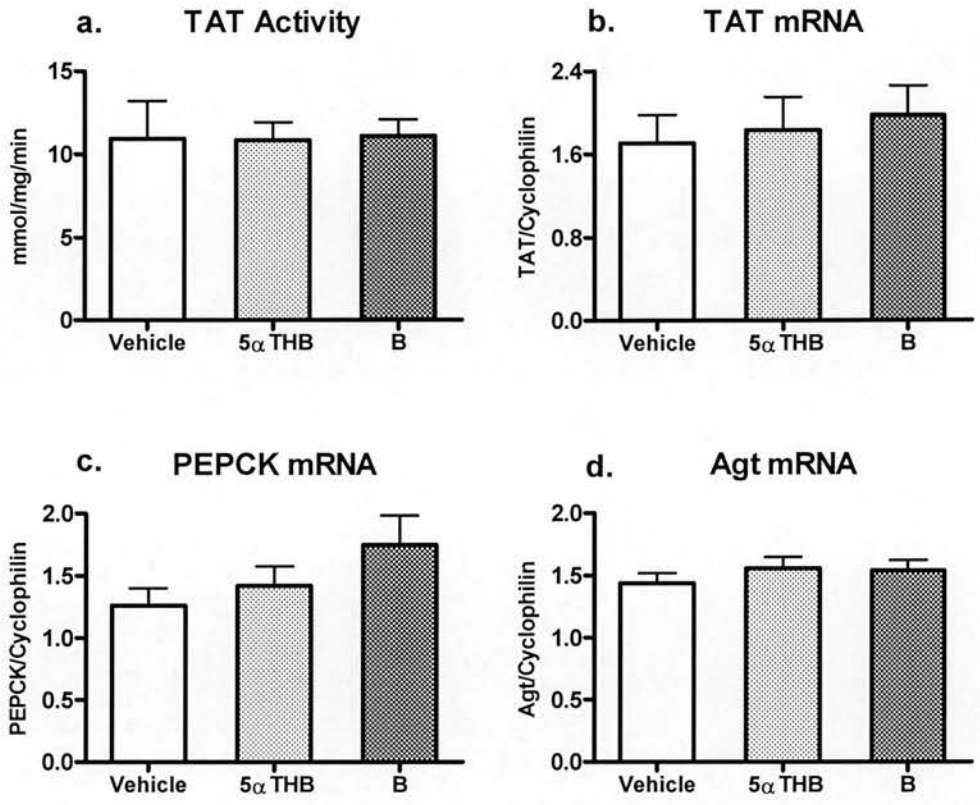

Figure 4.16 Hepatic TAT activity (a) and (b, c, d) mRNA abundance of hepatic glucocorticoid responsive genes, TAT, PEPCK and angiotensinogen (Agt), quantified by real-time PCR normalized against cyclophilin. None of these indices of hepatic genes or enzyme activity was altered significantly by B or 5αTHB. Data are mean ± SEM, analysed by one-way ANOVA, n=12.

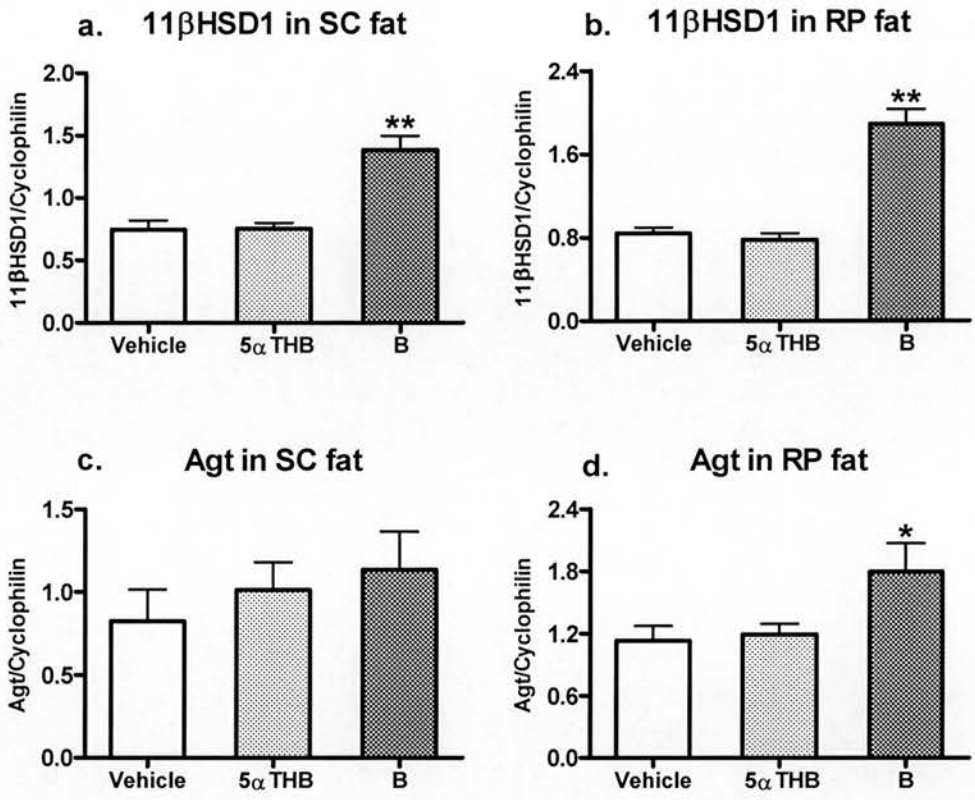

Figure 4.17 Transcript abundance of (a, b) glucocorticoid responsive gene 11β-HSD1 and (c, d) angiotensinogen (Agt) in subcutaneous (SC) and retroperitoneal (RP) adipose tissue. mRNAs were quantified by real-time PCR normalized against cyclophilin. 11β-HSD1 expression was significantly increased in both SC and RP fat in response to B infusion while increased Agt induction was only observed in RP fat. 5αTHB did not induce transcription of either gene in either fat pad. Data are mean ± SEM, n=12. *$p<0.05$, **$p<0.01$ versus vehicle, analysed by one-way ANOVA with Holm-Sidak post-hoc tests.

4.3.3.7 Cytokine expression in adipose tissues

Transcript abundances of pro-inflammatory cytokines TNFα, IL-6 and MCP-1 in adipose tissues, subcutaneous and retroperitoneal fats, were not significantly altered by any infusion (Figure 4.18).

4.3.3.8 Cytokine release in LPS stimulated whole blood

In whole blood stimulated by LPS in a range of concentrations, production of pro-inflammatory cytokines TNFα and IL-6 were significantly suppressed by corticosterone. 5αTHB exhibited suppressive effects on TNFα levels, and there was a trend for it to suppress IL-6 (Figure 4.19(1)). Secretion of MCP-1 and IL-10 was not affected by corticosterone or 5αTHB. The data pertaining to MCP-1 demonstrated a lot of variability in the vehicle group (Figure 4.19(2)).

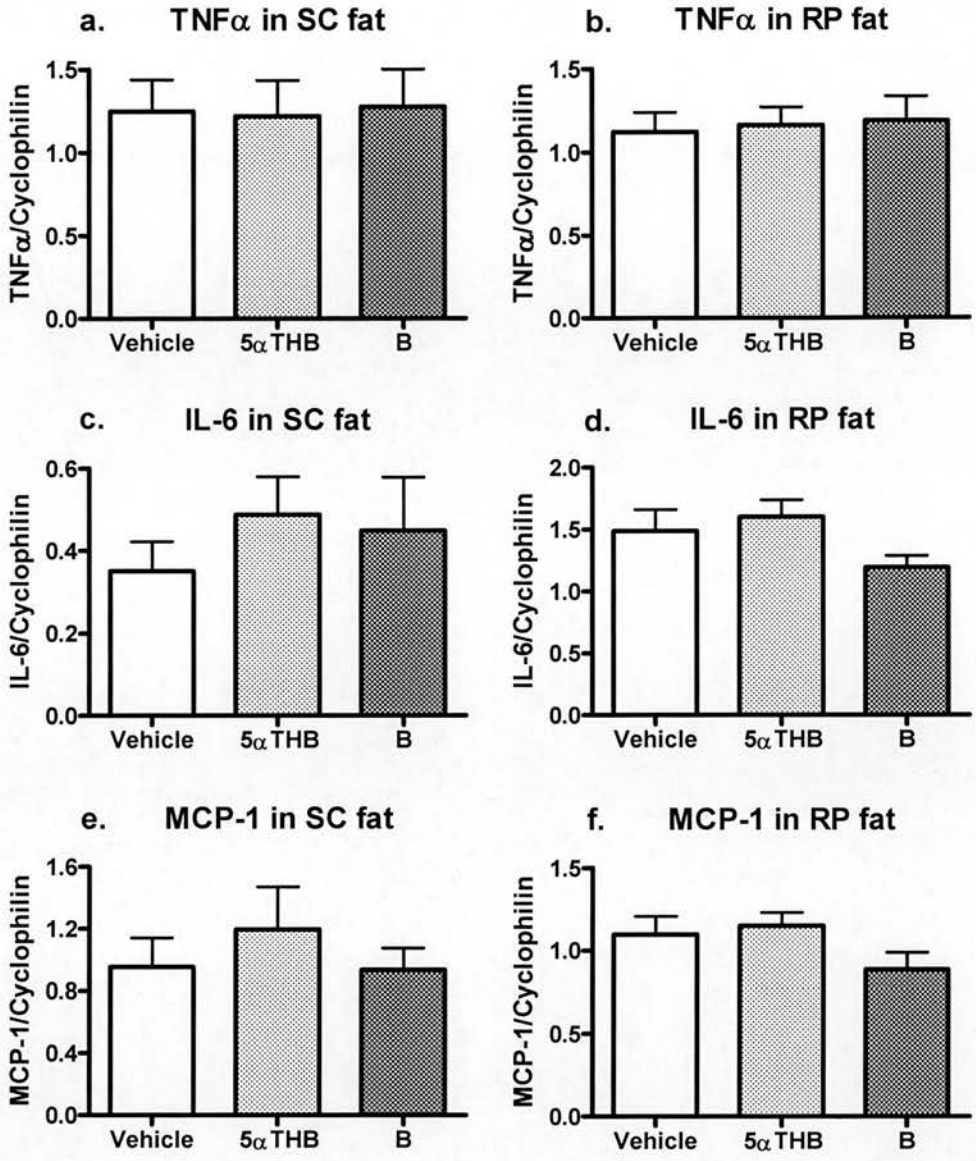

Figure 4.18 Transcript abundance of cytokines (a, b), TNFα; (c, d), IL-6; (e, f), MCP-1 in subcutaneous (SC) and retroperitoneal (RP) adipose tissue was measured by real-time PCR normalized against cyclophilin. The abundance of mRNAs of these cytokines was not altered significantly by any treatment. Data are mean ± SEM, n=12, analysed by one-way ANOVA.

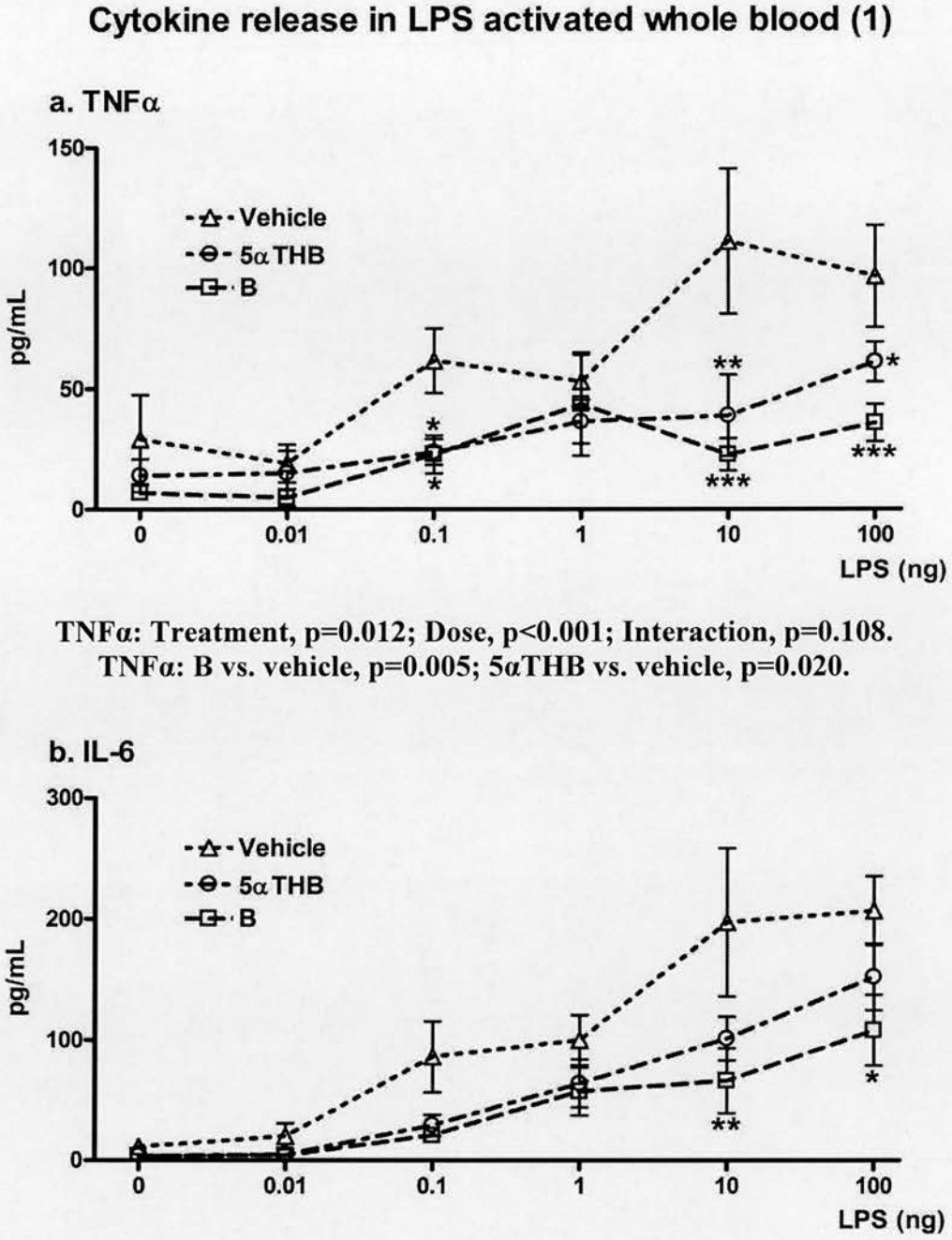

TNFα: Treatment, p=0.012; Dose, p<0.001; Interaction, p=0.108.
TNFα: B vs. vehicle, p=0.005; 5αTHB vs. vehicle, p=0.020.

IL-6: Treatment, p=0.224; Dose, p<0.001; Interaction, p=0.227.
IL-6: B vs. vehicle, p=0.030; 5αTHB vs. vehicle, p=0.090.

Figure 4.19 (1) Release of pro-inflammatory cytokines (a) TNFα and (b) IL-6 from LPS (0, 0.01, 0.1, 1, 10 and 100ng) activated whole blood that was collected from mice infused with B, 5αTHB or vehicle. TNFα and IL-6 were significantly suppressed by B. 5αTHB suppressed TNFα significantly, and there was a trend for it to suppress IL-6. Data are mean ± SEM, n=3-6. *p<0.05, **p<0.01, ***p<0.001 versus vehicle, analysed by two-way repeated measure ANOVA (one factor repetition) with Holm-Sidak post-hoc tests.

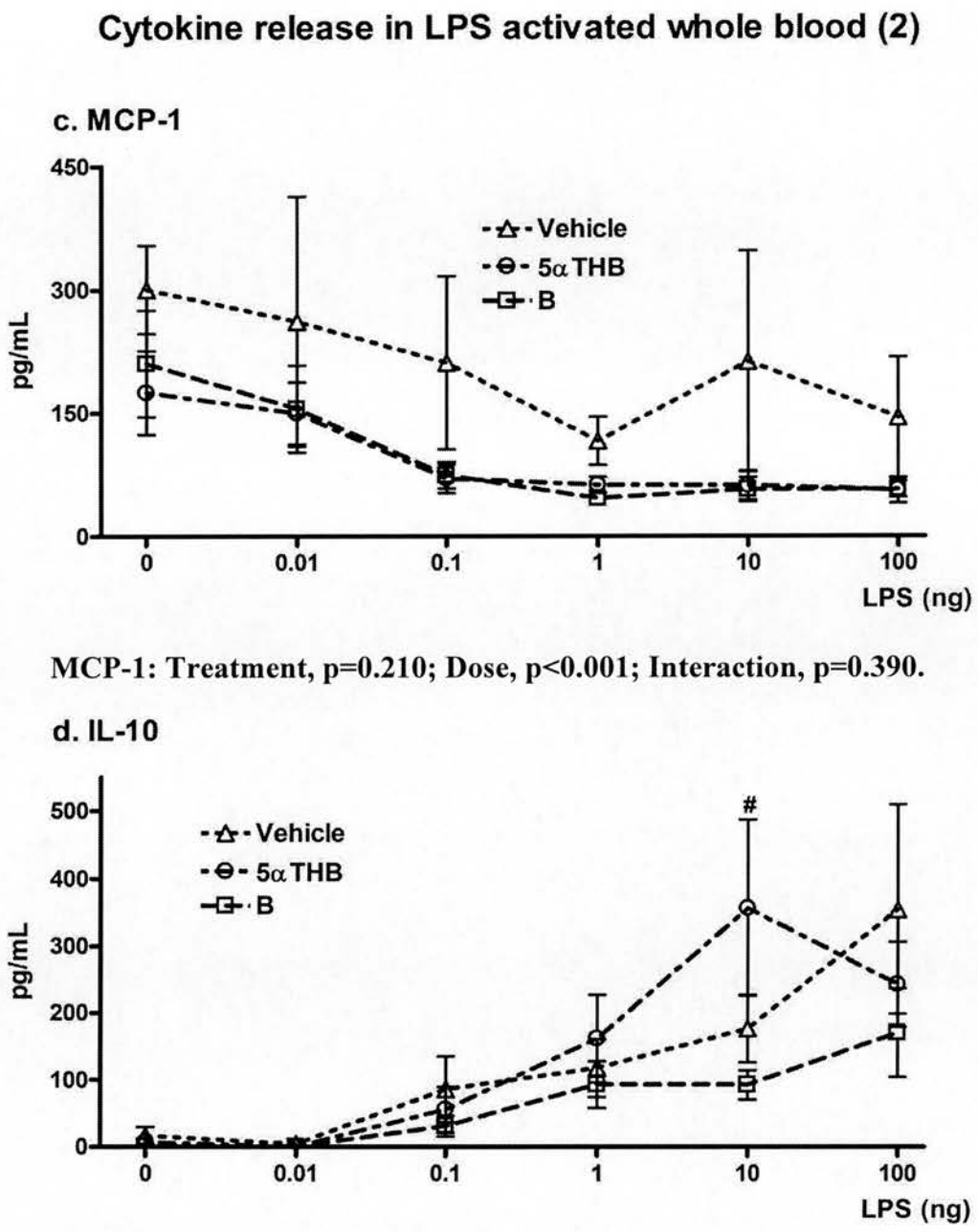

Figure 4.19 (2) Release of chemokine (c) MCP-1 and (d) anti-inflammatory cytokine IL-10 from LPS (0, 0.01, 0.1, 1, 10 and 100ng) activated whole blood that was collected from mice infused with B, 5αTHB or vehicle. Secretion of MCP-1 and IL-10 was not affected by B or 5αTHB. Data are mean ± SEM, n=3-6, #p<0.05 versus B, analysed by two-way repeated measure ANOVA (one factor repetition) with Holm-Sidak post-hoc tests.

4.4 Discussion

In this chapter, the effects of 5αTHB *in vivo* have been investigated by the approaches of acute administration or chronic infusion of 5αTHB into C57BL/6 mice, and compared to those of its parent hormone corticosterone. By means of acute administration, 5αTHB did not increase the hepatic TAT activities in time course or dose responses, or affect the circulating levels of glucose or insulin following administration. Chronic infusion of 5αTHB suppressed ACTH levels, as previously reported in rats (McInnes et al. 2004), but did not affect blood pressure, body or organ weight, nor did it affect the glucose tolerance or insulin sensitivity. Similar to the *in vitro* findings, 5αTHB did not induce the glucocorticoid transactivated genes in liver and adipose tissue, but had suppressive effects on the production of LPS-induced pro-inflammatory cytokines from blood immune cells. These findings support the hypothesis that 5αTHB is a "dissociated steroid", suppressing inflammation without influencing metabolism, while exerting negative feedback on the HPA axis.

4.4.1 Effects of 5αTHB by acute administration

To investigate the acute effects of 5αTHB, an injection method was established to eliminate the stress response to either the physical aspects of the injection or the vehicle solution of the injection. In the first attempt to establish the time course of 5αTHB action, steroid was dissolved in 100 μl of a mixture of DMSO, ethanol and saline (13:1:6, v/v). Following the injection, plasma corticosterone in animals receiving this steroid was elevated instantly, suggesting rapid transit of the injected corticosterone from subcutaneous tissue into system circulation, particularly given the time between injection and decapitation was within 30 seconds. This was followed by an induction of activity of TAT at 3h, which was a slower process since it involves GR activation, translocation, gene transcription and protein expression in hepatocytes. Circulating corticosterone and hepatic TAT activity returned to basal levels at 6 h, accompanied by an increase in insulin to maintain metabolic homeostasis.

Meaningful comparisons between the effects of corticosterone and 5αTHB were not possible in initial studies due to experimental confounders. At baseline, the levels of corticosterone in animals receiving 5αTHB or vehicle were not changed, however they did rise significantly over the first hour after treatment, albeit the peak levels in animals receiving corticosterone were significantly higher than those receiving 5αTHB or vehicle. This elevation in plasma corticosterone may have been generated from adrenals upon the activation of the HPA axis, stimulated by the psychological response to the stress of injection or the irritant nature of the injection solution. Lack of cross-reactivity of 5αTHB in the radioimmunoassay of corticosterone was confirmed. Increases in hepatic TAT activity were also detected at 3 h following injection of vehicle or 5αTHB, although again the largest increase was observed in animals receiving corticosterone. This response may have been induced by the elevated circulating corticosterone and/or the vehicle solution might have led to a direct stimulation of hepatic metabolism to eliminate the xenobiotic solvents. Interestingly, increased plasma corticosterone levels were sustained from 1 h to 3 h in the animals receiving 5αTHB injection, indicating a prolonged clearance of corticosterone caused by the exogenous 5αTHB, perhaps through competition for a shared route of elimination.

To address concerns about the effect of vehicle and hence afford a more stable and lower baseline, steps were taken to alleviate stressors. Thereafter, the injection method was modified in order to avoid the stress response, and finally 20 μl of DMSO was used as the solvent for further investigation of the dose response of TAT by corticosterone and 5αTHB. Under these conditions, the vehicle injection did not induce any change in TAT activities nor did it cause an increase in corticosterone levels. Further, corticosterone was not elevated following 5αTHB administration, by way of reassurance that 5αTHB cannot be metabolised in the reverse direction to corticosterone. Hepatic TAT activity was significantly increased in a dose dependent manner by corticosterone, showing a narrow dynamic range of induction. However, 5αTHB did not alter TAT activity at 3 h. Plasma glucose and insulin were not significantly changed at 3 h by any treatment.

In conclusion, 5αTHB did not increase the activity of the hepatic gluconeogenic enzyme TAT in this model system, mirroring the data generated *in vitro* in Chapter 3. However given the *in vitro* findings that 5αTHB took longer to induce GR translocation than corticosterone, it may not have been appropriate to investigate the effects of 5αTHB at the same time point as those of corticosterone. This is supported by McInnes' *in vivo* findings that an intraperitoneal injection of 5αTHB suppresses plasma ACTH levels 1 h later than that of corticosterone (McInnes et al. 2004). Therefore, an experiment with chronic administration of 5αTHB *in vivo* was necessary.

4.4.2 Effects of 5αTHB by chronic administration

Following chronic infusions of 5αTHB or corticosterone, a series of physiological and metabolic parameters were measured indicative of glucocorticoid action. Infusion of corticosterone dramatically increased plasma concentrations of this hormone, while treatment with 5αTHB and control did not, again confirming that 5α-dehydrogenation does not regenerate corticosterone from 5α-reduced metabolites. Furthermore, the mice were not exhibiting signs of global stress throughout the experiment. Circulating levels of 5αTHB were very low: only a few nM of 5αTHB were detected in animals receiving this compound, and it was un-detectable in animals of the other groups, suggesting the clearance of 5αTHB was more rapid than corticosterone. The concentrations of steroids in residual infusion solutions were checked and confirmed that both steroids remained stable in the infusate throughout the experiment.

Considering the low levels of plasma 5αTHB, it was striking to find that plasma ACTH was significantly suppressed by chronic infusion of 5αTHB. This confirms the previous finding that an acute intraperitoneal injection of 5αTHB (5 mg/kg BW) in adrenalectomized rats suppressed plasma ACTH albeit 1 h later than the emergence of the suppressive effect of corticosterone (McInnes et al. 2004). These results generated by the two approaches confirmed the ability of 5αTHB to induce negative feedback of the HPA axis, in which both the hypothalamus and pituitary can

be the target of negative regulation mediated by glucocorticoids. Surprisingly, the transcript abundance of POMC and CRH receptor type 1 in the pituitary were not directly affected by any infusion treatment. This was consistent with the *in vitro* findings with 5αTHB performed in the AtT20 cells, although in that model corticosterone did cause this change. Since POMC and CRH receptor 1 were down-, and up-, regulated by glucocorticoids and CRH respectively, it is likely that the inhibition of ACTH was a result of suppression of CRH in the hypothalamus induced by the glucocorticoids.

Adrenal size was reduced in animals receiving corticosterone but not 5αTHB. This discordance with plasma ACTH results may reflect the time of blood sampling. The animals of this experiment were culled in the morning when circulating ACTH were at their lowest (rodents are nocturnal with a circadian rhythm of HPA activity opposite to that of humans (Windle et al. 1998)). Since the adrenal size was clearly reduced in animals receiving the more potent glucocorticoid, corticosterone, it seems likely that 5αTHB levels were sufficient to suppress ACTH at the nadir, but perhaps not at the zenith thus allowing unsuppressed endogenous corticosterone levels to maintain the adrenals at their normal sizes. Thus further experiments to investigate the levels of corticosterone and ACTH in late afternoon could be performed.

Alternatively, rather than exert central suppressive effects, treatment of 5αTHB may affect the peripheral clearance of corticosterone by competition with liver enzymes, e.g. 20α- and 20β-HSDs that catalyze the reduction of both the hormone and its tetrahydro metabolites (Kawamura et al. 1981), thus may result in lower ACTH required to maintain the levels of corticosterone. As this may not be as profound to suppress ACTH-adrenal function as administration of corticosterone, adrenal shrinkage was not detectable.

At the molecular level, the mechanism of glucocorticoids inhibition of CRH transcription has been well documented. CRH induced increase in POMC transcription involves increased expression of *c-fos* and *c-jun* (Autelitano and Cohen 1996; Autelitano and Sheppard 1993), AP-1 nucleoproteins. Glucocorticoids inhibit

CRH gene transcription through a mechanism whereby GR monomer directly binds to the negative GRE in the CRH gene as well as to AP-1 (Malkoski and Dorin 1999; Malkoski, et al. 1997). Therefore, the suppressive effects of 5αTHB observed here during the circadian nadir may indicate the weak potency of 5αTHB to induce GR interactions between AP-1 and the negative GRE of CRH. Since the brains were collected from the animals receiving steroid infusions at cull, the expression of CRH in the hypothalamus could be measured by *in situ* hybridisation to address this hypothesis.

During the 14 days infusion of corticosterone, the anticipated metabolic responses were observed. Corticosterone suppressed body weight gain, indicating an increasing rate of proteolysis in skeletal muscles of animals receiving the hormone, although individual organ weights were not significantly changed. Decreased thymus size induced by corticosterone infusion was anticipated. It is well-recognised that circulating glucocorticoids invoke thymus involution (van den Brandt, et al. 2007). Fat was subtly redistributed to subcutaneous depots. Within the subcutaneous and retroperitoneal adipose depots, 11β-HSD1 mRNA (a glucocorticoid responsive gene in adipose) was upregulated. As a result, the activity of corticosterone was boosted in these adipose depots increasing lipolysis and release of free fatty acids and glycerol into circulation, contributing to hyperinsulinaemia and rebound hyperlipidemia in the glucose tolerance test. Since 5αTHB is not a substrate for 11β-HSD1 (Tomlinson and Stewart 2001), the activities of 5αTHB were not amplified. However, in liver, gluconeogenic genes PEPCK and TAT were not significantly upregulated and neither was TAT activity, perhaps because the liver samples were collected when animals were not fasted.

None of these effects of corticosterone were observed following infusion of 5αTHB (or vehicle) in agreement with the previous acute study and *in vitro* data, suggesting that this steroid does not alter metabolism when administered *in vivo*. It is important to recognise however that the circulating concentration achieved of 5αTHB was 10 fold lower than that of corticosterone and perhaps different results would be

encountered if their circulating concentrations were matched, as opposed to their infusion rates.

Additionally, angiotensinogen gene transcription was increased by infusion of corticosterone, not 5αTHB, in retroperitoneal adipose tissue. Angiotensinogen is a glucocorticoid responsive gene and present in liver and adipose tissue; it is the unique substrate of renin and the precursor of angiotensin II in the renin-angiotensin system (RAS), which plays an important role in the regulation of blood pressure as well as sodium and fluid balance (Aubert, et al. 1997). With chronic exposure to corticosterone in adipose tissue, increased 11β-HSD1 amplified the corticosterone action on angiotensinogen expression, thereby potentially contributing to the marginal hypertension induced by infusion of corticosterone (Masuzaki et al. 2003). However in this study, treatment of corticosterone did not significantly affect the systolic blood pressure, which is possibly due to the short term infusion period or the limited sensitivity of the blood pressure measurement. 5αTHB did not induce the activation of angiotensinogen expression, and also did not increase the blood pressure.

Besides angiotensinogen, adipose tissue also produces pro-inflammatory molecules, so-called "adipokines", such as TNFα, IL-6, TGF-β1, C-reactive protein, soluble ICAM, and MCP-1. The secretion of these proteins is significantly increased in adipose tissue of obese cohorts compared with lean individuals (Weisberg, et al. 2003), which plays a crucial role in the development of obesity-induced insulin resistance (Xu, et al. 2003). Thus, although glucocorticoids have adverse metabolic effects, they may, paradoxically, act to suppress inflammation and protect against metabolic syndrome. For example, it was reported that dexamethasone suppressed IL-6 production in cultured obese human adipocytes *ex vivo* (Fried, et al. 1998). Here in this thesis, in view of the *in vitro* evidence that 5αTHB could suppress secretion of pro-inflammatory cytokines and also stimulate IL-10 secretion, gene transcriptions of these adipokines were measured following infusion of corticosterone and 5αTHB. However, the adipokines were not affected by any treatment. The cytokine secretion

remained at basal levels in the tested fat depots. This may have been because the C57BL/6 mice in this study were not obese.

However, in marked contrast with the lack of effect of 5αTHB on cardiometabolic variables, the *in vitro* evidence of the effects of 5αTHB to modulate cytokine secretion was recapitulated in LPS-stimulated whole blood collected at cull from the animals receiving chronic infusion treatment of this compound. The concentrations of test glucocorticoids in the whole blood can be extrapolated from the plasma levels, such that elevated corticosterone was present only in samples collected from animals receiving corticosterone, whereas basal corticosterone and increased 5αTHB levels were present following treatment with 5αTHB. In the vehicle group, only basal corticosterone level was present. The leucocytes in whole blood included monocytes, lymphocytes, neutrophils, basophils, and eosinophils (Smits, et al. 1998). LPS is a powerful stimulant to induce secretion of cytokines mainly, but not exclusively, from monocytes; this can be inhibited by glucocorticoids and, for example, dexamethasone inhibits secretion of monokines more than it does to lymphokines in natural human whole blood (Franchimont, et al. 1998). Secretion of TNFα was significantly suppressed by corticosterone and 5αTHB in response to a wide range of LPS concentrations from 0.1 to 100 ng. Similarly, IL-6 secretion was suppressed by corticosterone with secretion also tending to be lower with 5αTHB treatment. These findings support and extend the *in vitro* study in which 5αTHB suppressed the secretion of LPS-induced TNFα and IL-6 from bone marrow derived macrophages (Chapter 3). The suppression of cytokine release from cells in whole blood by 5αTHB was similar to that of corticosterone indicating considerable potency given that circulating concentrations of 5αTHB are 10 fold lower than those of corticosterone. Therefore, this dose of 5αTHB achieved equivalent effects as 10 fold higher dose of corticosterone on cytokine suppression but not on fuel metabolism related glucocorticoid responsive genes.

4.4.3 Summary

To summarize, acute or chronic administration of 5αTHB did not induce any alterations of metabolic parameters normally associated with glucocorticoid excess,

but it did exhibit suppressive effects on the HPA axis as well as immune responses. The suppression of ACTH induced by 5αTHB was not through inhibition of POMC expression, and may be via reduced secretion of CRH or the influence of 5αTHB on corticosterone clearance by competition with liver enzymes. Moreover, 5αTHB suppressed the production of pro-inflammatory cytokines, TNFα and IL-6, from blood immune cells. Suppressive effects on CRH, TNFα and IL-6 involve a common mechanism whereby monomeric GR binds to NFκB or AP-1, suggesting that the physiological functions of 5αTHB may be exerted in this manner.

In the following chapter, the impact of hepatic 5α-reduction that produces the 5α-tetrahydro metabolites of glucocorticoids has been investigated using the 5αR1-null mice. The anti-inflammatory effects of 5αTHB following the peritoneal administration of LPS *in vivo* will be further investigated in Chapter 6.

Chapter 5

Investigation of the function of 5α-reductase type 1 (SRD5A1) using SRD5A1 knock-out mice

5.1 Introduction

Metabolism of glucocorticoids mainly takes place in liver through the A ring-reductases, including 5α-, and 5β-reductases, and 3α-HSDs. Reactions catalyzed by 5α- and 5β- reductases involve the irreversible *trans* and *cis*, respectively, reduction of the double bond at position $\Delta^{4,5}$ of A-ring, yielding *trans* 5α- and *cis* 5β- dihydro glucocorticoids, which are further reduced by 3α-HSD into 5α- and 5β- tetrahydro derivatives.

Two isozymes of 5α-reductases, 5αR1 and 5αR2, have been cloned from different genes, *SRD5A1* and *SRD5A2*. The isozymes are expressed in a tissue-specific pattern. In rats, 5αR1 is the only isozyme expressed in liver and adipose tissue (Normington and Russell 1992), and 5αR2 are mostly present in tissues of male reproductive system (Normington and Russell 1992; Russell and Wilson 1994). In general, the 5αR2 has 10-20 fold higher affinity for androgens, progesterone, and corticosterone than 5αR1. 5β-reductase is expressed predominantly in liver (Kondo et al. 1994).

In idiopathic obesity, abnormal glucocorticoid metabolism through A-ring reduction is associated with the adverse consequences of obesity. In obese humans, 5α-reductase activity is enhanced (Andrew et al. 1998); and decreased 5α-reductase activity is observed in weight loss (Tomlinson et al. 2008b). In obese Zucker rats, hepatic mRNA transcription of 5αR1 is increased, and insulin sensitization can ameliorate the increase in A-ring reductases (Livingstone et al. 2000; Livingstone et al. 2005). Thus in the context of the data presented earlier, the upregulation may modify adverse effects of glucocorticoids.

At the outset of this thesis, it was uncertain whether we would predict that 5αR1 deficiency results in exaggerated GR activation, due to accumulation of corticosterone in the liver, or attenuated GR activation, due to loss of the contribution made to GR activation by 5α-reduced corticosterone metabolites. Conversely, it was unclear if increased 5αR1 would amplify or attenuate GR activation. From the results of the previous chapters, it now appears that the consequences of variations in 5αR1

activity may be selective, with 5α-reduced corticosterone metabolites making a positive contribution to GR signalling with respect to inflammatory signalling but having a neutral effect on metabolic signalling. Consequences for HPA axis function are hard to predict since we have discordant *in vitro* and *in vivo* results and 5α-reduced corticosterone metabolites may act not only on central regulation of ACTH secretion but also may influence peripheral clearance of corticosterone, with secondary changes in the HPA axis.

Transgenic mice with 5αR1 knock-out have been generated and used as an animal model to specifically study the roles of this isozyme (Mahendroo et al. 1996). The male 5αR1 knock-out mice appear normal and can breed. Female mice can become pregnant, but exhibit parturition and fecundity defects due to elevated progesterone (Mahendroo et al. 1999) and estrogen (Mahendroo et al. 1997) levels, respectively, suggesting a critical role of 5αR1 in steroid metabolism. However, the metabolic consequences from loss of 5αR1 have not been explored and an overt phenotype is not observed when mice are maintained on a normal diet. Recently Livingstone et al. in our lab have investigated the effects of high-fat diet on 5αR1-null mice and found that inhibition of 5αR1 resulted in detrimental metabolic effects characterized by glucose intolerance and fatty liver (Livingstone et al. 2008), consistent with accumulation of the parent steroid in the liver. This raises the hypothesis that 5αR1 acts to protect against adverse changes in metabolism induced by glucocorticoids. Immune regulation in these animals has not been studied.

Aims

The aims of this chapter were to investigate the panel of metabolic, inflammatory and HPA axis variables used in Chapter 4 to assess the phenotype of 5αR1 knock-out mice, and to challenge these mice with chronic infusion of corticosterone to test whether their responses in each of these domains are modified in the absence of the capacity to generate 5α-reduced corticosterone metabolites.

5.2 Methods and materials

5.2.1 Background and maintenance of animals

5.2.1.1 Background

Steroid 5αR1 (SRD5A1) knock-out (*SRD5A1*$^{-/-}$) mice were of a mixed strain of C57BL/6J/129/SvEv, generated previously in the Russell laboratory (South Western University, Dallas, USA) by injection of blastocysts with modified ES cells (Mahendroo et al., 1996). Embryos were imported from the Jackson laboratory (Westgrove, PA, US), and a colony was generated by Dr Dawn Livingstone in our laboratory. To generate *SRD5A1*$^{-/-}$ mice, *SRD5A1* heterozygous females were routinely mated to heterozygous males to avoid problems of parturition in the homozygote mothers. Offspring of both sexes were produced with normal Mendelian ratios of wild type, heterozygous, and homozygous genotype with no abnormalities affecting sexual development or survival. The offspring of these matings were genotyped using a multiplex PCR assay (adapted from Mahendroo et al., 1996).

5.2.1.2 Maintenance

Male SRD5A1 knock-outs mice (*SRD5A1*$^{-/-}$) and their wild-type (*SRD5A1*$^{+/+}$) littermates were 20 weeks old and weighed 30±3 g at the start of the study. Animals were maintained under controlled conditions as described in Section 2.3.1.

5.2.2 Experimental design

Twenty-four male SRD5A1 knock-out mice and 24 wild-types were divided into two groups (n=12/group). Before mini-osmotic pump implantation, two pre-treatment blood pressure measurements were carried out. On Day 0, mice of each genotype were implanted with mini-pumps that infused either corticosterone (50 μg/day) or vehicle (DMSO: propylene glycol = 1:1, v/v). Mice were weighed on Days 0, 1, 4, 6 and 11, and blood pressure measured on Days 1, 4, 6, and 11. Glucose tolerance tests were carried out on Day 7. Animals were killed, and blood and tissues collected on Day 14.

5.2.3Animal procedures

5.2.3.1 Mini-osmotic pump implantation

All mice received their operations according to the surgical procedures described in Section 2.3.2.

5.2.3.2 Measurement of systolic blood pressure

Systolic blood pressure of each animal was measured as described in Section 2.4.1.

5.2.3.3 Insulin sensitivity

Glucose tolerance test was assessed as described in Section 2.4.2.

5.2.3.4 Terminal procedures

Animals were killed, and trunk blood and tissues collected as described in Section 2.4.3.

5.2.4 Activation of whole blood by LPS

Heparinized trunk blood was activated by incubation with increasing doses of LPS to study the impact of corticosterone on cytokine release from white blood cells. The experiment was performed as described in Section 2.4.4.

5.2.5 Molecular biology: quantification of mRNA abundance of genes of interest

Total RNAs were isolated from snap frozen livers (see 2.5.1.1), pituitaries (see 2.5.1.3), subcutaneous fat and retroperitoneal fat (see 2.5.1.2) before RNA quantification (see 2.5.2). Then the first strand cDNA was synthesised by reverse transcription (see 2.5.3). The mRNA abundances of TAT, PEPCK and angiotensinogen in liver, POMC and CRF receptor 1 in pituitary, 11β-HSD1, angiotensinogen, IL-6, TNFα and MCP-1 in subcutaneous and retroperitoneal fat

were quantified by real-time PCR (see 2.5.5) and normalised for the abundances of the housekeeping gene cyclophilin A.

5.2.6 Biochemical assays

5.2.6.1 Quantification of plasma corticosterone

Corticosterone in plasma prepared from trunk blood was quantified by RIA (see 2.6.1).

5.2.6.2 Quantification of plasma glucose

Glucose in plasma collected during the glucose tolerance test was quantified by hexokinase assay as described in Section 2.6.2.

5.2.6.3 Quantification of plasma insulin

Insulin in plasma collected during the glucose tolerance test was quantified by ELISA as described in Section 2.6.3.

5.2.6.4 Quantification of plasma NEFAs

NEFAs in plasma collected during the glucose tolerance test were quantified by spectrophotometry as described in Section 2.6.5.

5.2.6.5 Quantification of cytokines

Cytokines in samples collected in LPS-activated whole blood were quantified by CBA assay as described in Section 2.6.6.

5.2.7 Statistics

Data are presented as mean ± SEM and were analysed by one-way, two-way, or three-way ANOVA, or repeated measures ANOVA, followed by Holm-Sidak post-hoc test where appropriate.

5.3 Results

5.3.1 Infusion of steroid

Concentrations of corticosterone in knock-out mice infused with vehicle were two fold greater than wild-type mice although the difference was not statistically significant. When infused with corticosterone, plasma corticosterone levels were similar in wild-type and knock-out mice. Size of adrenal glands was not affected by genotype and was reduced to a similar degree following infusion of corticosterone, reflecting the suppression of the HPA axis (Figure 5.1).

The mRNA abundance of POMC and CRH receptor 1 in pituitary was quantified and corrected for abundance of cyclophilin which did not differ between groups ($p>0.05$). As shown in Figure 5.2, POMC mRNA was decreased in abundance by corticosterone in wild-type mice only. Suppression of CRH receptor 1 was not affected by any treatment in animals of either genotype. Analysis of plasma ACTH was not possible due to insufficient plasma.

5.3.2 Body weight and blood pressure

There were no significant differences observed in body weight gain or systolic blood pressures (Figure 5.3), either between genotypes or treatments. Animal body weights in this experiment may have been temporarily affected by the glucose tolerance test on Day 7 which required at least six hours fasting. Measurement of systolic blood pressure in mice on this genetic background was more variable than in C57BL/6 animals, and some values reflect stressed measurements and are difficult to interpret. Anecdotally the knock-out animals appeared to be more easily disturbed.

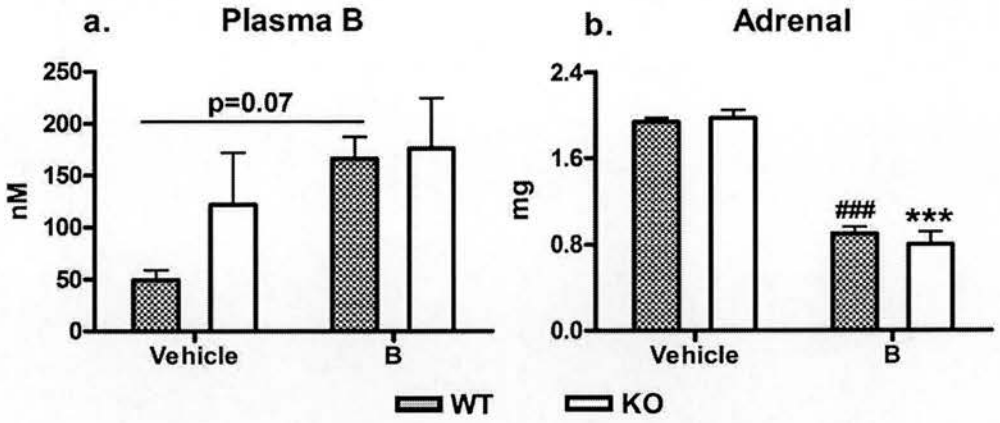

Plasma B: Treatment: p=0.049; Genotype, n.s.
Adrenal: Treatment: p<0.001; Genotype, n.s.

Figure 5.1 Following infusion of B (50 μg/day, 14 days) or vehicle, (a) plasma B, quantified by RIA, n=6-11, tended to be increased by infusion of B. (b) Formalin fixed right adrenal weights, n=12, was reduced by infusion of B. No significant difference was seen between genotypes following infusions. Data are mean ± SEM, analysed by two-way ANOVA with Holm-Sidak post-hoc tests. ***p<0.001 versus vehicle within KO; ###p<0.001 versus vehicle within WT.

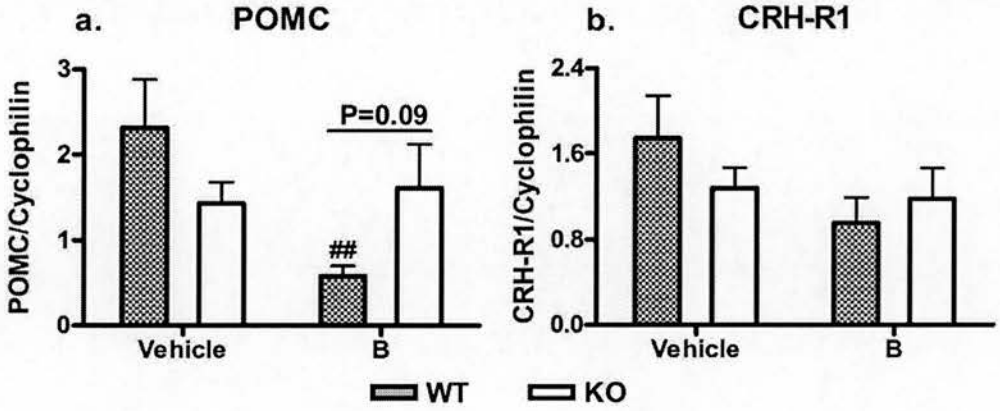

POMC: Treatment, p=0.073; Genotype × treatment: p=0.031.
CRH R1: n.s.

Figure 5.2 Following infusion of B (50 μg/day, 14 days) or vehicle, transcript abundances of (a) POMC and (b) CRH receptor 1 in pituitaries were quantified by real-time PCR. The mRNA abundance of POMC in pituitary was decreased only in WT animals receiving B infusion. The mRNA abundance of CRH receptor 1 was not affected by treatment or genotype. Data are mean ± SEM, n=5-6; ##p<0.05 versus vehicle within WT; analysed by two-way ANOVA with Holm-Sidak post-hoc tests.

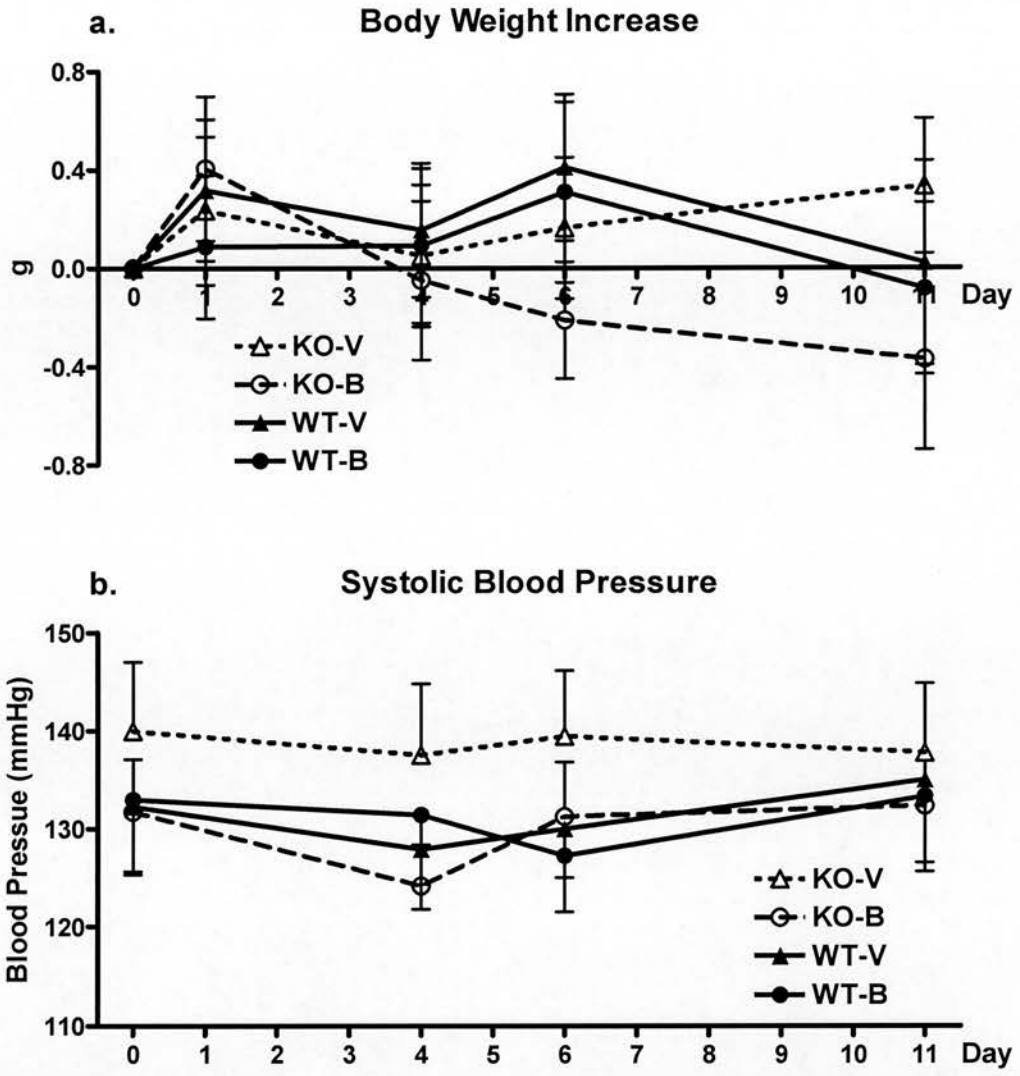

Body weight increase or Blood pressure: Treatment, Genotype or Time: n.s.

Figure 5.3 (a) Body weight change and (b) blood pressure during chronic infusion of vehicle or B (50 μg/day, 14 days). Neither parameter was affected. Data points on Day 0 were the average values from two pre-treatment measurements. Data are mean ± SEM, n=12, analysed by two-way repeated measure ANOVA.

5.3.3 Weights of organs

Organ and adipose tissue weights are shown in Figures 5.4 and 5.5 (presented as the actual weights or the percentage of body weight). No differences between genotypes were observed for any organ or adipose tissue. Weights of thymus and spleen were reduced in animals infused with corticosterone, and thymus was more sensitive to this change than spleen, typical of the pro-apoptotic effects of corticosterone. Decreased liver size was also seen in animals infused with corticosterone. Kidneys and quadriceps were not affected. Corticosterone caused a redistribution of fat to mesenteric and subcutaneous adipose tissue while other fat pads were not affected.

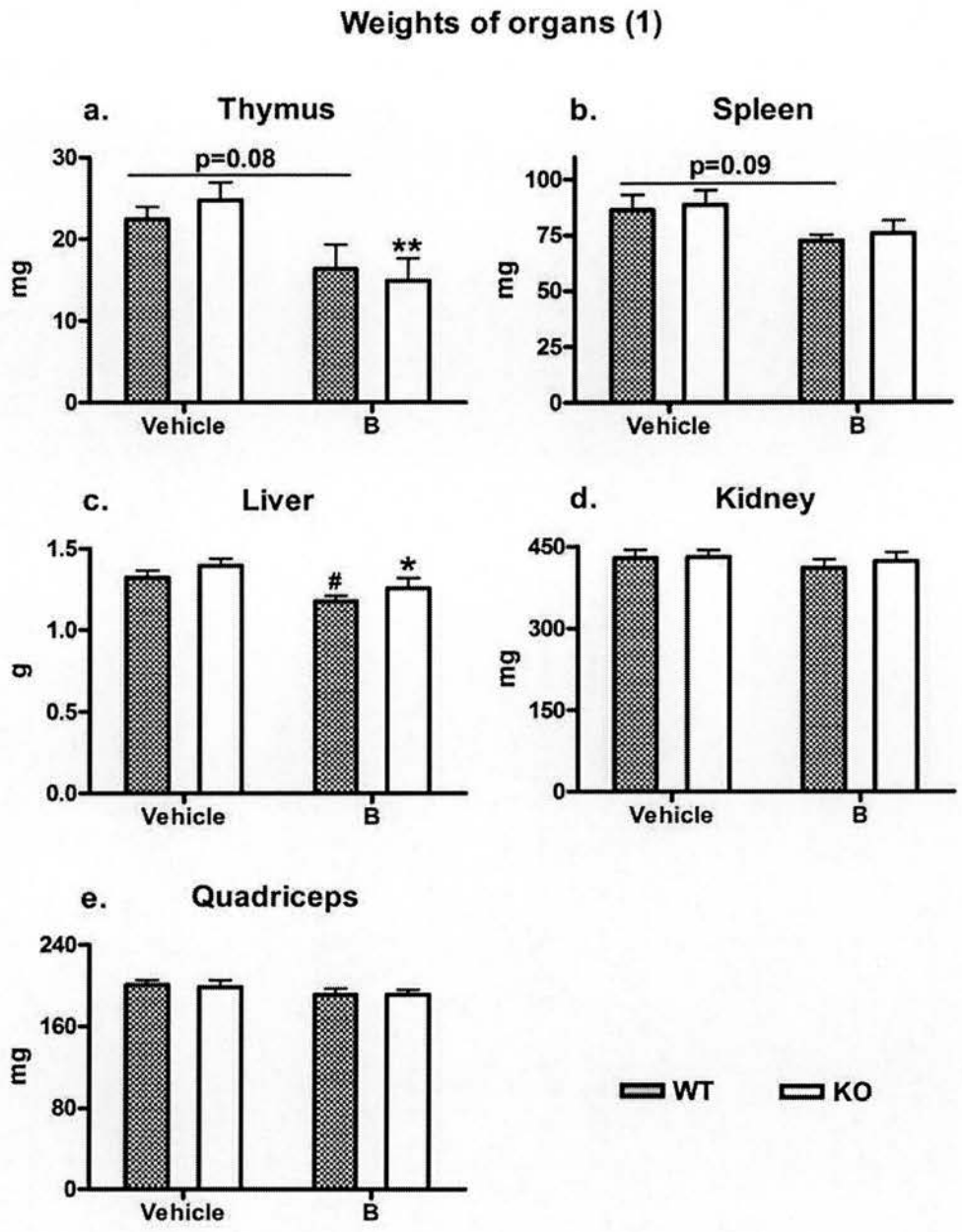

Thymus: Treatment, p=0.002; Spleen: Treatment, p=0.024; Liver: Treatment, p=0.004; Others: n.s.

Figure 5.4 (1) Weights of organs. (a) Thymus, (b) spleen and (c) liver were significantly reduced by B infusion, and (d) kidneys and (e) quadriceps were not affected. No effect of genotype was detected. Data are mean ± SEM, n=12, *p<0.05, **p<0.01 versus vehicle within KO; #p<0.05 versus vehicle within WT; analysed by two-way ANOVA with Holm-Sidak post-hoc tests.

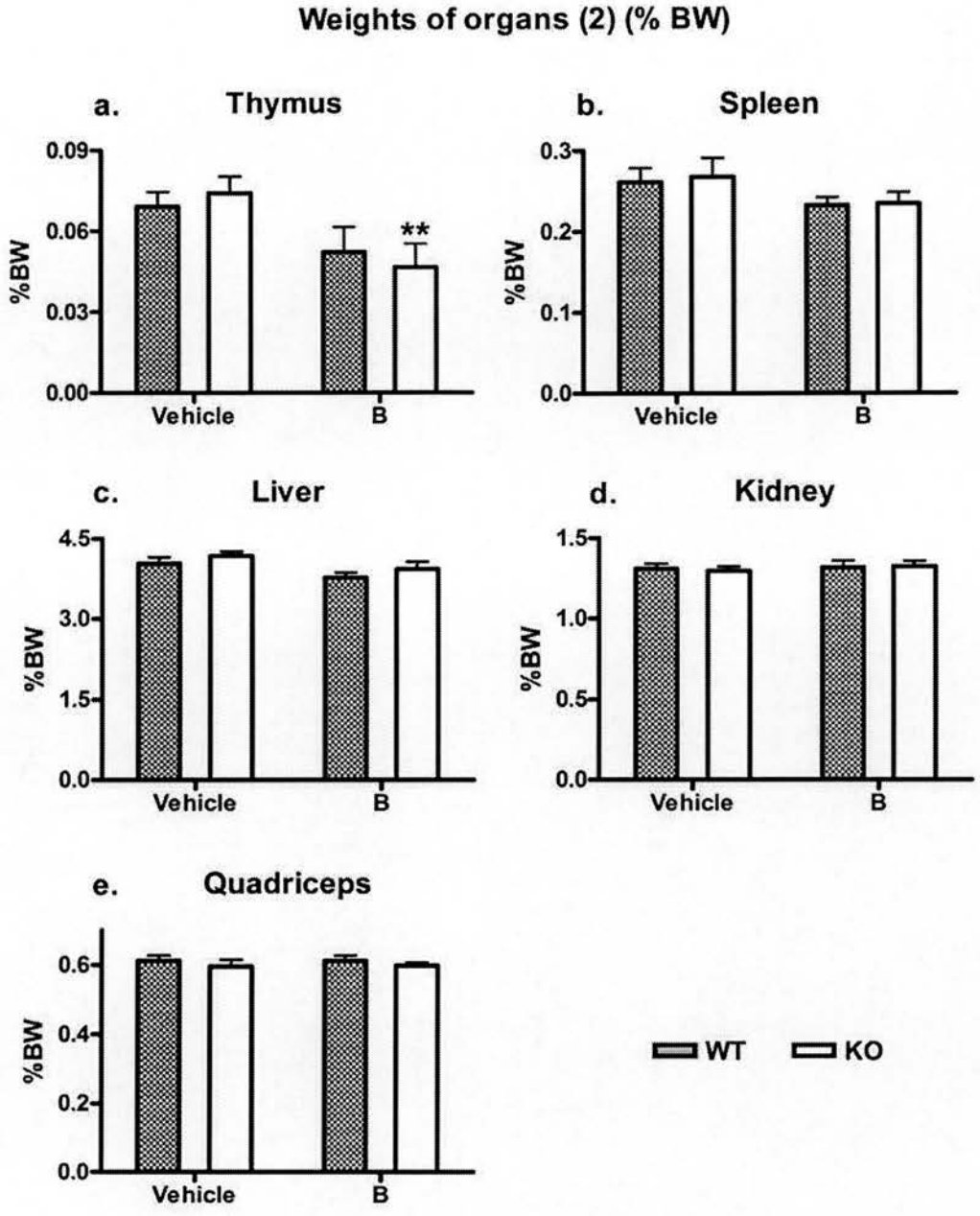

Thymus: Treatment, p=0.005; Liver: Treatment, p=0.026;
Others: n.s. (Spleen: Treatment, p=0.076)

Figure 5.4 (2) Weights of organs presented as percentage of body weight (Onate, et al.). (a) Thymus, (b) spleen and (c) liver were significantly reduced by B infusion, and (d) kidneys and (e) quadriceps were not affected. No effect of genotype was detected. Data are mean ± SEM, n=12, *p<0.05, **p<0.01 versus vehicle within KO; analysed by two-way ANOVA with Holm-Sidak post-hoc tests.

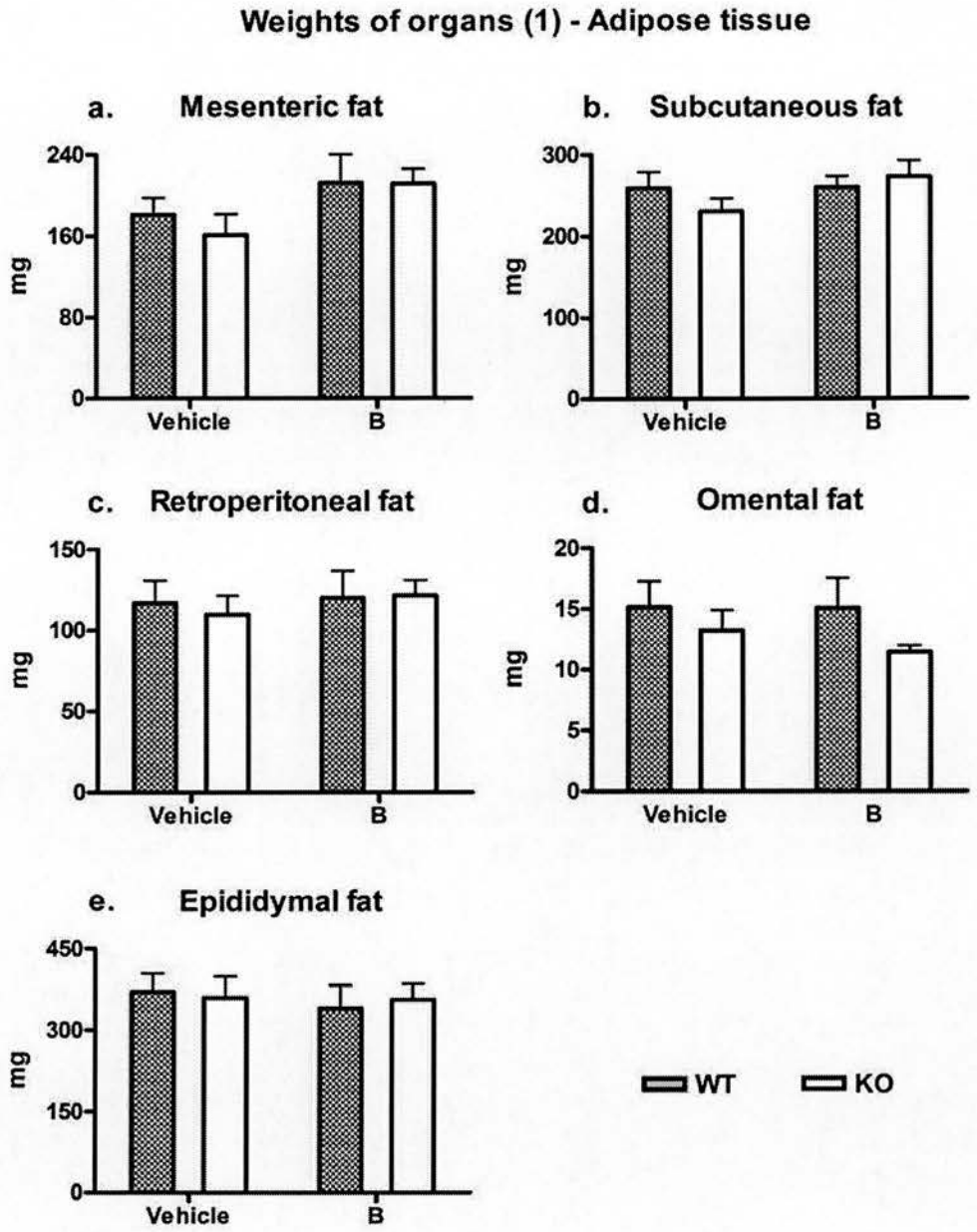

Mesenteric fat: Treatment: p=0.053. Others: n.s.

Figure 5.5 (1) Weights of adipose tissue. Five pads of adipose tissue (a) mesenteric; (b) subcutaneous; (c) retroperitoneal; (d) omental and (e) epididymal fat were weighed immediately after dissection on Day 14. No effect of genotype was detected. A trend to increased mesenteric adipose tissue was observed following B infusion. Other fat pads were not affected. Data are mean ± SEM, n=12, analysed by two-way ANOVA with Holm-Sidak post-hoc tests.

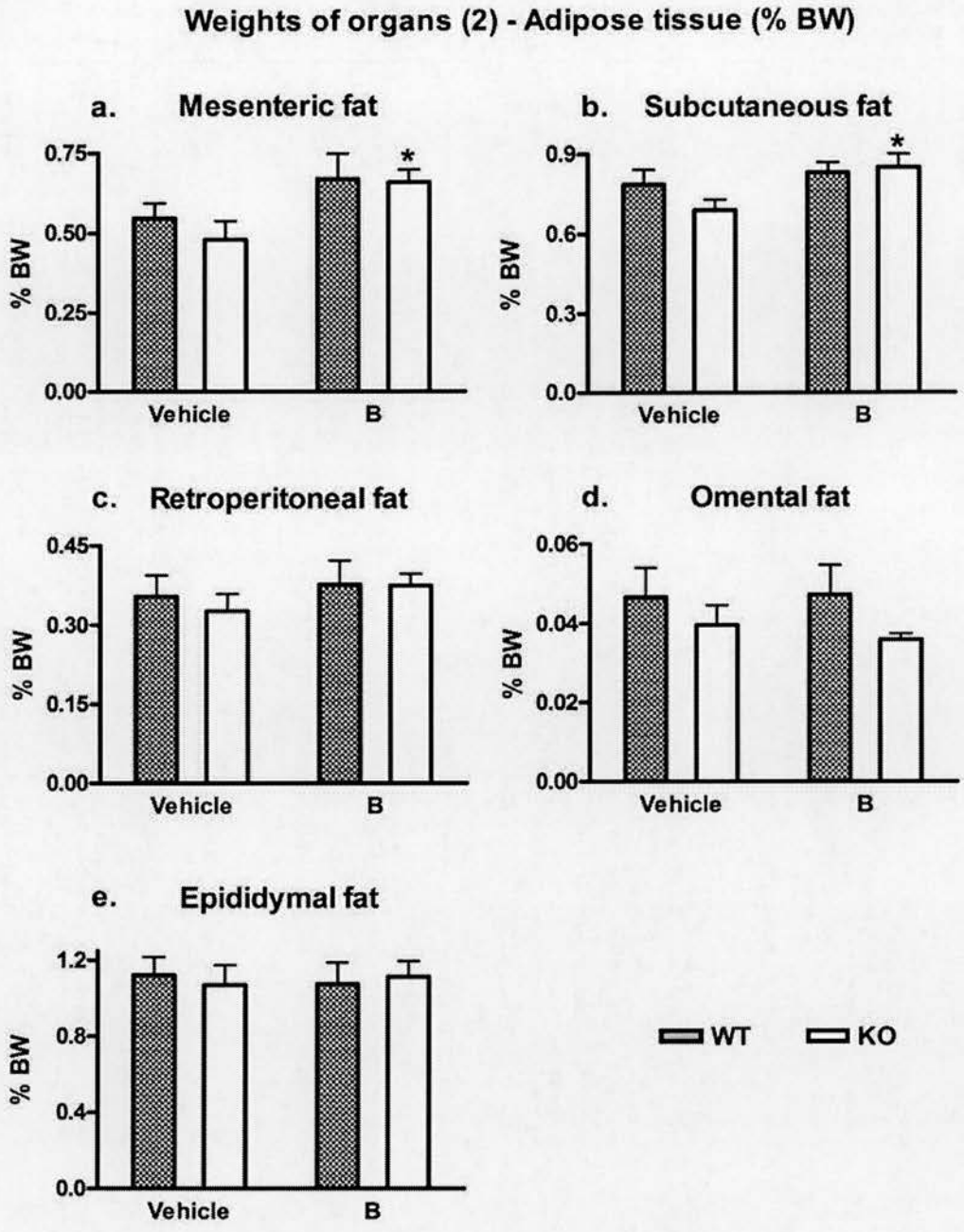

Figure 5.5 (2) Weights of adipose tissue presented as percentage of body weight (Onate et al.). Five pads of adipose tissue (a) mesenteric; (b) subcutaneous; (c) retroperitoneal; (d) omental and (e) epididymal fat were weighed immediately after dissection on Day 14. No effect of genotype was detected. Mesenteric and subcutaneous fat were increased following B infusion. Other fat pads were not affected. Data are mean ± SEM, n=12, analysed by two-way ANOVA with Holm-Sidak post-hoc tests.

5.3.4 Glucose tolerance test

After fasting for six hours, plasma glucose was not different between experimental groups; hyperinsulinaemia was observed in mice receiving corticosterone. Following an i.p. dose of glucose, circulating glucose concentrations were elevated reaching peak values at 15 min and then declined. No differences were observed in plasma glucose level between genotypes or treatments. Plasma insulin reached peak levels at 15min in mice of both genotypes. Animals receiving corticosterone had higher circulating insulin than animals receiving vehicle (Figure 5.6(1)). The data are presented also as area under curve (AUC) for both glucose and insulin responses. Animals which received corticosterone infusion showed hyperinsulinemia, but there was no statistical significance between genotypes and no effect of genotype or steroid treatment on glucose responses (Figure 5.6(2)).

Suppression of lipolysis, indicated by plasma NEFAs 0 min and 15 min, was also quantified (Figure 5.6(2)). Overall fasting circulating NEFAs were higher in animals receiving corticosterone treatment but were not affected by genotype. Following glucose administration, NEFA levels dropped rapidly during the first 15 min, at which time there were no differences between groups.

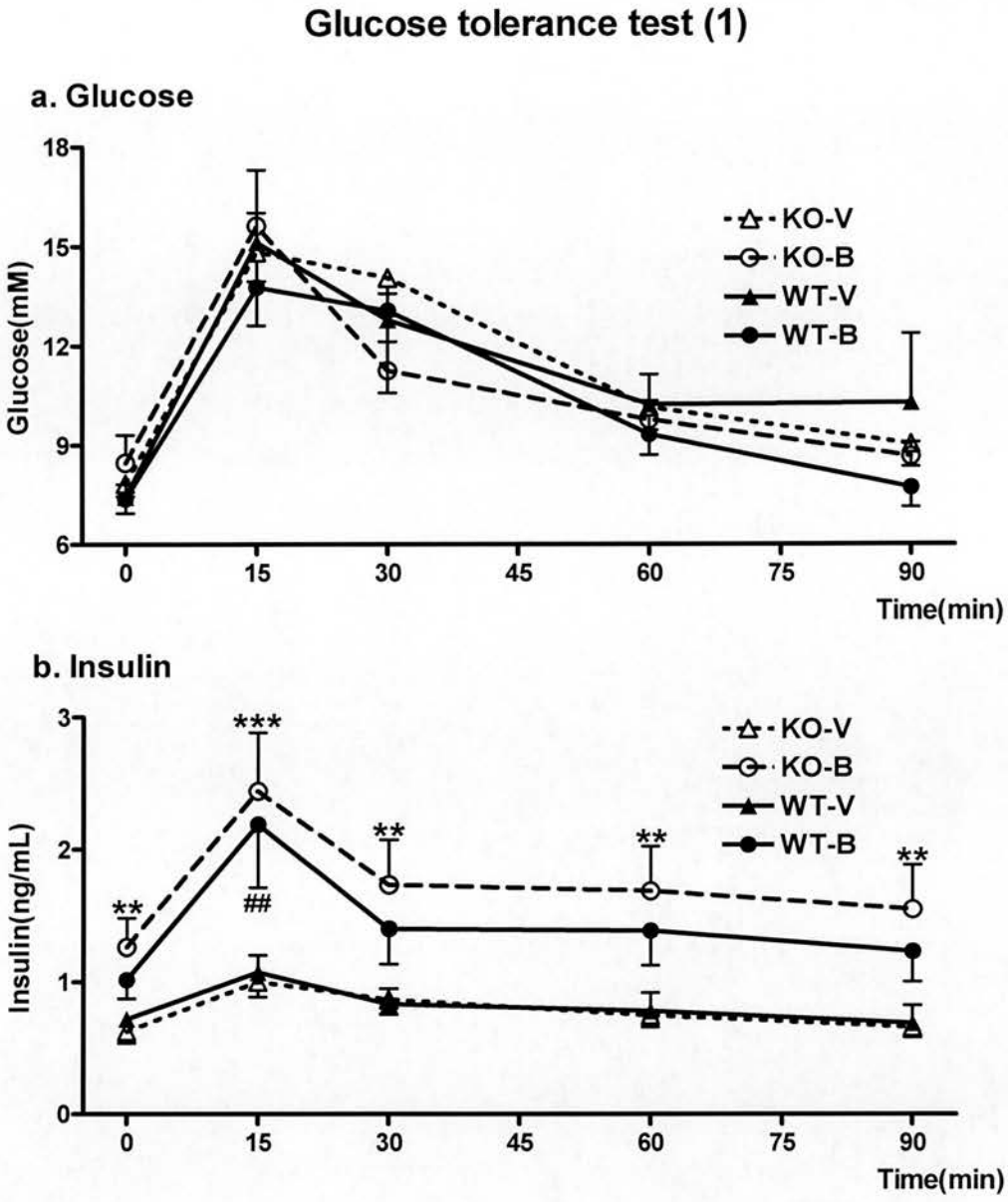

Insulin: Treatment, p<0.001; Time, p<0.001; Treatment×Time; p<0.001; Genotype, n.s.; Glucose, n.s.

Figure 5.6 (1) Plasma concentrations of (a) glucose and (b) insulin during a glucose tolerance test. Mice (WT and KO) received vehicle or B (50 µg/day) and were fasted for 6 h prior to being injected i.p. with glucose (2 g/kg BW). Samples were collected at 0, 15, 30, 60 and 90 min.Glucose was quantified by hexokinase assay, and insulin by ELISA. Plasma glucose was not different between genotypes or treatments. Animals receiving B showed hyperinsulinaemia compared to control mice. Data are mean ± SEM, n=12; **p<0.01 versus vehicle within KO; #P≤0.05, ##p<0.01 versus vehicle within WT; analysed by two-way repeated measure ANOVA with Holm-Sidak post-hoc tests.

Glucose tolerance test (2)

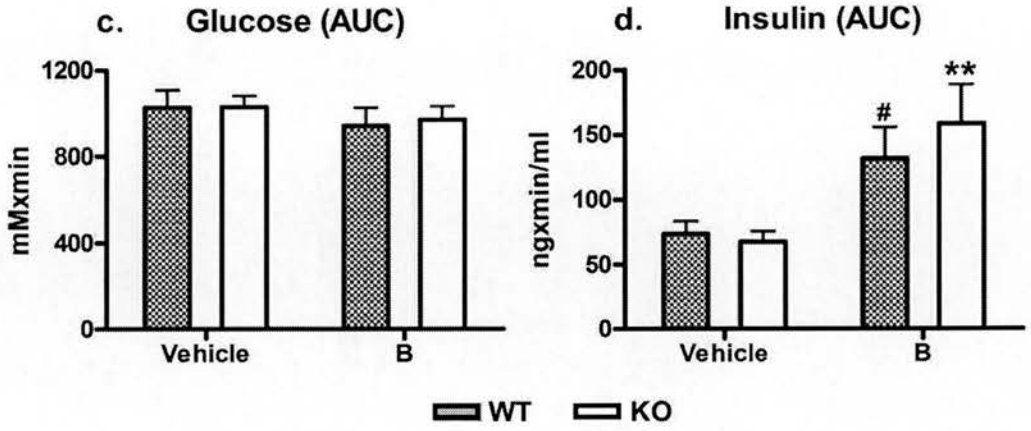

Insulin (AUC): Treatment, p<0.001.Others: n.s.

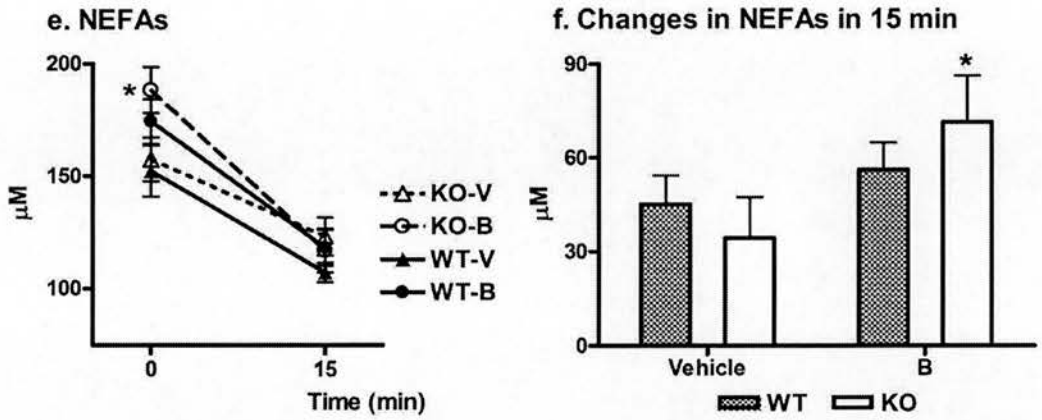

NEFAs: Treatment, p=0.029; Time, p<0.001; Genotype, n.s.
Changes in NEFAs: Treatment, p=0.046; Genotype, n.s.; Interaction, n.s.

Figure 5.6 (2) Plasma concentrations of (c) glucose, (d) insulin, (e) NEFAs, and (f) changes in NEFA concentrations from 0-15 min, during a glucose tolerance test. Glucose and insulin are presented as AUC generated from the graphs of Figure 5.6(1). Mice (WT and KO) receiving either vehicle or B (50 µg/day) were fasted for 6 h prior to being injected i.p. with glucose (2 g/kg BW). Samples were collected at 0, 15, 30, 60 and 90 min. Plasma glucose concentrations were not different between genotypes or treatments. Animals receiving B showed hyperinsulinaemia and hyperlipidemia compared to control mice. Significant differences of basal fasting NEFAs and NEFA suppression in 15 min were only observed not between genotypes. Data are mean ± SEM, n=12; **p<0.01 versus vehicle within KO; #P≤0.05, ##p<0.01 versus vehicle within WT; analysed by two-way ANOVA or two-way repeated measure ANOVA with Holm-Sidak post-hoc tests.

5.3.5 Glucocorticoid responsive genes in liver

The abundances of mRNAs of hepatic glucocorticoid responsive genes, TAT, PEPCK and angiotensinogen, were not significantly altered following the infusion of corticosterone, and no difference was observed between genotypes (Figure 5.7).

5.3.6 Glucocorticoid responsive genes in adipose tissue

The abundances of mRNAs of glucocorticoid responsive genes, 11β-HSD1 and angiotensinogen, were measured in mesenteric fat tissue (Figure 5.8). Basal expression of both genes was not affected by genotype. Corticosterone treatment did increase the expression of 11β-HSD1, an effect that was more marked in wild-type mice. In contrast, angiotensinogen expression was only increased by corticosterone in knock-out mice.

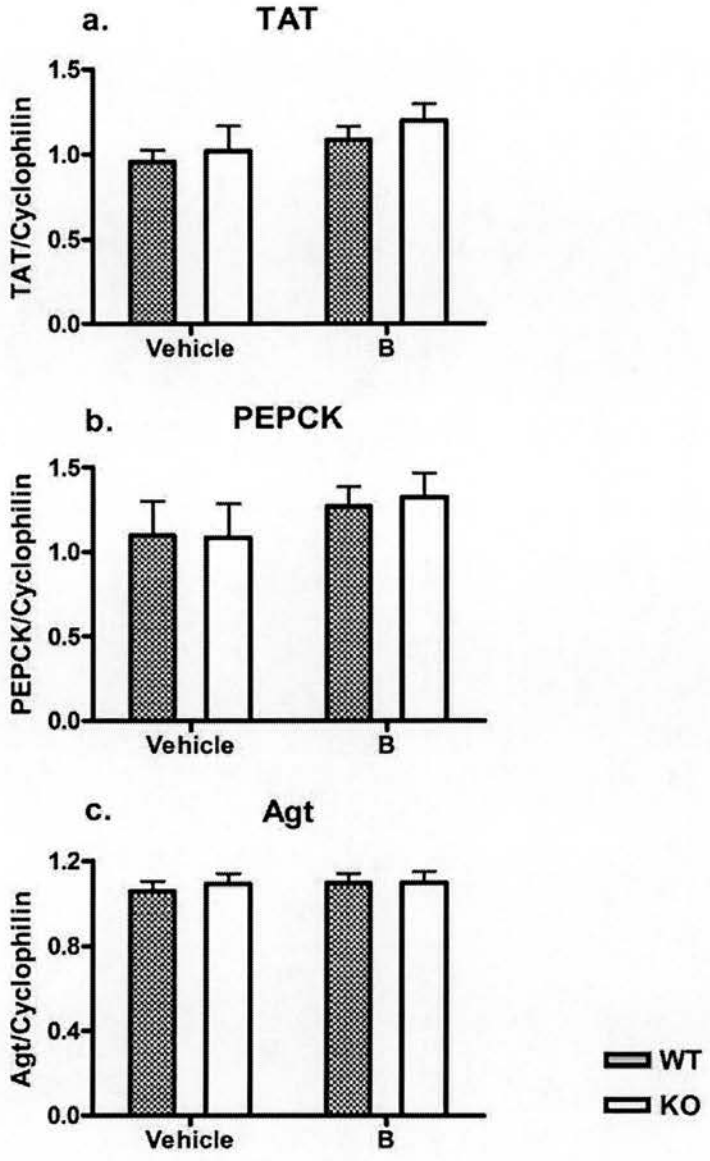

Genotype: n.s.; Treatment: n.s.; Interaction: n.s.

Figure 5.7 Transcript abundance of hepatic GC responsive genes, (a) TAT, (b) PEPCK, and (c) angiotensinogen (Agt), were quantified by real-time PCR normalized against cyclophilin. None of these hepatic genes were affected by genotype or steroid treatment. Data are mean ± SEM, analysed by two-way ANOVA, n=12.

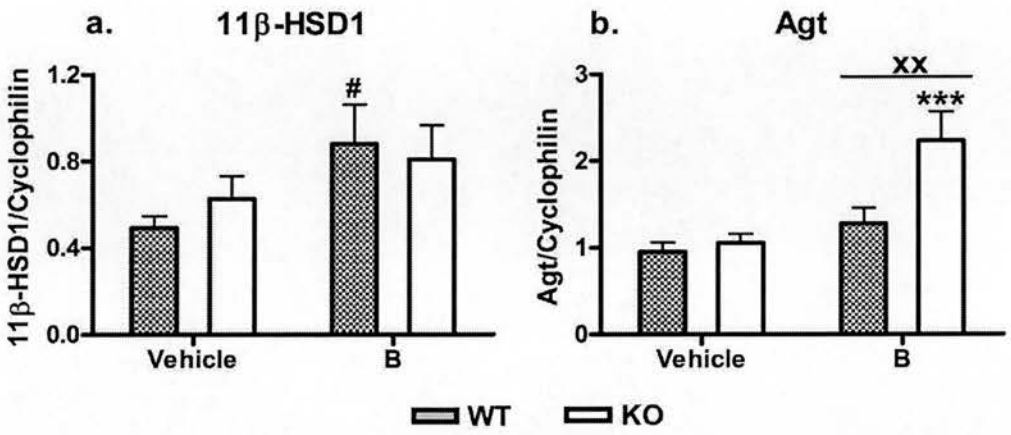

11β-HSD1: Treatment, p=0.041; others, n.s.;
Agt: Genotype, p=0.012; Treatment, p<0.001; Interaction, p=0.040.

Figure 5.8 Transcript abundances of (a) 11β-HSD1 and (b) Agt in mesenteric adipose tissue were quantified by real-time PCR normalized against cyclophilin. Both transcripts were significantly induced following B infusion. Changes of 11β-HSD1 were not different between genotypes, whereas Agt was highly induced by B in knock-out mice compared to wild-types. Data are mean ± SEM, n=12. ***$p<0.001$ versus vehicle within KO; #$p<0.05$ versus vehicle within WT, $^{XX}p<0.01$ versus the other genotype within the same treatment; analysed by two-way ANOVA with Holm-Sidak post-hoc tests.

5.3.7 Cytokine release in LPS activated whole blood

Cytokines were measured in whole blood samples when they were activated by increasing doses of LPS. As shown in Figure 5.9(1), proinflammatory cytokines TNFα and IL-6 were increasingly secreted as white blood cells were activated by LPS of 10 and 100ng, and they were significantly suppressed in samples collected from animals infused with corticosterone. However, there was no difference between by genotypes on either treatment.

Figure 5.9(2) shows results of chemokine MCP-1 and anti-inflammatory cytokine IL-10 measurements. The MCP-1 data were highly variable and no significant effect of genotype or steroid treatment was seen. Difference was not observed in the infusion treatments or genotypes. IL-10 in most samples was below the minimum detection limit of the CBA assay, although the higher concentrations of LPS did stimulate release.

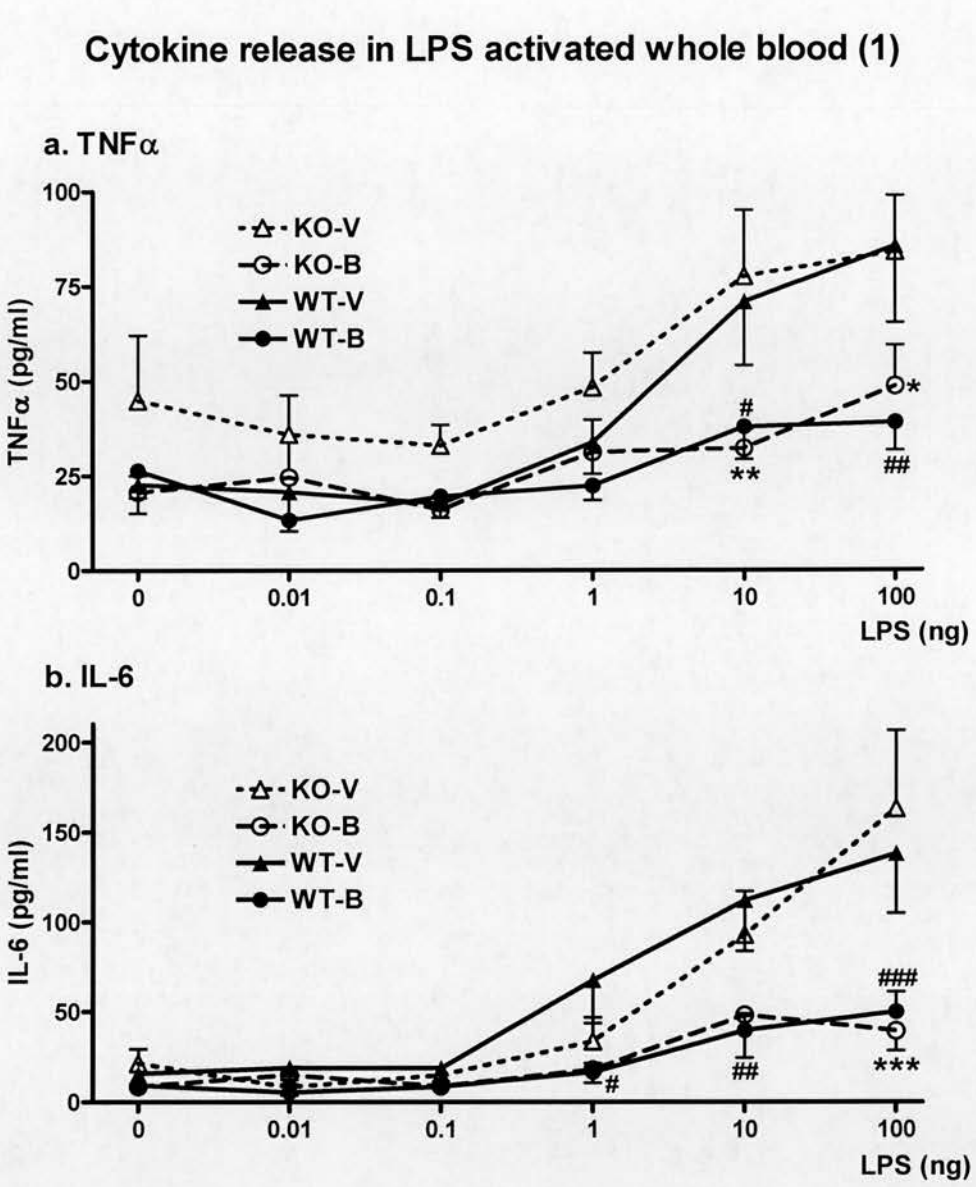

TNFα: Treatment, p=0.004; Dose of LPS, p<0.001; Treatment×LPS, p=0.015.
IL-6: Treatment, p=0.006; Dose of LPS, p<0.001; Treatment×LPS, p<0.001.
Genotype: n.s.

Figure 5.9(1) Release of proinflammatory cytokines (a) TNFα and (b) IL-6 from whole blood, activated by increasing doses of LPS (0, 0.01, 0.1, 1, 10 and 100ng), collected from mice (WT and KO) that were infused with B or vehicle for 14 days. They were quantified by CBA assay. TNFα and IL-16 were secreted in increased amounts as the dose of LPS increased. Their secretion was significantly suppressed in blood samples collected from animals infused with B. However, no difference was detected between genotypes. Data are mean ± SEM, n=5-12. *p<0.05, **p<0.01, ***p<0.001 versus vehicle within KO; #p<0.05, ##p<0.01 versus vehicle within WT; analysed by two-way repeated measure ANOVA with Holm-Sidak post-hoc tests.

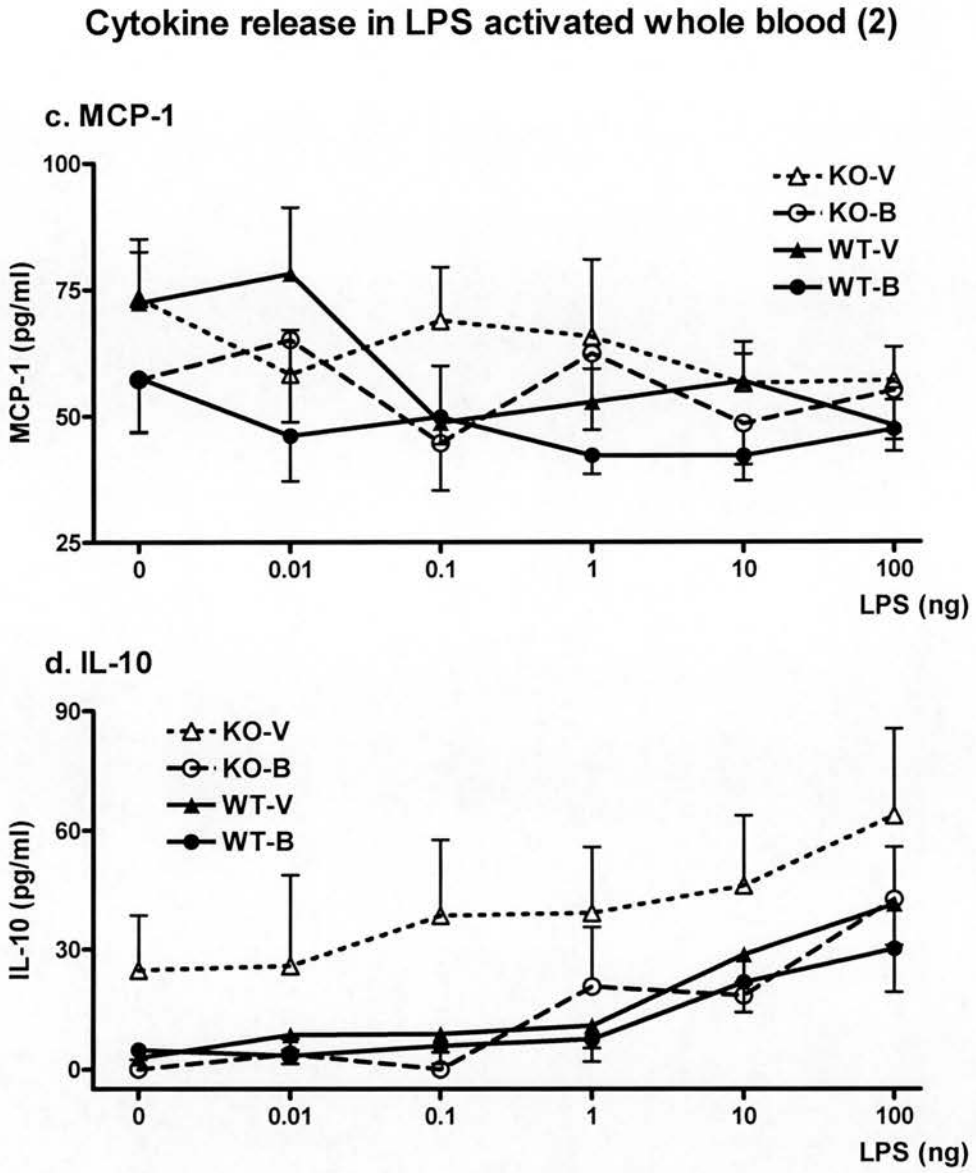

MCP-1 and IL-10: Dose of LPS: p<0.001; Treatment or genotype: n.s.

Figure 5.9(2) Release of chemokine (c) MCP-1 (n=3-12) and (d) anti-inflammatory cytokine IL-10 (n=3-10) from whole blood, activated by increasing doses of LPS (0, 0.01, 0.1, 1, 10 and 100 ng), from mice (WT and KO) that were infused with B or vehicle for 14 days. They were quantified by CBA assay. Secretion of MCP-1 and IL-10 was not significantly different in treatments of genotypes. Data are mean ± SEM, n=6-12, analysed by two-way repeated measure ANOVA (one factor repetition) with Holm-Sidak post-hoc tests.

5.4 Discussion

The role of 5αR1 in modulating tissue responses to glucocorticoid were investigated in *SRD5A1*$^{-/-}$ mice. Indices of the HPA axis, glucocorticoid target tissues, and glucose and lipid metabolism were measured, and cytokine production from leucocytes in the transgenic mice compared to wild-type mice was quantified. To summarise, there were no differences between wild type and 5αR1-knock-out mice in almost all variables measured during vehicle treatment. Animals infused with corticosterone showed changes typical of those reported in Chapter 4 but there were very few differences between wild-type and knock-out mice. In terms of the HPA axis, elevated circulating levels of corticosterone were accompanied by reduced adrenal size, independent of the presence of 5αR1. However, inhibited mRNA expression of POMC in pituitary was only detected in wild-type mice receiving corticosterone. In terms of metabolism, infusion of corticosterone resulted in smaller liver size and increased weights of mesenteric and subcutaneous fat depots in both genotypes. Moreover, animals receiving corticosterone exhibited elevated levels of insulin and free fatty acids during the glucose tolerance test, irrespective of genotype. In the mesenteric adipose tissue, expression of 11β-HSD1 was augmented following infusion of corticosterone in both genotypes, whereas angiotensinogen expression was only increased in 5αR1 knock-out mice receiving corticosterone. Immunosuppressive and anti-inflammatory effects of corticosterone were evident but not affected by transgenic disruption of 5αR1; weights of thymus and spleen were reduced by corticosterone treatment, regardless of genotype. Similarly, lack of 5αR1 did not alter the anti-inflammatory effects of corticosterone on suppression of LPS-induced cytokine production from blood leucocytes. It appears, therefore, that variations in the capacity to produce endogenous 5α-reduced corticosterone metabolites do not have a marked effect on glucocorticoid-sensitive variables or their response to exogenous corticosterone.

Corticosterone infusion increased circulating levels of the hormone to the same extent in both wild-type and knock-out mice, indicating that glucocorticoid clearance is not affected by genotypes. Since liver is the major organ for glucocorticoid

clearance and 5αR2 is not expressed in mouse livers (Mahendroo et al. 1996), 5β-reductase is the main metabolic enzyme, and 6β-hydroxylase and 20α- and 20β-HSDs are minor enzymes (Kawamura et al. 1981; Quattrochi and Guzelian 2001) in the liver of 5αR1 deficient mice. It appears that 5α-reductases and the other enzymes may be modulated concordantly to maintain a steady rate of hormone metabolism, and that they may be able to compensate for lack of 5αR1. It is known that hepatic 6β-hydroxylase (Quattrochi and Guzelian 2001) as well as renal 11β-HSD2 (Li et al. 1996; Suzuki et al. 2003) are substantially upregulated by glucocorticoids. Moreover, the Km of 5αR1 is in the low micromolar range and hence it will not be functioning at maximal velocity in the presence of normal baseline levels of corticosterone or even following corticosterone infusion. As circulating corticosterone was not different between genotypes, adrenal size in both genotypes was reduced similarly. 5αR2, not 5αR1, is the dominant 5α-reductase expressed in adrenals of male mice (Mahendroo et al. 1996) where it is thought to regulate steroidogenesis (Luu-The et al. 2005); therefore adrenal size is unlikely to be affected by local 5αR1 deficiency.

However, in the pituitary, POMC expression was only significantly suppressed in wild-type mice receiving corticosterone infusion; whereas in knock-out mice, exogenous corticosterone did not affect POMC expression. As the circulating levels of corticosterone were not different between genotypes, the differential response in POMC expression was possibly controlled by altered CRH however the reason was unclear and indeed there was no difference in the expression of CRH receptor 1 in the pituitary, although CRH itself was not quantified. It has been reported in rats that the 5αR1 is the dominant isozyme in the brain, including the regions of hypothalamus, cerebral cortex, subcortical white matter and purified myelin membranes (Poletti, et al. 1998). If the main role of 5αR1 in these areas was to inactivate corticosterone, then it might be anticipated that 5αR1 knock-out mice would be less able to inactivate corticosterone and induce greater suppression in these regions, in contrast to the findings here. However, as it has been shown in Chapter 4 as well as reported by McInnes et al. (2004), 5αTHB has the ability to suppress the release of ACTH and thus may play a key role in the set point of the HPA axis. As discussed previously in Chapter 4, 5αTHB may have the ability to

suppress CRH production via a mechanism whereby involves GR binding to the subunit of AP-1. Thus lack of this metabolite locally in the hypothalamus may reveal its contribution. Another explanation may be that 5αR2 is able to compensate for the lack of 5αR1 in the brain as it does in the male murine reproductive tract (Mahendroo et al. 1996). In support, 5αR2 is selectively expressed in the hypothalamus, and it is also expressed in hippocampus after acute stress (Poletti et al. 1998). Therefore, it could be possible that in 5αR1-deficient mice, the expression of 5αR2 was increased to compensate for the missing 5αR1 activity in the hypothalamus. 5αR2 has 10-20 fold higher affinity for corticosterone than 5αR1, allowing corticosterone to be cleared more efficiently in hypothalamus of knock-out mice, thereby ameliorating the decrease in POMC expression. These hypotheses have not been tested, although brains have been archived and could be studied to quantify CRH and 5αR2 at sites of negative feedback.

In terms of the peripheral actions of glucocorticoids, blood pressure was not different between 5αR1 knock-out and wild-type mice. Glucocorticoids increase blood pressure through regulation of vascular tone by increasing vasoconstrictive factors and decreasing vasodilatory proteins, and activating the renin-angiotensin system (Sato et al. 1994). In the kidney, glucocorticoids cause vasodilatation and increase glomerular filtration rate (De Matteo and May 1997), and enhance the activity of ion transporters in the proximal tubules (Brem 2001). The increase in circulating corticosterone in animals receiving this treatment did not translate into elevated blood pressure perhaps because of the limited sensitivity of the method of blood pressure measurement, and this could be improved using telemetry. It would also be of interest to see whether vascular reactivity and/or renal functions are affected in knockout mice (with and without corticosterone treatment).

Body weight gain was not changed significantly by genotype or treatment. However, corticosterone did affect the weight of several organ weights albeit without genotypic differences being revealed. Infusion of corticosterone caused atrophy of the thymus and spleen, supporting the fact that glucocorticoids have immunosuppressive effects on T-cell apoptosis (Ashwell et al. 2000). Lack of 5αR1 did not alter the extent of

changes which again are likely to be a function of circulating steroid concentrations, although the thymus does expresses 5αR1 to a small extent in adult animals (Borlak, et al. 2004). In the present study, liver weights were reduced by infusion of corticosterone regardless of genotype. This reduction contrasted with previous finding of glucocorticoid-induced increases in liver weight which were associated with hepatic triglyceride and glycogen storage (Santidrian and Young 1980; Mantha et al. 1999; Bollen et al. 1998; van Schaftingen and Gerin 2002). These increases are perhaps independent of hepatic 5αR1 and may require higher doses of glucocorticoid hormone. It is significant that infusions of low doses of corticosterone in the present studies did not provoke the changes in hepatic glucocorticoid responsive genes including PEPCK, TAT, and angiotensinogen which were observed in more acute studies with higher steroid doses.

In adipose tissue, among the five adipose depots, weights of mesenteric and subcutaneous fat pads were increased in animals receiving corticosterone, which was more evident when the data were presented as the percentage of body weight; this bears similarities to the animals in Chapter 4. Although lack of 5αR1 did not induce significant difference in adipose weights between genotypes, local levels of corticosterone in adipose tissue may have been differently regulated in knock-out mice. 5αR1 is expressed at this site (Normington and Russell 1992) and may act to inactivate corticosterone. As tested in mesenteric fat depots, expression of the glucocorticoid responsive gene angiotensinogen was dramatically increased in 5αR1 deficient mice receiving corticosterone treatment (without a change in blood pressure), whereas the expression in wild-types was not changed. In contrast however, 11β-HSD1 was upregulated by corticosterone in animals of both knock-out and wild-type receiving this hormone. It is not clear why the two glucocorticoid responsive genes were diversely regulated, but the effects on angiotensinogen suggest that within the intracellular compartments, glucocorticoid concentrations may be altered as a result of reduced 5αR1 activity. Interestingly, these changes were revealed in adipose which does not express other clearance mechanisms (e.g. 5βR, 5αR2, 11β-HSD2), in contrast to liver. Inside the adipocytes, corticosterone treatment increased the activity of 11β-HSD1 regenerating more active

corticosterone thus amplifying the action independent of 5αR1. In the adipose tissue of wild-type animals, excessive glucocorticoids may subsequently be inactivated by 5αR1 only. However in the 5αR1 knock-out mice receiving exogenous corticosterone, amplified corticosterone levels may have been cleared slowly in adipose tissue, and therefore angiotensinogen may be dramatically induced. This evidence suggested that the 5α-reduced metabolism inactivated glucocorticoid actions in adipose tissue and may play an important role in regulating glucocorticoid action in this tissue. Additionally, 11β-HSD1 is responsive to glucocorticoid only but angiotensinogen regulated by both glucocorticoid and estrogen (Kunapuli et al. 1987), the latter being higher in 5αR1 knock-out mice due to an increased accumulation of androgen precursors (Martin et al. 2003). This may also be responsible for the diverse regulation of the two genes. The elevated estrogen levels in the knock-out mice may have primed for the corticosterone treatment and cause additive effects on angiotensinogen expression.

Besides the overexpression of 11β-HSD1 and angiotensinogen, rates of lipolysis in adipose tissue were altered following glucocorticoid infusion. When treated with corticosterone, basal levels of NEFAs were significantly higher and suppression of lipolysis was greater during the glucose tolerance test, indicative of mild insulin resistance. Increased insulin and free fatty acids were also observed in animals receiving infusion of corticosterone. These changes were not significantly different between genotypes. However, the impact of 5αR1 deficiency on these variations could be revealed more clearly in 5αR1-null mice predisposed to the Metabolic Syndrome, e.g. following a high-fat diet, which has been demonstrated recently that 5αR1-null mice showed glucose intolerance and fatty liver (Livingstone et al. 2008).

Cytokine secretion was measured from the LPS stimulated whole blood collected from mice of 5αR1 knock-out or wild-type following infusion of corticosterone. Production of pro-inflammatory cytokines, TNFα and IL-6, were significantly suppressed by corticosterone treatment regardless of genotypes. These findings are consistent with the results shown in Chapter 4. Previously we showed that the 5α-reduced metabolites may also induce immune suppression and hypothesized that lack

of the enzyme may to predispose to inflammation. A difference in cytokine release was not detected between genotypes following infusion of corticosterone. Since most corticosterone is inactivated by first pass metabolism, corticosterone treatment does not subsequently elevate 5αTHB in blood (as demonstrated in Chapter 4); hence in the circulation, blood leucocytes (mainly monocytes/macrophages) would not have sensed the lack of this metabolite. Macrophages do not express 5αR1 (data shown in Chapter 3) and thus cannot locally synthesise the active metabolite.

These results lead to the conclusion that following chronic glucocorticoid excess, hepatic 5α-reductase deficiency may be compensated to some degrees by increased corticosterone metabolism by other routes. However, the adverse metabolic effects of glucocorticoids are similar in wild-type and 5αR1-knock-out mice, suggesting that variations in endogenous 5α-reduced corticosterone metabolites do not substantially modify GR metabolic signalling during glucocorticoid excess. Whether these metabolites are important during glucocorticoid deficiency has not been tested here. Regarding inflammatory signalling, in macrophages A-ring reductases, but not 11β-HSD1, are absent, so intact anti-inflammatory effects of glucocorticoids may be maintained and these cells are responsive to circulating steroid concentrations. It may only be when immune cells infiltrate tissues containing the enzyme e.g. liver and adipose, that the paracrine effects of 5αTHB to suppress inflammation come into play. The potential for interactions between 5αR1 and inflammation in liver and adipose deserve further exploration in models of the Metabolic Syndrome, e.g. with high fat feeding.

Chapter 6

Investigation of anti-inflammatory effects of 5αTHB *in vivo*

6.1 Introduction

As shown in previous chapters, 5αTHB could exert anti-inflammatory effects in isolated cells and also *ex vivo* following infusion in healthy mice. It increased the secretion of anti-inflammatory cytokine IL-10, and suppressed the production of LPS-induced pro-inflammatory cytokines TNFα and IL-6, from cultured bone marrow derived macrophages; and also suppressed LPS-induced release of TNFα and IL-6 from blood leucocytes harvested at cull, mainly monocytes/macrophages. However, the anti-inflammatory effects of 5αTHB *in vivo* have not been tested. As the investigation in previous chapters was carried out using LPS-stimulated inflammatory cell models, this chapter will further pursue the effects of 5αTHB on LPS-induced inflammation in animals. The hypothesis of the study in this chapter is that 5αTHB will be an immune suppressant during an inflammatory response *in vivo*.

Aims

The aim of this chapter was to investigate the anti-inflammatory effects of 5αTHB in mice following intraperitoneal administration of LPS.

6.2 Methods and materials

6.2.1 Maintenance of animals

Male C57BL/6 mice were maintained as described in Section 2.3.1.

6.2.2 Buffers and solutions

6.2.2.1 Steroid injection solutions

Corticosterone and 5αTHB (0.005 g) were dissolved thoroughly in DMSO (1 ml) on the day of experiment. Vehicle was DMSO only. They were loaded into Insulin pens (NovoPen®3, 30G) and stored at RT.

6.2.2.2 LPS injection solution

On the day of experiment, LPS (10 mg) was dissolved thoroughly in PBS (4 ml, see 2.2.4.2) and stored at -4 °C until required.

6.2.2.3 BSA buffer (0.1% w/v)

BSA (0.3g, fraction V) was dissolved in PBS (300ml, see 2.2.4.2).

6.2.3 Administration of steroid and LPS

At 14:00, animals were injected s.c. with corticosterone, 5αTHB (0.1 mg in 20 µl DMSO per mouse) or vehicle (DMSO, 20 µl), n=8. One hour later, all were injected i.p. with LPS (100 µl, approximately 10 mg/kg BW).

6.2.4 Terminal procedures

At 09:00 on the next day, 18h after the administration of LPS, mice were decapitated, and trunk blood was collected immediately into tubes containing EDTA (0.5 M).

Plasma was prepared thereafter by centrifugation (1000 g, 5 min, 4 °C) and stored at -20°C until required for quantification of corticosterone and ACTH.

6.2.5 Peritoneal lavage

Post mortem, mouse skin was removed from the abdomen so that the trunk was exposed. The peritoneal cavity was washed by injecting sterile saline (0.9%, 2 ml, Fisher Scientific) followed by gently massage on the abdomen. The cavity was washed for three times. The first lavage fluid was transferred into a 2 ml round-bottom microtube, and the last two lavages were combined in a 15 ml Falcon tube. All the tubes were placed on ice.

6.2.6 Preparation of lavage samples

Following centrifugation (1,000 g, 5 min, RT) of all the lavages, the supernatant from the first lavage fluid was aliquoted to three microtubes for quantification of cytokines. The supernatant from the other two lavages were discarded. Lavage was deemed unsuccessful if the peritoneal cavity was contaminated with blood, and the samples were not processed further.

The cell pellet remaining in the Falcon tubes was resuspended in BSA buffer (0.1% w/v, 0.5 ml) before cells were transferred into the corresponding microtube containing cells from the first lavage. Then cells from three lavages were combined and gently resuspended, and 10 µl was diluted in BSA buffer (0.1% w/v, 90 µl).

6.2.7 Quantification of inflammatory cells

The total number of inflammatory cells in the cell suspension (100 µl) was determined using a NucleoCassette and a NucleoCounter (ChemoMetec, Denmark). The reagents provided (Reagent A-100 (100 µl) followed by Reagent B (100 µl)) were added into the suspension and gently flicked to mix. Reagent A-100 (pH 1.25) was used as a lysis buffer that disaggregated cell clusters and disrupted cell membranes. Reagent B was a stabilizing buffer that raised the pH value and allowed

more efficient staining of DNA in the NucleoCassette. The disposable cassette was loaded with approximately 50 µl of the sample mixture. The fluorescent dye propidium iodide immobilized inside the flow channels of the cassette was dissolved and mixed with the sample, staining the DNA of cell nuclei. The loaded cassette was then placed in the NucleoCounter which is an integrated fluorescence microscope. The stained sample mixture (approximately 2 µl) passed into the measurement chamber of the cassette where the fluorescent image was recorded. The image as well as the total cell number was generated automatically by NucleoView Software (ChemoMetec, Denmark).

6.2.8 Cytospin and differential cell quantification

Approximately 4×10^4 cells were mixed into the BSA buffer (300 µl) and deposited by centrifugation (250 g, 3 min, RT) onto a microscope slide by Cytospin-3 (Shandon Scientific Limited, Cheshire, England). One cytospin was prepared per mouse. Cells on the air-dried slides were fixed in 100 % methanol for 1min and stained by eosin and methylene blue (Wright's stain) before being washed in distilled water and allowed to dry. A coverslip was mounted on the slide with the mounting medium and left over night for stabilization. Differential cell counts were performed by light microscopy (Model: Axioskop, Carl Zeiss, Germany; objective, Plan-Neofluar 40×/0.75; ocular lens, E-Pl 10×/20). At least 300 cells were counted per slide. Standard morphologic criteria were used to identify cell types as follows,

Polymorphonuclear cells:

PMNs, also called neutrophils, are mobile phagocytes that comprise the majority of blood leukocytes. Their nuclei are multilobed and they stain dark blue.

Eosinophils:

Eosinophils are granular leukocytes which stain with eosin. The cytoplasm contains numerous coarse, reddish-orange granules.

Basophils and mast cells:

Basophils and mast cells have similar morphology and functions. They are stained with basic dyes. There are large, dark-blue granules in the cytoplasm which are darker than the nuclei.

Lymphocytes:

Lymphocytes are stained with basic dyes and have very little cytoplasm. Their nuclei are generally round or oval.

Monocytes and macrophages:

Monocytes resemble lymphocytes but are larger. The cytoplasm is grey-blue and more abundant than in lymphocytes. Their nuclei are lobulated, indented or kidney-shaped.

Macrophages originate from monocytes. The mononuclear phagocyte system is composed of both macrophages and monocytes. Macrophages are large and variable-shaped cells, and have round nuclei and lysosomes in the cytoplasm.

6.2.9 Biochemical assays

6.2.9.1 Quantification of plasma ACTH

ACTH in plasma prepared from trunk blood was quantified by ELISA (see 2.6.4)

6.2.9.2 Quantification of cytokines

Cytokines in plasma and lavage fluid samples were quantified by CBA assay as described in Section 2.6.6.

6.3 Results

6.3.1 Activation of the HPA axis

Following the administration of steroids and induction of peritonitis, plasma ACTH and corticosterone were variable, and not significantly different between experimental groups (Figure 6.1).

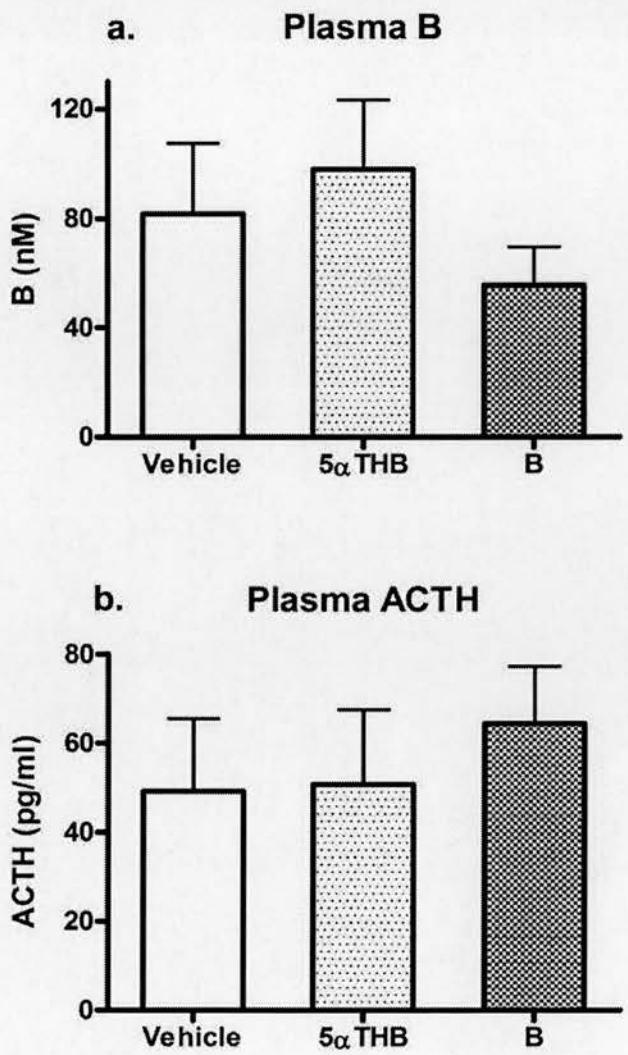

Figure 6.1 Plasma (a) ACTH and (b) B, quantified by ELISA and RIA respectively, in mice with 1 h pre-treatment of steroids followed by LPS-induce peritonitis after 18 h. ACTH and B were not significantly different between experimental groups. Data are mean ± SEM, n=8, analysed by one-way ANOVA.

6.3.2 Differential cell quantification

Inflammatory cells in the peritoneal lavages including PMNs, monocytes/macrophages (mono/macro), basophils/mast cells (baso/mast), lymphocytes and eosinophils were quantified and presented by actual cell numbers (Figure 6.2(1)) and percentage of total cells (Figure 6.2(2)). Neither steroid had any effect when compared with vehicle treated controls, although in some case cell numbers were variable.

6.3.3 Peritoneal cytokines

As shown in Figure 6.3, concentrations of IL-6 produced in the peritoneal cavity were substantially suppressed by both 5αTHB and B. Peritoneal MCP-1 levels were not different in animals between the treatment groups.

6.3.4 Plasma cytokines

As shown in Figure 6.4, circulating IL-6 concentrations were elevated in animals pre-treated by 5αTHB only. Plasma MCP-1 levels were not different in animals between the treatment groups.

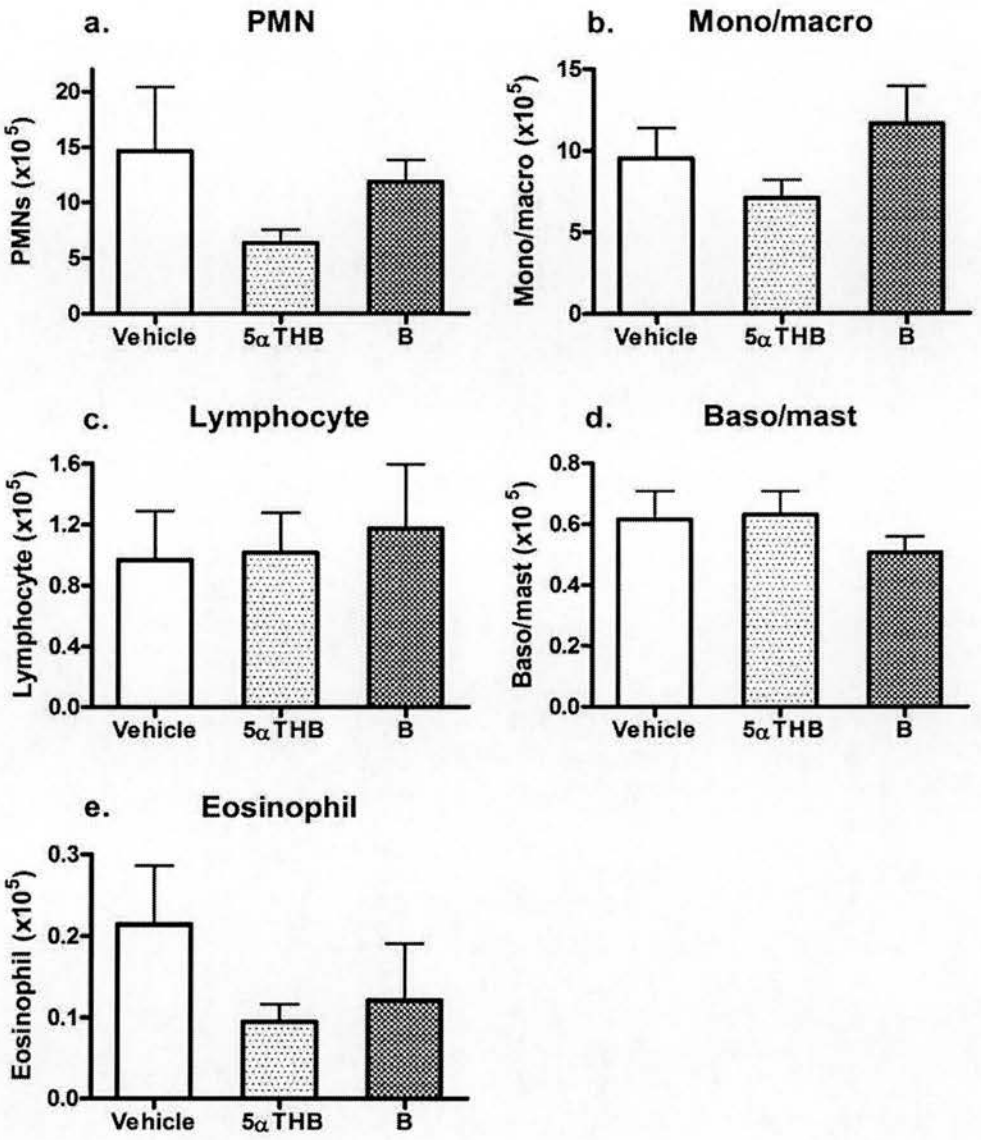

Figure 6.2 (1) Differential cells count of peritoneal lavages. (a) PMNs, (b) mono/macro, (c) lymphocytes, (d) baso/mast, and (e) eosinophils, were not affected by either steroid treatment when compared with vehicle treated controls. Data are mean ± SEM, n=8, analysed by one-way ANOVA.

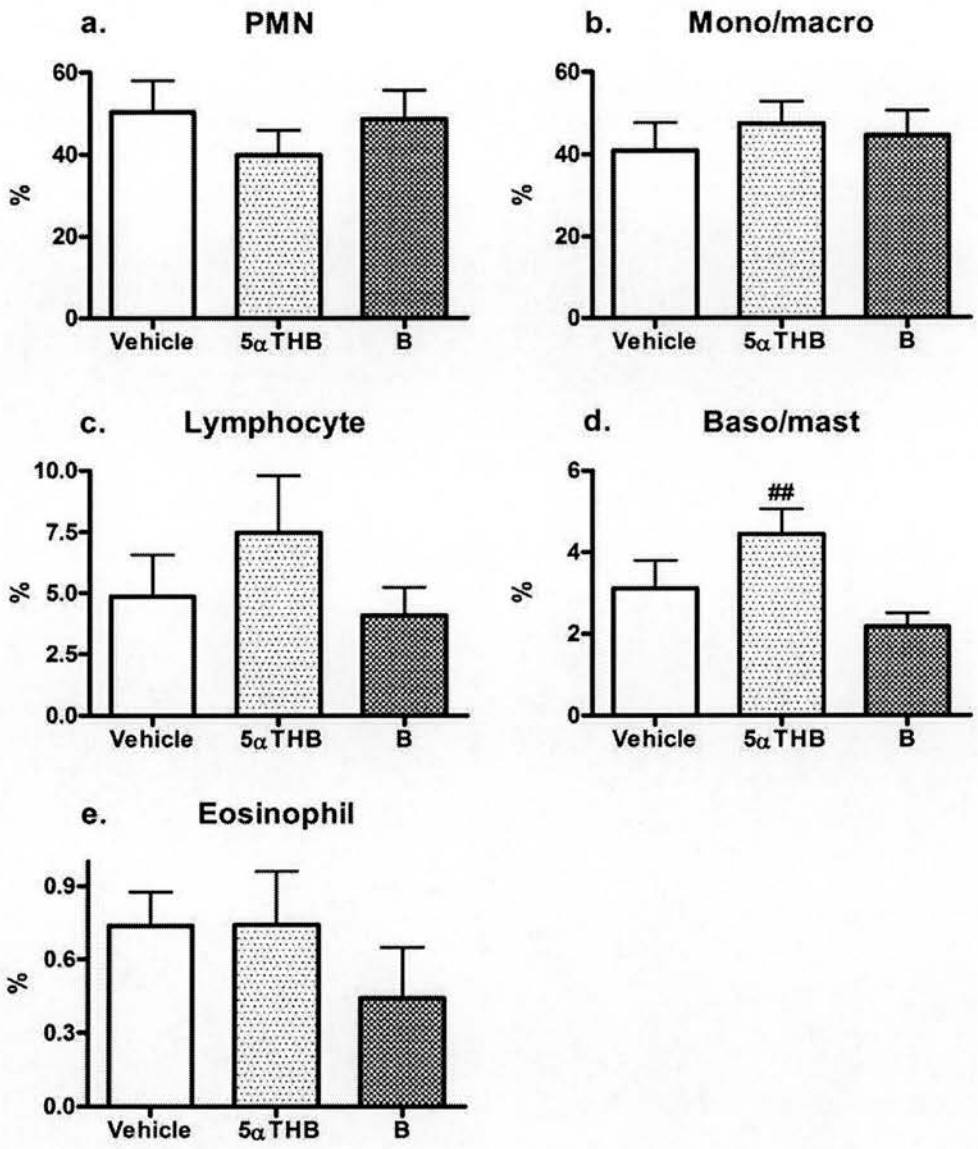

Figure 6.2 (2) Differential cells count of peritoneal lavages, presented by percentage of total cells, (a) PMNs, (b) mono/macro, (c) lymphocytes, (d) baso/mast, and (e) eosinophils. Neither steroid had any effect when compared with vehicle treated controls. Baso/mast cells were increased in animals pre-treated with 5αTHB compared to B. Data are mean ± SEM, n=8, ##$p<0.01$ versus B, analysed by one-way ANOVA with Holm-Sidak post-hoc tests.

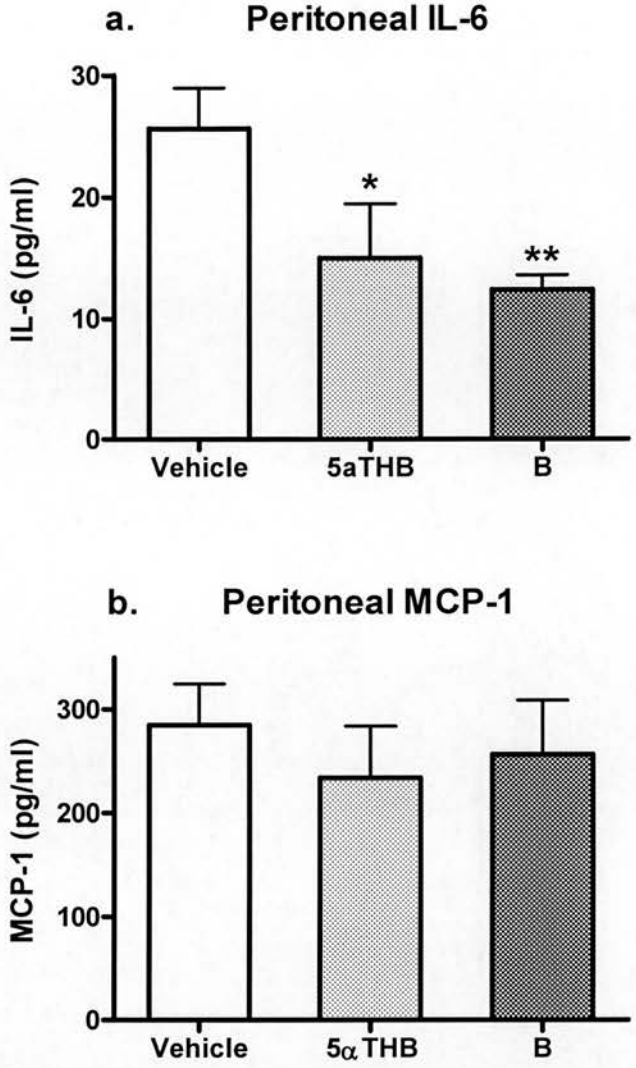

Figure 6.3 IL-6 and MCP-1 concentrations in the peritoneal cavity. (a) IL-6 and (b) MCP-1 were quantified in the peritoneal lavage fluid by CBA. IL-6 production was suppressed by 5αTHB and B. Peritoneal MCP-1 was not different between the treatment groups. Data are mean ± SEM, n=8; *$p<0.05$, **$p\leq0.01$ versus vehicle; analysed by one-way ANOVA with Holm-Sidak post-hoc tests.

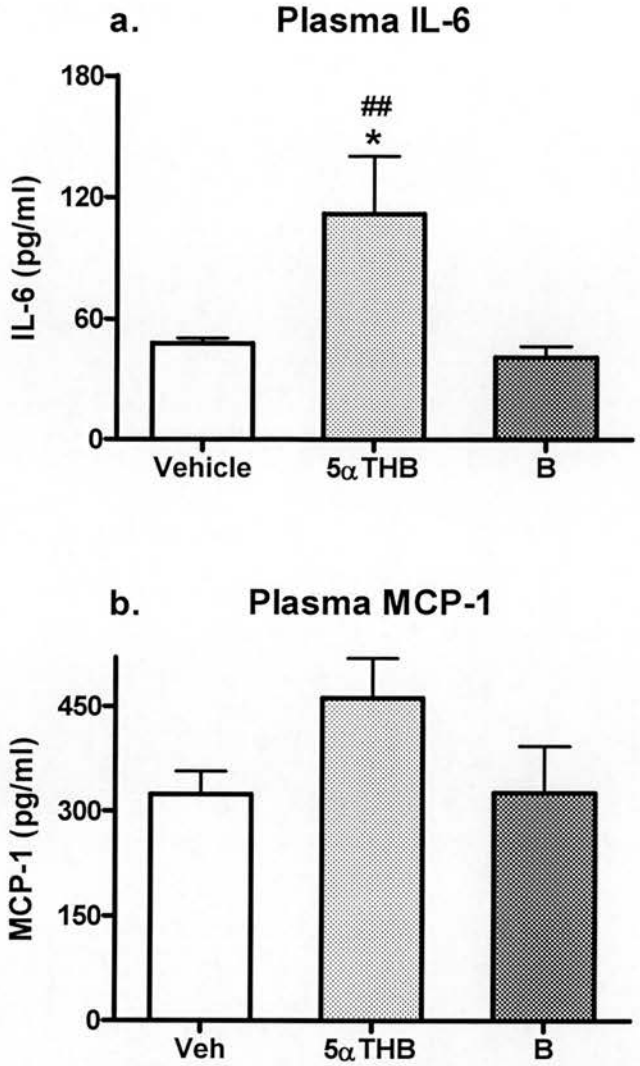

Figure 6.4 IL-6 and MCP-1 concentrations in the plasma. (a) IL-6 and (b) MCP-1 were quantified in the plasma by CBA. IL-6 production was elevated in animals pre-treated by 5αTHB only. Plasma MCP-1 was not significantly different between the treatment groups. Data are mean ± SEM, n=8; *$p<0.05$ versus vehicle, ##$p\leq0.01$ versus B; analysed by one-way ANOVA with Holm-Sidak post-hoc tests.

6.4 Discussion

Pharmaceutical doses of glucocorticoids have profound anti-inflammatory effects and exert pleiotropic actions on target cells. Neutrophils are among the first immune cells to be recruited in response to pathogens and injury. These cells, together with basophils and eosinophils, secrete proinflammatory cytokines and chemokines that attract other immune cells to the site of inflammation, and also remove foreign substances through phagocytosis. Glucocorticoids inhibit the chemotactic activity of neutrophils, induce apoptosis in basophils and eosinophils, and also suppress proinflammatory cytokines and chemokines production from these cells (Butts and Sternberg 2008; Goulding et al. 1998; Sorrells and Sapolsky 2007). Monocytes are antigen presenting cells with phagocytic properties; macrophages are the mature form of monocytes. They promote inflammatory responses by secreting proinflammatory cytokines including TNF-α, IL-6 and IL-1β. At the later stage of inflammation, macrophages remove the phagocytosing granulocytes that have undergone apoptosis. Glucocorticoids suppress the differentiation of monocyte into macrophages, macrophage phagocytosis, and secretion of proinflammatory cytokines (Baybutt and Holsboer 1990). Moreover, glucocorticoids induce apoptosis in T lymphocytes and shift phenotypes from Th1 (secreting IL-2 and IFN-γ) to Th2 (secreting IL-4 and IL-10) that reduces inflammation (Elenkov and Chrousos 2002). Lymphocyte trafficking is also inhibited by glucocorticoids (Milad et al. 1994; Tait et al. 2008).

As shown in previous chapters, 5αTHB was active to suppress the LPS-induced production of TNFα and IL-6 from cultured bone marrow derived macrophages and blood immune cells. In the present study, anti-inflammatory effects of 5αTHB *in vivo* were investigated, using the model of LPS induced peritonitis. Intra-peritoneal administration of LPS causes a dose-dependent endotoxemia and induces a variety of systemic responses including infiltration of immune cells. In the acute phase after administration of LPS, neutrophils enter the peritoneal cavity, however at later stages macrophages are attracted to the site of inflammation.

It appeared that in the experimental animals, inflammation had resolved at 18 h, since the numbers of immune cells in the peritoneal cavity were not elevated above vehicle, and did not differ between steroid treatments. However initial infiltration was not quantified. Baso/mast cells were increased in mice pre-treated with 5αTHB compared to those primed with corticosterone but not to the controls. These cells only represent a small population of the peritoneal immune cell family. Glucocorticoids can induce apoptosis in basophils, which may have occurred in response to corticosterone. Nonetheless these findings are weak and the general picture suggests a lack of change in peritoneal cells.

The activated immune cells release cytokines (e.g. TNFα, IL-1β, and IL-6) in response to LPS (Romanovsky, et al. 2000). Corticosterone as well as 5αTHB reduced the production of IL-6 within the peritoneal cavity even up to 18h later, suggesting the comparable local anti-inflammatory effects of 5αTHB and corticosterone. These findings support those in previous chapters, although the local concentrations of LPS and steroid in peritoneal cavity were unknown. MCP-1 was not suppressed, consistent with equivalent numbers of macrophages in the lavage fluid and also the weaker response of this chemokine in previous Chapters.

A different picture was observed in plasma, where circulating IL-6 was increased selectively by 5αTHB. There are two routes for LPS to escape from the peritoneal cavity, the hematogenous and the lymphogenous routes, which are via the portal vain and the lymph system, respectively (Romanovsky et al. 2000). Cytokines produced in the peritoneal cavity remain local, whereas those in circulation are primarily derived from immune cells outside the peritoneal cavity, mainly from monocytes or endothelial cells (Lenczowski et al. 1997). Appearance of LPS in the general circulation is a prerequisite for the elevation of circulating IL-6, which plays a critical signalling role in the LPS-induced activation of the HPA axis (Lenczowski et al. 1997), with subsequent release of ACTH and corticosterone into the circulation. In Lenczowski's study in rats, endotoxin appeared in the general circulation within 15 min of the intraperitoneal LPS injection, whereas elevations of plasma ACTH, corticosterone, and IL-6 concentrations were not detected until 90 min (Lenczowski

et al. 1997). Moreover, the elevated levels in circulating IL-6, ACTH and corticosterone correlated with circulating endotoxin, not with local LPS or cytokines within the peritoneal cavity (Lenczowski et al. 1997).

In the present study, circulating levels of ACTH and corticosterone at 18 hours following administration of LPS were not significantly different between experimental groups, perhaps simply because that peak time of ACTH elevation induced by LPS had passed. Animals were terminated at 9:00 a.m. at the circadian nadir for HPA hormones. The low levels of ACTH (<80 pg/ml) and corticosterone (<120nM) suggested that the HPA axis had returned to basal. However, 5αTHB pretreated mice exhibited higher plasma IL-6 compared to the vehicle and corticosterone pre-treated animals. The reason of the observed deviation of plasma ACTH, corticosterone and IL-6 is unknown, and the results were somewhat variable between individuals (variability was also great in Lenczowski's study), although an explanation might exist.

It has been reported in rats that the onset of ACTH suppression was observed at 2 h post-5αTHB injection compared with 1 h post-corticosterone injection. Also the 5αTHB effect lasted longer (up to 6 h, final time point tested) than that of corticosterone (up to 2 h) (McInnes et al. 2004). Plasma ACTH, corticosterone and IL-6 concentrations peak at about 2 h after intraperitoneal administration of LPS in rats (Lenczowski et al. 1997). In mice, plasma IL-6 also increased at 2 h post-challenge and returned to baseline by 6 h (Eskay, et al. 1990). Thus in the present experiment, the HPA axis would have been suppressed one hour after corticosterone treatment so that subsequent activation of the HPA axis by LPS may be impaired. The circulating corticosterone would be mainly exogenous and exert suppressive effects on IL-6 secretion. Following vehicle treatment, intraperitoneal administration of LPS would activate the HPA axis in response to cytokine production. Endogenous corticosterone in circulation would increase to suppress IL-6 production. Eighteen hours later, plasma IL-6 would already have returned to the basal levels in animals of the vehicle and corticosterone treated groups. However in animals receiving 5αTHB, the HPA axis would be suppressed in a slower and weaker manner so that LPS

activation of the HPA axis might only be partially suppressed. Therefore 5αTHB treated mice might produce less endogenous corticosterone than the vehicle treated mice. Circulating 5αTHB was not potent enough to suppress IL-6 secretion from monocytes/macrophages induced by a large dose of LPS, resulting in higher levels of plasma IL-6 compared to the IL-6 levels in the other groups. Further time course studies of responses of the HPA axis and cytokine release to LPS stimulation are required to validate this explanation.

Moreover, in previously reported studies, plasma levels of IL-6 at 12 h post LPS-challenge were at least 10^5 pg/ml (quantified by ELISA) (Bhattacharyya et al. 2007), far higher than the values observed in the present study (10^2 pg/ml, quantified by CBA). This might indicate that, in the present study, IL-6 levels in all animals had already returned to base line values by 18 h after LPS treatment.

In conclusion, these results performed *in vivo* demonstrated the potential suppressive effects of 5αTHB on LPS-induced production of IL-6 in the peritoneal cavity. Although the impact of 5αTHB pre-treatment on the general circulating levels of LPS was not tested, 5αTHB may suppress the HPA axis and somehow affect the resolution of inflammation *in vivo*, resulting in prolonged elevation of IL-6 in the circulation. Since intraperitoneal administration of endotoxin resulted in systemic sepsis rather than restricted inflammation, it was not an ideal animal model in which to study the anti-inflammatory effects of 5αTHB. Recently in our lab, these experiments have been taken forward using restricted peritonitis induced by thioglycollate which has produced reasonable dose-dependent responses of peritoneal immune cell numbers which could be suppressed by corticosterone. Use of this model will allow corroboration of these preliminary findings and investigation of more detailed dose responses.

Chapter 7

Summary and future work

The hypothesis of this thesis is that 5αTHB possesses some of the glucocorticoid agonist properties of its parent steroid corticosterone and hence is not an inert metabolite. The aims of this thesis were to assess the cellular effects of 5αTHB on transactivation and transrepression, and the physiological effects of 5αTHB on HPA axis, fuel metabolism, and immune responses. The work described in this thesis has demonstrated 5αTHB is a weak GR ligand with suppressive effects on immune responses but without metabolic effects. Effects on HPA axis were discordant between cell studies and *in vivo* studies and are most likely due to indirect effects. The molecular basis for the selectivity of 5αTHB for anti-inflammatory glucocorticoid action appears to lie in activation of GR-mediated protein interactions but not chromatin binding.

5αTHB induces GR translocation

Data in this thesis have demonstrated that 5αTHB is capable of inducing GR translocation into nuclei in a slower and weaker manner than corticosterone. Following translocation, GR ligated with 5αTHB has increased nuclear mobility assessed by FRAP, and faster nuclear export process after steroid withdrawl, suggesting 5αTHB has a low affinity for the receptor; and these properties are associated with decreased ability to bind GRE and thereby decreased transcriptional abilities (Carrigan et al. 2007; Kino et al. 2004; Sackey et al. 1996). These cellular properties were determined by the nature of the ligand (Meijsing et al. 2007) since 5αTHB has a less preferable structure for GR binding. 5αTHB has a hydroxyl group at the C3 position instead of the GR-favored ketone structure (Bledsoe et al. 2002). 5αDHB (with a ketone at position 3) may be a better ligand for GR than 5αTHB and future studies should investigate the effects of 5αDHB on GR translocation and transcriptional abilities. However the availability of 5αDHB in cells may be short-lived, given the widespread expression of 3αHSD.

5αTHB acted synergistically with corticosterone to induce GR nuclear translocation, suggesting corticosterone-ligated GR may somehow facilitate the process of 5αTHB induced translocation or vice-versa. However, the synergistic observation has not

been tested at the transcriptional levels, and should be further investigated, e.g. induction of TAT in H4IIE cells.

5αTHB does not have metabolic effects through gene transactivation

5αTHB did not increase the expression of mRNAs or activities of proteins of any of the glucocorticoid responsive metabolic genes that were tested. Since the adverse metabolic effects of glucocorticoids are mainly mediated via a GR induced transactivation mechanism (Schacke, et al. 2002), 5αTHB appears inactive in this respect. The *in vitro* findings were confirmed in animals receiving acute or chronic administration of 5αTHB. Indeed, in this thesis 5αTHB did not influence metabolic profiles, including body and organ weights, blood pressure, glucose tolerance, insulin sensitivity, or lipid metabolism.

5α-Reductase inactivates glucocorticoids in liver and adipose tissues

5α-Reduction of glucocorticoids in liver or adipose tissue produces the inert 5α-reduced metabolites, thus inactivating glucocorticoids giving protection from adverse effects on metabolism. In obesity, although circulating glucocorticoids are normal, intracellular concentrations of glucocorticoids may be elevated by conversion of 11-dehydrocorticosterone (or cortisone in human) to corticosterone (or cortisol in human) by local expression of 11β-HSD1, thereby amplifying the glucocorticoid actions. 11β-HSD1 activity has been found to be decreased in liver but enhanced in adipose tissue (Livingstone et al. 2000; Rask et al. 2001), whereas 5αR1 activity is increased in liver (Andrew et al. 1998; Livingstone et al. 2000; Livingstone et al. 2005), of obese Zucker rats and humans. Increased hepatic 5αR1 can be interpreted as a compensating mechanism to inactivate locally regenerated glucocorticoids, and to increase the clearance rates of glucocorticoids together with the impaired hepatic 11β-HSD1 activities. When animals were challenged with chronic corticosterone excess, deletion of 5αR1 may be compensated by increased metabolic rates of corticosterone through other routes, so that the adverse metabolic effects of

glucocorticoids are not significantly different between 5αR1-deficient mice and wild-types.

5αTHB suppresses the HPA axis

It was demonstrated in this thesis that 5αTHB suppresses the circulating ACTH *in vivo*, consistent previous findings in rats (McInnes et al. 2004). The negative feedback of glucocorticoids is regulated through the hypothalamus and corticotroph cells in pituitary. We have found that 5αTHB does not suppress the mRNA expression of pituitary POMC *in vitro* and *in vivo*. Therefore, it is reasonable to conclude that 5αTHB may influence the synthesis and secretion of CRH in the hypothalamus. However, this hypothesis has not been pursued in this thesis and requires further proof. CRH is synthesized in the PVN of hypothalamus, and its levels of expression can be detected by *in situ* hybridization. The brains from animals receiving chronic steroid infusions were collected at cull. Thus the suppression of expression of CRH in response to 5αTHB infusion could be tested in the future experiment.

Alternatively, chronic treatment of 5αTHB may not have central effects to suppress the HPA axis but may influence the peripheral clearance of corticosterone by competition with liver enzymes. This hypothesis needs further investigation in the future by measuring the hepatic enzymes of steroid metabolism such as A-ring reductases, 6β-hydroxylase, 20α- and 20β-HSDs and the metabolites of these glucocorticoid metabolic pathways.

5αTHB has anti-inflammatory effects

Data in this thesis have demonstrated that 5αTHB has anti-inflammatory effects *in vitro* and *in vivo*. 5αTHB can increase the release of anti-inflammatory cytokine IL-10 and suppress the LPS-activated production of pro-inflammatory cytokines TNFα and IL-6 in the *in vitro* conditions described in this thesis. 5αTHB also suppressed the IL-6 levels in the peritoneal fluid in mice following intra-peritoneal

administration of LPS. Because systemic use of 5αTHB can drive negative feedback of the HPA axis and LPS activates the HPA axis to a variable degree (Lenczowski et al. 1997), animal models with non-systemic inflammation may be a better model system to further investigate the anti-inflammatory effects of 5αTHB. Very recently in our lab, restricted peritonitis induced by thioglycollate has been proved to be a better animal model to investigate more detailed effects of 5αTHB. Similarly, croton oil-induced inflammation in mouse ears also provides a good model to study the effects of 5αTHB on topical inflammation (Gabor and Razga 1989).

5αTHB was effective through GR-protein binding mechanism?

As described in previous chapters, glucocorticoids exert their genomic effects through GRs. After translocation, GR binds to the positive or negative GRE of the target genes, or to a second transcription factors such as NFκB, AP-1 or STATs (i.e. GR-protein binding) to exert transactivation and transrepression effects. In this thesis, all the glucocorticoid responsive genes that were modulated by GR-GRE binding (e.g. PEPCK, TAT, MMTV, PNMT, 11β-HSD1, angiotensinogen, POMC, and CRH receptor 1) did not respond to 5αTHB, whereas all the cytokines tested that were modulated through a GR-protein binding mechanism (e.g. TNFα, IL-6 and IL-10) were down- or up- regulated appropriately by 5αTHB. These results suggest that 5αTHB is active through GR-protein binding mechanism as opposed to GR-GRE binding. Moreover, it is interested to find that RU486 augmented the suppressive effects of 5αTHB on LPS-induced IL-6 secretion in BMDMØ. Although the mechanism is unknown, further study using RU486 to investigate the GR-protein interaction may gain further mechanistic insight. The suppressive effects of 5αTHB can also be investigated in the future by transfection assays with reporter driven by the collagenase promoter, which is mediated by the GR-protein transrepression mechanism involving GR binding to AP-1 (Yang-Yen, et al. 1990).

5αTHB-bound GR could not dimerize?

It has long been recognized that transrepression effects of glucocorticoids on NFκB and AP-1 are mediated by GR-protein binding mechanism independent of GR dimerization, e.g. through GR monomer (Heck, et al. 1997; Heck, et al. 1994). This has been demonstrated in a number of studies using mutations on the interface of GR dimer, such as A458T (mutation of alanine 458 to threonine in the second zinc finger in the DBD of the GR) (Heck et al. 1994; Reichardt, et al. 1998) and I628A (mutation of isoleucine 628 to alanine at the core hydrophobic dimer interface in the LBD of the GR) (Bledsoe et al. 2002). GR with a dimerization-defective mutation in either the DBD or LBD fails to transactivate gene expression but is capable of transrepression as efficiently as the wild-type GR. Based on observations using mice with a GR mutation of A458T in the DBD, GR induced transactivation of MKP-1 to suppress the LPS-induced p38 MAPK signalling has also been shown to be dimerization independent (Abraham et al. 2006). Similarly in this thesis, 5αTHB does not transactivate genes requiring GR dimerization but may transactivate or transrepress genes independent of dimerization. This leads to the possibility that 5αTHB does not induce a sufficient conformational change of GR structure which would allow GR to dimerize.

This reasoning may also explain why 5αTHB is able to suppress the expression of CRH in the hypothalamus. It is known that glucocorticoid repression of CRH involves direct DNA binding of monomeric GR and AP-1 at discrete adjacent sites in the promoter region (Malkoski and Dorin 1999). This also leads weight to proposition that 5αTHB induces transrepression through GR monomer. It will be interesting to investigate this hypothesis in the future study using the brain samples described above.

5αTHB is a dissociated steroid

In conclusion, 5αTHB is a GR ligand that is competent to induce transrepressive effects through monomeric GR-protein mechanism as opposed to GR homodimer mediated transactivation. Pharmacological dose of 5αTHB selectively induces anti-inflammatory effects with limited metabolic adverse effects. Thus 5αTHB could be a

potential "dissociated steroid" which could be used for long-term treatment for inflammatory diseases. Nowadays, about 1-3% of adults worldwide are taking long-term glucocorticoids (McDonough, et al. 2008). Treatment of high-dose glucocorticoids is associated with 2.5-fold greater risk for cardiovascular events, including myocardial infarction, angina, angioplasty or coronary revascularization, stroke, transient ischemic attack, congestive cardiac failure, or cardiovascular death (Wei, et al. 2004). It has also been revealed that glucocorticoid users in general have spent more money than non-users on treating glucocorticoid-associated adverse events (Pisu, et al. 2005). Therefore the development of new "dissociated steroids" with reduced side effects are highly desirable and would allow safer and more effective treatments for patients requiring long-term glucocorticoids therapy. The study in this thesis on the mechanisms and effects of 5αTHB actions not only discovered the dissociated properties of 5αTHB itself, but also provided a potential steroid model with limited ability to induce GR binding in favor of anti-inflammatory actions.

References

Abraham SM, Lawrence T, Kleiman A, Warden P, Medghalchi M, Tuckermann J, Saklatvala J & Clark AR 2006 Antiinflammatory effects of dexamethasone are partly dependent on induction of dual specificity phosphatase 1. *J Exp Med* **203** 1883-1889.

Adams M, Meijer OC, Wang J, Bhargava A & Pearce D 2003 Homodimerization of the glucocorticoid receptor is not essential for response element binding: activation of the phenylethanolamine N-methyltransferase gene by dimerization-defective mutants. *Mol Endocrinol* **17** 2583-2592.

Affolter HU & Reisine T 1985 Corticotropin releasing factor increases proopiomelanocortin messenger RNA in mouse anterior pituitary tumor cells. *J Biol Chem* **260** 15477-15481.

Agarwal AK, Monder C, Eckstein B & White PC 1989 Cloning and expression of rat cDNA encoding corticosteroid 11 beta-dehydrogenase. *J Biol Chem* **264** 18939-18943.

Alberts P, Engblom L, Edling N, Forsgren M, Klingstrom G, Larsson C, Ronquist-Nii Y, Ohman B & Abrahmsen L 2002 Selective inhibition of 11beta-hydroxysteroid dehydrogenase type 1 decreases blood glucose concentrations in hyperglycaemic mice. *Diabetologia* **45** 1528-1532.

Albiston AL, Obeyesekere VR, Smith RE & Krozowski ZS 1994 Cloning and tissue distribution of the human 11 beta-hydroxysteroid dehydrogenase type 2 enzyme. *Mol Cell Endocrinol* **105** R11-17.

Andersson S, Berman DM, Jenkins EP & Russell DW 1991 Deletion of steroid 5 alpha-reductase 2 gene in male pseudohermaphroditism. *Nature* **354** 159-161.

Andersson S & Russell DW 1990 Structural and biochemical properties of cloned and expressed human and rat steroid 5 alpha-reductases. *Proc Natl Acad Sci USA* **87** 3640-3644.

Andrew R, Phillips DI & Walker BR 1998 Obesity and gender influence cortisol secretion and metabolism in man. *J Clin Endocrinol Metab* **83** 1806-1809.

Andrews RC & Walker BR 1999 Glucocorticoids and insulin resistance: old hormones, newt argets. *Clinical Science* **96** 513–523.

Antoni FA, Hoyland J, Woods MD & Mason WT 1992 Glucocorticoid inhibition of stimulus-evoked adrenocorticotrophin release caused by suppression of intracellular calcium signals. *J Endocrinol* **133** R13-16.

Aoki Y, Iwasaki Y, Katahira M, Oiso Y & Saito H 1997 Regulation of the rat proopiomelanocortin gene expression in AtT-20 cells. I: effects of the common secretagogues. *Endocrinology* **138** 1923-1929.

Ashwell JD, Lu FW & Vacchio MS 2000 Glucocorticoids in T cell development and function. *Annu Rev Immunol* **18** 309-345.

Aubert J, Darimont C, Safonova I, Ailhaud G & Negrel R 1997 Regulation by glucocorticoids of angiotensinogen gene expression and secretion in adipose cells. *Biochem J* **328 (Pt 2)** 701-706.

Auphan N, DiDonato JA, Rosette C, Helmberg A & Karin M 1995 Immunosuppression by glucocorticoids: inhibition of NF-kappa B activity through induction of I kappa B synthesis. *Science* **270** 286-290.

Autelitano DJ & Cohen DR 1996 CRF stimulates expression of multiple fos and jun related genes in the AtT-20 corticotroph cell. *Mol Cell Endocrinol* **119** 25-35.

Autelitano DJ & Sheppard KE 1993 Corticotrope responsiveness to glucocorticoids is modulated via rapid CRF-mediated induction of the proto-oncogene c-fos. *Mol Cell Endocrinol* **94** 111-119.

Banchereau J & Steinman RM 1998 Dendritic cells and the control of immunity. *Nature* **392** 245-252.

Barnes P 1998 Anti-inflammatory actions of glucocorticoids: molecular mechanisms. *Clinical Science* **94** 557-572.

Bartholome B, Spies CM, Gaber T, Schuchmann S, Berki T, Kunkel D, Bienert M, Radbruch A, Burmester GR, Lauster R, Scheffold A, Buttgereit F 2004 Membrane glucocorticoid receptors (mGCR) are expressed in normal human peripheral blood mononuclear cells and up-regulated after *in vitro* stimulation and in patients with rheumatoid arthritis. *FASEB J* **18** 70-80.

Baum M, Moe OW, Gentry DL & Alpern RJ 1994 Effect of glucocorticoids on renal cortical NHE-3 and NHE-1 mRNA. *Am J Physiol* **267** F437-442.

Baxter JD & Forsham PH 1972 Tissue effects of glucocorticoids. *Am J Med* **53** 573-589.

Baxter JD & Tomkins GM 1971 Specific cytoplasmic glucocorticoid hormone receptors in hepatoma tissue culture cells. *Proc Natl Acad Sci USA* **68** 932-937.

Baybutt HN & Holsboer F 1990 Inhibition of macrophage differentiation and function by cortisol. *Endocrinology* **127** 476-480.

Beato M & Klug J 2000 Steroid hormone receptors: an update. *Hum Reprod Update* **6** 225-236.

Best R, Nelson SM & Walker BR 1997 Dexamethasone and 11-dehydrodexamethasone as tools to investigate the isozymes of 11 beta-hydroxysteroid dehydrogenase *in vitro* and *in vivo*. *J Endocrinol* **153** 41-48.

Bhattacharyya S, Brown DE, Brewer JA, Vogt SK & Muglia LJ 2007 Macrophage glucocorticoid receptors regulate Toll-like receptor 4-mediated inflammatory responses by selective inhibition of p38 MAP kinase. *Blood* **109** 4313-4319.

Bland R, Worker CA, Noble BS, Eyre LJ, Bujalska IJ, Sheppard MC, Stewart PM & Hewison M 1999 Characterization of 11beta-hydroxysteroid dehydrogenase activity and corticosteroid receptor expression in human osteosarcoma cell lines. *J Endocrinol* **161** 455-464.

Bledsoe RK, Montana VG, Stanley TB, Delves CJ, Apolito CJ, McKee DD, Consler TG, Parks DJ, Stewart EL, Willson TM, Lambert MH, Moore JT, Pearce KH, Xu HE 2002 Crystal structure of the glucocorticoid receptor ligand binding domain reveals a novel mode of receptor dimerization and coactivator recognition. *Cell* **110** 93-105.

Bollen M, Keppens S & Stalmans W 1998 Specific features of glycogen metabolism in the liver. *Biochem J* **336 (Pt 1)** 19-31.

Borlak J, Schulte I & Thum T 2004 Androgen metabolism in thymus of fetal and adult rats. *Drug Metab Dispos* **32** 675-679.

Boullu-Ciocca S, Paulmyer-Lacroix O, Fina F, Ouafik L, Alessi MC, Oliver C & Grino M 2003 Expression of the mRNAs coding for the glucocorticoid receptor isoforms in obesity. *Obes Res* **11** 925-929.

Brem AS 2001 Insights into glucocorticoid-associated hypertension. *Am J Kidney Dis* **37** 1-10.

Brem AS, Bina RB, Mehta S & Marshall J 1999 Glucocorticoids inhibit the expression of calcium-dependent potassium channels in vascular smooth muscle. *Mol Genet Metab* **67** 53-57.

Brown RW, Chapman KE, Kotelevtsev Y, Yau JL, Lindsay RS, Brett L, Leckie C, Murad P, Lyons V, Mullins JJ, Edwards CR, Seckl JR 1996a Cloning and production of antisera to human placental 11 beta-hydroxysteroid dehydrogenase type 2. *Biochem J* **313 (Pt 3)** 1007-1017.

Brown RW, Chapman KE, Murad P, Edwards CR & Seckl JR 1996b Purification of 11 beta-hydroxysteroid dehydrogenase type 2 from human placenta utilizing a novel affinity labelling technique. *Biochem J* **313 (Pt 3)** 997-1005.

Buren J, Liu HX, Jensen J & Eriksson JW 2002 Dexamethasone impairs insulin signalling and glucose transport by depletion of insulin receptor substrate-1, phosphatidylinositol 3-kinase and protein kinase B in primary cultured rat adipocytes. *Eur J Endocrinol* **146** 419-429.

Buttgereit F & Scheffold A 2002 Rapid glucocorticoid effects on immune cells. *Steroids* **67** 529-534.

Butts CL & Sternberg EM 2008 Neuroendocrine factors alter host defense by modulating immune function. *Cell Immunol* **252** 7-15.

Carlstedt-Duke J, Gustafsson JA, Gustafsson SA & Wrange O 1977 Interactions of corticosterone, 5alpha-dihydrocorticosterone and dexamethasone with proteins in rat-liver cytosol. *Eur J Biochem* **73** 231-238.

Carrigan A, Walther RF, Salem HA, Wu D, Atlas E, Lefebvre YA & Hache RJ 2007 An active nuclear retention signal in the glucocorticoid receptor functions as a strong inducer of transcriptional activation. *J Biol Chem* **282** 10963-10971.

Catley M 2007 Dissociated steroids. *Scientific World Journal* **7** 421-430.

Chen F, Watson CS & Gametchu B 1999 Association of the glucocorticoid receptor alternatively-spliced transcript 1A with the presence of the high molecular weight membrane glucocorticoid receptor in mouse lymphoma cells. *J Cell Biochem* **74** 430-446.

Christenson LK & Strauss JF, 3rd 2001 Steroidogenic acute regulatory protein: an update on its regulation and mechanism of action. *Arch Med Res* **32** 576-586.

Chung BC, Picado-Leonard J, Haniu M, Bienkowski M, Hall PF, Shively JE & Miller WL 1987 Cytochrome P450c17 (steroid 17 alpha-hydroxylase/17,20 lyase): cloning of human adrenal and testis cDNAs indicates the same gene is expressed in both tissues. *Proc Natl Acad Sci USA* **84** 407-411.

Cole TJ 1995 Cloning of the mouse 11 beta-hydroxysteroid dehydrogenase type 2 gene: tissue specific expression and localization in distal convoluted tubules and collecting ducts of the kidney. *Endocrinology* **136** 4693-4696.

Cooper MS, Walker EA, Bland R, Fraser WD, Hewison M & Stewart PM 2000 Expression and functional consequences of 11beta-hydroxysteroid dehydrogenase activity in human bone. *Bone* **27** 375-381.

Coppack SW, Jensen MD & Miles JM 1994 *In vivo* regulation of lipolysis in humans. *J Lipid Res* **35** 177-193.

Cox G 1995 Glucocorticoid treatment inhibits apoptosis in human neutrophils. Separation of survival and activation outcomes. *J Immunol* **154** 4719-4725.

Croxtall JD, Choudhury Q & Flower RJ 2000 Glucocorticoids act within minutes to inhibit recruitment of signalling factors to activated EGF receptors through a receptor-dependent, transcription-independent mechanism. *Br J Pharmacol* **130** 289-298.

Cushing H 1912 The pituitary body and its disorders. Philadelphia, Lippincott.

de Castro M, Elliot S, Kino T, Bamberger C, Karl M, Webster E & Chrousos GP 1996 The non-ligand binding beta-isoform of the human glucocorticoid receptor (hGR beta): tissue levels, mechanism of action, and potential physiologic role. *Mol Med* **2** 597-607.

de Kloet ER, de Jong IE & Oitzl MS 2008 Neuropharmacology of glucocorticoids: focus on emotion, cognition and cocaine. *Eur J Pharmacol* **585** 473-482.

De Matteo R & May CN 1997 Glucocorticoid-induced renal vasodilatation is mediated by a direct renal action involving nitric oxide. *Am J Physiol* **273** R1972-1979.

de Wet JR, Wood KV, DeLuca M, Helinski DR & Subramani S 1987 Firefly luciferase gene: structure and expression in mammalian cells. *Mol Cell Biol* **7** 725-737.

Degtiar WG & Kushlinsky NE 2001 3alpha-Hydroxysteroid dehydrogenase in animal and human tissues. *Biochemistry (Mosc)* **66** 256-266.

DeRijk RH, Schaaf M & de Kloet ER 2002 Glucocorticoid receptor variants: clinical implications. *J Steroid Biochem Mol Biol* **81** 103-122.

Diamondstone TI 1966 Assay of tyrosine transaminase activity by conversion of p-hydroxyphenylpyruvate to p-hydroxybenzaldehyde. *Analytical Biochemistry* **16** 395-401.

Doering DD, Steckelbroeck S, Doering T & Klingmuller D 2002 Effects of butyltins on human 5alpha-reductase type 1 and type 2 activity. *Steroids* **67** 859-867.

Domalik LJ, Chaplin DD, Kirkman MS, Wu RC, Liu WW, Howard TA, Seldin MF & Parker KL 1991 Different isozymes of mouse 11 beta-hydroxylase produce mineralocorticoids and glucocorticoids. *Mol Endocrinol* **5** 1853-1861.

Dostert A & Heinzel T 2004 Negative glucocorticoid receptor response elements and their role in glucocorticoid action. *Curr Pharm Des* **10** 2807-2816.

Drouin J, Sun YL, Chamberland M, Gauthier Y, De Lean A, Nemer M & Schmidt TJ 1993a Novel glucocorticoid receptor complex with DNA element of the hormone-repressed POMC gene. *EMBO J* **12** 145-156.

Drouin J, Sun YL, Chamberland M, Gauthier Y, Léan AD, Nemer M & Schmidt TJ 1993b Novel glucocorticoid receptor complex with DNA element of the hormone-repressed POMC gene. *EMBO Jounal* **12** 145-156.

Drouin J, Sun YL, Tremblay S, Lavender P, Schmidt TJ, de Lean A & Nemer M 1992 Homodimer formation is rate-limiting for high affinity DNA binding by glucocorticoid receptor. *Mol Endocrinol* **6** 1299-1309.

Ducy P, Desbois C, Boyce B, Pinero G, Story B, Dunstan C, Smith E, Bonadio J, Goldstein S, Gundberg C, Bradley A, Karsenty G 1996 Increased bone formation in osteocalcin-deficient mice. *Nature* **382** 448-452.

Dufort I, Soucy P, Labrie F & Luu-The V 1996 Molecular cloning of human type 3 3 alpha-hydroxysteroid dehydrogenase that differs from 20 alpha-hydroxysteroid dehydrogenase by seven amino acids. *Biochem Biophys Res Commun* **228** 474-479.

Duma D, Jewell CM & Cidlowski JA 2006 Multiple glucocorticoid receptor isoforms and mechanisms of post-translational modification. *J Steroid Biochem Mol Biol* **102** 11-21.

Eckel RH, Grundy SM & Zimmet PZ 2005 The metabolic syndrome. *Lancet* **365** 1415-1428.

Edwards CR, Stewart PM, Burt D, Brett L, McIntyre MA, Sutanto WS, de Kloet ER & Monder C 1988 Localisation of 11 beta-hydroxysteroid dehydrogenase--tissue specific protector of the mineralocorticoid receptor. *Lancet* **2** 986-989.

Eijken M, Hewison M, Cooper MS, de Jong FH, Chiba H, Stewart PM, Uitterlinden AG, Pols HA & van Leeuwen JP 2005 11beta-Hydroxysteroid dehydrogenase expression and glucocorticoid synthesis are directed by a molecular switch during osteoblast differentiation. *Mol Endocrinol* **19** 621-631.

Eijken M, Koedam M, van Driel M, Buurman CJ, Pols HA & van Leeuwen JP 2006 The essential role of glucocorticoids for proper human osteoblast differentiation and matrix mineralization. *Mol Cell Endocrinol* **248** 87-93.

Elenkov IJ & Chrousos GP 2002 Stress hormones, proinflammatory and antiinflammatory cytokines, and autoimmunity. *Ann N Y Acad Sci* **966** 290-303.

Elliott P, Peters RF & White AM 1971 A study of the relationship between glucocorticoid-induced weight loss in rats and the activity of skeletal-muscle and cardiac-muscle ribosomes *in vitro*. *Biochem J* **125** 106P-107P.

Encio IJ & Detera-Wadleigh SD 1991 The genomic structure of the human glucocorticoid receptor. *J Biol Chem* **266** 7182-7188.

Eskay RL, Grino M & Chen HT 1990 Interleukins, signal transduction, and the immune system-mediated stress response. *Adv Exp Med Biol* **274** 331-343.

Evans AL, Brown W, Kenyon CJ, Maxted KJ & Smith DC 1994 Improved system for measuring systolic blood pressure in the conscious rat. *Med Biol Eng Comput* **32** 101-102.

Exton JH 1979 Regulation of gluconeogenesis by glucocorticoids. *Monogr Endocrinol* **12** 535-546.

Eyre LJ, Rabbitt EH, Bland R, Hughes SV, Cooper MS, Sheppard MC, Stewart PM & Hewison M 2001 Expression of 11 beta-hydroxysteroid dehydrogenase in rat osteoblastic cells: pre-receptor regulation of glucocorticoid responses in bone. *J Cell Biochem* **81** 453-462.

Falardeau P & Martineau A 1989 Prostaglandin I2 and glucocorticoid-induced rise in arterial pressure in the rat. *J Hypertens* **7** 625-632.

Falduto MT, Hickson RC & Young AP 1989 Antagonism by glucocorticoids and exercise on expression of glutamine synthetase in skeletal muscle. *FASEB J* **3** 2623-2628.

Fang H, Pengal RA, Cao X, Ganesan LP, Wewers MD, Marsh CB & Tridandapani S 2004 Lipopolysaccharide-induced macrophage inflammatory response is regulated by SHIP. *J Immunol* **173** 360-366.

Fassler R, Sasaki T, Timpl R, Chu ML & Werner S 1996 Differential regulation of fibulin, tenascin-C, and nidogen expression during wound healing of normal and glucocorticoid-treated mice. *Exp Cell Res* **222** 111-116.

Fietta P 2007 Glucocorticoids and brain functions. *Riv Biol* **100** 403-418.

Fleig WE, Noether-Fleig G, Roeben H & Ditschuneit H 1984 Hormonal regulation of key gluconeogenic enzymes and glucose release in cultured hepatocytes: effects of dexamethasone and gastrointestinal hormones on glucagon action. *Arch Biochem Biophys* **229** 368-378.

Franchimont D 2004 Overview of the actions of glucocorticoids on the immune response: a good model to characterize new pathways of immunosuppression for new treatment strategies. *Ann N Y Acad Sci* **1024** 124-137.

Franchimont D, Louis E, Dewe W, Martens H, Vrindts-Gevaert Y, De Groote D, Belaiche J & Geenen V 1998 Effects of dexamethasone on the profile of cytokine secretion in human whole blood cell cultures. *Regul Pept* **73** 59-65.

Freeman L, Hewison M, Hughes SV, Evans KN, Hardie D, Means TK & Chakraverty R 2005 Expression of 11beta-hydroxysteroid dehydrogenase type 1 permits regulation of glucocorticoid bioavailability by human dendritic cells. *Blood* **106** 2042-2049.

Fried SK, Bunkin DA & Greenberg AS 1998 Omental and subcutaneous adipose tissues of obese subjects release interleukin-6: depot difference and regulation by glucocorticoid. *J Clin Endocrinol Metab* **83** 847-850.

Fried SK, Russell CD, Grauso NL & Brolin RE 1993 Lipoprotein lipase regulation by insulin and glucocorticoid in subcutaneous and omental adipose tissues of obese women and men. *J Clin Invest* **92** 2191-2198.

Fukao T & Koyasu S 2003 PI3K and negative regulation of TLR signaling. *Trends Immunol* **24** 358-363.

Fuller PJ & Young MJ 2005 Mechanisms of mineralocorticoid action. *Hypertension* **46** 1227-1235.

Funder JW, Pearce PT, Smith R & Smith AI 1988 Mineralocorticoid action: target tissue specificity is enzyme, not receptor, mediated. *Science* **242** 583-585.

Gabor M & Razga Z 1989 Influence of nonsteroidal antiphlogistics on mouse ear inflammation induced with croton oil. *Arch Int Pharmacodyn Ther* **299** 241-246.

Galigniana MD, Scruggs JL, Herrington J, Welsh MJ, Carter-Su C, Housley PR & Pratt WB 1998 Heat shock protein 90-dependent (geldanamycin-inhibited) movement of the glucocorticoid receptor through the cytoplasm to the nucleus requires intact cytoskeleton. *Mol Endocrinol* **12** 1903-1913.

Gametchu B, Watson CS & Wu S 1993 Use of receptor antibodies to demonstrate membrane glucocorticoid receptor in cells from human leukemic patients. *FASEB J* **7** 1283-1292.

Gathercole LL, Bujalska IJ, Stewart PM & Tomlinson JW 2007 Glucocorticoid modulation of insulin signaling in human subcutaneous adipose tissue. *J Clin Endocrinol Metab* **92** 4332-4339.

Giambartolomei GH, Dennis VA, Lasater BL, Murthy PK & Philipp MT 2002 Autocrine and exocrine regulation of interleukin-10 production in THP-1 cells stimulated with Borrelia burgdorferi lipoproteins. *Infect Immun* **70** 1881-1888.

Gilmour JS, Coutinho AE, Cailhier JF, Man TY, Clay M, Thomas G, Harris HJ, Mullins JJ, Seckl JR, Savill JS, Chapman KE 2006 Local amplification of glucocorticoids by 11 beta-hydroxysteroid dehydrogenase type 1 promotes macrophage phagocytosis of apoptotic leukocytes. *J Immunol* **176** 7605-7611.

Gingras MC & Margolin JF 2000 Differential expression of multiple unexpected genes during U937 cell and macrophage differentiation detected by suppressive subtractive hybridization. *Exp Hematol* **28** 350.

Golf SW, Bepperling F & Graef V 1984 Effect of 5 alpha-dihydrocorticoids on enzymes of gluconeogenesis in rat liver. *Steroids* **43** 85-91.

Goodwin B, Gauthier KC, Umetani M, Watson MA, Lochansky MI, Collins JL, Leitersdorf E, Mangelsdorf DJ, Kliewer SA & Repa JJ 2003 Identification of bile acid precursors as endogenous ligands for the nuclear xenobiotic pregnane X receptor. *Proc Natl Acad Sci USA* **100** 223-228.

Gorlich D & Kutay U 1999 Transport between the cell nucleus and the cytoplasm. *Annu Rev Cell Dev Biol* **15** 607-660.

Gorsline J, Harnik M, Tresco PA & Morris DJ 1986 Hypertensinogenic activities of ring A-reduced metabolites of aldosterone. *Hypertension Suppl I* **8** I-187-191.

Gorsline J, Latif SA & Morris DJ 1988 Changes in 5 alpha- and 5 beta-reductase pathways of aldosterone metabolism by dietary sodium. *Am J Hypertens* **1** 272-275.

Goulding NJ, Euzger HS, Butt SK & Perretti M 1998 Novel pathways for glucocorticoid effects on neutrophils in chronic inflammation. *Inflamm Res* **47 Suppl 3** S158-165.

Grange T, Cappabianca L, Flavin M, Sassi H & Thomassin H 2001 *In vivo* analysis of the model tyrosine aminotransferase gene reveals multiple sequential steps in glucocorticoid receptor action. *Oncogene* **20** 3028-3038.

Grange T, Roux J, Rigaud G & Pictet R 1991 Cell-type specific activity of two glucocorticoid responsive units of rat tyrosine aminotransferase gene is associated with multiple binding sites for C/EBP and a novel liver-specific nuclear factor. *Nucleic Acids Res* **19** 131-139.

Grundy WN, Bailey TL, Elkan CP & Baker ME 1997 Hidden Markov model analysis of motifs in steroid dehydrogenases and their homologs. *Biochem Biophys Res Commun* **231** 760-766.

Gwynne JT, Hess B, Hughes T, Rountree R & Mahaffee D 1984 The role of serum high density lipoproteins in adrenal steroidogenesis. *Endocr Res* **10** 411-430.

Haffner SM 2006 Relationship of metabolic risk factors and development of cardiovascular disease and diabetes. *Obesity (Silver Spring)* **14 Suppl 3** 121S-127S.

Haller J, Mikics E & Makara GB 2008 The effects of non-genomic glucocorticoid mechanisms on bodily functions and the central neural system. A critical evaluation of findings. *Front Neuroendocrinol* **29** 273-291.

Hara A, Matsuura K, Tamada Y, Sato K, Miyabe Y, Deyashiki Y & Ishida N 1996 Relationship of human liver dihydrodiol dehydrogenases to hepatic bile-acid-binding protein and an oxidoreductase of human colon cells. *Biochem J* **313 (Pt 2)** 373-376.

Heck S, Bender K, Kullmann M, Gottlicher M, Herrlich P & Cato AC 1997 I kappaB alpha-independent downregulation of NF-kappaB activity by glucocorticoid receptor. *EMBO J* **16** 4698-4707.

Heck S, Kullmann M, Gast A, Ponta H, Rahmsdorf HJ, Herrlich P & Cato AC 1994 A distinct modulating domain in glucocorticoid receptor monomers in the repression of activity of the transcription factor AP-1. *EMBO J* **13** 4087-4095.

Hench PS 1950 The reversibility of certain rheumatic and non-rheumatic conditions by the use of cortisone or of the pituitary adrenocorticotrophic hormone. In *Nobel Lectures, Physiology or Medicine*, pp 1942–1962. Amsterdam: Elsevier.

Hench PS & Kendall EC 1949 The effect of a hormone of the adrenal cortex (17-hydroxy-11-dehydrocorticosterone; compound E) and of pituitary adrenocorticotropic hormone on rheumatoid arthritis. *Mayo Clin Proc* **24** 181-197.

Higashijima M, Nawata H, Kato K & Ibayashi H 1987 Studies on lipoprotein and adrenal steroidogenesis: I. Roles of low density lipoprotein- and high density lipoprotein-cholesterol in steroid production in cultured human adrenocortical cells. *Endocrinol Jpn* **34** 635-645.

Hillgartner FB, Salati LM & Goodridge AG 1995 Physiological and molecular mechanisms involved in nutritional regulation of fatty acid synthesis. *Physiol Rev* **75** 47-76.

Hollenberg SM, Weinberger C, Ong ES, Cerelli G, Oro A, Lebo R, Brad Thompson E, Rosenfeld MG & Evans RM 1985 Primary structure and expression of a functional human glucocorticoid receptor cDNA. *Nature* **318** 635-641.

Holmes MC, Sangra M, French KL, Whittle IR, Paterson J, Mullins JJ & Seckl JR 2006 11beta-Hydroxysteroid dehydrogenase type 2 protects the neonatal cerebellum from deleterious effects of glucocorticoids. *Neuroscience* **137** 865-873.

Holmes MC & Seckl JR 2006 The role of 11beta-hydroxysteroid dehydrogenases in the brain. *Mol Cell Endocrinol* **248** 9-14.

Hosoe S, Ogura T, Hayashi S, Komuta K, Ikeda T, Shirasaka T, Kawase I, Masuno T & Kishimoto S 1989 Induction of tumoricidal macrophages from bone marrow cells of normal mice or mice bearing a colony-stimulating-factor-producing tumor. *Cancer Immunol Immunother* **28** 116-122.

Howlett TA, Drury PL, Perry L, Doniach I, Rees LH & Besser GM 1986 Diagnosis and management of ACTH-dependent Cushing's syndrome: comparison of the features in ectopic and pituitary ACTH production. *Clin Endocrinol (Oxf)* **24** 699-713.

Htun H, Barsony J, Renyi I, Gould DL & Hager GL 1996 Visualization of glucocorticoid receptor translocation and intranuclear organization in living cells with a green fluorescent protein chimera. *Proc Natl Acad Sci USA* **93** 4845-4850.

Iredale PA & Duman RS 1997 Glucocorticoid regulation of corticotropin-releasing factor1 receptor expression in pituitary-derived AtT-20 cells. *Mol Pharmacol* **51** 794-799.

Joels M 2007 Role of corticosteroid hormones in the dentate gyrus. *Prog Brain Res* **163** 355-370.

Justesen J, Mosekilde L, Holmes M, Stenderup K, Gasser J, Mullins JJ, Seckl JR & Kassem M 2004 Mice deficient in 11beta-hydroxysteroid dehydrogenase type 1 lack bone marrow adipocytes, but maintain normal bone formation. *Endocrinology* **145** 1916-1925.

Kanelakis KC, Shewach DS & Pratt WB 2002 Nucleotide binding states of hsp70 and hsp90 during sequential steps in the process of glucocorticoid receptor.hsp90 heterocomplex assembly. *J Biol Chem* **277** 33698-33703.

Kawamura J, Tanimoto T, Fukuda H & Hayakawa T 1981 Structural requirements in 20-oxo-steroids for interaction with the binding site of 20beta-hydroxysteroid dehydrogenase. *Chem Pharm Bull (Tokyo)* **29** 476-484.

Kennedy B & Ziegler MG 1991 Cardiac epinephrine synthesis. Regulation by a glucocorticoid. *Circulation* **84** 891-895.

Kenyon C, Saccoccio N, Harnik M & Morris D 1985 The effects of long-term infusions of the reduced derivatives of aldosterone on water and electrolyte metabolism. *The Adrenal Gland and Hypertension* **27** 209-214.

Kenyon CJ, Brem AS, McDermott MJ, Deconti GA, Latif SA & Morris DJ 1983 Antinatriuretic and kaliuretic activities of the reduced derivatives of aldosterone. *Endocrinology* **112** 1852-1856.

Khanna M, Qin KN, Wang RW & Cheng KC 1995 Substrate specificity, gene structure, and tissue-specific distribution of multiple human 3 alpha-hydroxysteroid dehydrogenases. *J Biol Chem* **270** 20162-20168.

Kino T, Liou SH, Charmandari E & Chrousos GP 2004 Glucocorticoid receptor mutants demonstrate increased motility inside the nucleus of living cells: time of fluorescence recovery after photobleaching (FRAP) is an integrated measure of receptor function. *Mol Med* **10** 80-88.

Knolle PA, Uhrig A, Protzer U, Trippler M, Duchmann R, Meyer zum Buschenfelde KH & Gerken G 1998 Interleukin-10 expression is autoregulated at the transcriptional level in human and murine Kupffer cells. *Hepatology* **27** 93-99.

Kondo KH, Kai MH, Setoguchi Y, Eggertsen G, Sjoblom P, Setoguchi T, Okuda KI & Bjorkhem I 1994 Cloning and expression of cDNA of human delta 4-3-oxosteroid 5 beta-reductase and substrate specificity of the expressed enzyme. *Eur J Biochem* **219** 357-363.

Kotelevtsev Y, Brown RW, Fleming S, Kenyon C, Edwards CR, Seckl JR & Mullins JJ 1999 Hypertension in mice lacking 11beta-hydroxysteroid dehydrogenase type 2. *J Clin Invest* **103** 683-689.

Kotelevtsev Y, Holmes MC, Burchell A, Houston PM, Schmoll D, Jamieson P, Best R, Brown R, Edwards CR, Seckl JR, Mullins JJ 1997 11beta-hydroxysteroid dehydrogenase type 1 knockout mice show attenuated glucocorticoid-inducible responses and resist hyperglycemia on obesity or stress. *Proc Natl Acad Sci USA* **94** 14924-14929.

Krsek M, Rosicka M, Nedvidkova J, Kvasnickova H, Hana V, Marek J, Haluzik M, Lai EW & Pacak K 2006 Increased lipolysis of subcutaneous abdominal adipose tissue and altered noradrenergic activity in patients with Cushing's syndrome: an in-vivo microdialysis study. *Physiol Res* **55** 421-428.

Kunapuli SP, Benedict CR & Kumar A 1987 Tissue specific hormonal regulation of the rat angiotensinogen gene expression. *Arch Biochem Biophys* **254** 642-646.

Lacey DL, Timms E, Tan HL, Kelley MJ, Dunstan CR, Burgess T, Elliott R, Colombero A, Elliott G, Scully S, Hsu H, Sullivan J, Hawkins N, Davy E, Capparelli C, Eli A, Qian YX, Kaufman S, Sarosi I, Shalhoub V, Senaldi G, Guo J, Delaney J, Boyle WJ 1998 Osteoprotegerin ligand is a cytokine that regulates osteoclast differentiation and activation. *Cell* **93** 165-176.

Landfield PW, Baskin RK & Pitler TA 1981 Brain aging correlates: retardation by hormonal-pharmacological treatments. *Science* **214** 581-584.

Landfield PW, Waymire JC & Lynch G 1978 Hippocampal aging and adrenocorticoids: quantitative correlations. *Science* **202** 1098-1102.

Lane NE, Sanchez S, Modin GW, Genant HK, Pierini E & Arnaud CD 1998 Parathyroid hormone treatment can reverse corticosteroid-induced osteoporosis. Results of a randomized controlled clinical trial. *J Clin Invest* **102** 1627-1633.

LaPier TK 1997 Glucocorticoid-induced muscle atrophy. The role of exercise in treatment and prevention. *J Cardiopulm Rehabil* **17** 76-84.

Laplace JR, Husted RF & Stokes JB 1992 Cellular responses to steroids in the enhancement of Na+ transport by rat collecting duct cells in culture. Differences between glucocorticoid and mineralocorticoid hormones. *J Clin Invest* **90** 1370-1378.

Lazar MA 2002 Mechanism of action of hormones that act on nuclear receptors. In *Williams textbook of endocrinology*, edn 10th, pp 35-44. Eds PR Larsen, HM Kronenberg, S Melmed & KS Polonsky. Philadelphia: Saunders.

Lee YC, Lin HH & Tang MJ 1995 Glucocorticoid upregulates Na-K-ATPase alpha- and beta-mRNA via an indirect mechanism in proximal tubule cell primary cultures. *Am J Physiol* **268** F862-867.

Lefebvre P, Berard DS, Cordingley MG & Hager GL 1991 Two regions of the mouse mammary tumor virus long terminal repeat regulate the activity of its promoter in mammary cell lines. *Mol Cell Biol* **11** 2529-2537.

Lemonde HA, Custard EJ, Bouquet J, Duran M, Overmars H, Scambler PJ & Clayton PT 2003 Mutations in SRD5B1 (AKR1D1), the gene encoding delta(4)-3-oxosteroid 5beta-reductase, in hepatitis and liver failure in infancy. *Gut* **52** 1494-1499.

Lenczowski MJ, Van Dam AM, Poole S, Larrick JW & Tilders FJ 1997 Role of circulating endotoxin and interleukin-6 in the ACTH and corticosterone response to intraperitoneal LPS. *Am J Physiol* **273** R1870-1877.

Lewis-Tuffin LJ & Cidlowski JA 2006 The physiology of human glucocorticoid receptor beta (hGRbeta) and glucocorticoid resistance. *Ann N Y Acad Sci* **1069** 1-9.

Lewis-Tuffin LJ, Jewell CM, Bienstock RJ, Collins JB & Cidlowski JA 2007 Human glucocorticoid receptor beta binds RU-486 and is transcriptionally active. *Mol. Cell. Biol.* **27** 2266-2282.

Li KX, Smith RE, Ferrari P, Funder JW & Krozowski ZS 1996 Rat 11 beta-hydroxysteroid dehydrogenase type 2 enzyme is expressed at low levels in the placenta and is modulated by adrenal steroids in the kidney. *Mol Cell Endocrinol* **120** 67-75.

Liberman AC, Druker J, Perone MJ & Arzt E 2007 Glucocorticoids in the regulation of transcription factors that control cytokine synthesis. *Cytokine Growth Factor Rev* **18** 45-56.

Lin HK, Hung CF, Moore M & Penning TM 1999 Genomic structure of rat 3alpha-hydroxysteroid/dihydrodiol dehydrogenase (3alpha-HSD/DD, AKR1C9). *J Steroid Biochem Mol Biol* **71** 29-39.

Lin HK, Jez JM, Schlegel BP, Peehl DM, Pachter JA & Penning TM 1997 Expression and characterization of recombinant type 2 3 alpha-hydroxysteroid dehydrogenase (HSD) from human prostate: demonstration of bifunctional 3 alpha/17 beta-HSD activity and cellular distribution. *Mol Endocrinol* **11** 1971-1984.

Lindsay RS, Lindsay RM, Edwards CR & Seckl JR 1996a Inhibition of 11-beta-hydroxysteroid dehydrogenase in pregnant rats and the programming of blood pressure in the offspring. *Hypertension* **27** 1200-1204.

Lindsay RS, Lindsay RM, Waddell BJ & Seckl JR 1996b Prenatal glucocorticoid exposure leads to offspring hyperglycaemia in the rat: studies with the 11 beta-hydroxysteroid dehydrogenase inhibitor carbenoxolone. *Diabetologia* **39** 1299-1305.

Livingstone DE, Jones GC, Smith K, Jamieson PM, Andrew R, Kenyon CJ & Walker BR 2000 Understanding the role of glucocorticoids in obesity: tissue-specific alterations of corticosterone metabolism in obese Zucker rats. *Endocrinology* **141** 560-563.

Livingstone DE, McInnes KJ, Walker BR & Andrew R 2005 Increased A-ring reduction of glucocorticoids in obese Zucker rats: effects of insulin sensitization. *Obes Res* **13** 1523-1526.

Livingstone DE, Walker BR & Andrew R 2008 Increased susceptibility to liver fat accumulation and insulin resistance, but not obesity, induced by high fat diet in 5 alpha-reductase type 1 knock-out mice. In *The Endocrine Society's Annual Meeting*. San Francisco.

Loechner KJ, Knox RJ, McLaughlin JT & Dunlap K 1999 Dexamethasone-mediated inhibition of calcium transients and ACTH release in a pituitary cell line (AtT-20). *Steroids* **64** 404.

Lowenberg M, Stahn C, Hommes DW & Buttgereit F 2008 Novel insights into mechanisms of glucocorticoid action and the development of new glucocorticoid receptor ligands. *Steroids* **73** 1025-1029.

Lupien SJ, de Leon M, de Santi S, Convit A, Tarshish C, Nair NP, Thakur M, McEwen BS, Hauger RL & Meaney MJ 1998 Cortisol levels during human aging predict hippocampal atrophy and memory deficits. *Nat Neurosci* **1** 69-73.

Lupien SJ, Maheu F, Tu M, Fiocco A & Schramek TE 2007 The effects of stress and stress hormones on human cognition: Implications for the field of brain and cognition. *Brain Cogn* **65** 209-237.

Luu-The V, Pelletier G & Labrie F 2005 Quantitative appreciation of steroidogenic gene expression in mouse tissues: new roles for type 2 5alpha-reductase, 20alpha-hydroxysteroid dehydrogenase and estrogen sulfotransferase. *J Steroid Biochem Mol Biol* **93** 269-276.

Macfarlane DP, Forbes S & Walker BR 2008 Glucocorticoids and fatty acid metabolism in humans: fuelling fat redistribution in the metabolic syndrome. *J Endocrinol* **197** 189-204.

Mackenzie SM, Huda SS, Sattar N, Fraser R, Connell JM & Davies E 2008 Depot-specific steroidogenic gene transcription in human adipose tissue. *Clin Endocrinol (Oxf)* **69** 848-854.

MacPhee IA, Antoni FA & Mason DW 1989 Spontaneous recovery of rats from experimental allergic encephalomyelitis is dependent on regulation of the immune system by endogenous adrenal corticosteroids. *J Exp Med* **169** 431-445.

Mahendroo MS, Cala KM, Hess DL & Russell DW 2001 Unexpected virilization in male mice lacking steroid 5 alpha-reductase enzymes. *Endocrinology* **142** 4652-4662.

Mahendroo MS, Cala KM, Landrum DP & Russell DW 1997 Fetal death in mice lacking 5alpha-reductase type 1 caused by estrogen excess. *Mol Endocrinol* **11** 917-927.

Mahendroo MS, Cala KM & Russell DW 1996 5 alpha-reduced androgens play a key role in murine parturition. *Mol Endocrinol* **10** 380-392.

Mahendroo MS, Porter A, Russell DW & Word RA 1999 The parturition defect in steroid 5alpha-reductase type 1 knockout mice is due to impaired cervical ripening. *Mol Endocrinol* **13** 981-992.

Malkoski SP & Dorin RI 1999 Composite glucocorticoid regulation at a functionally defined negative glucocorticoid response element of the human corticotropin-releasing hormone gene. *Mol Endocrinol* **13** 1629-1644.

Malkoski SP, Handanos CM & Dorin RI 1997 Localization of a negative glucocorticoid response element of the human corticotropin releasing hormone gene. *Mol Cell Endocrinol* **127** 189-199.

Mancini T, Doga M, Mazziotti G & Giustina A 2004 Cushing's syndrome and bone. *Pituitary* **7** 249-252.

Mantha L, Palacios E & Deshaies Y 1999 Modulation of triglyceride metabolism by glucocorticoids in diet-induced obesity. *Am J Physiol* **277** R455-464.

Martin RM, Lin CJ, Nishi MY, Billerbeck AE, Latronico AC, Russell DW & Mendonca BB 2003 Familial hyperestrogenism in both sexes: clinical, hormonal, and molecular studies of two siblings. *J Clin Endocrinol Metab* **88** 3027-3034.

Masuzaki H, Yamamoto H, Kenyon CJ, Elmquist JK, Morton NM, Paterson JM, Shinyama H, Sharp MG, Fleming S, Mullins JJ, Seckl JR, Flier JS 2003 Transgenic amplification of glucocorticoid action in adipose tissue causes high blood pressure in mice. *J Clin Invest* **112** 83-90.

McDonough AK, Curtis JR & Saag KG 2008 The epidemiology of glucocorticoid-associated adverse events. *Curr Opin Rheumatol* **20** 131-137.

McEwen BS & Magarinos AM 2001 Stress and hippocampal plasticity: implications for the pathophysiology of affective disorders. *Hum Psychopharmacol* **16** S7-S19.

McInnes KJ, Kenyon CJ, Chapman KE, Livingstone DE, Macdonald LJ, Walker BR & Andrew R 2004 5alpha-reduced glucocorticoids, novel endogenous activators of the glucocorticoid receptor. *J Biol Chem* **279** 22908-22912.

McNally JG, Muller WG, Walker D, Wolford R & Hager GL 2000 The glucocorticoid receptor: rapid exchange with regulatory sites in living cells. *Science* **287** 1262.

Meijsing SH, Elbi C, Luecke HF, Hager GL & Yamamoto KR 2007 The ligand binding domain controls glucocorticoid receptor dynamics independent of ligand release. *Mol Cell Biol* **27** 2442-2451.

Milad MA, Ludwig EA, Anne S, Middleton E, Jr. & Jusko WJ 1994 Pharmacodynamic model for joint exogenous and endogenous corticosteroid suppression of lymphocyte trafficking. *J Pharmacokinet Biopharm* **22** 469-480.

Mirescu C & Gould E 2006 Stress and adult neurogenesis. *Hippocampus* **16** 233-238.

Mitchell BM & Webb RC 2002 Impaired vasodilation and nitric oxide synthase activity in glucocorticoid-induced hypertension. *Biol Res Nurs* **4** 16-21.

Molenkamp R, van der Ham A, Schinkel J & Beld M 2007 Simultaneous detection of five different DNA targets by real-time Taqman PCR using the Roche LightCycler480: Application in viral molecular diagnostics. *J Virol Methods* **141** 205-211.

Morton NM, Holmes MC, Fievet C, Staels B, Tailleux A, Mullins JJ & Seckl JR 2001 Improved lipid and lipoprotein profile, hepatic insulin sensitivity, and glucose tolerance in 11beta-hydroxysteroid dehydrogenase type 1 null mice. *J Biol Chem* **276** 41293-41300.

Morton NM, Paterson JM, Masuzaki H, Holmes MC, Staels B, Fievet C, Walker BR, Flier JS, Mullins JJ & Seckl JR 2004 Novel adipose tissue-mediated resistance to diet-induced visceral obesity in 11 beta-hydroxysteroid dehydrogenase type 1-deficient mice. *Diabetes* **53** 931-938.

Naray-Fejes-Toth A & Fejes-Toth G 1990 Glucocorticoid receptors mediate mineralocorticoid-like effects in cultured collecting duct cells. *Am J Physiol* **259** F672-678.

Naray-Fejes-Toth A & Fejes-Toth G 1994 11 beta-Hydroxysteroid dehydrogenase in renal collecting duct cells. *Steroids* **59** 105-110.

Necela BM & Cidlowski JA 2003 Crystallization of the human glucocorticoid receptor ligand binding domain: a step towards selective glucocorticoids. *Trends Pharmacol Sci* **24** 58-61.

Nelson MT & Quayle JM 1995 Physiological roles and properties of potassium channels in arterial smooth muscle. *Am J Physiol* **268** C799-822.

Nieman LK & Chanco Turner ML 2006 Addison's disease. *Clin Dermatol* **24** 276-280.

Nishi M & Kawata M 2007 Dynamics of glucocorticoid receptor and mineralocorticoid receptor: implications from live cell imaging studies. *Neuroendocrinology* **85** 186-192.

Normington K & Russell DW 1992 Tissue distribution and kinetic characteristics of rat steroid 5 alpha- reductase isozymes. Evidence for distinct physiological functions. *J Biol Chem* **267** 19548-19554.

Nuglozeh E, Mbikay M, Stewart DJ & Legault L 1997 Rat natriuretic peptide receptor genes are regulated by glucocorticoids *in vitro*. *Life Sci* **61** 2143-2155.

O'Donnell ME & Owen NE 1994 Regulation of ion pumps and carriers in vascular smooth muscle. *Physiol Rev* **74** 683-721.

Oakley RH, Sar M & Cidlowski JA 1996 The human glucocorticoid receptor beta isoform. *J Cell Biol* **271** 9550-9559.

Ogishima T, Suzuki H, Hata J, Mitani F & Ishimura Y 1992 Zone-specific expression of aldosterone synthase cytochrome P-450 and cytochrome P-45011 beta in rat adrenal cortex: histochemical basis for the functional zonation. *Endocrinology* **130** 2971-2977.

Okuda A & Okuda K 1984 Purification and characterization of delta 4-3-ketosteroid 5 beta-reductase. *J Biol Chem* **259** 7519-7524.

Olefsky JM 1975 Effect of dexamethasone on insulin binding, glucose transport, and glucose oxidation of isolated rat adipocytes. *J Clin Invest* **56** 1499-1508.

Onate S, Tsai S, Tsai M & O'Malley B 1995 Sequence and characterization of a coactivator for the steroid hormone receptor superfamily. *Science* **270** 1354-1357.

Ong JM, Simsolo RB, Saffari B & Kern PA 1992 The regulation of lipoprotein lipase gene expression by dexamethasone in isolated rat adipocytes. *Endocrinology* **130** 2310-2316.

Ooi GT, Tawadros N & Escalona RM 2004 Pituitary cell lines and their endocrine applications. *Mol Cell Endocrinol* **228** 1-21.

Palermo M, Marazzi MG, Hughes BA, Stewart PM, Clayton PT & Shackleton CH 2008 Human Delta4-3-oxosteroid 5beta-reductase (AKR1D1) deficiency and steroid metabolism. *Steroids* **73** 417-423.

Paterson JM, Morton NM, Fievet C, Kenyon CJ, Holmes MC, Staels B, Seckl JR & Mullins JJ 2004 Metabolic syndrome without obesity: Hepatic overexpression of 11beta-hydroxysteroid dehydrogenase type 1 in transgenic mice. *Proc Natl Acad Sci USA* **101** 7088-7093.

Penning TM 1999 Molecular determinants of steroid recognition and catalysis in aldo-keto reductases. Lessons from 3alpha-hydroxysteroid dehydrogenase. *J Steroid Biochem Mol Biol* **69** 211-225.

Penning TM, Smithgall TE, Askonas LJ & Sharp RB 1986 Rat liver 3 alpha-hydroxysteroid dehydrogenase. *Steroids* **47** 221-247.

Perez P, Page A, Bravo A, Del Rio M, Gimenez-Conti I, Budunova I, Slaga TJ & Jorcano JL 2001 Altered skin development and impaired proliferative and inflammatory responses in transgenic mice overexpressing the glucocorticoid receptor. *FASEB J* **15** 2030-2032.

Phair RD & Misteli T 2001 Kinetic modelling approaches to *in vivo* imaging. *Nat Rev Mol Cell Biol* **2** 898.

Picado-Leonard J & Miller WL 1987 Cloning and sequence of the human gene for P450c17 (steroid 17 alpha-hydroxylase/17,20 lyase): similarity with the gene for P450c21. *DNA* **6** 439-448.

Pierotti S, Gandini L, Lenzi A & Isidori AM 2008 Pre-receptorial regulation of steroid hormones in bone cells: insights on glucocorticoid-induced osteoporosis. *J Steroid Biochem Mol Biol* **108** 292-299.

Pisu M, James N, Sampsel S & Saag KG 2005 The cost of glucocorticoid-associated adverse events in rheumatoid arthritis. *Rheumatology (Oxford)* **44** 781-788.

Poletti A, Coscarella A, Negri-Cesi P, Colciago A, Celotti F & Martini L 1998 5 alpha-reductase isozymes in the central nervous system. *Steroids* **63** 246-251.

Pratt WB, Galigniana MD, Harrell JM & DeFranco DB 2004 Role of hsp90 and the hsp90-binding immunophilins in signalling protein movement. *Cell Signal* **16** 857-872.

Pratt WB, Morishima Y, Murphy M & Harrell M 2006 Chaperoning of glucocorticoid receptors. *Handb Exp Pharmacol* 111-138.

Prima V, Depoix C, Masselot B, Formstecher P & Lefebvre P 2000 Alteration of the glucocorticoid receptor subcellular localization by non steroidal compounds. *J Steroid Biochem Mol Biol* **72** 1-12.

Quattrochi LC & Guzelian PS 2001 Cyp3A regulation: from pharmacology to nuclear receptors. *Drug Metab Dispos* **29** 615-622.

Rabbitt EH, Lavery GG, Walker EA, Cooper MS, Stewart PM & Hewison M 2002 Prereceptor regulation of glucocorticoid action by 11beta-hydroxysteroid dehydrogenase: a novel determinant of cell proliferation. *FASEB J* **16** 36-44.

Rask E, Olsson T, Soderberg S, Andrew R, Livingstone DE, Johnson O & Walker BR 2001 Tissue-specific dysregulation of cortisol metabolism in human obesity. *J Clin Endocrinol Metab* **86** 1418-1421.

Reichardt HM, Kaestner KH, Tuckermann J, Kretz O, Wessely O, Bock R, Gass P, Schmid W, Herrlich P, Angel P, Schutz G 1998 DNA binding of the glucocorticoid receptor is not essential for survival. *Cell* **93** 531-541.

Roland BL, Krozowski ZS & Funder JW 1995 Glucocorticoid receptor, mineralocorticoid receptors, 11 beta-hydroxysteroid dehydrogenase-1 and -2 expression in rat brain and kidney: *in situ* studies. *Mol Cell Endocrinol* **111** R1-7.

Romanovsky AA, Ivanov AI, Lenczowski MJ, Kulchitsky VA, Van Dam AM, Poole S, Homer LD & Tilders FJ 2000 Lipopolysaccharide transport from the peritoneal cavity to the blood: is it controlled by the vagus nerve? *Auton Neurosci* **85** 133-140.

Ross ME, Evinger MJ, Hyman SE, Carroll JM, Mucke L, Comb M, Reis DJ, Joh TH & Goodman HM 1990 Identification of a functional glucocorticoid response element in the phenylethanolamine N-methyltransferase promoter using fusion genes introduced into chromaffin cells in primary culture. *J Neurosci* **10** 520-530.

Ruiz OS, Wang LJ, Pahlavan P & Arruda JA 1995 Regulation of renal Na-HCO3 cotransporter: III. Presence and modulation by glucocorticoids in primary cultures of the proximal tubule. *Kidney Int* **47** 1669-1676.

Russell DW & Wilson JD 1994 Steroid 5 alpha-reductase: two genes/two enzymes. *Annu Rev Biochem* **63** 25-61.

Russell SB, Trupin JS, Kennedy RZ, Russell JD & Davidson JM 1995 Glucocorticoid regulation of elastin synthesis in human fibroblasts: down-regulation in fibroblasts from normal dermis but not from keloids. *J Invest Dermatol* **104** 241-245.

Sackey FN, Hache RJ, Reich T, Kwast-Welfeld J & Lefebvre YA 1996 Determinants of subcellular distribution of the glucocorticoid receptor. *Mol Endocrinol* **10** 1191-1205.

Samra JS, Clark ML, Humphreys SM, MacDonald IA, Bannister PA & Frayn KN 1998 Effects of physiological hypercortisolemia on the regulation of lipolysis in subcutaneous adipose tissue. *J Clin Endocrinol Metab* **83** 626-631.

Sandeep TC, Yau JL, MacLullich AM, Noble J, Deary IJ, Walker BR & Seckl JR 2004 11Beta-hydroxysteroid dehydrogenase inhibition improves cognitive function in healthy elderly men and type 2 diabetics. *Proc Natl Acad Sci USA* **101** 6734-6739.

Santidrian S & Young VR 1980 Effect of corticosterone and protein malnutrition on muscle protein breakdown *in vivo* in rats as measured by the urinary excretion of 3-methylhistidine. *Rev Esp Fisiol* **36** 205-214.

Sapolsky RM, Romero LM & Munck AU 2000 How do glucocorticoids influence stress responses? Integrating permissive, suppressive, stimulatory, and preparative actions. *Endocr Rev* **21** 55-89.

Sarnstrand B, Brattsand R & Malmstrom A 1982 Effect of glucocorticoids on glycosaminoglycan metabolism in cultured human skin fibroblasts. *J Invest Dermatol* **79** 412-417.

Sato A, Suzuki H, Murakami M, Nakazato Y, Iwaita Y & Saruta T 1994 Glucocorticoid increases angiotensin II type 1 receptor and its gene expression. *Hypertension* **23** 25-30.

Sawmynaden P & Perretti M 2006 Glucocorticoid upregulation of the annexin-A1 receptor in leukocytes. *Biochem Biophys Res Commun* **349** 1351-1355.

Schaaf MJM, Champagne D, van Laanen IHC, van Wijk DCWA, Meijer AH, Meijer OC, Spaink HP & Richardson MK 2008 Discovery of a functional glucocorticoid receptor beta-isoform in zebrafish. *Endocrinology* **149** 1591-1599.

Schaaf MJM & Cidlowski JA 2003 Molecular determinants of glucocorticoid receptor mobility in living cells: the importance of ligand affinity. *Mol Cell Biol* **23** 1922-1934.

Schacke H, Docke WD & Asadullah K 2002 Mechanisms involved in the side effects of glucocorticoids. *Pharmacol Ther* **96** 23-43.

Schacke H, Schottelius A, Docke W-D, Strehlke P, Jaroch S, Schmees N, Rehwinkel H, Hennekes H & Asadullah K 2004 Dissociation of transactivation from transrepression by a selective glucocorticoid receptor agonist leads to separation of therapeutic effects from side effects. *Proc Natl Acad Sci USA* **101** 227-232.

Schleimer RP & Bochner BS 1994 The effects of glucocorticoids on human eosinophils. *J Allergy Clin Immunol* **94** 1202-1213.

Schoneveld OJ, Gaemers IC & Lamers WH 2004 Mechanisms of glucocorticoid signalling. *Biochim Biophys Acta* **1680** 114-128.

Seckl JR & Walker BR 2004 11beta-hydroxysteroid dehydrogenase type 1 as a modulator of glucocorticoid action: from metabolism to memory. *Trends Endocrinol Metab* **15** 418-424.

Shneider BL, Setchell KD, Whitington PF, Neilson KA & Suchy FJ 1994 Delta 4-3-oxosteroid 5 beta-reductase deficiency causing neonatal liver failure and hemochromatosis. *J Pediatr* **124** 234-238.

Silvestrini G, Ballanti P, Patacchioli FR, Mocetti P, Di Grezia R, Wedard BM, Angelucci L & Bonucci E 2000 Evaluation of apoptosis and the glucocorticoid receptor in the cartilage growth plate and metaphyseal bone cells of rats after high-dose treatment with corticosterone. *Bone* **26** 33-42.

Smith L & Smith JB 1994 Regulation of sodium-calcium exchanger by glucocorticoids and growth factors in vascular smooth muscle. *J Biol Chem* **269** 27527-27531.

Smith SS, Gong QH, Hsu FC, Markowitz RS, ffrench-Mullen JM & Li X 1998 GABA(A) receptor alpha4 subunit suppression prevents withdrawal properties of an endogenous steroid. *Nature* **392** 926-930.

Smits HH, Grunberg K, Derijk RH, Sterk PJ & Hiemstra PS 1998 Cytokine release and its modulation by dexamethasone in whole blood following exercise. *Clin Exp Immunol* **111** 463-468.

Smoak KA & Cidlowski JA 2004 Mechanisms of glucocorticoid receptor signaling during inflammation. *Mech Ageing Dev* **125** 697-706.

Song IH & Buttgereit F 2006 Non-genomic glucocorticoid effects to provide the basis for new drug developments. *Mol Cell Endocrinol* **246** 142-146.

Sorrells SF & Sapolsky RM 2007 An inflammatory review of glucocorticoid actions in the CNS. *Brain Behav Immun* **21** 259-272.

Stahn C, Lowenberg M, Hommes DW & Buttgereit F 2007 Molecular mechanisms of glucocorticoid action and selective glucocorticoid receptor agonists. *Mol Cell Endocrinol* **275** 71-78.

Stewart PM 2002 The adrenal cortex. In *Williams textbook of endocrinology*, edn 10th, pp 491-551. Eds PR Larsen, HM Kronenberg, S Melmed & KS Polonsky. Philadelphia: Saunders.

Stewart PM, Boulton A, Kumar S, Clark PM & Shackleton CH 1999 Cortisol metabolism in human obesity: impaired cortisone-->cortisol conversion in subjects with central adiposity. *J Clin Endocrinol Metab* **84** 1022-1027.

Stewart PM, Corrie JE, Shackleton CH & Edwards CR 1988 Syndrome of apparent mineralocorticoid excess. A defect in the cortisol-cortisone shuttle. *J Clin Invest* **82** 340-349.

Stewart PM, Wallace AM, Valentino R, Burt D, Shackleton CH & Edwards CR 1987 Mineralocorticoid activity of liquorice: 11-beta-hydroxysteroid dehydrogenase deficiency comes of age. *Lancet* **2** 821-824.

Stravitz RT & Sanyal AJ 2003 Drug-induced steatohepatitis. *Clin Liver Dis* **7** 435-451.

Sugiyama T, Scott DK, Wang JC & Granner DK 1998 Structural requirements of the glucocorticoid and retinoic acid response units in the phosphoenolpyruvate carboxykinase gene promoter. *Mol Endocrinol* **12** 1487-1498.

Suzuki S, Koyama K, Darnel A, Ishibashi H, Kobayashi S, Kubo H, Suzuki T, Sasano H & Krozowski ZS 2003 Dexamethasone upregulates 11beta-hydroxysteroid dehydrogenase type 2 in BEAS-2B cells. *Am J Respir Crit Care Med* **167** 1244-1249.

Tai TC, Claycomb R, Her S, Bloom AK & Wong DL 2002 Glucocorticoid responsiveness of the rat phenylethanolamine N-methyltransferase gene. *Mol Pharmacol* **61** 1385-1392.

Tait AS, Butts CL & Sternberg EM 2008 The role of glucocorticoids and progestins in inflammatory, autoimmune, and infectious disease. *J Leukoc Biol* **82** 924-931.

Todd-Turla KM, Schnermann J, Fejes-Toth G, Naray-Fejes-Toth A, Smart A, Killen PD & Briggs JP 1993 Distribution of mineralocorticoid and glucocorticoid receptor mRNA along the nephron. *Am J Physiol* **264** F781-791.

Tomlinson JW, Finney J, Gay C, Hughes BA, Hughes SV & Stewart PM 2008a Impaired glucose tolerance and insulin resistance are associated with increased

adipose 11beta-hydroxysteroid dehydrogenase type 1 expression and elevated hepatic 5alpha-reductase activity. *Diabetes* **57** 2652-2660.

Tomlinson JW, Finney J, Hughes BA, Hughes SV & Stewart PM 2008b Reduced glucocorticoid production rate, decreased 5alpha-reductase activity, and adipose tissue insulin sensitization after weight loss. *Diabetes* **57** 1536-1543.

Tomlinson JW & Stewart PM 2001 Cortisol metabolism and the role of 11beta-hydroxysteroid dehydrogenase. *Best Pract Res Clin Endocrinol Metab* **15** 61-78.

Tomlinson JW, Walker EA, Bujalska IJ, Draper N, Lavery GG, Cooper MS, Hewison M & Stewart PM 2004 11beta-hydroxysteroid dehydrogenase type 1: a tissue-specific regulator of glucocorticoid response. *Endocr Rev* **25** 831-866.

Torres JM & Ortega E 2003 Differential regulation of steroid 5alpha-reductase isozymes expression by androgens in the adult rat brain. *FASEB J* **17** 1428-1433.

Truss M & Beato M 1993 Steroid hormone receptors: interaction with deoxyribonucleic acid and transcription factors. *Endocr Rev* **14** 459-479.

Ulick S, Levine LS, Gunczler P, Zanconato G, Ramirez LC, Rauh W, Rosler A, Bradlow HL & New MI 1979 A syndrome of apparent mineralocorticoid excess associated with defects in the peripheral metabolism of cortisol. *J Clin Endocrinol Metab* **49** 757-764.

Unterberger C, Staples KJ, Smallie T, Williams L, Foxwell B, Schaefer A, Kempkes B, Hofer TP, Koeppel M, Lohrum M, Stunnenberg H, Frankenberger M, Ziegler-Heitbrock L 2008 Role of STAT3 in glucocorticoid-induced expression of the human IL-10 gene. *Mol Immunol* **45** 3230-3237.

van den Brandt J, Luhder F, McPherson KG, de Graaf KL, Tischner D, Wiehr S, Herrmann T, Weissert R, Gold R & Reichardt HM 2007 Enhanced glucocorticoid receptor signaling in T cells impacts thymocyte apoptosis and adaptive immune responses. *Am J Pathol* **170** 1041-1053.

van Schaftingen E & Gerin I 2002 The glucose-6-phosphatase system. *Biochem J* **362** 513-532.

Vayssiere BM, Dupont S, Choquart A, Petit F, Garcia T, Marchandeau C, Gronemeyer H & Resche-Rigon M 1997 Synthetic glucocorticoids that dissociate

transactivation and AP-1 transrepression exhibit antiinflammatory activity *in vivo*. *Mol Endocrinol* **11** 1245-1255.

Walker BR 2000 Deflazacort: towards selective glucocorticoid receptor modulation? *Clin Endocrinol (Oxf)* **52** 13-15.

Walker BR 2006 Cortisol--cause and cure for metabolic syndrome? *Diabet Med* **23** 1281-1288.

Walker BR 2007a Extra-adrenal regeneration of glucocorticoids by 11beta-hydroxysteroid dehydrogenase type 1: physiological regulator and pharmacological target for energy partitioning. *Proc Nutr Soc* **66** 1-8.

Walker BR 2007b Glucocorticoids and cardiovascular disease. *Eur J Endocrinol* **157** 545-559.

Wei L, MacDonald TM & Walker BR 2004 Taking glucocorticoids by prescription is associated with subsequent cardiovascular disease. *Ann Intern Med* **141** 764-770.

Weisberg SP, McCann D, Desai M, Rosenbaum M, Leibel RL & Ferrante AW, Jr. 2003 Obesity is associated with macrophage accumulation in adipose tissue. *J Clin Invest* **112** 1796-1808.

Wilfinger WW, Mackey K & Chomczynski P 1997 Effect of pH and ionic strength on the spectrophotometric assessment of nucleic acid purity. *Biotechniques* **22** 474-476, 478-481.

Windle RJ, Wood SA, Shanks N, Lightman SL & Ingram CD 1998 Ultradian rhythm of basal corticosterone release in the female rat: dynamic interaction with the response to acute stress. *Endocrinology* **139** 443-450.

Wiper-Bergeron N, Salem HA, Tomlinson JJ, Wu D & Hache RJ 2007 Glucocorticoid-stimulated preadipocyte differentiation is mediated through acetylation of C/EBPbeta by GCN5. *Proc Natl Acad Sci USA* **104** 2703-2708.

Woods MD, Shipston MJ, Mullens EL & Antoni FA 1992 Pituitary corticotrope tumor (AtT20) cells as a model system for the study of early inhibition by glucocorticoids. *Endocrinology* **131** 2873-2880.

Wurtman RJ & Axelrod J 1966 Control of enzymatic synthesis of adrenaline in the adrenal medulla by adrenal cortical steroids. *J Biol Chem* **241** 2301-2305.

Xu H, Barnes GT, Yang Q, Tan G, Yang D, Chou CJ, Sole J, Nichols A, Ross JS, Tartaglia LA, Chen H 2003 Chronic inflammation in fat plays a crucial role in the development of obesity-related insulin resistance. *J Clin Invest* **112** 1821-1830.

Yang J, Liu J & DeFranco DB 1997 Subnuclear trafficking of glucocorticoid receptors *in vitro*: chromatin recycling and nuclear export. *J Cell Biol* **137** 523-538.

Yang-Yen HF, Chambard JC, Sun YL, Smeal T, Schmidt TJ, Drouin J & Karin M 1990 Transcriptional interference between c-Jun and the glucocorticoid receptor: mutual inhibition of DNA binding due to direct protein-protein interaction. *Cell* **62** 1205-1215.

Yasunari K, Kohno M, Murakawa K, Yokokawa K & Takeda T 1990 Glucocorticoids and atrial natriuretic factor receptors on vascular smooth muscle. *Hypertension* **16** 581-586.

Yau JL, Noble J, Kenyon CJ, Hibberd C, Kotelevtsev Y, Mullins JJ & Seckl JR 2001 Lack of tissue glucocorticoid reactivation in 11beta -hydroxysteroid dehydrogenase type 1 knockout mice ameliorates age-related learning impairments. *Proc Natl Acad Sci USA* **98** 4716-4721.

Yoshimura C, Miyamasu M, Nagase H, Iikura M, Yamaguchi M, Kawanami O, Morita Y, Iwata T, Yamamoto K & Hirai K 2001 Glucocorticoids induce basophil apoptosis. *J Allergy Clin Immunol* **108** 215-220.

Zhang TY & Daynes RA 2007 Glucocorticoid conditioning of myeloid progenitors enhances TLR4 signaling via negative regulation of the phosphatidylinositol 3-kinase-Akt pathway. *J Immunol* **178** 2517-2526.

Zhang TY, Ding X & Daynes RA 2005 The expression of 11 beta-hydroxysteroid dehydrogenase type I by lymphocytes provides a novel means for intracrine regulation of glucocorticoid activities. *J Immunol* **174** 879-889.

Zheng Y, Ye LB, Liu J, Jing W, Timani KA, Yang XJ, Yang F, Wang W, Gao B & Wu ZH 2005 Gene expression profiles of HeLa Cells impacted by hepatitis C virus non-structural protein NS4B. *J Biochem Mol Biol* **38** 151-160.